Reactor Engineering
Division

Thermophysical Properties of Uranium Dioxide

by J. K. Fink and M. C. Petri
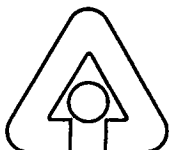
Argonne National Laboratory, Argonne, Illinois 60439
operated by The University of Chicago
for the United States Department of Energy under Contract W-31-109-Eng-38

Argonne National Laboratory, with facilities in the states of Illinois and Idaho, is owned by the United States government, and operated by The University of Chicago under the provisions of a contract with the Department of Energy.

Reactor Engineering Division
Argonne National Laboratory
9700 South Cass Avenue
Argonne, Illinois 60439

THERMOPHYSICAL PROPERTIES OF URANIUM DIOXIDE

VERSION 0 FOR PEER REVIEW

by

J. K. Fink and M. C. Petri

February 1997

DISCLAIMER

Portions of this document may be illegible
in electronic image products. Images are
produced from the best available original
document.

<p style="text-align:center">TABLE OF CONTENTS</p>

TABLE OF CONTENTS
(contd)

TABLE OF CONTENTS
(contd)

LIST OF FIGURES

LIST OF FIGURES
(contd)

LIST OF FIGURES

(contd)

LIST OF TABLES

THERMOPHYSICAL PROPERTIES OF URANIUM DIOXIDE
VERSION 0 FOR PEER REVIEW

by

J. K. Fink and M. C. Petri

ABSTRACT

Data on thermophysical properties of solid and liquid UO_2 have been reviewed and critically assessed to obtain consistent thermophysical property recommendations for inclusion in the International Nuclear Safety Center Database on the World Wide Web (http://www.insc.anl.gov.). Thermodynamic properties that have been assessed are enthalpy, heat capacity, melting point, enthalpy of fusion, thermal expansion, density, surface tension, and vapor pressure. Transport properties that have been assessed are thermal conductivity, thermal diffusivity, viscosity, and emissivity. Summaries of the recommendations with uncertainties and detailed assessments for each property are included in this report and in the International Nuclear Safety Center Database for peer review. The assessments includes a review of the experiments and data, an examination of previous recommendations, the basis for selecting recommendations, a determination of uncertainties, and a comparison of recommendations with data and with previous recommendations. New data and research that have led to new recommendations include thermal expansion and density measurements of solid and liquid UO_2, derivation of physically-based equations for the thermal conductivity of solid UO_2, measurements of the heat capacity of liquid UO_2, and measurements and analysis of the thermal conductivity of liquid UO_2.

INTRODUCTION

BACKGROUND ON THE INSC DATABASE

The International Nuclear Safety Center (INSC) has been established at Argonne National Laboratory to promote continuing improvement in nuclear safety and nuclear technology through collaboration in research, analyses, and development and through the open exchange of nuclear safety information. As an integral part of the INSC, the International Nuclear Safety Center Database has been established to provide an open exchange of safety data, tools, and information needed for reactor safety analyses and to support plant safety evaluation activities. Information in the database is maintained with the Oracle Relational Database Management System. An Internet interface provides international interactive access to the INSC Database via standard World Wide Web browsers. The INSC Database is located on the World Wide Web at http://www.insc.anl.gov.

Information that is being added to the INSC Database includes:

(1) thermophysical and mechanical properties of reactor materials for safety analyses;

(2) plant-specific operating, and design data;

(3) bibliography of available safety evaluations and risk assessments;

(4) documentation on computer codes, analysis methods, and input data for codes;

(5) network links to other information sources and databases.

MATERIAL PROPERTIES INCLUDED IN THE INSC DATABASE

One role of the INSC Database is to provide recommended thermophysical and mechanical property data of water reactor materials for normal operation, accident, and severe accident conditions. Materials that have been identified for inclusion in the database are:

Fuel: UO_2, UO_2-PuO_2, UO_2-Gd_2O_3, Irradiated UO_2, SIMFUEL, (UO_2/PuO_2)-ThO_2, PuO_2-ZrO_2, and Cermet(UO_2-Zr);

Cladding: Zirconium alloys (Zircaloy-2, Zircaloy-4), Zr-Nb alloys (Zr-1%Nb, Zr-2.5%Nb, Zr-3% Nb);

Absorbers: Ag-In-Cd, B_4C;

Structural Materials:	LWR vessel materials (e.g. stainless steels),
	VVER vessel materials,
	HWR pressure tube materials (Zr-2.5% Nb),
	HWR calandria tube materials (Zircaloy-2),
	steam generator materials (Inconels);
Liquid Mixtures:	combinations of UO_2, Zr, ZrO_2, stainless steel, absorber materials, concrete
Concrete:	limestone/common sand, siliceous, limestone.

Properties identified for inclusion in the database are most thermodynamic, transport, and mechanical properties. However, not all properties would be included for each material. Selection would be based on need for reactor safety calculations and risk assessments. Possible properties are listed below:

Thermodynamic Properties:

> enthalpy,
>
> heat capacity,
>
> density,
>
> thermal expansion,
>
> solidus/liquidus and/or melting point,
>
> enthalpy of fusion,
>
> vapor pressure,
>
> boiling point,
>
> enthalpy of vaporization,
>
> surface tension, and
>
> phase diagram information for mixtures.

Transport Properties:

> thermal conductivity,
>
> thermal diffusivity,
>
> viscosity,

emissivity, and

electrical conductivity.

Mechanical Properties:

Young's modulus,

shear modulus,

Poisson's ratio,

flow stress,

yield strength,

tensile strength,

creep strength, and

biaxial creep rupture strength.

A survey of material property needs of analysts and experimenters doing reactor safety research at Argonne National Laboratory has been used to rank the material properties for inclusion in the INSC database. This ranking has set the order of assessment. Selected thermodynamic and transport properties of UO_2 were ranked the highest.

CRITICAL ASSESSMENT AND PEER REVIEW PROCESS

The material property recommendations in the INSC database are based on the following critical assessment of the material property data and peer review process:

(1)   collection and critical assessment of all available property data;

(2)   recommendation of equations (which requires assessment of existing recommendations and, when appropriate, development of new equations by fitting data);

(3)   comparison of recommendations with previous recommendations;

(4)   determination of the uncertainties in recommended equations from errors in fitting the data, uncertainties in the data, and uncertainties in the theory used to fit the data;

(5)   inclusion of recommendations in the database for peer review (version 0);

(6)   international peer review of recommendations;

(7)   iteration of steps 2 through 6 until a consensus is reached;

(8)   inclusion of peer reviewed recommendation in the database (version 1).

As new data or new theories relevant to any material property in the database become available, the critical assessment and peer review process, outlined above, will be repeated so that the recommendations in the database remain current.

For the UO_2 thermophysical properties, critical assessments through step 5 (given above) have been completed. These assessments and recommendations are ready for peer review. They are available in the INSC database and have been documented in this report to facilitate the peer review process. All information relevant to each material property has been included under each material property in the INSC database and in each subsection of this report so that the reviewer or user needs only read the subsection for the property being reviewed. All tables and graphs given in this report are available in the INSC Database. The graphs in the INSC Database are in color for ease of identification of data and curves. Peer review comments may be sent to the main author of this report by mail or by electronic mail at the electronic mail address given at the bottom of each page in the material property section of this report.

REPORT ORGANIZATION

This report has been organized by thermophysical property. Thermodynamic properties of solid and liquid UO_2 are given in the first six sections. These sections cover enthalpy and heat capacity, melting point, enthalpy of fusion, thermal expansion and density, surface tension, and vapor pressure. Transport properties are given in the last three sections. Section 7 includes solid and liquid thermal conductivity and thermal diffusivity. Section 8 covers liquid viscosity. Section 9 covers emissivity and optical constants. When appropriate, sections are subdivided into solid and liquid properties. The section on thermal expansion and density is divided into five subsections that cover solid thermal expansion, solid density, liquid thermal expansion, liquid density, and thermodynamic relations between density and thermal expansion. The subsections for each property include a summary with recommended equation, uncertainties in the recommendation, recommended property values tabulated as a function of temperature (when appropriate), a graph of the recommendation with uncertainties, a detailed discussion of the assessment and recommendation, and a list of references. The summary is given first so that users of the INSC database not interested in the details of the assessment will be able to locate property data quickly.

THERMODYNAMIC PROPERTIES

1. ENTHALPY AND HEAT CAPACITY OF URANIUM DIOXIDE

1.1 ENTHALPY AND HEAT CAPACITY OF SOLID UO_2

Summary and Recommended Equations

Recommended equations for the enthalpy and heat capacity of solid UO_2 are from the assessment by Fink et al.[1-3] of the experimental enthalpy data[4-10] from 483 to 3112 K and the heat capacity data[11-16] from 5 to 1006 K and from the assessment by Harding et al.[17] The UO_2 phase transition at 2670 K, included in these equations, has been confirmed by high-temperature neutron diffraction and scattering experiments reported by Hutchings et al.[18-19] and by thermal analysis of $UO_{2\pm x}$ cooling curves from 2300 to 3000 K by Hiernaut et al.[20] Thermal analysis of cooling curves for stoichiometric $UO_{2.00}$ indicated a second order λ–transition peak at 2670 K. Cooling curves of substoichiometric uranium dioxide (UO_{2-x}) indicated a first order λ–transition whose temperature varied with stoichiometry while no transition was observed in cooling curves of UO_{2+x}.

The equations of Fink et al. for the enthalpy of UO_2 relative to the enthalpy at 298.15 K are
For 298.15 K $\leq T \leq$ 2670 K,

$$H(T)-H(298.15K) = C_1\theta\left[(e^{\theta/T}-1)^{-1}-(e^{\theta/298.15}-1)^{-1}\right]$$
$$+C_2\left[T^2-(298.15)^2\right] \tag{1}$$
$$+C_3k\left(Te^{-E_a/kT}-298.15e^{-E_a/k298.15}\right)$$

where
$\theta = 516.12$ K,

$C_1 = 78.215$ J $\cdot$ mol^{-1} $\cdot$ K^{-1},

$C_2 = 3.8609$ x 10^{-3} J $\cdot$ mol^{-1} $\cdot$ K^{-2},

$C_3 = 3.4250$ x 10^8 J $\cdot$ mol^{-1} $\cdot$ eV^{-1},

$E_a = 1.9105$ eV,

$k = 8.6144$ x 10^{-5} eV $\cdot$ K^{-1}, is the Boltzmann constant,

T is in K, and the enthalpy increment is in J $\cdot$ mol^{-1}.

For 2670 K ≤ T ≤ 3120 K,

$$H(T) - H(298.15K) = 167.04T - 218342. \tag{2}$$

where T is in K and the enthalpy increment is in $J \cdot mol^{-1}$.

The heat capacity of solid UO_2 is well represented by the temperature derivative of the equations for the enthalpy increments because, for solid UO_2, the other thermodynamic contributions to the heat capacity are small.[1-2]   The equations of Fink et al. for the heat capacity of UO_2 are as follows:

For 298.15 K ≤ T < 2670 K,

$$C_P = \frac{C_1 \theta^2 e^{\theta/T}}{T^2 (e^{\theta/T} - 1)^2} + 2C_2 T + C_3 ke^{-E_d/kT} \left(1 + \frac{E_a}{kT} \right) \tag{3}$$

where the symbols are defined above for Eq. (1), T is in K, and C_P is in $J \cdot mol^{-1} \cdot K^{-1}$.
For 2670 K < T ≤ 3120 K,

$$C_p = 167.04 \ J \cdot mol^{-1} \cdot K^{-1} \tag{4}$$

Values for enthalpy in $J \cdot mol^{-1}$ and heat capacity in $J \cdot mol^{-1} \cdot K^{-1}$ calculated from these equations are tabulated as a function of temperature in Table 1.1.1. Tabulated values for enthalpy in $J \cdot kg^{-1}$ and heat capacity in $J \cdot kg^{-1} \cdot K^{-1}$ are given in Table 1.1.2. Figure 1.1.1 compares the enthalpy increments from these equations with the experimental data.[4-6] Recommended values for the heat capacity with uncertainties are shown in Figure 1.1.2.

The polynomial equations for the enthalpy and heat capacity of solid UO_2 given by Harding et al.[17] fit the data with about the same standard deviations, except at low temperatures. Thus, the equations given by Harding et al.[17] are suggested as reasonable alternatives to the recommended equations of Fink et al. because of the simpler mathematical form of the equations by Harding et al. The following equations are given by Harding et al. for the enthalpy increment in $J \cdot mol^{-1}$:

For 298.15 K $\leq$ T $\leq$ 2670 K,

$$H(T) - H(298\,K) = -\,22528 + 201296\tau + 138884\tau^2 + 5498.6\tau^3$$
$$-\,329758\tau^4 + 322837\tau^5 + 186.3\tau^{-1} \tag{5}$$

where τ is the reduced temperature defined as $\tau = T/T_m$ and T_m is the melting point, 3120 K.
For 2670 < T < 3120 K,

$$H(T) - H(298K) = 521159\tau - 220041. \tag{6}$$

where τ is the reduced temperature and the enthalpy increment H(T) - H(298 K) is in J $\cdot$ mol^{-1}.

The recent analysis by Ronchi and Hyland[21] of heat capacity data from 1000 to 3000 K provides the best physically based analysis available, but the complexity of the functional forms for the contributions of each physical process as a function of temperature makes it unsuitable for numerous repetitive calculations required in computer codes used in reactor safety analyses.

Uncertainties

The uncertainty in the recommended enthalpy increments is 1% from 298.15 K to the melting point at 3120 K. The heat capacity uncertainty is 2% from 298.15 to 2000 K; 5% from 2600 K to near the phase transition. From 2000 to 2600 K, the uncertainty increases linearly. The recommended equations are discontinuous at the 2670 K $\lambda-$ phase transition. Because no attempt has been made to calculate the heat capacity peak at this transition, as was done in the detailed analysis by by Ronchi and Hyland,[21] the heat capacity equations and uncertainties are not valid for temperatures close to the λ–phase transition. The heat capacity uncertainty above the transition is 8%.

Discussion

No new analysis of the experimental data has been done for this assessment. The recommendations are based on assessments of existing equations, comparisons with available data, and recent theoretical considerations. In addition to the experimental data[4-16] on which the existing equations are based, new experimental data[18-20] confirm the existence of the phase transition first suggested by Bredig[22] at 0.8 T_m and adopted in the equations of Fink et al. and of Harding et al.

Experimental Data - Fink et al.[2-3] reviewed the experimental enthalpy and heat capacity data available prior to 1980. Their comparison of the available enthalpy data showed that the data of Hein and Flagella[6] (from 1174 to 3112 K) are in good agreement with that of Leibowitz, Mishler and Chasanov[4] (from 2561 to 3088 K) and with the data of Fredrickson and Chasanov[5] (from 674 to 1436 K). Data given by Hein, Sjodahl and Szwarz[7] is identical with that reported by Hein and Flagella.[6] Data reported by Conway and Hein[8] in 1965 are preliminary results of the data published in 1968. The 1947 measurements by Moore and Kelley (from 483 to 1464 K) do not agree well with the data of Fredrickson and Chasanov.[5] The data of Ogard and Leary (from 1339 to 2306 K) do not agree well with the data of Hein and Flagella[6] or that of Fredrickson and Chasanov.[5]

The heat capacity data of Hunzicker and Westrum[12] (5 to 346 K) and that of Gronvold et al.[11] (304-1006 K) are in good agreement in the temperature range of overlap. However, between 500 and 800 K, the data of Gronvold et al.[11] are high because of contamination of the sample by U_4O_9. The heat capacity data of Affortit and Marcon[15] and of Affortit[16] clearly disagree with other data. Data of Popov et al.[13] (433 to 876 K) are consistently high. Data of Engel[14] (300 to 1000 K) appear to have a systematic error because they differ from other data by a normalization factor.

The recent high-temperature thermal analysis of cooling curves of $UO_{2\pm x}$ by Hiernaut et al.[20] have shown the existence of a solid phase transition in stoichiometric $UO_{2.00}$ and in UO_{2-x} and provided heat capacity data in the vicinity of this transition. The high-temperature laser pulse-heating experiments by Ronchi et al.[23] to determine the heat capacity of liquid UO_2 to 8000 K included measurements of the solid at the melting point. Ronchi[24] reports $640 \, J \cdot kg^{-1} \cdot K^{-1}$ as the heat capacity of the solid for the experimental point nearest the solidus. In their analysis of the heat capacity data of solid and liquid UO_2, Ronchi and Hyland[21] estimated an 8% error in the heat capacity data above the 2670 K solid phase transition.

Hiernaut et al.[20] found that the transition temperature in nominally stoichiometric $UO_{2.00}$ is 2670 ± 30 K, which is coincident with the transition temperature proposed by Bredig[22] but higher than the 2610 K value proposed by Ralph and Hyland.[25] The scatter in their data was approximately twice the precision of the temperature measurement. The transition was identified as a first-order phase transition from cooling curves in the temperature range of 2300 to 3000 K. However, when the sample was initially heated above its melting point, no transition appeared, even in subsequent

heatings of the sample to submelting temperatures. They found that for substoichiometric urania (UO_{2-x}) the transition temperature increased with increasing x (i.e., reduction of the sample in a 3% hydrogen atmosphere) and the cooling curves exhibit undercooling indicative of a first-order transition. No transition was detected in UO_{2+x}.

Heirnaut et al.[20] found that the phase transition in stoichiometric $UO_{2.00}$ was consistent with that in stoichiometric non-actinide fluorites (e.g., $SrCl_2$), where the high-temperature phase is established rapidly but continuously. They modeled the λ-like phase transition in $UO_{2.00}$ as a second-order transition involving oxygen Frenkel disorder. Their model is consistent with the second-order λ transition in $UO_{2.00}$ converting to a first-order phase transition in UO_{2-x}. Although no transition was detected in UO_{2+x}, their model is consistent with a second-order transition that decreases with increasing x from T=2670 K at x=0 to cross the U_4O_9 phase boundary near 973 K, where a diffuse order-disorder transition is observed in the U_4O_9 oxygen sublattice. They suggested that the second-order λ transition in $UO_{2.00}$ is the stoichiometric counterpart of the interstitial superlattice transition in U_4O_9. Heirnaut et al[20] stated that they did not experimentally observe a transition in UO_{2+x} because, according to their model, the transition rapidly decreases in peak height and increases in peak width with x. Based on their experimental results and their model, Heirnaut et al.[19] have modified the U-O phase diagram to include these transitions.

High-temperature neutron diffraction, coherent diffuse, and inelastic scattering experiments on UO_2 and ThO_2 at temperatures from 293 to 2930 K reported by Hutchings et al.[18-19] provide direct evidence for thermally induced Frenkel oxygen lattice disorder at temperatures above approximately 2000 K. The disorder has been identified as dynamic Frenkel type similar to that in halide fluorites with a Frenkel pair formation energy of 4.6 ± 0.5 eV. Hutchings[18] suggested that the high oxygen vacancy concentrations and their mobility at high temperatures may be related to the observed high creep rate[26] and softening or plasticity of UO_2 above 2500 K. He also reported that inelastic magnetic scattering on lowest magnetic energy levels of U^{4+} indicate that excitation of these levels makes a significant contribution to the heat capacity in UO_2.

Theory and Equations - An excellent discussion of the current theoretical understanding of the contributions to the heat capacity of UO_2 is given by Ronchi and Hyland.[21] The dominant

contributions in each of four temperature intervals for the solid discussed in detail by Ronchi and Hyland are summarized below.

(1)   From room temperature to 1000 K, the increase in heat capacity is governed by the harmonic lattice vibrations, which may be approximated by a Debye model. By 1000 K, this contribution becomes constant. A smaller contribution is provided by thermal excitation of localized electrons of U^{4+} $(5f)^2$ in the crystal field levels. This crystal field contribution is proportional to T at low temperatures, but becomes temperature independent at high temperatures where the concentration of U^{4+} decreases as the concentrations of U^{3+} and U^{5+} increase.

(2)   From 1000 to 1500 K, the heat capacity increases because of increases in the anharmonicity of the lattice vibrations as evidenced in the thermal expansion. This contribution has been previously referred to as the thermal expansion or dilation contribution.

(3)   From 1500 to 2670 K, the increase in heat capacity is due to formation of lattice and electronic defects. The peak in the heat capacity at 2670 K (85.6% of the melting point) has been attributed to Frenkel defects both from theoretical considerations[21] and neutron scattering measurements of the oxygen defect concentration as a function of temperature as discussed by Hutchings.[18] A similar discontinuity and anion behavior was observed for ThO_2.[18,19] Harding et al.[17] commented that, because no excess enthalpy is evident in ThO_2 below the corresponding transition, it is reasonable to suggest that the increase in UO_2 below the phase transition is due to coupling between electronic disorder and Frenkel disorder. Ronchi et al.[21] pointed out that the increase in the electrical conductivity in this temperature interval indicates a contribution from electronic defects, but the small polaron contribution from electron-hole interactions is minor compared to contributions due to Frenkel defects.

(4)   Above the phase transition temperature, the peak of the heat capacity drops sharply due to rapid saturation of the defect concentration. From 2700 K to the melting point, Schottky defects become important.

The UO_2 heat capacity calculations of Ronchi and Hyland[21] from 1000 K to the melting point have a sound theoretical basis and provide good agreement with the high-temperature heat capacity data. They are the only available calculations that include a calculation of the peak in the

heat capacity. Figure 1.1.3 shows heat capacities calculated by Ronchi and Hyland,[21] experimental data (shown in their graph[21]), and their tabulated smoothed experimental data. The experimental data shown in their graph was obtained from differentiation of enthalpy data below the phase transition, the measurements of Hiernaut et al.[20] in the vicinity of the λ-transition peak, and the measurements by Ronchi et al.[23] just below the solidus. The values of the heat capacity calculated from Eqs. (3) and (4) of Fink et al. have been included in Figure 1.1.3 for comparison.

Although the calculations of Ronchi and Hyland[21] are the best theoretical description of the temperature dependence of the heat capacity of UO_2, their complexity limits their usefulness for the repetitive calculations required by reactor safety computer codes. Consequently, other existing equations have been examined. Figure 1.1.4 shows the heat capacities determined by the Kerrisk and Clifton[27] equation recommended by MATPRO[28] for the entire temperature range, the equations of Fink et al.[1-3] and of Harding et al.,[17] and the assessed experimental data as given by Ronchi and Hyland.[21] Note that Kerrisk and Clifton limited their equation to the temperature range of 298 to 1500 K. Its use for the entire temperature range, as suggested in MATPRO, is not recommended because this equation does not include a phase transition at 2670 K. Figure 1.1.4 shows that the heat capacity equation given in MATPRO deviates significantly from experimental data above 2670 K. Although the enthalpy increments calculated from the equations given in these three assessments do not appear to differ significantly, as shown in Figure 1.1.5, examination of their deviations from the experimental data shows differences. Figures 1.1.6 through 1.1.8 show the percent deviations of the equations given by MATPRO,[28] Harding et al.,[17] and Fink et al.[1-3] from the experimental enthalpy data.[4-6] The deviations of the MATPRO-recommended Kerrisk and Clifton equation (Figure 1.1.6) appear to be systematic both below and above 2670 K. Equations of Fink et al. and of Harding et al. have similar deviations. The chi-square deviations of the data from these equations are 56 for MATPRO, 25 for Harding et al., and 20 for Fink et al.

Phase transitions have been included in both the assessments of Fink et al. and of Harding et al. Their enthalpy equations above the phase transition [Eqs. (2) and (6) shown above] give values that agree within 1% and the difference in their heat capacities above 2670 K is not statistically significant. The heat capacities of Harding et al. do not differ significantly from those of Fink et al. except at low temperatures. Both agree well with the calculations of Ronchi and Hyland below the

phase transition. The polynomial equation given by Harding et al., Eq. (5), contains seven parameters, whereas Eq. (1) of Fink et al. contains five parameters but only four of them are free. One of the parameters in Eq. (1) is set by the constraint that the heat capacity at 298.15 K equals the heat capacity measured by Huntzicker and Westrum,[12] 63.60 J·mol^{-1}·K^{-1}. The form of equation used by Fink et al. constrains the enthalpy increment at 298.15 K to zero. The equation of Harding et al. gives a zero enthalpy increment at 298 K but gives 66.21 J·mol^{-1}·K^{-1} for the heat capacity at 298.15 K. This value is high relative to the experimental data by 4%. The equations of Fink et al. have been recommended because of their better fit to the enthalpy data (X^2= 20) with the use of fewer parameters. However, the 7-term polynomial and linear equations given by Harding et al. fit the available data almost as well (X^2 = 25), except for low temperature heat capacities, and provide a simpler analytical form for programming.

The forms of equations selected by Kerrisk and Clifton[27] and used by Rand et al.[29] and Fink et al.[1-3] to describe the enthalpy data below the 2670 K phase transition include terms that have traditionally been identified with contributions to the enthalpy and heat capacity from different physical processes. The first term in Eq. (1) approximate the harmonic lattice contribution, the second term accounts for the anharmonicity of the lattice as given by dilation, and the last term gives an anomalous contribution due to defects. The recent neutron diffraction and scattering experiments[18-19] have shown that the phase transition at 2670 K arises from Frenkel defects, and calculations by Ronchi and Hyland[21] show that contributions to the heat capacity due to Frenkel defects are much larger than the electronic small-polaron contribution. The mathematical form of the third term selected by Fink et al. is more appropriate for describing electronic defects than Frenkel defects. Frenkel defects are more appropriately described by a term of the form used by Rand et al.[29] and by Kerrisk and Clifton,[27] which is $C\,e^{-E/kT}$. Although the equations of Rand et al.[29] had been considered in the assessment by Fink et al., they chose the form used in Eq. (1) because it provided a better fit to the available data.[1-2] Browning et al.[30] have commented that the ability to calculate the magnitude of each contribution to the enthalpy from physical principles, as was done by Ronchi and Hyland,[21] makes analysis of the enthalpy data based on fitting procedures used by Fink et al. and Rand et al. obsolete. They also stated that attribution of the terms of equations used by Rand et al. and by Fink et al. to any physical process is only a rough

approximation because these equations do not account for all physical processes and, therefore, the fitting procedure gives values for parameters in these equations that differ from the known physical values. For example, the Debye and Einstein temperatures of UO_2 are well known and different from the values obtained in such a fitting procedure. However, Browning et al. concurred that the best fit to the experimental data below 2500 K is obtained with equations of the form used by Rand et al. and by Fink et al. These forms of equations provide a better fit to the experimental data than do fits using polynomials.

REFERENCES

1.   J. K. Fink, *Enthalpy and Heat Capacity of the Actinide Oxides,* Int. J. Thermophys. **3**(2), 165-200 (1982).

2.   J. K. Fink, M. G. Chasanov, and L. Leibowitz, *Thermophysical Properties of Uranium Dioxide,* J. Nucl. Mater. **102,** 17-25 (1981); also as ANL Report **ANL-CEN-RSD-80-3,** Argonne National Laboratory (April 1981).

3.   J. K. Fink, M. G. Chasanov, and L. Leibowitz, *Enthalpy and Heat Capacity of Solid UO$_2$,* ANL Report **ANL-CEN-RSD-81-2,** Argonne National Laboratory (May 1981).

4.   L. Leibowitz, L. W. Mishler, and M. G. Chasanov, J. Nucl. Mater. **29,** 356 (1969).

5.   D. R. Fredrickson and M. G. Chasanov, J. Chem. Thermodynamics **2,** 263 (1970).

6.   R. A. Hein and P. N. Flagella, *Enthalpy Measurements of UO$_2$ and Tungsten to 3260 K,* GE Report **GEMP-578,** General Electric, February 16, 1968.

7.   R. A. Hein, L. A. Sjodahl, and R. Szwarc, J. Nucl. Mater. **25,** 99 (1968).

8.   J. B. Conway and R. A. Hein, J. Nucl. Mater. **15,** 149 (1965).

9.   G. E. Moore and K. K. Kelly, J. Am. Chem. Soc. **69,** 2105 (1947).

10. A. E. Ogard and J. A. Leary, *High-Temperature Heat Content and Heat Capacity of Uranium Dioxide and Uranium Dioxide-Plutonium Dioxide Solid Solutions,* in Thermodynamics of Nuclear Materials 1967, IAEA, Vienna, p. 651 (1969).

11. F. Gronvold, N. J. Kvseth, A. Sveen, and J. Tichy', J. Chem. Thermo. **2,** 665 (1970).

12. J. J. Hunzicker and E. F. Westrum, J. Chem. Thermo. **3,** 61 (1971).

13. M. M. Popov, G. L. Gal'chenko, and M. D. Seniv, Zh. Neorg. Khim. **3,** 1734 (1958); [Trans. J. Inorg. Chem., USSR **3,** 18 (1958)].

14. T. K. Engel, J. Nucl. Mater. **31,** 211 (1969).

15. C. Affortit and J. Marcon, Rev. Int. Hautes Temp. et Refract. **7,** 236 (1970).

16. C. Affortit, High Temp.-High Pressures **1,** 27-33 (1969).

17.   J. H. Harding, D. G. Martin, and P. E. Potter, *Thermophysical and Thermochemical Properties of Fast Reactor Materials,* Commission of the European Communities Report **EUR 12402 EN** (1989).

18.   M. T. Hutchings, *High-Temperature Studies of UO₂ and ThO₂ Using Neutron Scattering Techniques,* J. Chem. Soc. Faraday Trans. II **83**, 1083-1103 (1987).

19.   M. T. Hutchings, K. Clausen, M. H. Dicken, W. Hayes, J. K. Kjems, P. G. Schnabel, and C. Smith, J. Phys. C **17**, 3903 (1984).

20.   J. P. Hiernaut, G. J. Hyland, and C. Ronchi, *Premelting Transition in Uranium Dioxide,* Int. J. Thermophys. **14**(2), 259-283 (1993).

21.   C. Ronchi and G. J. Hyland, *Analysis of Recent Measurements of the Heat Capacity of Uranium Dioxide,* J. of Allys and Compounds **213/214** 159-168 (1994).

22.   M. A. Bredig, *L'Etude des Transformations Crystalline a Hautes Temperatures,* Proceedings of a Conference held in Odeillo, France, 1971 (CNRS, Paris, 1972), p. 183

23.   C. Ronchi, J. P. Hiernaut, R. Selfslag, and G. J. Hyland, *Laboratory Measurement of the Heat Capacity of Urania up to 8000 K: I. Experiment,* Nucl. Sci. and Eng. **113**, 1-19 (1993).

24.   C. Ronchi, J. Phys. *On the Thermal Conductivity and Diffusivity of Solid and Liquid Uranium Dioxide,* Condens. Mater. **6**, L561-L567 (1994).

25.   J. Ralph and G. J. Hyland, *Empirical Confirmation of a Bredig Transition in UO₂,* J. Nucl. Mater. **132**, 76 (1985).

26.   L. Leibowitz, J. K. Fink, and O. D. Slagle, *Phase Transitions, Creep, and Fission Gas Behavior in Actinide Oxides,* J. Nucl. Mater. **116**, 324-325 (1983).

27.   J. F. Kerrisk and D. G. Clifton, *Smoothed Values of the Enthalpy and Heat Capacity of UO₂,* Nucl. Technol. **16**, 531 (1972).

28.   J. K. Horhorst, editor, *SCADAP/RELAP5/MOD2 Code Manual Vol. 4: MATPRO - a Library of Materials Properties for Light-Water-Reactor Accident Analysis,* **NUREG/CR-5273** (1990).

29.   M. H. Rand, R. J. Ackermann, F. Gronvold, F. L. Oetting, A. Pattoret, *The Thermodynamic Properties of the Urania Phase,* Rev. Int. Hautes Temp. Refract. **15**, 355-365 (1978).

30.   P. Browning, G. J. Hyland, and J. Ralph, *The Origin of the Specific Heat Anomaly in Solid Urania,* High Temp.-High Pressures **15**, 169-178 (1983).

Table 1.1.1 Enthalpy and Heat Capacity of UO_2 per mole of UO_2

Temperature K	Enthalpy H(T)-H(298.15 K) kJ/mol	Heat Capacity C_P J/(mol K)
298.15	0.00	63.60
300	0.12	63.79
400	6.91	71.30
500	14.27	75.49
600	21.96	78.20
700	29.89	80.17
800	37.98	81.74
900	46.22	83.06
1000	54.59	84.22
1100	63.07	85.29
1200	71.65	86.29
1300	80.32	87.26
1400	89.10	88.21
1500	97.97	89.21
1600	106.94	90.31
1700	116.04	91.64
1800	125.28	93.33
1900	134.72	95.59
2000	144.43	98.68
2100	154.49	102.88
2200	165.05	108.53
2300	176.26	116.03
2400	188.33	125.75
2500	201.50	138.13
2600	216.06	153.56
2670	227.25	166.39
2670	227.65	167.04
2700	232.67	167.04
2800	249.37	167.04
2900	266.07	167.04
3000	282.78	167.04
3100	299.48	167.04
3120	302.82	167.04

Table 1.1.2 Enthalpy and Heat Capacity of UO$_2$ per kg of UO$_2$

Temperature K	Enthalpy H(T)-H(298.15 K) kJ/kg	Heat Capacity C$_P$ J/(kg K)
298.15	0.00	235.55
300	0.44	236.27
400	25.61	264.07
500	52.85	279.58
600	81.34	289.63
700	110.69	296.93
800	140.68	302.72
900	171.20	307.62
1000	202.18	311.94
1100	233.58	315.89
1200	265.35	319.60
1300	297.49	323.17
1400	329.99	326.71
1500	362.84	330.40
1600	396.08	334.50
1700	429.77	339.40
1800	464.01	345.68
1900	498.97	354.05
2000	534.92	365.47
2100	572.20	381.02
2200	611.30	401.98
2300	652.82	429.73
2400	697.52	465.76
2500	746.30	511.58
2600	800.22	568.72
2670	841.65	616.27
2670	843.17	618.67
2700	861.73	618.67
2800	923.59	618.67
2900	985.46	618.67
3000	1047.33	618.67
3100	1109.19	618.67
3120	1121.57	618.67

Figure 1.1.1 Enthalpy of Solid UO$_2$

Legend:
— Recommended Eq. (Fink et al.)
□ Fredrickson & Chasanov
▲ Hein & Flagella
● Leibowitz, Mischler, & Chasanov

X-axis: Temperature, K
Y-axis: H(T)-H(298.15), J/(mol K)
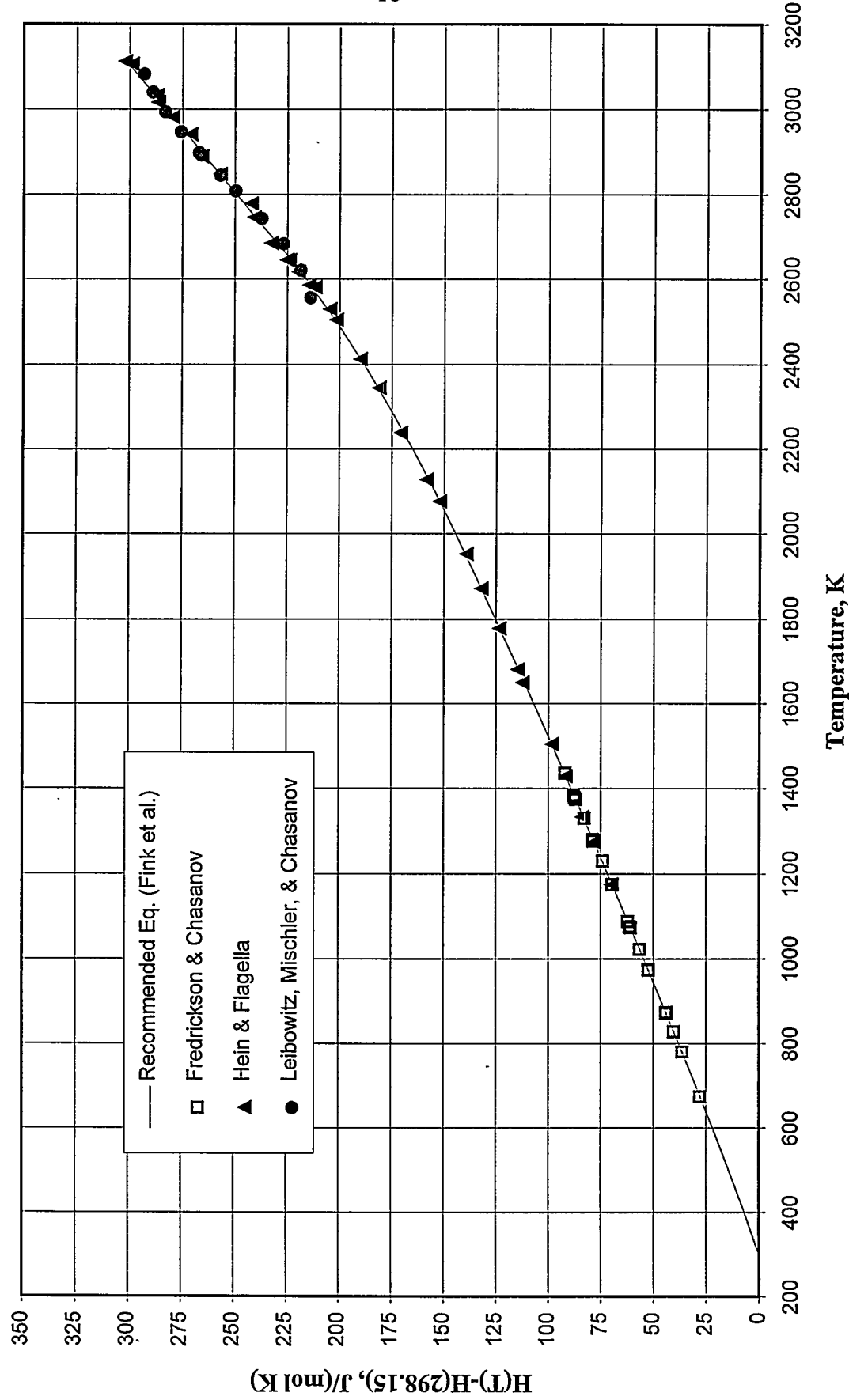
Figure 1.1.2 Recommended Heat Capacity of Solid UO₂ with Uncertainties
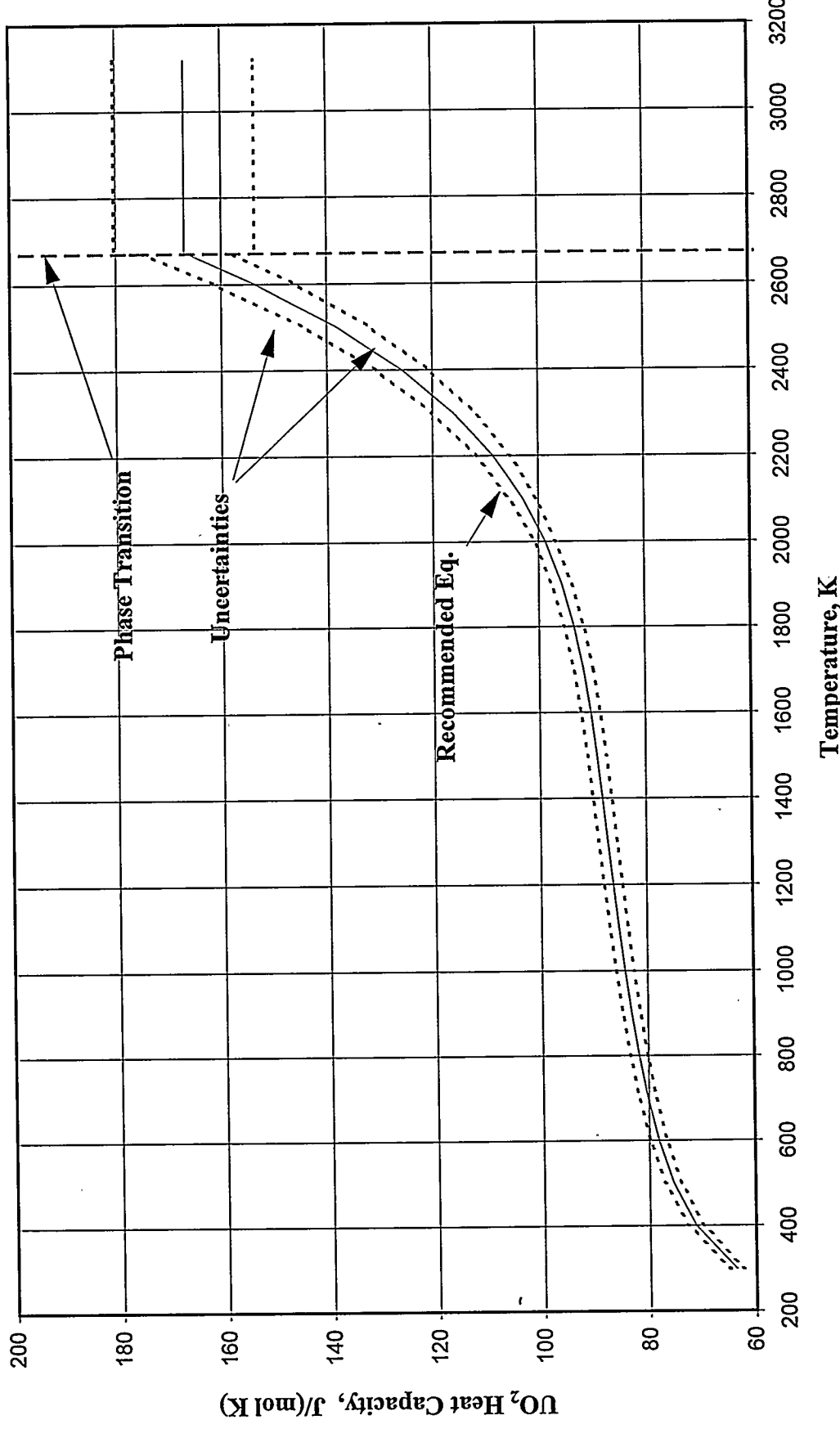
Figure 1.1.3 Heat Capacity of Solid UO_2 Calculated by Ronchi and Hyland
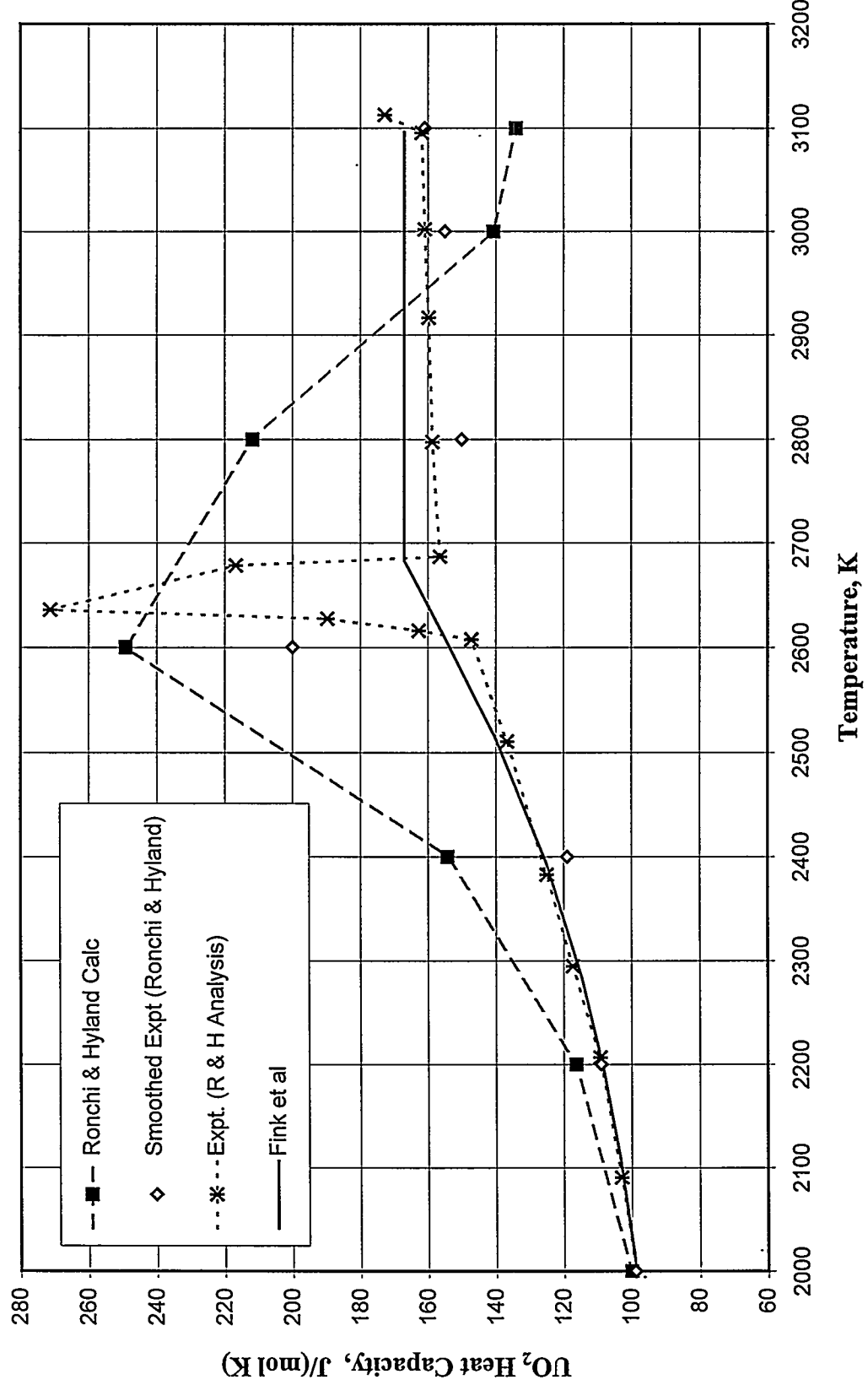
Figure 1.1.4 Comparison of Equations for the Heat Capacity of Solid UO$_2$
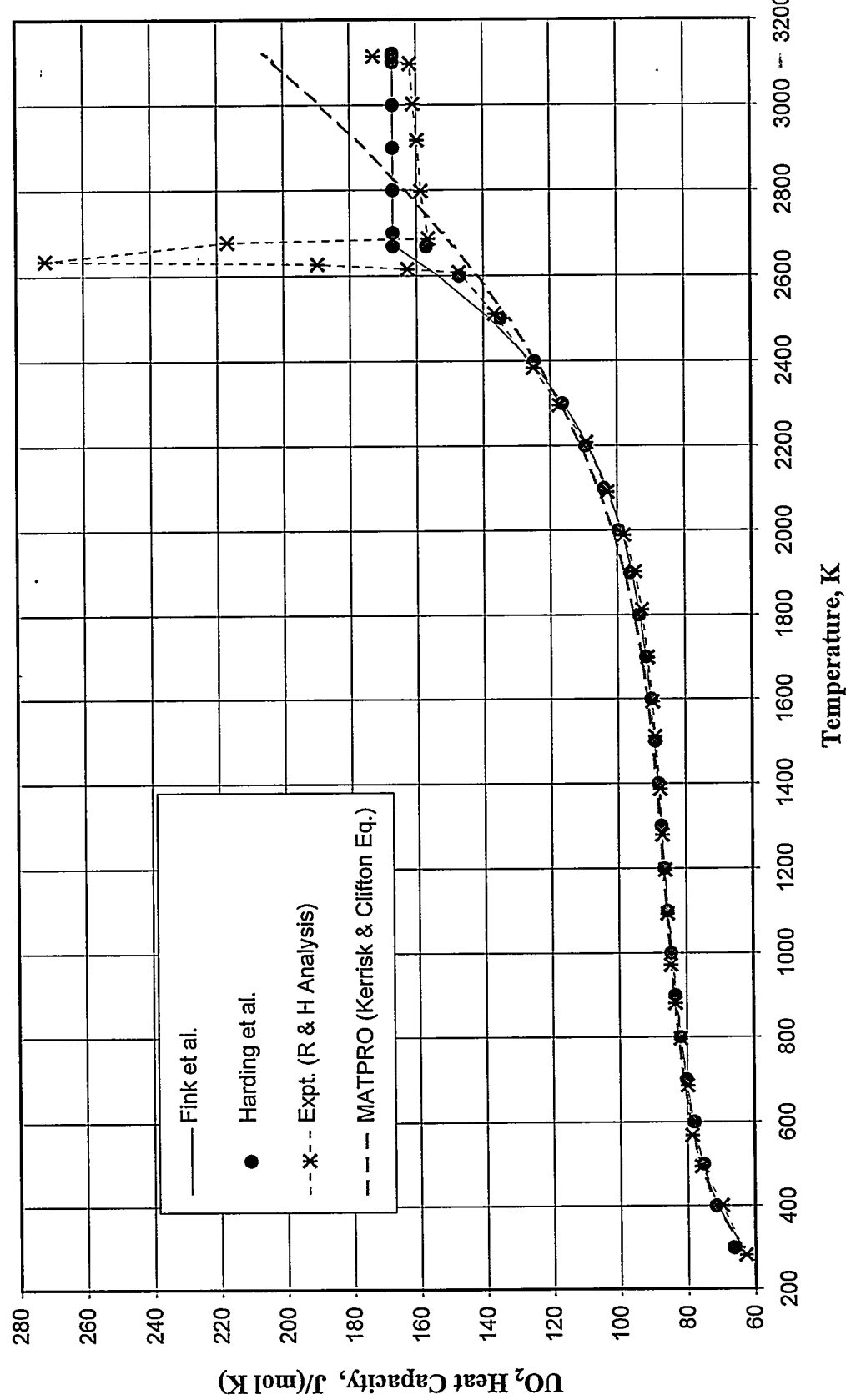
Figure 1.1.5 Comparison of Equations for the Enthalpy of Solid UO_2

Temperature, K

H(T)-H(298.15), J/(mol K)

Fink et al.

● Harding et al.

—⊞— MATPRO (Kerrisk & Clifton Eq.)
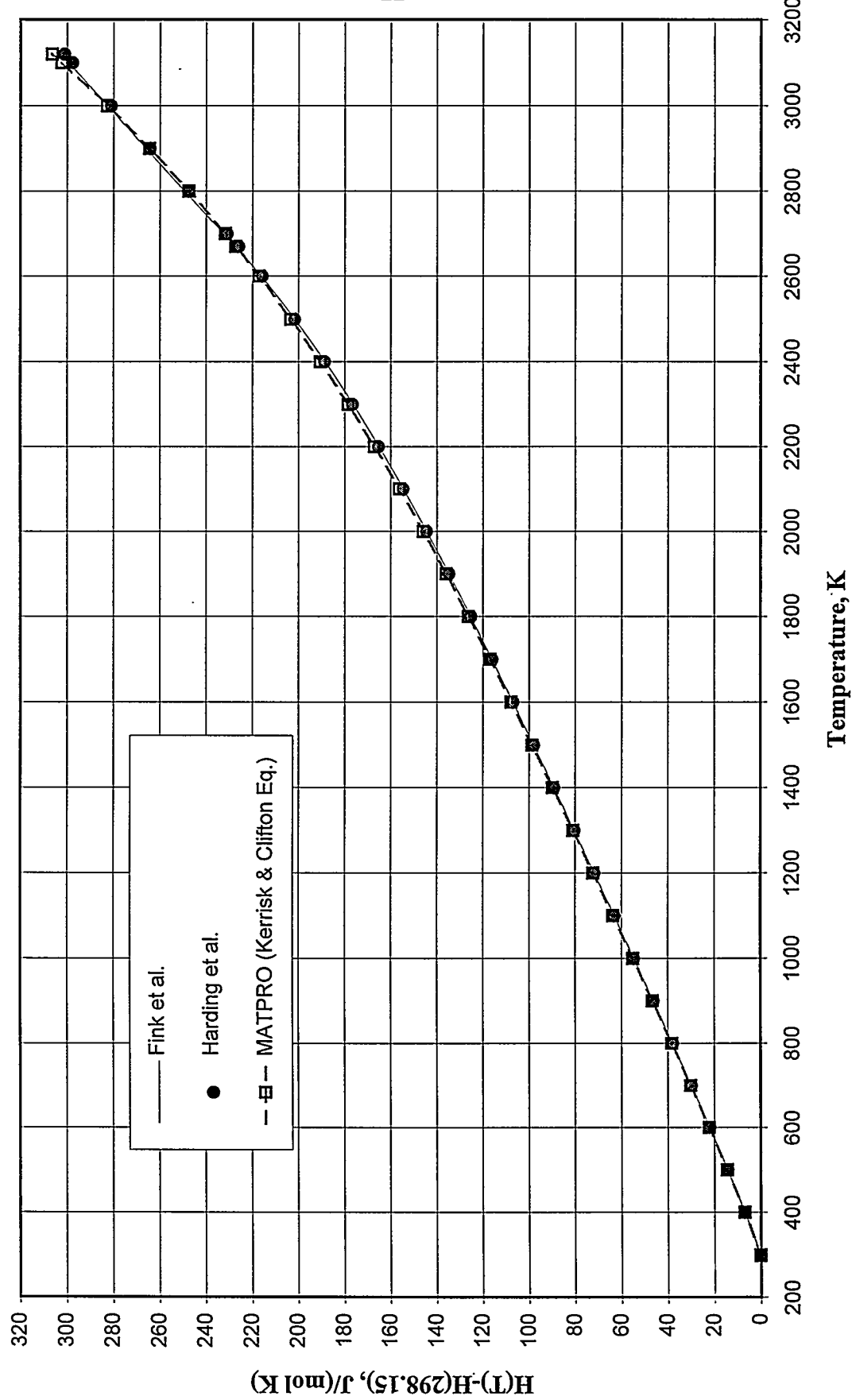
Figure 1.1.6 UO$_2$ Enthalpy Data Deviations from the MATPRO Equation

Legend:
□ Fredrickson & Chasanov
▲ Hein & Flagella
● Leibowitz, Mischler, & Chasanov

UO$_2$ Enthalpy Deviations, %

Temperature, K
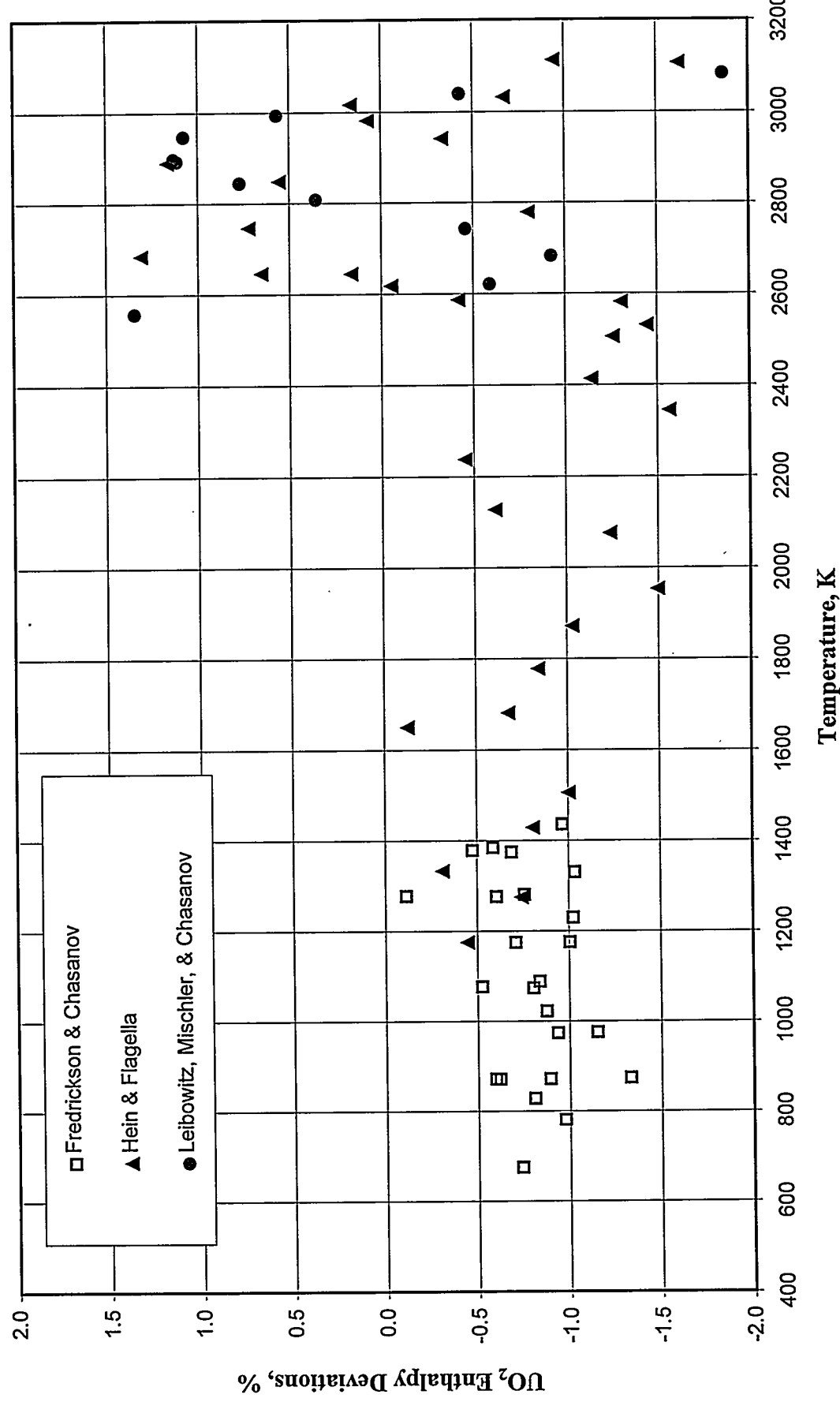
Figure 1.1.7 Enthalpy Data Deviations from the Equations of Harding et al.
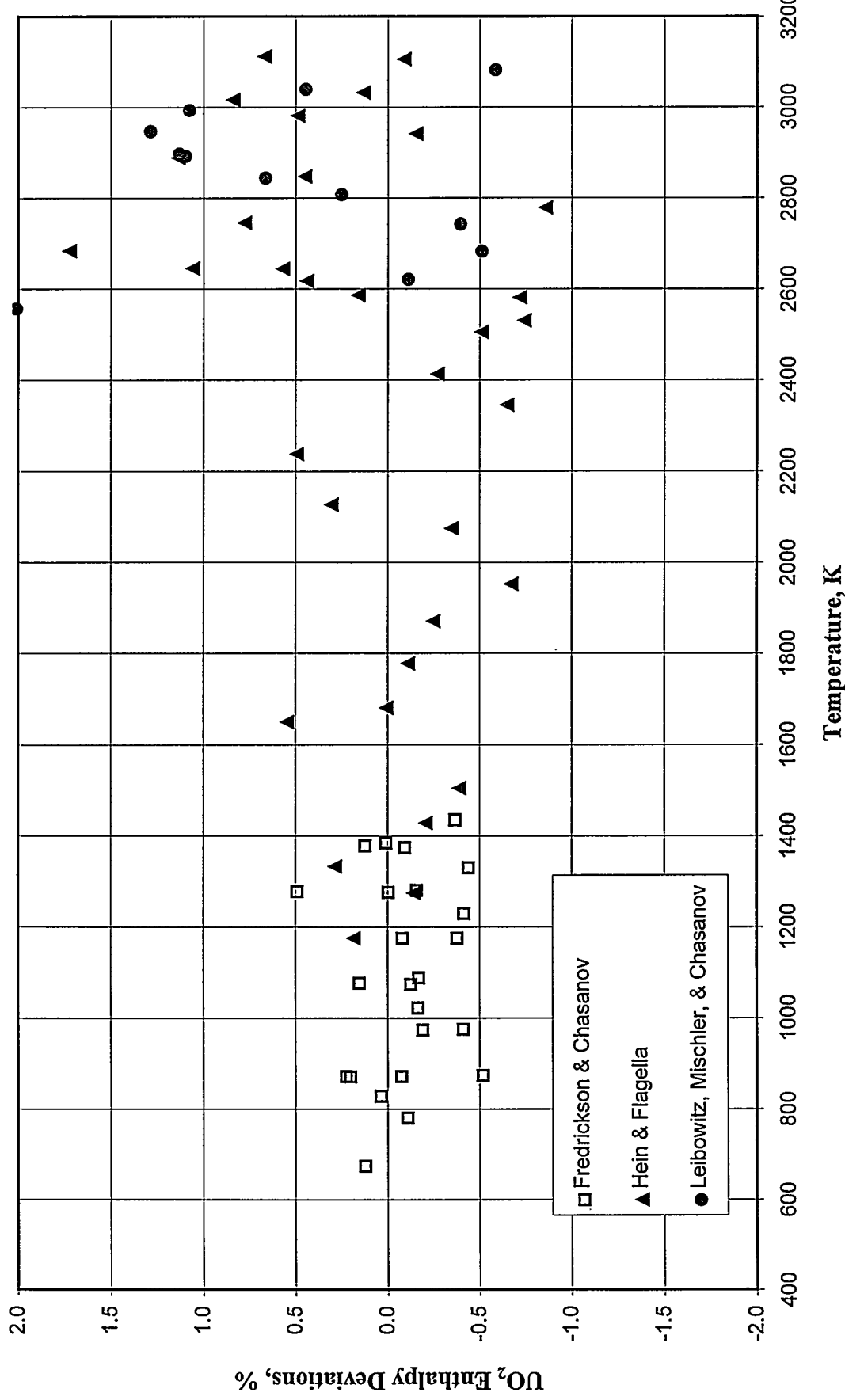
Figure 1.1.8 UO$_2$ Enthalpy Data Deviations from Equations of Fink et al.

Temperature, K

UO$_2$ Enthalpy Deviations, %

□ Fredrickson & Chasanov

▲ Hein & Flagella

● Leibowitz, Mischler, & Chasanov

Version 0 for Peer Review
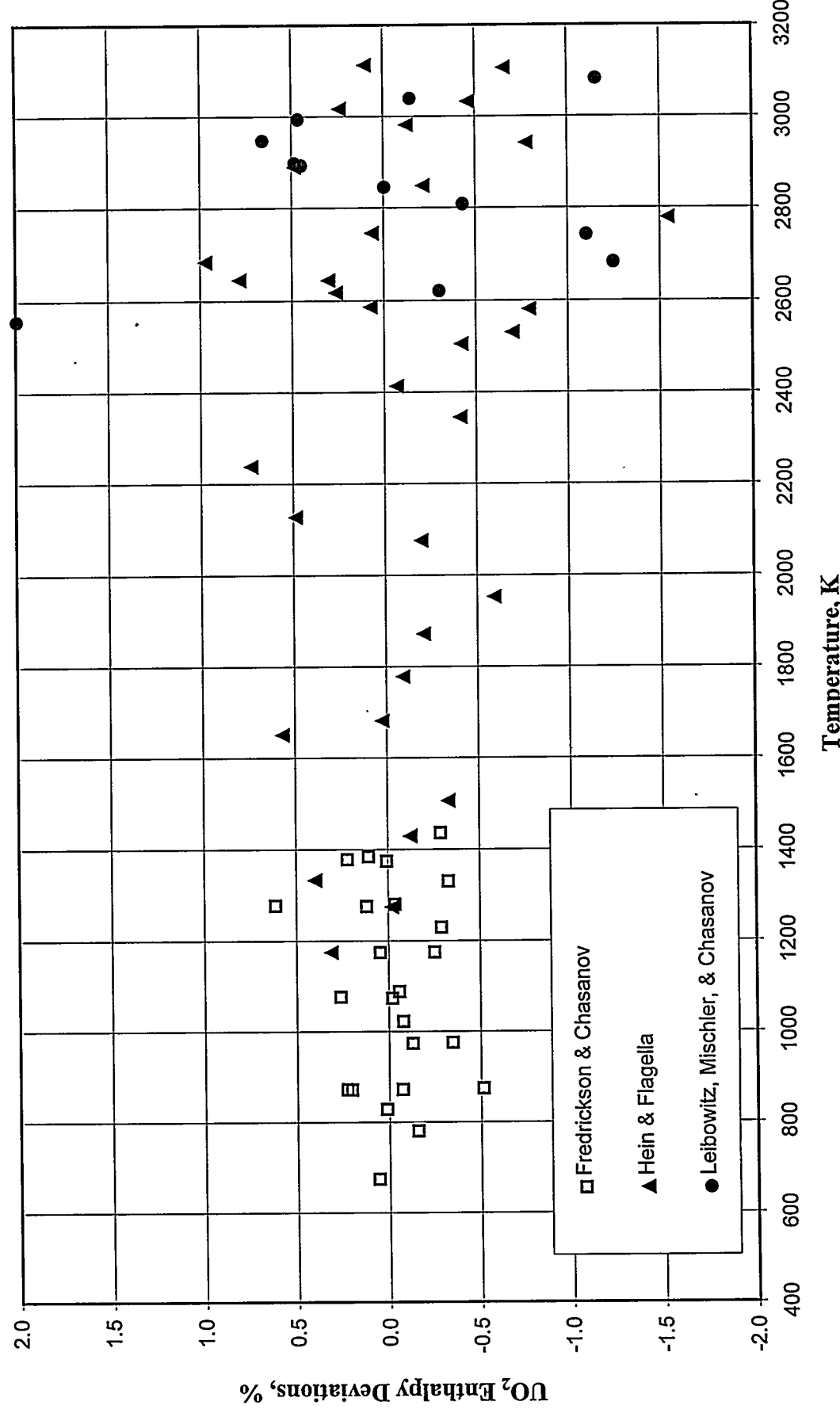
1.2   ENTHALPY AND HEAT CAPACITY OF LIQUID UO$_2$

Recommendation

The recommended equations for the enthalpy and heat capacity of liquid UO$_2$ are a least squares fit to the combined enthalpy data of Leibowitz et al.[1](3173 - 3523 K) and of Hein and Flagella[2] (3123 - 3260 K) and the heat capacity data of Ronchi et al.[3] (3100 - 4500 K). The data were weighted according to their uncertainties. Although measurements were made by Ronchi et al. to 8000 K, the data fit was limited to the temperature range 3100 to 4500 K because the range of interest for reactor safety calculations is from the melting point (3120 K) to 4500 K and the uncertainties in the determined heat capacities increase significantly with temperature above 4500 K.

For the temperature range 3120 to 4500 K, the recommended equation for the enthalpy increment of liquid UO$_2$ in J mol^{-1} is:

$$H(T) - H(298.15K) = 8.0383x10^5 - 8.4199x10^{-2}T - \frac{1.3288x10^9}{T} \qquad (1)$$

The heat capacity at constant pressure is the temperature derivative of the enthalpy. For 3120 to 4500 K, the recommended equation for the heat capacity, C_P, in J mol^{-1} K^{-1} is:

$$C_P = -8.4199x10^{-2} + \frac{1.3288x10^9}{T^2} \qquad (2)$$

In Eqs.(1) and (2), the temperature, T, is in K. Recommended values of the enthalpy increment in J mol^{-1} and the heat capacity in J mol^{-1} K^{-1} are tabulated in Table 1.2.1 and shown in Figures 1.2.1 and 1.2.2.

The recommended equations for the enthalpy increment in J kg^{-1} and the heat capacity at constant pressure in J kg^{-1}K^{-1} are

$$H(T) - H(298.15K) = 2.9768x10^6 - 0.31182T - \frac{4.9211x10^9}{T} \qquad (3)$$

and

$$C_P = -0.31182 + \frac{4.9211 \times 10^9}{T^2} \tag{4}$$

where temperature, T, is in K. Table 1.2.2 gives values for the enthalpy increment in J kg^{-1} and the heat capacity in J kg^{-1}K^{-1}.

Uncertainties

The uncertainty in the recommended values for the enthalpy of liquid UO_2 is 2% from 3120 to 3500 K and 10% in the extrapolated range from 3500 through 4500 K. The recommended values for the heat capacity of liquid UO_2 have larger uncertainties. From 3120 through 3400 K, the uncertainty is 10%. The uncertainty increases linearly from 10% at 3400 K to 25% at 4500 K. Uncertainties have been included in Figures 1.2.1 and 1.2.2.

Discussion

Enthalpy Experiments - Both Leibowitz et al.[1] and Hein and Flagella[2] used drop calorimetry to measure the enthalpy increments of molten UO_2 encapsulated in tungsten. Leibowitz et al. made six measurements from 3173 to 3523 K; Hein and Flagella made six measurements in the temperature range from 3123 to 3264 K but the datum at 3124 K was low relative to other data and discarded by Hein and Flagella. These two sets of data are in excellent agreement even though the samples differed in stoichiometry. The sample of Hein and Flagella had an O/M = 2.003 ± 0.003 at the start of the measurements and an O/M = 2.000 ± 0.003 at the end of the experiments, whereas the sample of Leibowitz et al. had an O/M = 2.015 at the start and an O/M = 1.98 at the end of the experiments. Although the change in O/M was greater in the experiments of Leibowitz et al. than in those of Hein and Flagella, the range in O/M is well within the range expected for variations of O/M in reactor fuel. The greater variation in the O/M in the experiments of Leibowitz et al. is most likely due to reduction from tungsten at high temperatures (~3500 K) because the effect of tungsten would increase as the melting point of tungsten (3685 K) is approached. Four of the six measurements of Leibowitz et al. were above the highest temperature measured by Hein and Flagella. Rand et al.[4] fit the data of Leibowitz et al.[1] and of Hein and Flagella[2] to a linear equation:

$$H(T) - H(298.15K) = 130.95\,T - 3091 \qquad (5)$$

where the enthalpy increment is in J mol^{-1} and temperature (T) is in K. This equation fits the data with a standard deviation of 0.41%. This equation has been recommended for the enthalpy of liquid UO_2 by Fink et al.[5] and by Harding, Martin, and Potter.[6] The data of Leibowitz et al.[1] and of Hein and Flagella[2] and the linear equation of Rand et al.[4] are shown in Figure 1.2.3.

Heat Capacity Experiments - The heat capacity of molten UO_2 has been determined by Ronchi et al.[3] from the analysis of cooling curves of 0.5- to 1-mm-diameter UO_2 microspheres heated to 3100-8000 K by four tetrahedrally oriented Nd:YAG lasers. The sintered UO_2 microspheres were suspended on a tungsten needle in an inert atmosphere autoclave at pressures up to 1000 bar (100 MPa). Analysis of the experiments was based on an energy balance of the rate of input energy and the enthalpy increase of the sample. The determination of the heat capacity is based on the measurement of the sample surface-temperature history during heating and cooling. Since, in most cases, the laser-energy deposition rate cannot be assessed with precision, the cooling branch of the curve is used preferentially.[7] Consequently, these difficult experiments required accurate (1) measurements of the sample temperature during and after laser pulse heating, (2) evaluation of energy loss rates, and (3) determination of the heat transport in the sample.

The experimenters took great care to minimize measurement errors as much as possible and to assess all energy losses. In an effort to reduce the errors due to optical absorption by the vapor surrounding the sample,[8] temperatures were measured using a six-wavelength optical pyrometer. Melting experiments of oxides and refractory metals, including tungsten, indicated that the accuracy of the temperature measurement was within ± 10 K. Measurements of the freezing temperature of UO_2 on various samples indicated that it was in the interval 3070 ± 20 K for samples heated in an inert atmosphere with up to 0.1 bar (0.01 MPa) of oxygen. Higher melting temperatures (3140 ± 20 K) were obtained for samples in an inert atmosphere without oxygen. This trend is consistent with the effect of change of O/U ratio on the melting temperature. The melting point of stoichiometric UO_2 is 3120 ±30 K. This value, recommended by Rand et al.[4] from their analysis of fourteen experimental studies (over a period of 20 years), has been accepted internationally.

Although Ronchi et al.[3] cited accurate measurements of lower values[9] (3075 ±30 K), Adamson et al.[10] found in their examination of melting behavior of UO_2 and $(U,Pu)O_2$ as a function of stoichiometry and irradiation that these measurements used a V-filament method, which yields consistently low melting temperatures. The V-filament method is a measurement on uncontained samples supported on a tungsten needle analogous to the method used for heat capacity measurements by Ronchi et al.[3] Adamson et al.[10] stated that in the V-filament method pronounced compositional changes occur in the small uncontained samples as a result of rapid incongruent vaporization and in some cases interactions involving oxygen exchange between either the atmosphere or the tungsten support. These changes lead to surface emissivity changes which cause an error in the temperature measurement. Ronchi et al. did not determine the stoichiometry of the microspheres before or after the heat capacity measurements because of the small size of the samples. They commented that oxidation to stoichiometries of O/U ≈ 2.03 cannot be excluded, but no evidence in the formation of U_4O_9 was observed in x-ray analysis. Although increases in stoichiometry may have occurred during heating at high pressure in an atmosphere of an inert gas plus oxygen, reductions could have occurred from heating in contact with tungsten in an inert atmosphere. Diffusion of tungsten from the supporting needle into the UO_2 was observed above 3000 K. The thickness of the UO_2/tungsten interaction region was a function of the pulse time. For a 20 ms pulse creating central melting, the chemical interaction only affected a 10 to 20 μm region near the tungsten needle and was, therefore, negligible. With repeated pulses, the tungsten precipitates migrated to the outer surface of the microsphere.

Heat losses taken into account during the pulse included radiation losses, evaporation losses, and convective losses. The experimenters observed that the plasma that surrounded their samples was significantly affected by laser excitation (inverse bremsstrahlung and photoeffects). Because the vapor partial pressure of liquid UO_2 is high and evaporation of atoms presented a serious experimental complication, the experiments had to be done under high pressures to prevent significant vaporization and mass loss. The type and pressure of the gas in the autoclave was selected based on the equation of state of Fischer[11] to reduce losses from vaporization to <1% of the radiative losses. Heat losses due to heat conduction and convection in the buffer gas were

determined from similar experiments using tungsten, which has a well-known heat capacity. Convective losses were dominant up to 4000 K.

In analysis of the experiments, Ronchi et al. used an iterative numerical method to find the unique heat capacity $C_p(T)$ that satisfies at any time the heat transport equation with the measured temperature boundary conditions and the one-dimensional unsteady energy conservation equation:

$$\frac{dH}{dt} = \int_0^{r_o} 4\pi r^2 \rho(T) C_p(T) \frac{\partial T(r)}{\partial t} dr = \text{losses} \tag{6}$$

where H is the enthalpy, $\rho(T)$ is the density as a function of temperature, $C_p(T)$ is the heat capacity at constant pressure as a function of temperature, T is the temperature, t is the time, and r_o is the radius of the UO_2 microsphere. The losses in Eq.(6) are defined by the following boundary condition:

For $r = r_o$ and $t > 0$,

$$-k\frac{\partial T}{\partial r} = \epsilon\sigma(T_S^4 - T_A^4) + D(T_S - T_A) - \phi_L(t) \tag{7}$$

where

$\quad k$ = thermal conductivity of the sphere,

$\quad T_S$ = sphere surface temperature,

$\quad T_A$ = ambient temperature,

$\quad \sigma$ = Stefan-Boltzmann constant,

$\quad \epsilon$ = total hemispherical emissivity,

$\quad r_o$ = outer radius of the sphere,

$\quad D$ = coefficient of convective and conductive heat losses to the environment,

and $\quad \phi_L$ = laser energy flux deposited onto the surface.

The quality of the experiments and selection of analyzed pulses was based on post-test metallographic examination of the microsphere to determine the integrity of the zone beneath the

measured area. Because severe cracking and large voids influenced temperature measurements, data from samples with defects in the vicinity of the measured area were discarded. Of 120 laser shots, only 20 were considered of sufficient quality for data analysis. Figure 1.2.4 shows the heat capacity data and uncertainties from Ronchi et al. The data were extracted from Figure 14 of Reference 3 because the experimenters did not tabulate their data. The points designated as "Ronchi (Not Used)" in the legend of Figure 1.2.4 indicate data that the experimenters considered to be in error and were discarded in their data analysis. They fit their data to the equation:

$$C_P = 277 + \frac{1.1 \times 10^7}{T^2} \exp\left(\frac{15500 \pm 1000}{T}\right)$$
$$+ \frac{1.0 \times 10^{12}}{T^2} \exp\left(-\frac{35500 \pm 4000}{T}\right)$$

(8)

where T is the temperature in K and C_P is the heat capacity in J kg^{-1} K^{-1}. Heat capacities calculated with this equation are shown in Figure 1.2.4 as the curve labeled "RHSH Eq."

The experimenters commented[3] that the accuracy of the heat capacities obtained from their data analysis depended on the spherical symmetry and the precision of the physical properties used in the analysis. The data reduction and analysis by Ronchi et al.[3] assumed spherical symmetry of the heat pulse, spherical symmetry of the temperature distribution in the microsphere, and maintenance of the spherical shape of the microsphere throughout the measurement. Because the surface temperature was measured on only a small area of the sample, the analysis is only viable if this temperature can be assumed to be homogeneous and if the internal temperature field can be considered spherically symmetric.[7] Although the experimenters commented that post-test examination of their samples showed that the melting front was approximately circular, it is not clear from the paper that all the necessary spherical symmetries were always maintained throughout the measurements. Peak surface temperatures of 3100 to 7850 K were achieved using input laser powers of 40 to 500 MW/m^2 with pulse durations ranging from 153 to 10 ms. The experimenters commented that the pulse duration was limited because the liquid adhered to the supporting tungsten needle for only a few tens of milliseconds before dropping. It is not clear how long the spherical

symmetry of the liquid was maintained because the liquid drop must deform prior to dropping from the needle in tens of milliseconds. The plume of hot gas around the sample during the laser heating, shown in photographs in Figure 6 of Reference 3 and Figure 4 of Reference 7, was not spherical. It is not clear if this departure from spherical symmetry was due to (1) gas flow in the autoclave, (2) nonspherical energy input and heat transfer, (3) change in the sample shape from that of a sphere, or some combination of these mechanisms.

Because the reliability of the calculated heat capacities depends on the accuracy of the physical properties used in the data analysis, the equations used for thermal conductivity and density have been compared with literature recommendations. Ronchi et al[3] calculated the density of solid UO_2 from

$$\rho^S(T) = 10970[1 + 2.04x10^{-5}(T-273) + 8.7x10^{-9}(T-273)^2]^{-1} \qquad (9)$$

where density ρ^S is in kg m^{-3} and T is in K. Densities calculated with this equation agree within 2% with values recommended in the recent assessment by Martin.[12] The thermal conductivity of solid UO_2 in W m^{-1} K^{-1} was obtained from the equation of Hyland:[13]

$$k(T) = (2.3\pm0.4) + \frac{2.25x10^5}{T}\exp\left(-\frac{12410}{T}\right) \qquad (10)$$

where T is in K. Values calculated with this equation agree within 8% with the values recently recommended by Harding and Martin.[14] Both are in good agreement with the available data.

Ronchi et al[3] calculated the liquid density of UO_2 from their least-squares fit to the data of Christensen[15] and Drotning:[16]

$$\rho^L(T) = 10970[1 + 9.30x10^{-5}(T-273)]^{-1} \qquad (11)$$

where density is in kg m^{-3} and T is in K. The form selected for this equation is the same as that for the solid density. Values calculated with this equation differ significantly from those obtained from the equation recommended by Drotning and the recent equation of Breitung and Reil,[17] which is

based on in-reactor measurements of the density and thermal expansion from the melting point to 8000 K. The equation of Breitung and Reil[17] is

$$\rho^L = 8860 - 0.9285(T - 3120) \qquad (12)$$

where density (ρ^L) is in kg m^{-3} and T is in K. Densities obtained from the equation by Breitung and Reil are in good agreement with values recommended by Drotning (within 1.2% from 3120 to 7600 K), and within 2.5% of the densities recommended from the melting point to 7600 K in an independent assessment by Harding, Martin, and Potter.[6] In Figure 1.2.5, densities calculated with the equation given by Ronchi et al.[3] are compared with the experimental data of Drotning and of Christensen, and with the equation recommended by Breitung and Reil. Densities calculated with the equation used by Ronchi et al. show a systematic deviation compared to densities calculated from the equation of Breitung and Reil. They deviate by -2% at the melting point, +4% at 4500 K, +16% at 6000 K, and +40% at 7600 K. Although the analytical form of equation selected by Ronchi et al. gives decreasing densities with increasing temperature, the densities do not decrease as fast as in the linear equations recommended by Breitung and Reil and by Christensen. Fischer[11] commented that the linear decrease with temperature of the liquid density is well established by existing experiments and the only physical reason for the liquid density to deviate from a straight line is due to the approach of the critical point where the deviation is more negative. The critical temperature and density given by Fischer[11] are respectively 10600 K and 1560 kg m^{-3}. The possibility exists that the density equation used by Ronchi et al. includes the increase of density with pressure since experiments at higher temperatures were performed at high pressure. However, Ronchi et al. made no mention of including the effects of pressure in their equation for the liquid density. They simply stated that the data of Drotning and of Christensen were fit to Eq. (11). Breitung and Reil have commented that along the saturation line the change in density due to increasing pressure is much smaller than the change in density due to thermal expansion.[17] Even at 8000 K, the correction of density for saturation pressure is only a few percent,[17] so the effects of pressure can be ignored. Thus, it is unclear why the equation given by Ronchi et al.[3] for the liquid density or UO$_2$ deviates

so greatly from the expected liquid density behavior and recommended densities at high temperatures.

For the thermal conductivity of liquid UO_2, Ronchi et al. used 2.5 W m^{-1} K^{-1}, which is the value obtained just above the melting point in recent measurements by Tasman[18] at the Institute for Transuranium Elements. This value is in agreement with the average value of 2.2 W m^{-1} K^{-1} previously obtained by Tasman et al.[19] for the temperature range 3103-3473 K. In these earlier measurements, a thermal conductivity of 2.4 W m^{-1} K^{-1} was obtained in an experiment in which the maximum top center temperature of the molten pool was 3473 K. In addition to the thermal conductivity measurements of Tasman et al.[18, 19] UO_2 thermal diffusivity measurements were made by Kim et al.[20] from 3187 to 3310 K and by Otter and Damien[21] in the temperature range of 3133 to 3273 K. The available experimental data on the thermal diffusivity and thermal conductivity[19] of UO_2 were reassessed in 1985 by Fink and Leibowitz,[22] who recommended 5.6 W m^{-1} K^{-1} for the thermal conductivity from the melting point to 3500 K. In this reassessment, Fink and Leibowitz used 131 J mol^{-1} K^{-1} (485 J kg^{-1} K^{-1}), the constant heat capacity given by the enthalpy equation of Rand et al.[4] If the heat capacities given by Ronchi et al. had been used in the reassessment, lower thermal conductivity values (3.3 to 5.8 W m^{-1} K^{-1}) would have been obtained in the assessment of these data. Ronchi et al. commented that the existence of a systematic error in the experimental measurements of Tasman cannot be excluded. At low temperatures, their calculated heat capacity is approximately inversely proportional to the thermal conductivity. Thus, selection of a higher thermal conductivity in this low temperature region would give lower heat capacities.

Ronchi et al. have assumed a constant thermal conductivity based on the assumption that thermal conductivity of liquids obey the Lorenz rule and are therefore only a weak function of temperature. Because no temperature dependence was evident in any of the thermal diffusivity data and no information is available on variation of thermal conductivity with temperature from the measurements of Tasman, there is no basis to assess this assumption. Wakeham[23] commented that the thermal conductivities of a number of liquids at high pressure are stronger functions of density change with pressure than functions of temperature. In their analysis, Ronchi et al. did not consider the effects of changes in pressure on the thermal conductivity, although the high temperature

measurements were done at pressures on the order of 100 MPa (1000 bar). Wakeham[23] found that for pressure variations from 0.1 to 700 MPa, the reduced thermal conductivity decreased as a function of increasing reduced molar volume (inverse reduced density).

Relationship Between Enthalpy and Heat Capacity Measurements, C_P and C_σ - The enthalpy measurements by Leibowitz et al.[1] and by Hein and Flagella[2] were performed on encapsulated samples so that the liquid was maintained in equilibrium with a small amount of vapor, giving the enthalpy along the saturation curve. The temperature derivative of these enthalpies is the heat capacity along the saturation curve, C_σ, which is related to the heat capacity at constant pressure, C_P, by

$$\left(\frac{\partial H}{\partial T} \right)_\sigma = C_\sigma = C_P - \frac{(T\alpha_P - 1)}{\rho} \left(\frac{\partial P}{\partial T} \right)_\sigma \qquad (13)$$

where P is the vapor pressure, ρ is the density, α_P is the instantaneous thermal expansion coefficient, T is the temperature, and the subscript σ designates the saturation curve. For most liquids, the difference between C_P and C_σ is not significant at temperatures below 75% of the critical temperature. Recent vapor pressure measurements by Breitung and Reil[17] and equation-of-state calculations by Fischer[11] indicate that the critical temperature for UO_2 is 10600 K. Thus, differences between C_P and C_σ are not significant below 7950 K. So for the temperature range of the UO_2 enthalpy data, the temperature derivative of the equation that fits the enthalpy measurements may be considered as the heat capacity at constant pressure.

The heat capacity measurements of Ronchi et al. were not done at constant pressure because measurements at constant pressure would have resulted in complete vaporization of the sample as the temperature was increased. Ronchi et al. used the saturated and total pressures from the equation of state of Fischer[11] to determine the pressure needed to prevent large losses from vaporization. However, the extent of pressure increase beyond the saturation pressure is not clear from the description of the experiment. In the analysis of Ronchi et al. and in the analysis below, the heat capacities reported by Ronchi et al. are assumed to be equivalent to C_P.

Combined Analysis of Enthalpy and Heat Capacity Data - Ronchi et al.[3] stated that the enthalpy data of Hein and Flagella and of Leibowitz et al. are consistent with their Equation 20, which will subsequently be referred to as "RHSH Eq. 20":

$$C_P(T) = 277 + \frac{(2370 \pm 290)}{(T/1000)^2} \qquad (14)$$

where heat capacity is in J kg^{-1} K^{-1} and temperature is in K. The first term of this equation is the Neumann-Kropp heat capacity value for a harmonic triatomic lattice (9R) which was fixed so that the only free parameter in the fitting procedure was the coefficient for the second term. They fit their heat capacity data from 3200 to 4500 K to an equation of the same form allowing both parameters to vary, giving their Equation 21, which will be referred to as "RHSH Eq. 21":

$$C_P(T) = 67.7 + \frac{(3831 \pm 300)}{(T/1000)^2} \qquad (15)$$

where heat capacity is in J kg^{-1} K^{-1} and temperature is in K. A graph of this fit has been included in Figure 1.2.4 for comparison with the fit given by Ronchi et al. for the entire temperature range 3100 to 8000 K.

A weighted combined fit has been performed for the enthalpy data of Leibowitz et al.[1] from 3173 to 3523 K and of Hein and Flagella[2] from 3123 to 3260 K and the heat capacity data of Ronchi et al.[3] from 3100 to 4500 K. Only the heat capacities at or below 4500 K have been included in this combined analysis because:

1.   above 4500 K, the deviations of the densities used by Ronchi et al. increases above 4% from accepted liquid densities;

2.   at higher temperatures, the pressure in the autoclave was increased significantly to prevent sample vaporization;

3.   at 4500 K and above, oxygen was added to the gas in an attempt to control the change in sample stoichiometry arising from vaporization, so greater uncertainty exists in the stoichiometry of the sample and in the temperature measurements;

4.   as the temperature increases, sample loss due to laser ablation and ionization effects from the laser heating become more pronounced;

5.   data above 4500 K are not needed for light water nuclear reactor severe accident analysis because higher temperatures are unlikely in these accident scenarios.

The form of the equation for the heat capacity used in this combined analysis is that suggested by Ronchi et al. in their data analysis in this temperature range. A weighted chi-squared minimization was used to determine the coefficients with the constraint that the enthalpy increment at the accepted melting point (3120 K) equals that given by the enthalpy equation of Rand et al.[4] This constraint provides consistency with the accepted heats of fusion at the accepted melting point. The data have been weighted by the inverse of their uncertainties. Because the enthalpy data are in excellent agreement in the two independent experiments,[1,2] which used standard techniques with calibration standards, and the stoichiometry change in these enthalpy experiments were within the variation for reactor fuel, these data were considered to be of higher quality than the heat capacity data. The uncertainty in the enthalpy data has been estimated as 2%. Ronchi et al. stated that the uncertainty in the heat capacity data is on the order of 15 to 20% from 3000 to 5000 K. A 15% uncertainty has been assumed for the heat capacity data. Thus, the enthalpy chi-squared has been weighted by a factor of 50 relative to the heat capacity chi-squared in the combined chi-squared minimization.

Equations (1) and (2) are, respectively, the enthalpy and heat capacity equations obtained from this weighted chi-squared minimization. In Figure 1.2.6, this weighted fit to enthalpy and heat capacity data is compared with the enthalpy data, the linear equation of Rand et al., the RHSH Eq. 20, and the enthalpies obtained by Ronchi et al. from fitting the heat capacity data from the melting point to 8000 K adjusted to a melting point of 3120 K and the enthalpy increment of Rand et al. (labeled "RHSH rel 3120"). This weighted equation fits the data to within 0.6% except for the data at and above 3475 K which are fit to 1.6 %. The greater deviation for the higher temperature data is acceptable because the stoichiometry variation detected by Leibowitz et al. most likely occurred during these high temperature measurements.

In Figure 1.2.7, the heat capacity data of Ronchi et al. from the melting point to 4500 K are plotted as a function of the square of the inverse temperature. Included for comparison with the data are the constant heat capacity of Rand et al., RHSH Eq. 20 (which fits the enthalpy data with one free parameter), RHSH Eq. 21 (which fits the heat capacity data with two free parameters), the fit by Ronchi et al. to all the heat capacity data (labeled "RHSH"), and the recommended weighted combined fit to the enthalpy and heat capacity data. This combined fit is much better than the fit to the enthalpy data alone (RHSH Eq. 20) and fits the data as well as the fit given by Ronchi et al. to the heat capacity data for the entire temperature range.

Figure 1.2.8 shows the heat capacity data with the error bars given by Ronchi et al., the fit by Ronchi et al. to data up to 4500 K (RHSH Eq. 21), the fit by Ronchi et al. to the heat capacities for the entire temperature range (RHSH), and the weighted combined fit to the enthalpy and heat capacities. The combined fit is within the error bars of most of the heat capacity data. Data with error bars that do not intersect this combined fit are also not well represented by the RHSH Eq. 21, indicating that they are not consistent with other heat capacity data in this temperature range. Deviations of the data from the combined fit are within the estimated uncertainty shown in Figure 1.2.2 except for isolated data near 3370 K, 3700 K, and 4370 K.

REFERENCES

1.   L. Leibowitz, M. G. Chasanov, L. W. Mishler, and D. F. Fischer, *Enthalpy of Liquid Uranium Dioxide to 3500 K,* J. Nucl. Mater. **39** 115-116 (1971).

2.   R. A. Hein and P. N. Flagella, *Enthalpy Measurements of UO_2 and Tungsten to 3260 K,* General Electric Report **GEMP-578** (February 16, 1968).

3.   C. Ronchi, J. P. Hiernaut, R. Selfslag, and G. J. Hyland, *Laboratory Measurement of the Heat Capacity of Urania up to 8000 K: I. Experiment,* Nuclear Science and Engineering **113**, 1-19 (1993).

4.   M. H. Rand, R. J. Ackermann, F. Gronvold, F. L. Oetting, A. Pattoret, *The Thermodynamic Properties of the Urania Phase,* Rev. Int. Hautes Temp. Refract. **15**, 355-365 (1978).

5.   J. K. Fink, M. G. Chasanov, and L. Leibowitz, *Thermophysical Properties of Uranium Dioxide,* J. Nucl. Mater. **102,** 17-25 (1981); also as ANL Report **ANL-CEN-RSD-80-3,** Argonne National Laboratory (April 1981).

6.   J. H. Harding, D. G. Martin, and P. E. Potter, *Thermophysical and Thermochemical Properties of Fast Reactor Materials,* Commission of the European Communities Report **EUR 12402 EN** (1989).

7.   J. P. Hiernaut, and C. Ronchi, *Calorimetric Measurements with Acoustic Levitation in High-Temperature Heating Experiments with Pulsed Laser Beams,* High Temps-High Pressures **21**, 119-130 (1989).

8.   C. Ronchi, R, Beukers, H. Heinz, J. P. Hiernaut, and R. Selfslag, *Graphite Melting Under Laser Pulse Heating,* Int. J. Thermophys. **13** (1) 107-129 (1992).

9.   J. L. Bates, Proc. IAEA Symp. Thermodynamics, Vienna, July 22-27 1965, Vol. II, p. 73, International Atomic Energy Agency, Vienna (1966); as referenced by C. Ronchi, J. P. Hiernaut, R. Selfslag, and G. J. Hyland, *Laboratory Measurement of the Heat Capacity of Urania up to 8000 K: I. Experiment,* Nuclear Science and Engineering **113**, 1-19 (1993).

10.   M. G. Adamson, E. A. Aitken, and R. W. Caputi, *Experimental and Thermodynamic Evaluation of the Melting Behavior of Irradiated Oxide Fuels,* J. Nucl. Mater. **130**, 349-365 (1985).

11.   E. A. Fischer, *Evaluation of the Urania Equation of State Based on Recent Vapour Pressure Measurements,* Kernforschungszentrum Karlsruhe GmbH Report **KfK 4084** (September 1987); Nuclear Science and Engineering **101**, 97-116 (1989).

12.   D. G. Martin, *The Thermal Expansion of Solid UO₂ and (U,Pu) Mixed Oxides - A Review and Recommendations,* J. Nucl. Mater. **152**, 94-101 (1988).

13.   G. J. Hyland, *Thermal Conductivity of Solid UO₂: Critique and Recommendation,* J. Nucl. Mater. **113**, 125-132 (1983).

14.   J. H. Harding and D. G. Martin, *A Recommendation for the Thermal Conductivity of UO₂,* J. Nucl. Mater. **166**, 223-226 (1989).

15.   J. A. Christensen, *Thermal Expansion and Change in Volume of Uranium Dioxide on Melting,* J. Am. Ceram. Soc. **46**, 607-608 (1963).

16.   W. D. Drotning, *Thermal Expansion of Molten Uranium Dioxide,* Proceedings of the Eighth Symp. On Thermophysical Properties, Gaithersburg, Maryland, June 15-18, 1981, J. V. Sengers, Ed., ASME, New York, Vol. II, pp 245-249 (1981).

17.   W. Breitung and K. O. Reil, *The Density and Compressibility of Liquid (U,Pu)-Mixed Oxide,* Nuclear Science and Engineering **105**, 205-217 (1990).

18.   H. A. Tasman, *Thermal Conductivity of Liquid UO₂,* Commission of the European Communities Joint Research Centre Annual Report **TUAR88**, Karlsruhe, Germany EUR-12385, p. 80 (1989), as referenced by C. Ronchi in *On the Thermal Conductivity and Diffusivity of Solid and Liquid Uranium Dioxide,* J. Phys. Condens. Matter **6**, L561-L567 (1994).

19.   H. A. Tasman, D. Pel, J. Richter, and H. E. Schmidt, *Measurement of the Thermal Conductivity of Liquid UO₂,* High Temp.–High Pressures **15**, 419-431 (1983).

20.   C. S. Kim, R. A. Haley, J. Fischer, M. G. Chasanov, and L. Leibowitz, *Measurement of Thermal Diffusivity of Molten UO₂,* Proc. Seventh Symp. On Thermophysical Properties, A. Cezairliyan, Ed., ASME, New York, p. 338-343 (1977).

21.   C. Otter and D. Damien, *Mesure de la Diffusivite Thermique de UO₂ Fondu,* High Temp.–High Pressures **16**, 1-6 (1984).

22.   J. K. Fink and L. Leibowitz, *An Analysis of Measurements of the Thermal Conductivity of Liquid Urania,* High Temp.–High Pressures **17**, 17-26 (1985).

23.   W. A. Wakeham, *Thermal Conductivity of Liquids Under Pressure,* High Temp.–High Pressures **21**, 249-259 (1989).

Table 1.2.1   Enthalpy and Heat Capacity of Liquid UO$_2$ per mole of UO$_2$

Temperature K	Enthalpy $H(T) - H(298.15 \text{ K})$ kJ mol^{-1}	Heat Capacity C_P J mol^{-1} K^{-1}
3120	378	136
3150	382	134
3200	388	130
3250	395	126
3300	401	122
3350	407	118
3400	413	115
3450	418	112
3500	424	108
3550	429	105
3600	434	102
3650	439	100
3700	444	97.0
3750	449	94.4
3800	454	91.9
3850	458	89.6
3900	463	87.3
3950	467	85.1
4000	471	83.0
4050	475	80.9
4100	479	79.0
4150	483	77.1
4200	487	75.2
4250	491	73.5
4300	494	71.8
4350	498	70.1
4400	501	68.6
4450	505	67.0
4500	508	65.5

Table 1.2.2   Enthalpy and Heat Capacity of Liquid UO_2 per kg of UO_2

Temperature K	Enthalpy $H(T) - H(298.15 \text{ K})$ kJ mol^{-1}	Heat Capacity C_P J mol^{-1} K^{-1}
3120	1399	505
3150	1414	496
3200	1438	480
3250	1462	466
3300	1485	452
3350	1507	438
3400	1528	425
3450	1549	413
3500	1570	401
3550	1589	390
3600	1609	379
3650	1627	369
3700	1646	359
3750	1663	350
3800	1681	340
3850	1697	332
3900	1714	323
3950	1730	315
4000	1745	307
4050	1760	300
4100	1775	292
4150	1790	285
4200	1804	279
4250	1818	272
4300	1831	266
4350	1844	260
4400	1857	254
4450	1870	248
4500	1882	243

Figure 1.2.1 Recommended Values for the Enthalpy of Liquid UO$_2$
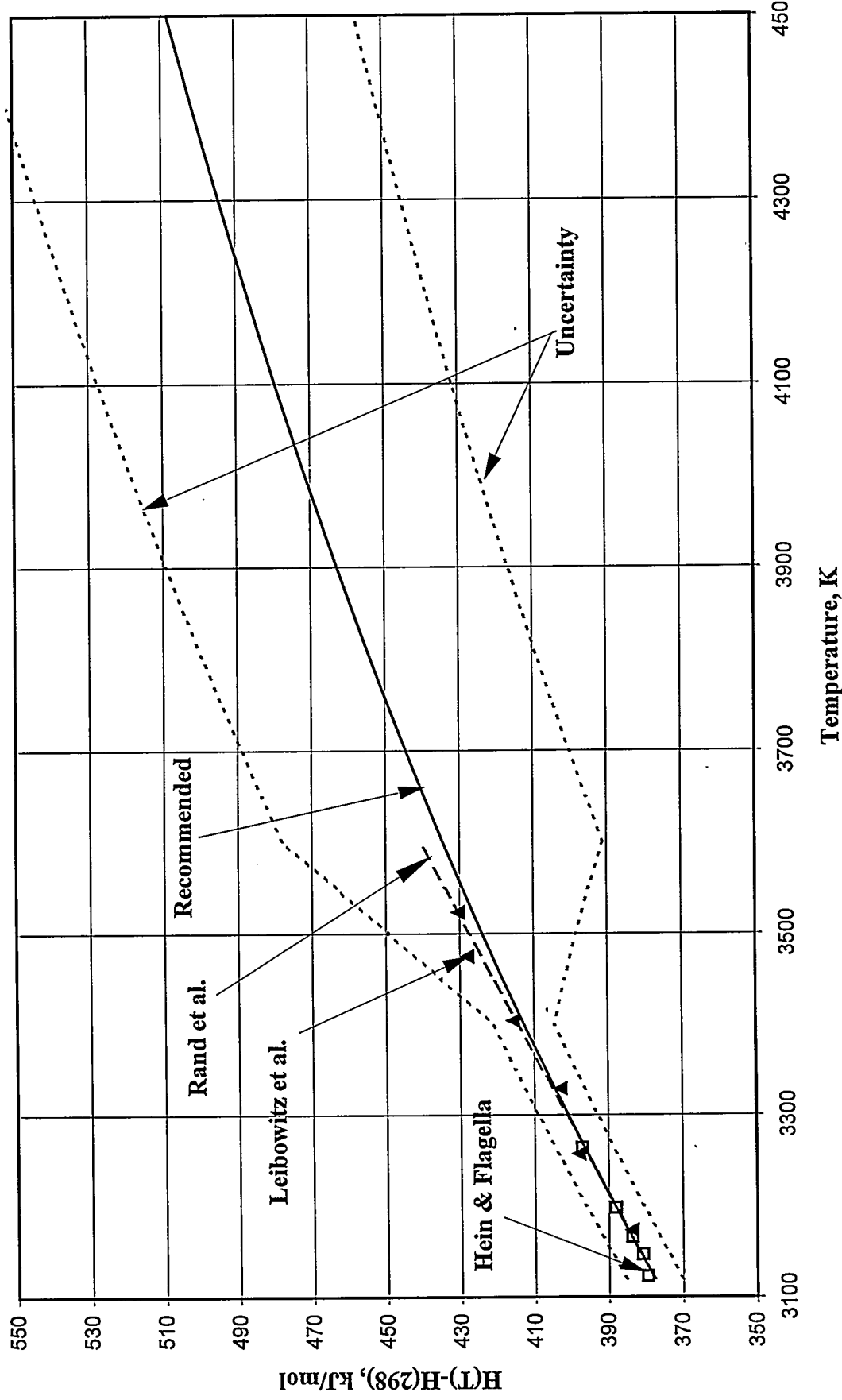
Figure 1.2.2 Liquid UO₂ Heat Capacity
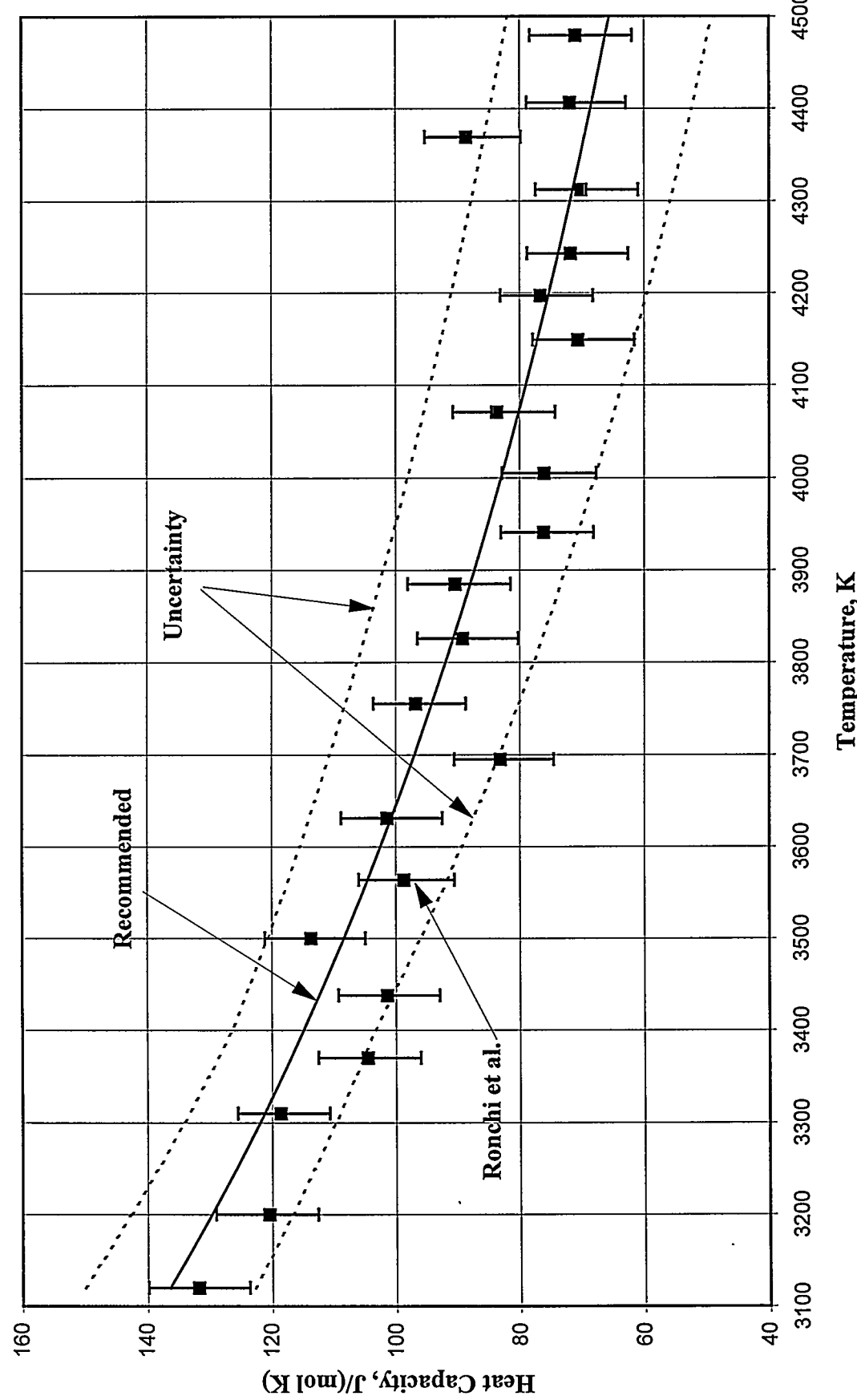
Figure 1.2.3 Fit of the Enthalpy of Liquid UO_2 by Linear Equation of Rand et al.
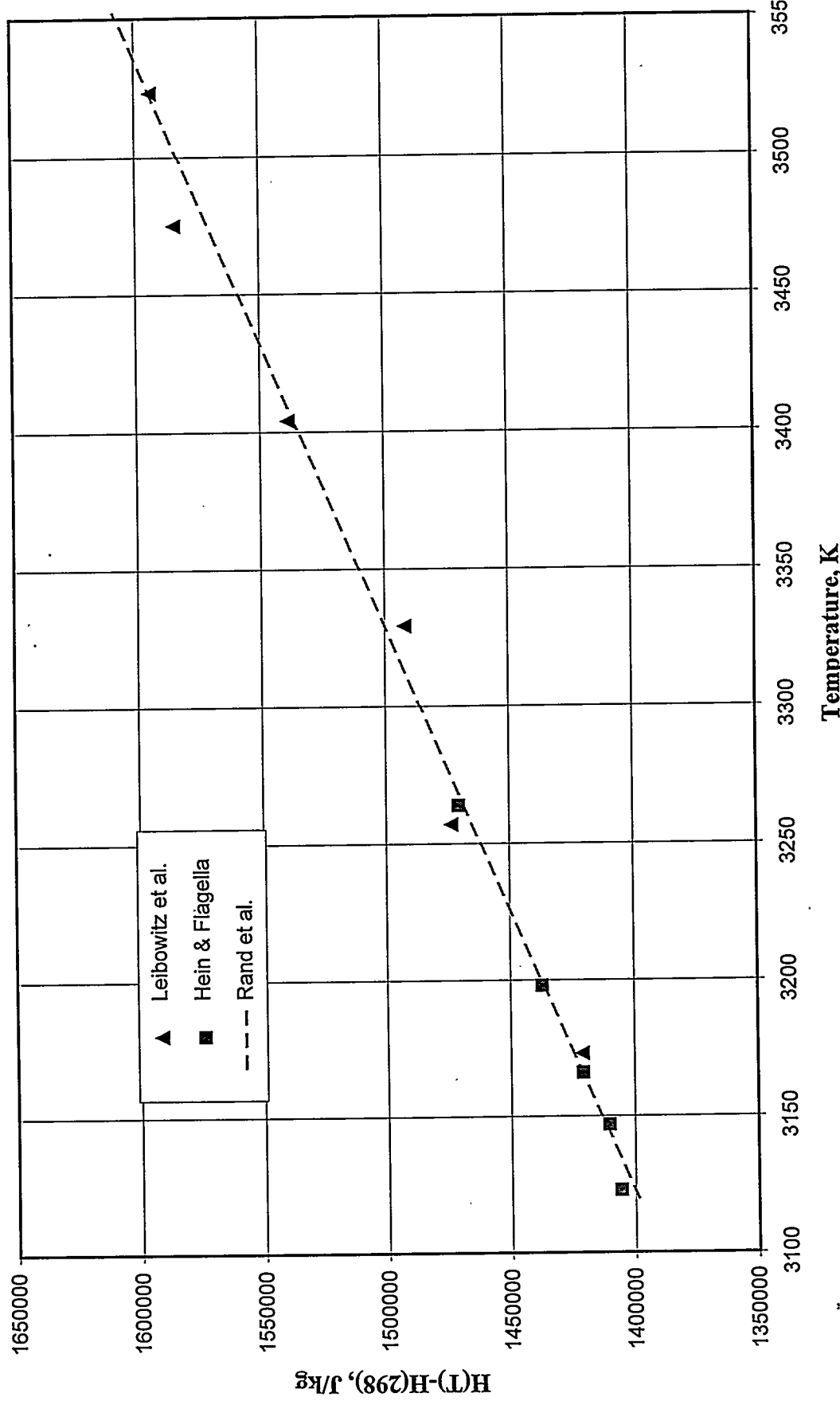
Figure 1.2.4 Liquid UO$_2$ Heat Capacity Measurements of Ronchi et al.

Legend:
- ■ Ronchi et al.
- ◆ Ronchi (Not Used)
- —— RHSH Eq.
- - - - Rand et al.

x-axis: Temperature, K

y-axis: UO$_2$ Heat Capacity, J/(kg-K)

10/96

Figure 1.2.5 Liquid Density of UO₂

Figure 1.2.5 Liquid Density of UO₂

Temperature, K

UO₂ Density, Mg/m³

Legend:
— Breitung & Reil Eq
● Christensen
▲ Drotning
····· Uncertainty
····· Uncertainty
– – – Ronchi et al
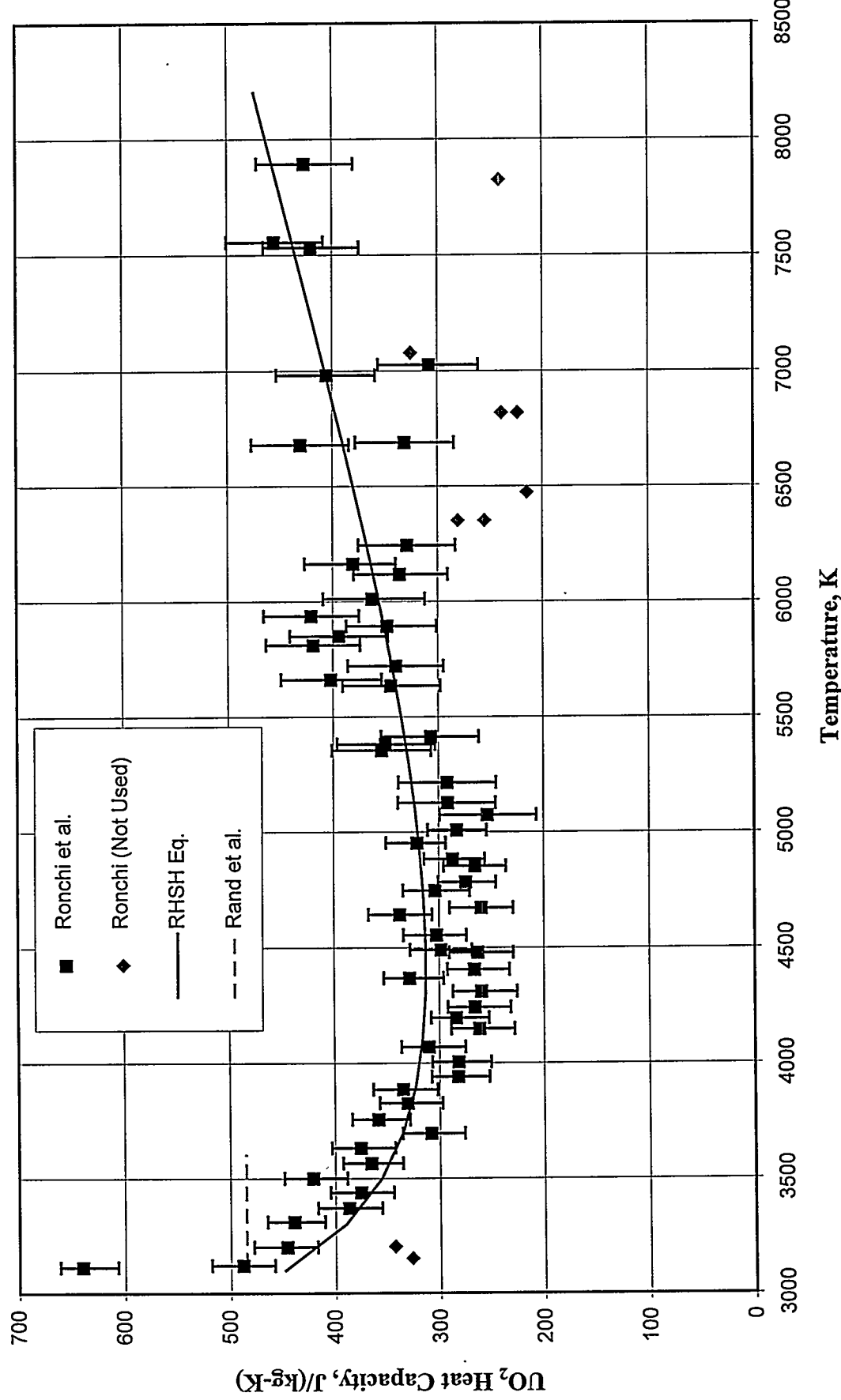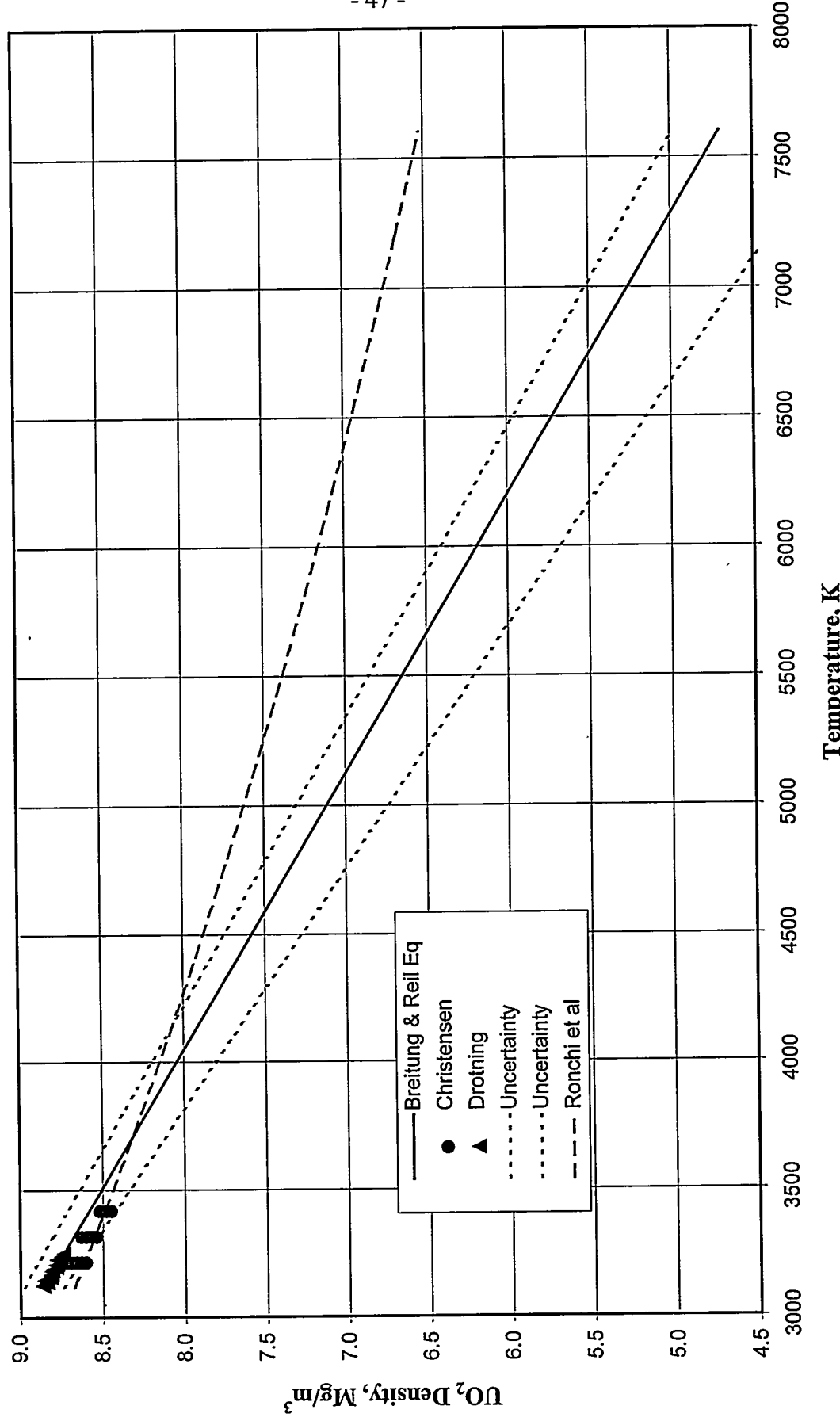
Figure 1.2.6 Comparison of Equations for the Enthalpy of Liquid UO$_2$
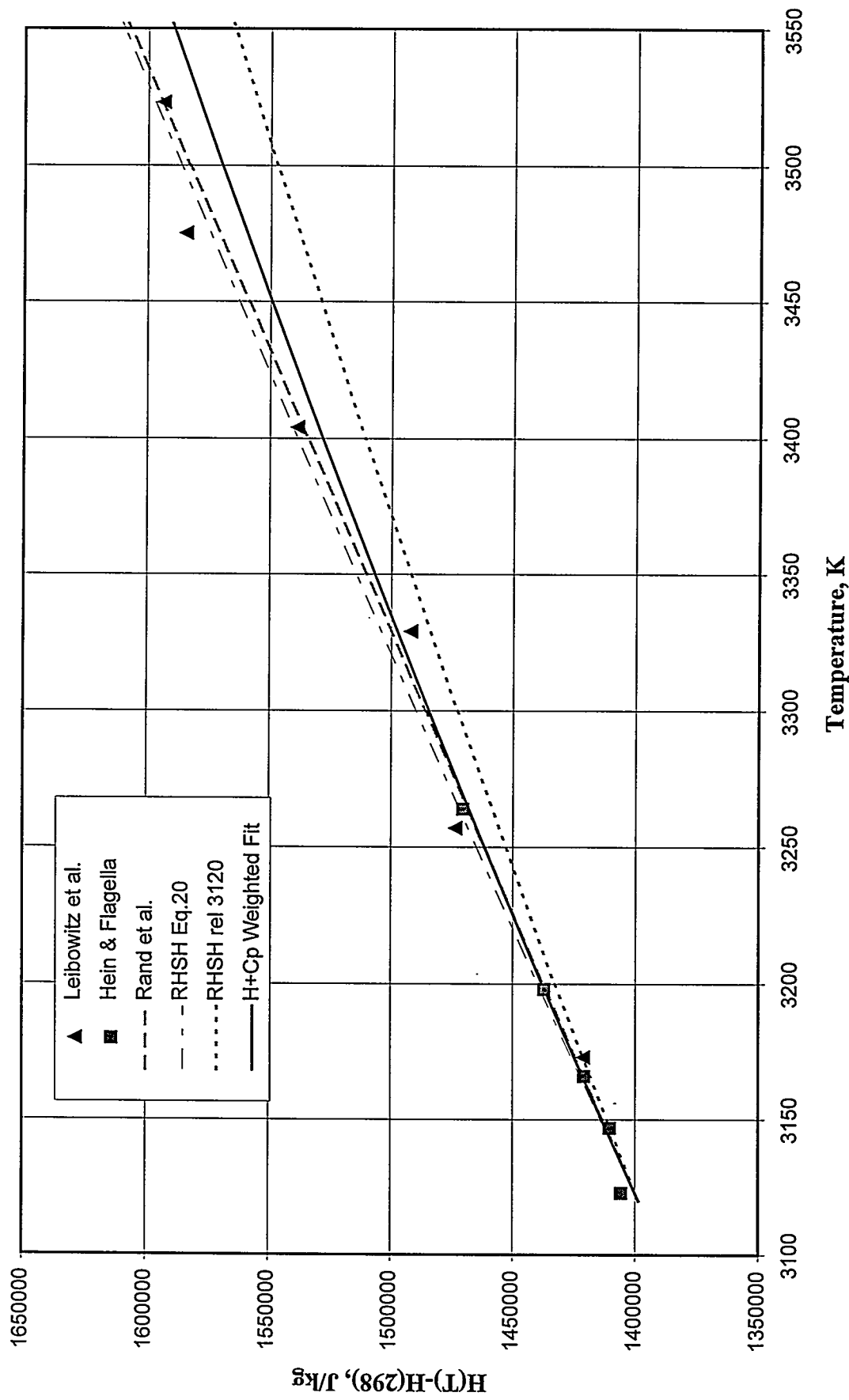
Figure 1.2.7 Comparison of Equations for the Heat Capacity of Liquid UO$_2$
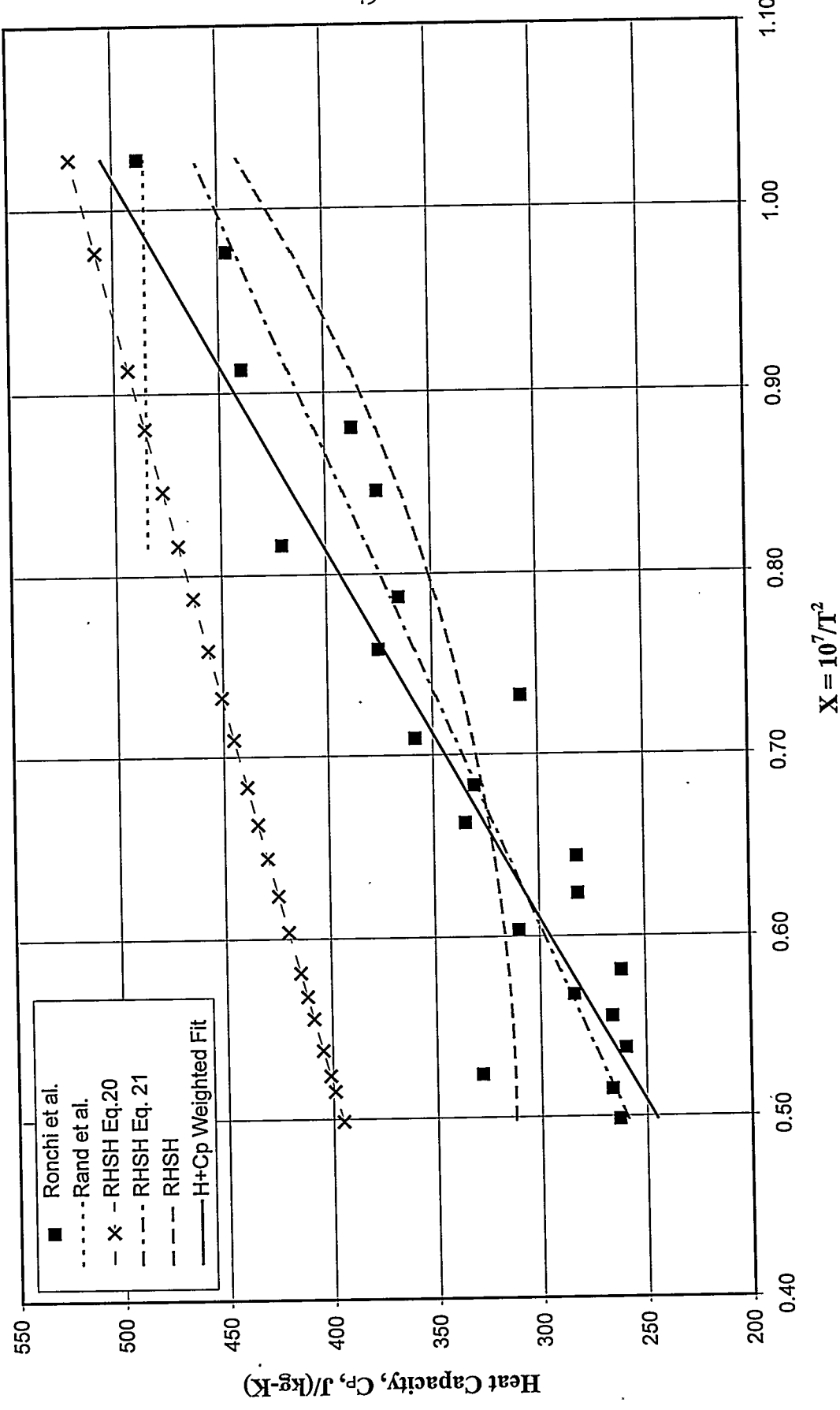
Figure 1.2.8 Liquid UO$_2$ Heat Capacity
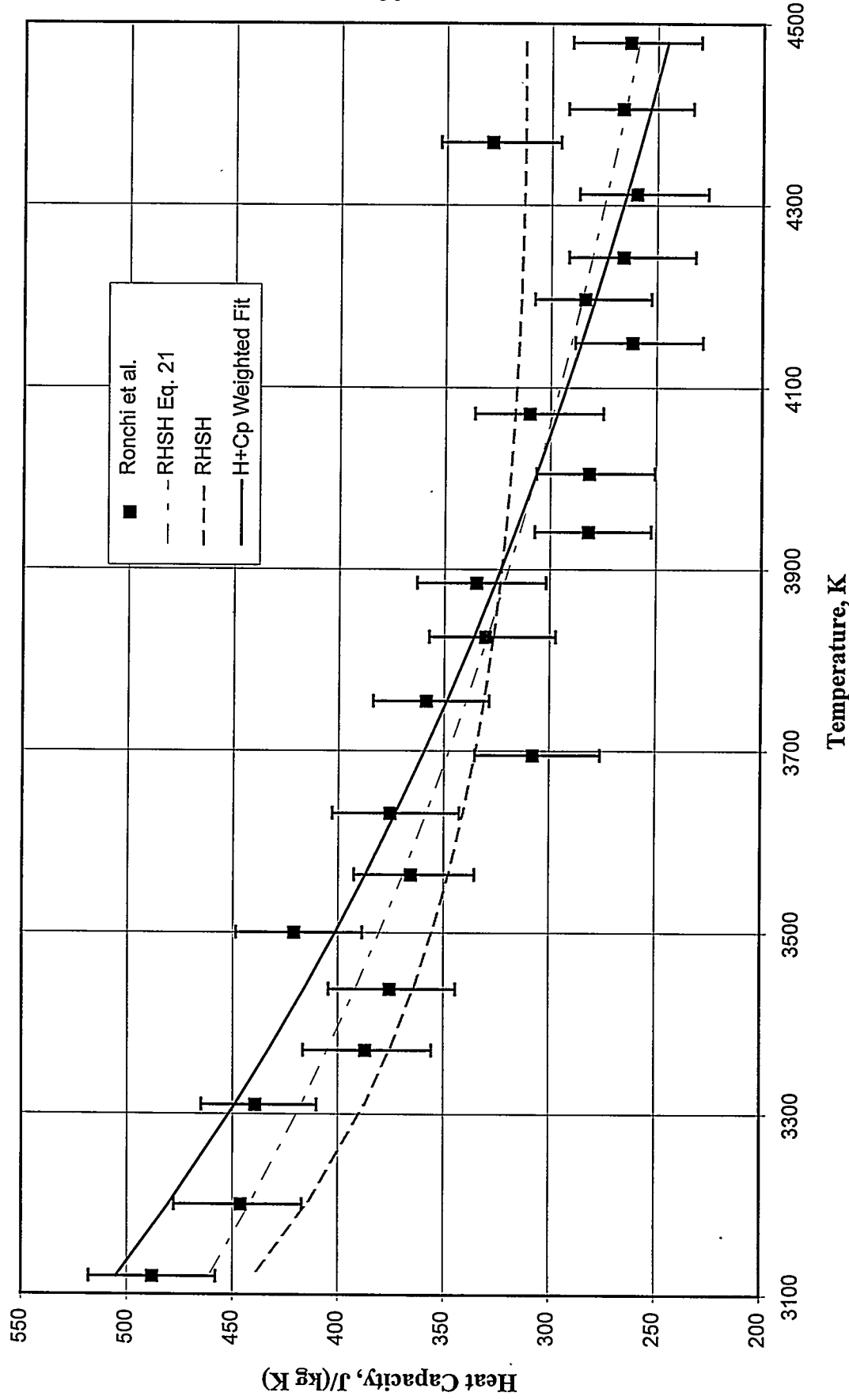
2.   MELTING POINT OF URANIUM DIOXIDE

Recommendation

The recommended value for the melting temperature of $UO_{2.00}$ is:

$$T_m = 3120 \pm 30 \text{ K (IPTS-68 scale)}$$

This value has been recommended by Rand et al.[1] from their analysis of fourteen experimental studies (over a period of 20 years) of the melting temperature of UO_2. This recommendation of Rand et al. has been accepted by international agreement and was recommended in the assessment of UO_2 properties by Fink et al. in 1981,[2,3] and by Harding, Martin, and Potter[4] in their 1989 review of material properties for fast reactor safety.

Discussion of Recommendation and Effects of Burnup

In their review of experimental measurements on the melting of UO_2, Rand et al. noted that the range in the values for the melting temperature decreased with time. Measurements prior to 1965 were reviewed by Hausner.[5] Measurements since 1965 include measurements by Latta and Fryxell,[6] Lyon and Baily,[7] and Bates.[8] Measurements have been made using a 'V'-filament method and by thermal arrest methods. The latter method is more reliable since the sample is encapsulated and vaporization is not a problem. Of the thermal arrest data, those of Latta and Fryxell appear to be the best. Their value, 3138 ± 15 K, agrees within experimental errors with the value reported by Lyon and Baily, 3113 ± 20 K.

In their 1985 review of experimental data on the melting of irradiated oxide fuels, Adamson et al.[9] commented that the 'V'-filament method appears to give consistently low melting temperatures when applied to variable-stoichiometry oxides such as $UO_{2\pm x}$ and $(U,Pu)O_{2\pm x}$. They attributed the low melting (solidus) temperatures obtained with the 'V'-filament technique, which use small uncontained samples, to pronounced compositional changes that arise from rapid incongruent vaporization and oxygen exchange with the supporting atmosphere (Ar or He) and/or tungsten support. The compositional changes cause changes in the surface emissivity which lead to measurement errors. Adamson et al.[9] commented that measurements made by Bates[8] and by Christensen[10,11] on unirradiated samples of stoichiometric UO_2 gave melting temperatures in the

range of 3063-3073 K which are approximately 50 K lower than its true melting point. The measurements of Bates[8] and Christensen[10,11] on irradiated UO_2 gave solidus temperature changes from zero to +130 K for low burnup ($\leq$ 1%) and - 120 K for high burnup (6 to 11%). These data were rejected by Adamson et al. in their assessment because of the unreliability of the 'V'-filament measurements. Adamson et al. concluded that the effect of burnup on the melting behavior is not large. They developed a model for mixed oxide fuel that predicts variations in the solidus as a function of burnup. For burnups up to 10%, the solidus of ($U_{0.75} Pu_{0.25} O_2$) is reduced by 22 K.[9]

In recent experimental measurements of the heat capacity of liquid UO_2 using laser heating of a 0.5 to 0.8 mm diameter UO_2 sphere, Ronchi et al.[12] made several measurements of the freezing temperature of UO_2 on different samples. For specimens in an inert gas atmosphere with up to 0.1-bar of oxygen, they obtained melting points in the interval 3070 $\pm$ 20 K. Higher melting temperatures (3140 $\pm$ 20 K) were obtained for samples in an inert gas atmosphere without oxygen. The variation in melting temperature is in accord with the expected lower oxygen to uranium (O/U) ratio in the latter samples. The O/U ratio of the samples used in these experiments was not determined but the experimenters cannot exclude a slight oxidation up to O/U=2.03.

The melting point of UO_2 given in MATPRO[13] is 3113.15 K. This temperature is based on measurements by Brassfield et al.[14] and the equations for the solidus and liquidus boundaries of the UO_2-PuO_2 phase diagram given by Lyon and Baily.[7] Properties in the MATPRO library are used in the SCDAP/RELAP5 code.

Uncertainties

The uncertainty in the recommended temperature of UO_2 is $\pm$1% (1σ) The experimental results of Latta and Fryxell[6] and of Lyon and Baily[7] are well within this uncertainty.

REFERENCES

1. J. K. Fink, M. G. Chasanov, and L. Leibowitz, *Properties for Reactor Safety Analysis,* **ANL-CEN-RSD-80-3**, Argonne National Laboratory Report (1981).

2. J. K. Fink, M. G. Chasanov, and L. Leibowitz, *Thermophysical Properties of Uranium Dioxide,* J. Nucl. Mater. **102** 17-25 (1981).

3. M. H. Rand, R. J. Ackermann, F. Gronvold, F. L. Oetting, A. Pattoret, Rev. Int. Des Hautes Temperatures et des Refractories **15**, 355 (1978).

4. J. H. Harding, D. G. Martin, and P. E. Potter, *Thermophysical and Thermochemical Properties of Fast Reactor Materials,"* Commission of European Communities Report **EUR 12402** (1989).

5. A. Hausner, J. Nucl. Mater. **15**, 179 (1965).

6. R. E. Latta and R. E. Fryxell, J. Nucl. Mater. **35**, 195 (1970).

7. W. L. Lyon and W. E. Bailey, *The Solid-Liquid Phase Diagram for the UO_2-PuO_2 System,* J. Nucl. Mater. **22**, 332 (1967).

8. J. L. Bates, J. Nucl. Mater. **36**, 234 (1970).

9. M. G. Adamson, E. A. Aitken, and R. W. Caputi, *Experimental and Thermodynamic Evaluation of the Melting Behavior of Irradiated Oxide Fuels,* J. Nucl. Mater. **130**, 349-365 (1985).

10. J. A. Christensen, R. J. Allio, and A. Biancheria, Trans. American Nuclear Society **7**, 390 (1964); also United States Report **WCAP-6065** (1965).

11. J. A. Christensen, *Irradiation Effects on Uranium Dioxide Melting,* United States Report **HW-69234** (1964).

12. C. Ronchi, J. P. Hiernaut, R. Selfslag, and G. J. Hyland, *Laboratory Measuremnt of the Heat Capacity of Urania up to 8000 K: I. Experiment,* Nucl. Sci. Eng. **113**, 1-19 (1993).

13. J. K. Hohorst (Editor), *SCDAP/RELAP5/MOD2 Code Manual, Vol 4: MATPRO- A Library of Materials Properties for Light-Water-Reactor Accident Analysis,"* Section 2.1 Melting Temperature, **NUREG/CR-5273** (1990).

14. H. C. Brassfield et al., *Recommended Property and Reactor Kinetics Data for Use in Evaluating a Light-Water-Coolant Reactor Loss-of-Coolant Incident Involving Zircaloy-4 or 304-SS-Clad UO_2,* **GEMP-482** (April 1968).

3. ENTHALPY OF FUSION OF URANIUM DIOXIDE

Recommendation

The recommended value for the enthalpy of fusion of $UO_{2.00}$ is:

$$\Delta H_f = 74.8 \pm 1 \text{ kJ mol}^{-1}$$

or $277.1 \pm 3.7 \text{ kJ kg}^{-1}$. The enthalpy of fusion was calculated from the following equations for the enthalpy of solid[1,2] and of liquid UO_2 at the melting point of 3120 K:

Solid UO_2; $2670 \text{ K} \le T \le 3120 \text{ K}$,

$$H(T) - H(298.15K) = 167.04T - 218342; \tag{1}$$

Liquid UO_2; $3120 \text{ K} \le T \le 4500 \text{ K}$,

$$H(T) - H(298.15K) = 2.64630x10^6 + 41.612T - \frac{4.2980x10^9}{T}; \tag{2}$$

where T is in K and enthalpy is in J mol^{-1}.

Discussion of Recommendation

Equation (2) for the enthalpy of liquid UO_2, is a combined fit of the recent liquid UO_2 heat capacity data of Ronchi et al.[3] and the enthalpy data of Leibowitz et al.[4] and of Hein and Flagella.[5] The fit to these data has been constrained to give the same enthalpy of the liquid at the melting point as that obtained from the linear equation of Rand[6] for the enthalpy of liquid UO_2:

Liquid UO_2; $3120 \text{ K} \le T \le 3550 \text{ K}$,

$$H(T) - H(298.15K) = 130.95T - 30911. \tag{3}$$

The recommended value for the enthalpy of fusion is identical to that recommended by Fink et al.[2] based on Eq. (1) and Eq. (3). It is consistent with experimental results of enthalpy measurements of Chikalla,[7] Leibowitz et al.,[4] and Hein and Flagella.[5] The enthalpy of fusion given in MATPRO[8] is 274.0 kJ kg^{-1} which is 74.0 kJ mol^{-1}.

<u>Uncertainty</u>

The uncertainty in the recommended enthalpy of fusion of UO_2 is $\pm 1\%$ (1σ).

REFERENCES

1. J. K. Fink, *Enthalpy and Heat Capacity of the Actinide Oxides,* Int. J. Thermophys. 3(2), 165-200 (1982); J. K. Fink, M. G. Chasanov, and L. Leibowitz, *Enthalpy and Heat Capacity of Solid UO_2,* ANL Report **ANL-CEN-RSD-81-2**, Argonne National Laboratory (May 1981).

2. J. K. Fink, M. G. Chasanov, and L. Leibowitz, *Thermophysical Properties of Uranium Dioxide,* J. Nucl. Mater. **102,** 17-25 (1981); also as ANL Report **ANL-CEN-RSD-80-3**, Argonne National Laboratory (April 1981).

3. C. Ronchi, J. P. Hiernaut, R. Selfslag, and G. J. Hyland, *Laboratory Measurement of the Heat Capacity of Urania up to 8000 K: I. Experiment,* Nucl. Sci. Eng. **113**, 1-19 (1993).

4. L. Leibowitz, M. G. Chasanov, L. W. Mishler, and D. F. Fischer, J. Nucl. Mater. **39** 115-116 (1971).

5. R. A. Hein and P. N. Flagella, *Enthalpy Measurements of UO_2 and Tungsten to 3260 K,* GE Report **GEMP-578**, General Electric, February 16, 1968.

6. M. H. Rand, R. J. Ackermann, F. Gronvold, F. L. Oetting, A. Pattoret, *The Thermodynamic Properties of the Urania Phase,* Rev. Int. Hautes Temp. Refract. **15**, 355-365 (1978).

7. T. D. Chikalla, *The Liquidus for the System UO_2-PuO_2,* General Electric Co. Hanford Atomic Products Operation Report **HW-698322** (June 1961).

8. J. K. Horhorst, editor, *SCADAP/RELAP5/MOD2 Code Manual Vol. 4: MATPRO - a library of materials properties for light-water reactor accident analysis,* EG&G Idaho Report **NUREG/CR-5273** (1990).

4.   THERMAL EXPANSION OF DENSITY OF URANIUM DIOXIDE

4.1   THERMAL EXPANSION OF SOLID UO$_2$

Summary and Recommended Equations

The recommended equations for the thermal expansion of solid uranium dioxide are from the 1988 assessment by D. G. Martin[1] which included the high temperature neutron diffraction data of Hutchings[2] that were not available to previous assessments.[3,4] Martin compared data from lattice parameter measurements and macroscopic length changes from 15 references,[2,5-18] made corrections to macroscopic thermal expansion measurements that exhibited a zero error, and excluded data that did not agree with the common consensus. Martin fit the remaining data to two cubic polynomials.

The recommended equations for the linear thermal expansion of solid UO$_2$ are

For 273 K $\leq$ T $\leq$ 923 K,

$$L = L_{273} \, (9.9734\text{x}10^{-1} + 9.802\text{x}10^{-6}T - 2.705\text{x}10^{-10}T^2$$
$$+ \, 4.291\text{x}10^{-13}T^3); \tag{1}$$

For 923 K $\leq$ T $\leq$ 3120 K,

$$L = L_{273} \, (9.9672\text{x}10^{-1} + 1.179\text{x}10^{-5}T - 2.429\text{x}10^{-9}T^2$$
$$+ \, 1.219\text{x}10^{-12}T^3); \tag{2}$$

where L and L_{273} are the lengths at temperatures T(K) and 273 K, respectively. The fractional change in the linear thermal expansion of UO$_2$, $\Delta L/L_{273}$, expressed as a percent, is shown in Figure 4.1.1 with the uncertainties recommended by Martin given as dotted lines. Recommended values for the fractional change in linear thermal expansion, $\Delta L/L_{273}$, are tabulated in Table 4.1.1. Values for the fractional change in volumetric thermal expansion of UO$_2$, $\Delta V/V_{273}$, are given in Table 4.1.2.

From assessment of the available data on hyperstoichiometric uranium dioxide (UO$_{2+x}$), Martin recommended using these equations for the linear thermal expansion of UO$_{2+x}$ for x in the ranges 0 to 0.13 and 0.23 to 0.25.

Version 0 for Peer Review

The recommended equations for the instantaneous linear thermal expansion coefficients, $\alpha_p(l)$, are cubic polynomial approximations[1] to the exact partial differentials $(1/L)\,(dL/dT)_p$ of Eqs. (1) and (2). These approximations do not differ by more than 0.6% from the exact differentials over the given temperature range. Martin recommended:

For $273\ K \leq T \leq 923\ K$,

$$\alpha_p(l) = 9.828 \times 10^{-6} - 6.390 \times 10^{-10} T + 1.330 \times 10^{-12} T^2$$
$$+ 1.757 \times 10^{-17} T^3; \tag{3}$$

For $923\ K \leq T \leq 3120\ K$,

$$\alpha_p(l) = 1.1833 \times 10^{-5} - 5.013 \times 10^{-9} T + 3.756 \times 10^{-12} T^2$$
$$+ 6.125 \times 10^{-17} T^3; \tag{4}$$

where $\alpha_p(l)$ is the coefficient of thermal expansion in K^{-1}. Recommended values of the instantaneous linear thermal expansion coefficient of UO_2 are shown in Figure 4.1.2 and tabulated as a function of temperature in Table 4.1.1. Dotted lines in Figure 4.1.2 represent the uncertainties suggested by Martin. Values for the instantaneous volumetric thermal expansion coefficient (the thermodynamic quantity, α_p) are given in Table 4.1.2. Equations relating the linear and volumetric thermal expansion coefficients and fractional changes in length, volume, and density with temperature are given in the Section 4.5 of this report.

Uncertainties

Martin gave the uncertainty in the fractional linear expansions $(L/L_{273} -1)$ as $\pm 2.6 \times 10^{-4}$ for 293 to 1273 K, $\pm 4.4 \times 10^{-4}$ for 1273 to 2273 K, and $\pm 7 \times 10^{-4}$ for 2273 to 2929 K. In terms of percents of the linear expansion as a function of temperature, the uncertainties are 105% at 298 K, 12% at 500 K, 3.6% at 1000 K, 3.4% at 1500 K, 2.2% at 2000 K, 2.3% at 2500 K, and 1.6% at 3000 K.

The corresponding uncertainties in the instantaneous linear thermal expansion, $\alpha_p(l)$, are $\pm 0.11 \times 10^{-6}$, $\pm 0.22 \times 10^{-6}$, and $\pm 1.1 \times 10^{-6}$ for the temperature ranges 293 to 1273 K, 1273 to 2273 K, and 2273 to 2929 K, respectively.

Discussion of Recommended Equations for UO$_2$

Martin[1] reviewed and compared UO$_2$ thermal expansion data from macroscopic length changes,[5-13] neutron diffraction,[2,18] and x-ray diffraction measurements[17] except for the recent x-ray diffraction results by Momin et al.[19] In his thorough data assessment, Martin examined the macroscopic expansion data for possible zero errors and made corrections to the data of Lambertson and Hanwerk[6], data of Brett and Russell[9], and data of Murray and Thackery.[10] He found good agreement between the data from macroscopic length changes and lattice parameter measurements so that these data could be combined in the final analysis. The good agreement between data from macroscopic measurements by Conway et al. and the lattice parameter measurements of Hutchings[2] led Martin to conclude that at least up to 2523 K, the contribution to the macroscopic expansion due to Schottky defects is negligible. In formulating equations to represent the linear thermal expansion of UO$_2$, Martin excluded data that did not agree with the common consensus. Data excluded by Martin were data of Bell et al.,[5] data of Christensen,[11] data of Halden et al.,[12] data above 1871 K from measurements by Baldock et al.,[17] and data from 1118 to 1200 K from measurements by Hoch and Momin.[15] Figure 4.1.3 shows most of the thermal expansion data fit by Martin and his recommended equations, expressed as the percent change in length relative to the length at 273 K, ie. ($\Delta L/L_{273}$, %).

Percent deviations of the data from the recommended equations of Martin are shown in Figure 4.1.4. Percent deviations in Figure 4.1.4 are defined as

$$Deviation(\%) = \frac{\dfrac{\Delta L(Data)}{L} - \dfrac{\Delta L(Martin)}{L}}{\dfrac{\Delta L(Martin)}{L}} \cdot 100\% \qquad (5)$$

The uncertainties given by Martin are included in Figure 4.1.4, expressed as percents, for comparison with the deviations of Martin's equations from the analyzed data.

Since this analysis by Martin,[1] Momin et al.[19] reported equations for the variation in the lattice parameter from 298 through 1600 K for UO_2 and UO_2 doped with fission products. These equations were based on x-ray diffraction measurements. The results by Momin et al. for UO_2, expressed as $\Delta L/L_{273}$, are compared with the recommendation of Martin in Figure 4.1.5. Values calculated from the equations of Momin et al. are consistently lower than the recommended values. Deviations, determined in accord with Eq. (5), range from -24% at 298 K to -0.5% at 1600 K. Momin et al. reported 0.5469 nm for the lattice parameter of UO_2 at room temperature. This is slightly lower than the 0.54704 nm value at 293 K obtained by Gronvold[16] and the 0.5470 nm value at 293 K obtained by Hutchings.[2] Thus, the results reported by Momin et al. appear to be low relative to other data as well as compared to the recommendation of Martin.

Comparison of UO_2 Recommendation with Previous Recommendations

The 1981 recommendation of Fink, Chasanov, and Leibowitz[3] and the recommendation of MATPRO[4] were based on an analysis by Olsen[4] which used the data of Conway et al.[13] from 1263 to 2535 K and that of Christensen[11] from 1473 to 3073 K. Although the data of Christensen showed much scatter, they were the only data available in 1981 above 2535 K. The recent data of Hutchings[2] are in much better agreement with that of Conway et al. than the data of Christensen and show that the data of Christensen are not reliable. Figure 4.1.6 compares $\Delta L/L_{273}$ from these three sets of data with the recommended equations of Martin and the 1981 recommendation. Differences are significant at high temperatures where the fits are based on different sets of data. From 2800 through 3120 K, deviations increase from 3% to 6.5%. These deviations are greater than the uncertainties given by Martin, which are 1.9% at 2800 K and 1.5% at 3120 K. In the temperature range of 500 to 1200 K, deviations between these two recommendations range from 18% to 5%. These are higher than the uncertainties given by Martin for his recommended values in this temperature range.

The recommended instantaneous linear thermal expansion coefficient given by Martin[1] is compared in Figure 4.1.7 with the 1981 recommended values. Deviations between these instantaneous linear thermal expansion coefficients are even greater than the deviations between

the fractional changes in linear thermal expansion $(\Delta L/L_{273})$ because the linear instantaneous thermal expansion coefficient is the temperature derivative of the linear thermal expansion.

Discussion of Hyperstoichiometric Uranium Dioxide (UO_{2+x})

Martin has examined the x-ray lattice parameter measurements of UO_{2+x} of Gronvold[16] for O/M ratios of 2.00, 2.10, 2.25, and 2.60; of Roth et al.[20] for O/M ratios of 2.08 and 2.24; of Fergusson et al.[21] for O/M = 2.235; and the macroscopic expansion studies on UO_{2+x} by Murray and Thackery[10] for O/M=2.00 and 2.13 and those by Leblanc and Andriessen[7] for O/M=2.00, 2.10, and 2.21. He made a zero error correction to the data of Murray and Thackery. He excluded the data of Gronvold with an O/M ratio of 2.60 on the basis that these data relate to an orthorhombic (U_3O_8) structure, not a fluorite structure. From comparison of the remaining data to his equations for the thermal expansion of $UO_{2.00}$, Martin concluded that the thermal expansion of UO_{2+x} is the same as that of $UO_{2.00}$ for x values of 0-0.13 and 0.235-0.25 up to 1520 K. Figure 4.1.8, which compares some of the UO_{2+x} data with Martin's recommended percent change in the linear thermal expansion of $UO_{2.00}$, shows that Martin's conclusion is justified. The data for UO_{2+x} are very close to the recommendation for $UO_{2.00}$ with deviations and scatter similar to that for the $UO_{2.00}$ thermal expansion data. Because no data for UO_{2+x} exist above 1520 K, Martin speculated that his conclusion for thermal expansion at lower temperatures may be extended to the melting point.

REFERENCES

1.   D. G. Martin, *The Thermal Expansion of Solid UO$_2$ and (U,Pu) Mixed Oxides - A Review and Recommendations,* J. Nucl. Mater. **152** 94-101 (1988).

2.   M. T. Hutchings, *High-Temperature Studies of UO$_2$ and ThO$_2$ Using Neutron Scattering Techniques,* J. Chem. Soc. Faraday Trans. II **83,** 1083-1103 (1987).

3.   J. K. Fink, M. G. Chasanov, and L. Leibowitz, *Thermophysical Properties of Uranium Dioxide,* J. Nucl. Mater. **102** 17-25 (1981).

4.   C. S. Olsen, *Fuel Thermal Expansion (FTHEXP)* in *MATPRO- Version 11: A Handbook of Materials Properties for Use in the Analysis of Light Water Reactor Fuel Rod Behavior,* ed. D. R. Hagraman and G. A. Reymann, US Nuclear Regulatory Commission Rep. **NUREG/CR-0497** (February 1979); also revision (1981).

5.   I. P. Bell and s. M. Makin, R. And D. B. (C), Tech. Note No. 70, Culcheth Laboratories, UK (1954), as referenced by D. G. Martin, *The Thermal Expansion of Solid UO$_2$ and (U,Pu) Mixed Oxides - A Reveiw and Recommendations,* J. Nucl. Mater. **152** 94-101 (1988).

6.   W. A. Lambertson and J. H. Hanwerk, *The Fabrication and Physical Properties of Urania Bodies,* Argonne National Laboratory Report **ANL-5053** (1963).

7.   J. M. Leblanc and H. Andriessen, EURATOM/USA Report **EURAEC-434** (1962).

8.   M. D. Burdick and H. S. Parker, J. Am. Ceram. Soc. **39,** 181-187 (1956).

9.   N. H. Brett and L. E. Russell, *The Thermal Expansion of PuO$_2$ and Some Other Actinide Oxides between Room Temperature and 1000°C,* in *Plutonium 1960,* pp. 397-410, E. Grison, W. B. H. Lord, and R. D. Fowler, eds., Cleaver Hyne Oress Ltd., London (1961).

10.   P. Murray and R. W. Thackray, *The Thermal Expansion of Sintered UO$_2$,* Harwell memo **AERE M/M22** (1950).

11.   J. A. Christensen, *Thermal Expansion and Change in Volume of Uranium Dioxide on Melting,* J. Am. Ceram. Soc. **46,** 607-608 (1963).

12.   F. A. Halden, H. C. Wohlers, and R. H. Reinhart, *Thermal Expansion of Uranium Dioxide,* Stanford Research Institute Report No. **SRI A-6,** available from Technical Information Services Oak Ridge National Laboratory Report **TID 5722** (1959).

13. J. B. Conway, R. M. Fincel, and R. A. Hein, *The Thermal Expansion and Heat Capacity of UO_2 to* 2200°C, Trans. Am. Nucl. Soc. **6**, 153 (1963).

14. C. P. Kempter and R. O. Elliot, J. Chem. Phys. **30**, 1524 (1959), as referenced by D. G. Martin, *The Thermal Expansion of Solid UO_2 and (U,Pu) Mixed Oxides - A Reveiw and Recommendations,* J. Nucl. Mater. **152** 94-101 (1988).

15. M. Hoch and A. C. Momin, *High Temperature Thermal Expansion of UO_2 and ThO_2,* High Temp.-High Press. **1**, 401-407 (1969).

16. F. Gronvold, J. Inorg. Nucl. Chem. **1**, 357 (1955).

17. P. J. Baldock, W. E. Spindler, and T. W. Baker, *The X-Ray Thermal Expansion of Near - Stoichiometric UO_2,* J. Nucl. Mater. **18** 305-313 (1966).

18. A. Albinati, M. J. Cooper, K. D. Rouse, M. W. Thomas, and B. T. M. Willis, Acta Crystallogr. **A36**, 265 (1980).

19. A. C. Momin, E. B. Miza, and M. D. Mathews, *High Temperature X-ray Diffractometric Studies on the Lattice Thermal Expansion Behaviour of UO_2, ThO_2, and $(U_{0.2}Th_{0.8})O_2$ Doped with Fission Product Oxides,* J. Nucl. Mater. **185**, 308-310 (1991).

20. J. Roth and E. K. Halteman, Nuclear Materials and Equipment Corp. Report **NUMEC-2389-9** (1965).

21. I. F. Ferguson and R. S. Street, Harwell memo **AERE M 1192** (1963) as referenced by D. G. Martin, *The Thermal Expansion of Solid UO_2 and (U,Pu) Mixed Oxides - A Reveiw and Recommendations,* J. Nucl. Mater. **152** 94-101 (1988).

Table 4.1.1 Recommended Linear Thermal Expansion of UO_2

Temperature, K	$\Delta L/L$ %	$\alpha_p(l) \times 10^6$, K^{-1}
273	0.000	9.74
298	0.025	9.74
300	0.027	9.74
400	0.125	9.76
500	0.223	9.81
600	0.322	9.89
700	0.422	9.99
800	0.523	10.12
900	0.626	10.27
1000	0.730	10.51
1100	0.837	10.78
1200	0.948	11.12
1300	1.062	11.53
1400	1.181	12.01
1500	1.305	12.56
1600	1.436	13.18
1700	1.573	13.86
1800	1.718	14.62
1900	1.871	15.45
2000	2.034	16.34
2100	2.206	17.30
2200	2.388	18.33
2273	2.528	19.12
2273	2.528	19.12
2300	2.582	19.43
2400	2.788	20.59
2500	3.006	21.82
2600	3.238	23.11
2670	3.409	24.06
2670	3.409	24.06
2700	3.484	24.47
2800	3.745	25.90
2900	4.021	27.39
3000	4.314	28.94
3100	4.624	30.56
3120	4.688	30.89

Table 4.1.2 Recommended Volumetric Thermal Expansion of UO_2

Temperature, K	$\Delta V/V$ %	$\alpha_p \times 10^6$, K^{-1}
298	0.075	29.22
300	0.080	29.22
400	0.374	29.29
500	0.670	29.44
600	0.969	29.66
700	1.271	29.97
800	1.578	30.35
900	1.891	30.81
1000	2.206	31.54
1100	2.533	32.35
1200	2.870	33.36
1300	3.220	34.59
1400	3.585	36.03
1500	3.968	37.67
1600	4.370	39.53
1700	4.794	41.59
1800	5.243	43.87
1900	5.720	46.34
2000	6.226	49.02
2100	6.764	51.91
2200	7.337	54.99
2273	7.779	57.37
2273	7.779	57.37
2300	7.947	58.28
2400	8.598	61.77
2500	9.292	65.46
2600	10.032	69.34
2670	10.578	72.18
2670	10.578	72.18
2700	10.820	73.42
2800	11.660	77.70
2900	12.556	82.17
3000	13.509	86.83
3100	14.524	91.69
3120	14.734	92.68

Figure 4.1.1 Recommended UO_2 Linear Thermal Expansion, $\Delta L/L_{273}$
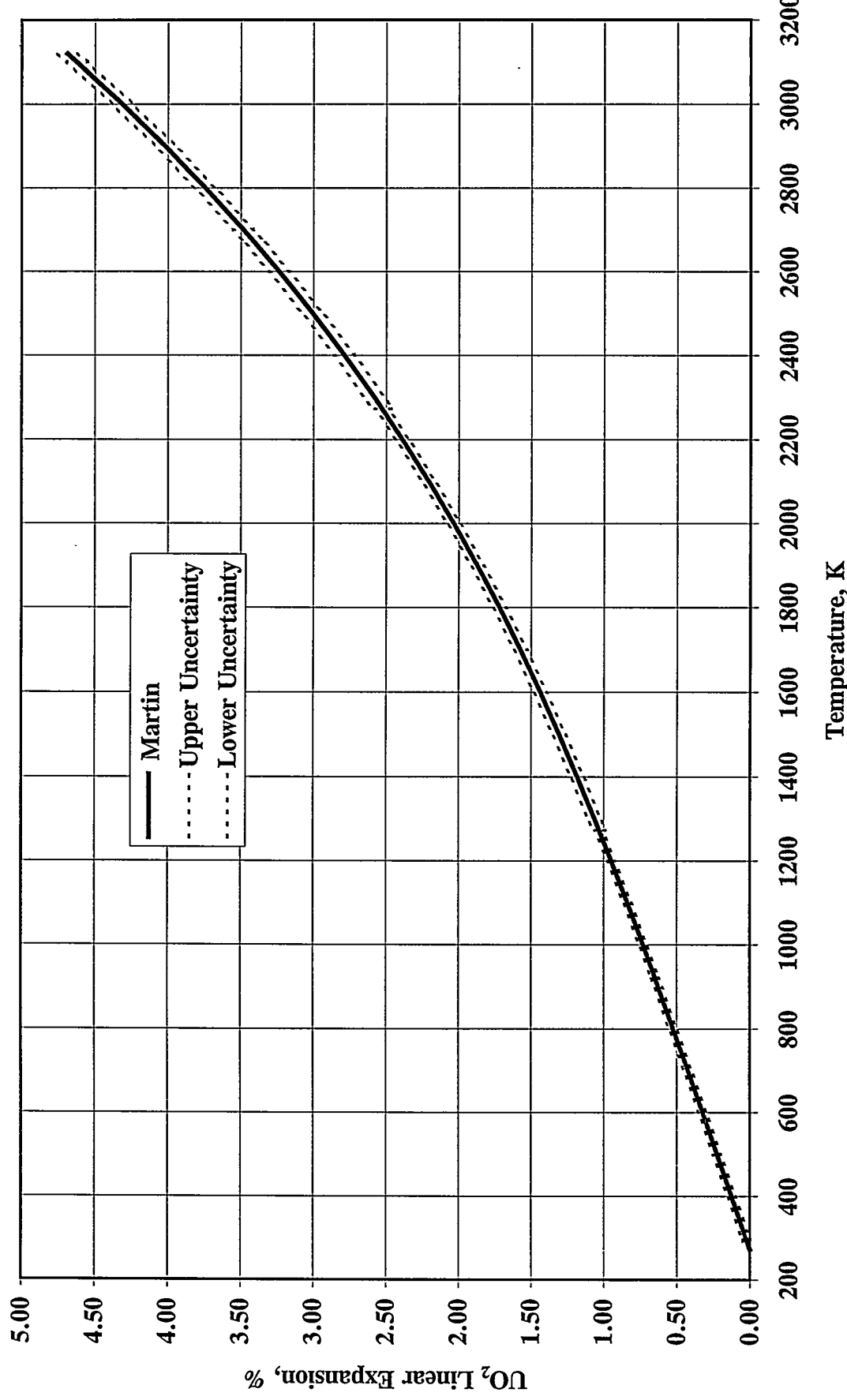
Figure 4.1.2 UO$_2$ Instantaneous Linear Thermal Expansion Coefficient
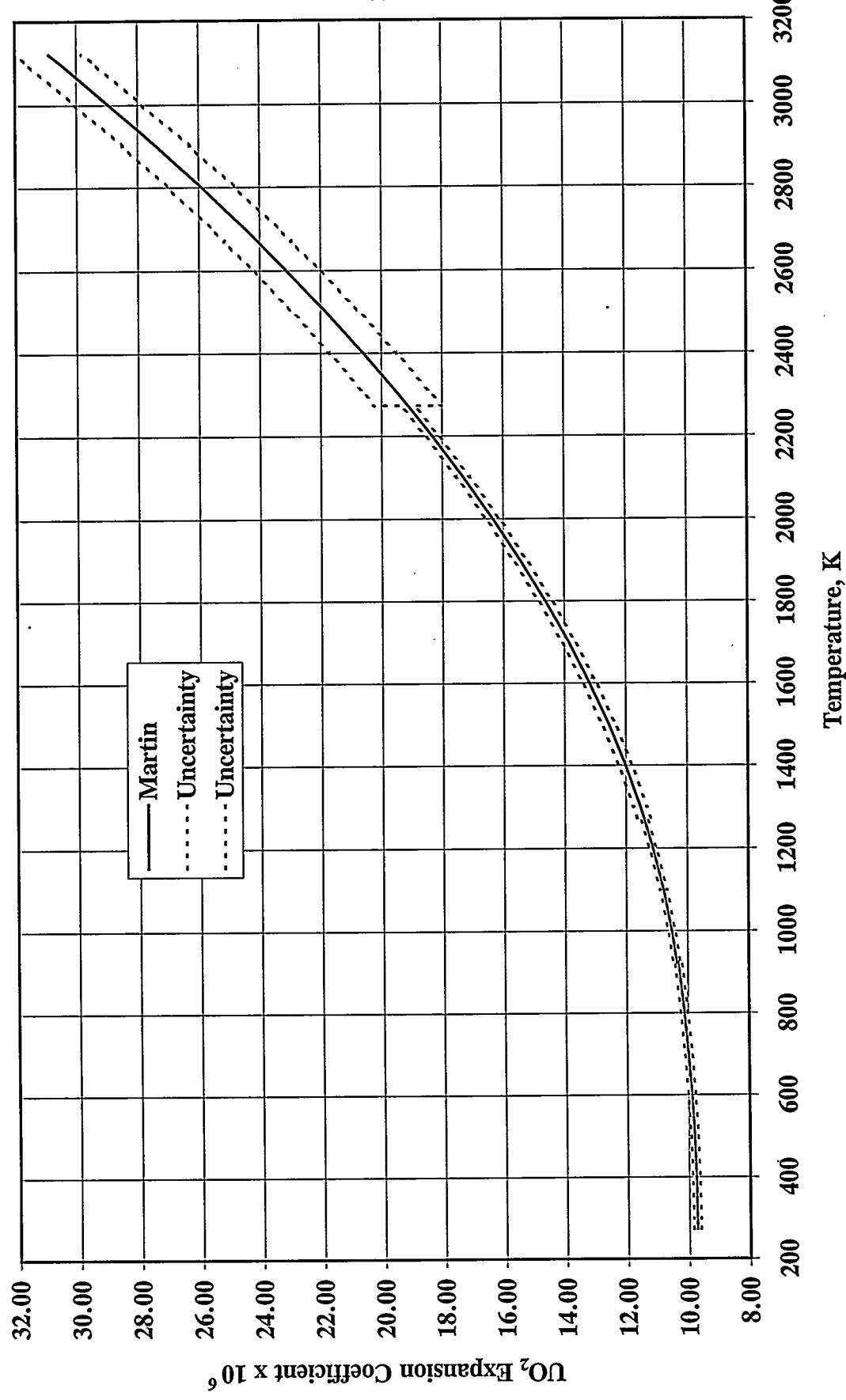
Figure 4.1.3 Recommended UO$_2$ Thermal Expansion Eq. Compared with Data Fit

4/96
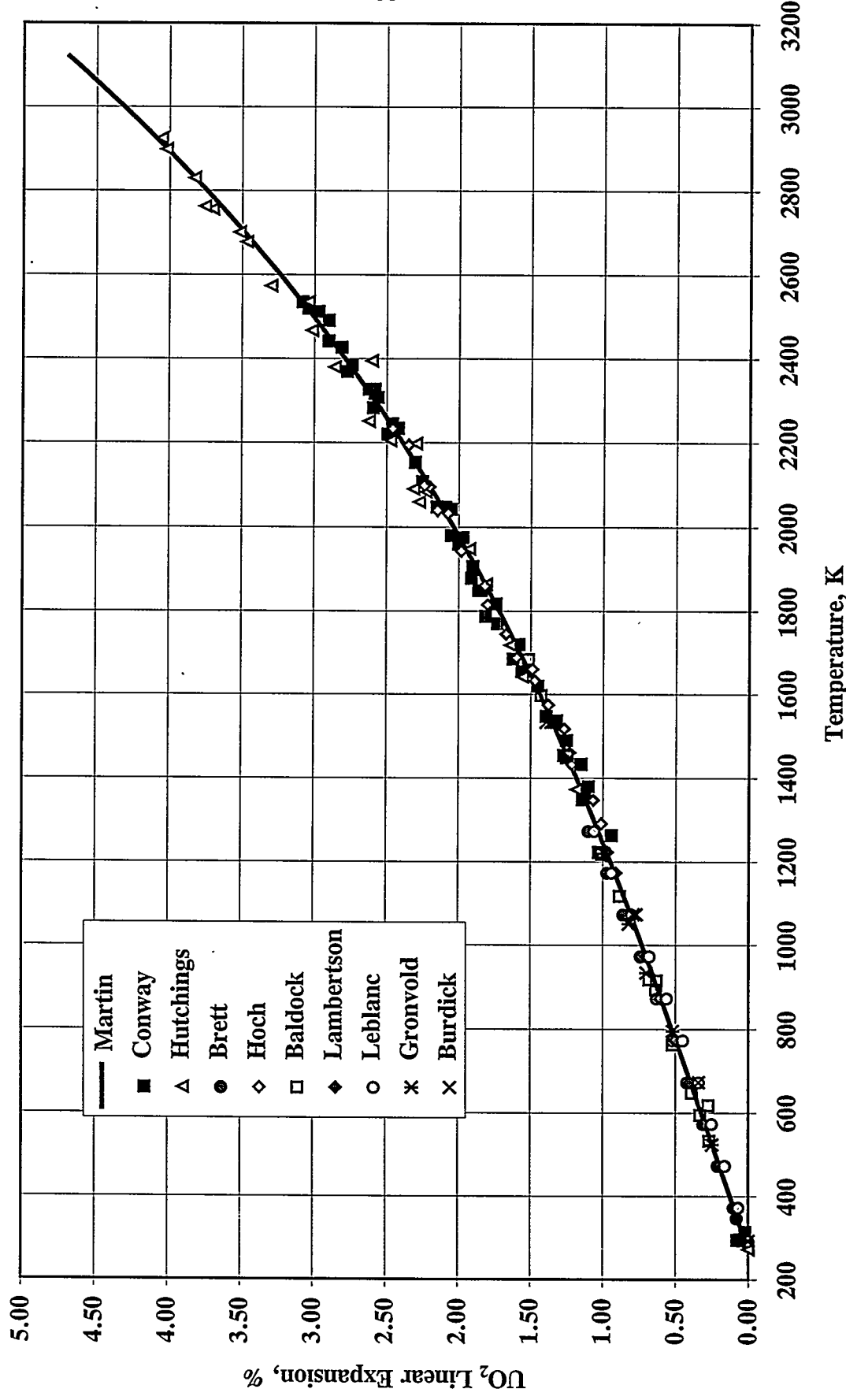
Figure 4.1.4 Deviations of UO$_2$ Linear Thermal Expansion Data from Recommendation

Send Comments to
jkfink@anl.gov

Version 0 for Peer Review
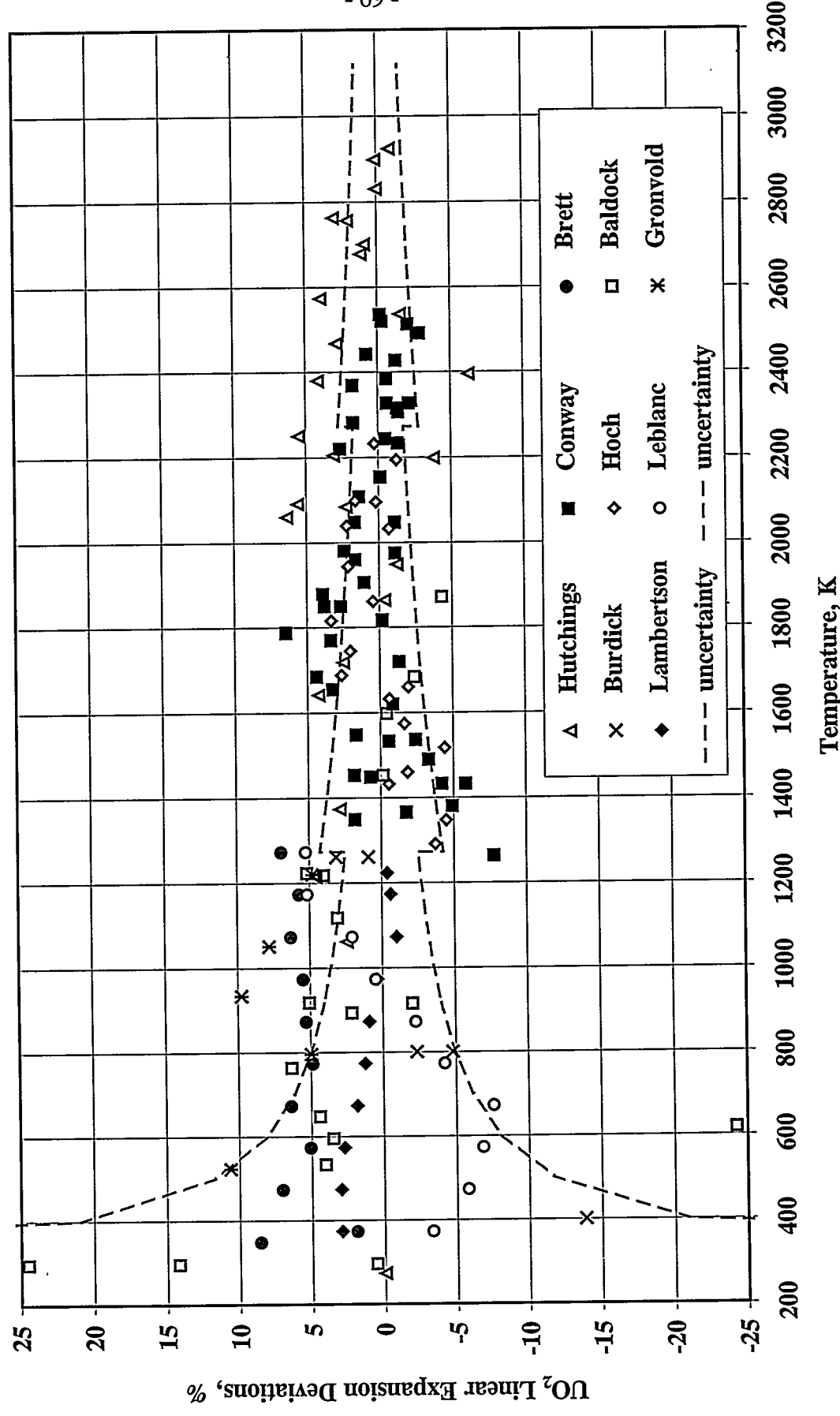
Figure 4.1.5 Comparison of UO$_2$ Thermal Expansion of Martin and of Momin et al.
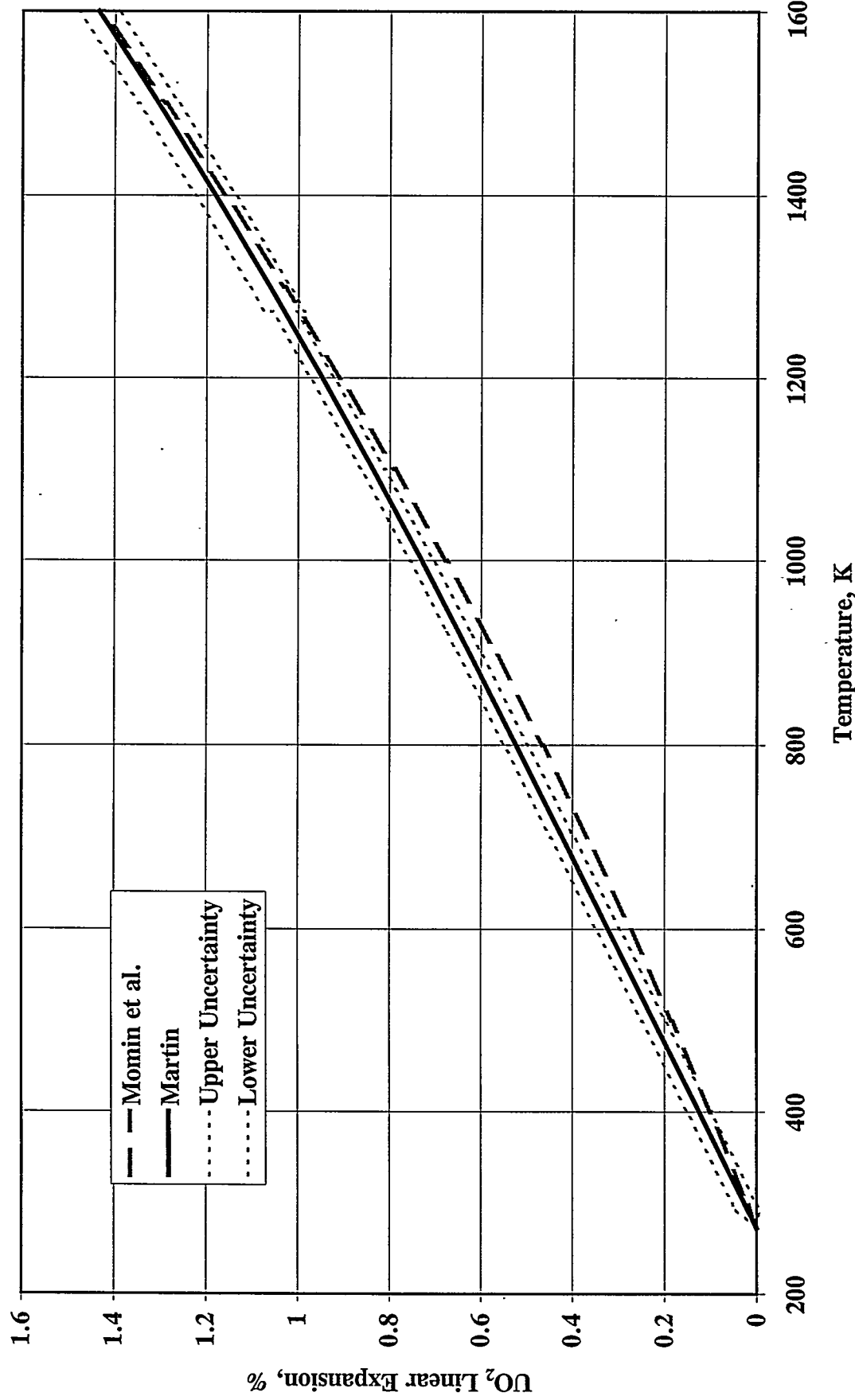
Figure 4.1.6 Comparison of Recommended UO_2 Thermal Expansion with Previous Recommendation and Data of Christensen, Conway, and Hutchings
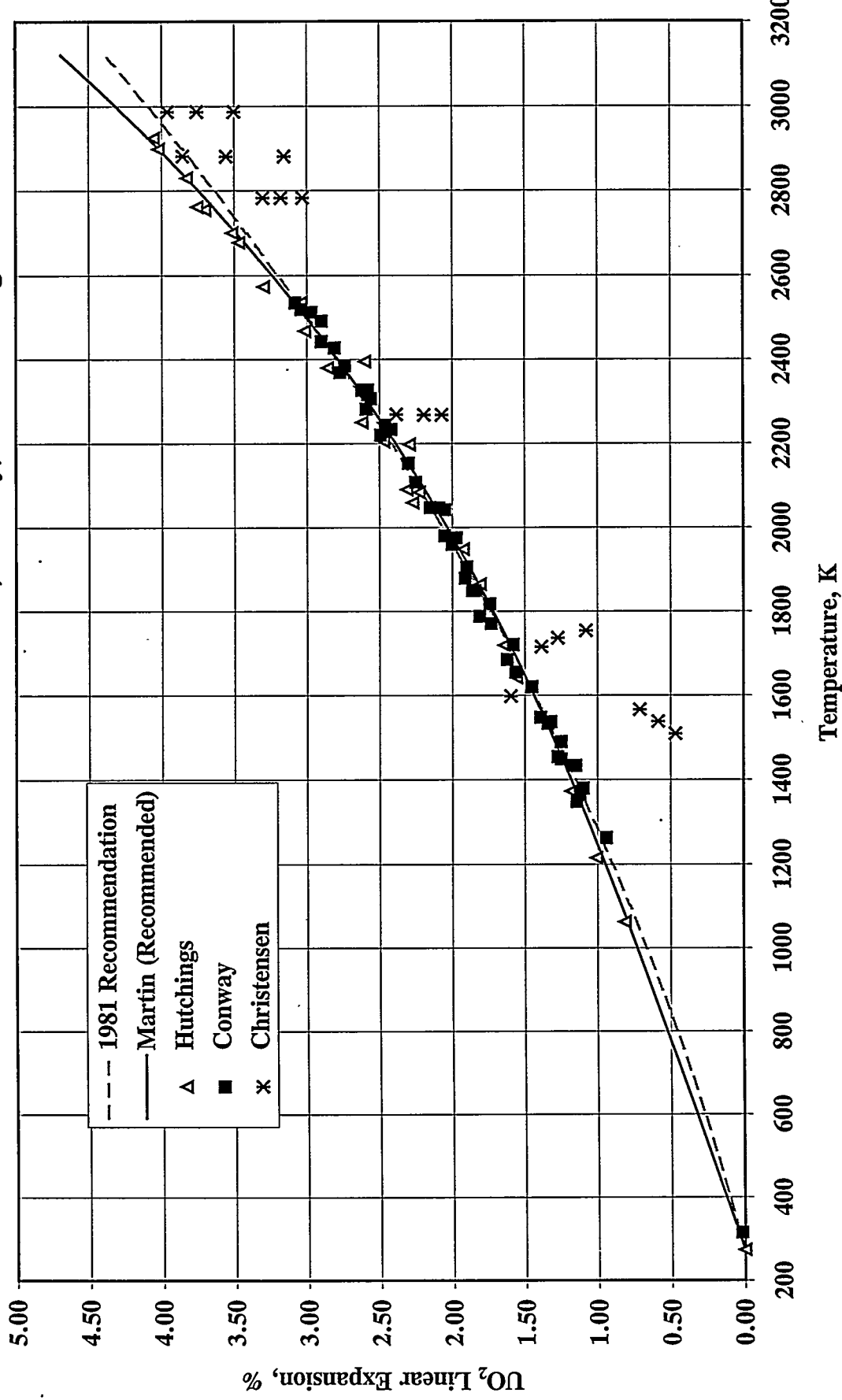
Figure 4.1.7 Comparison of Recommended UO₂ Linear Thermal Expansion Coefficient of Martin with Previous Recommendation
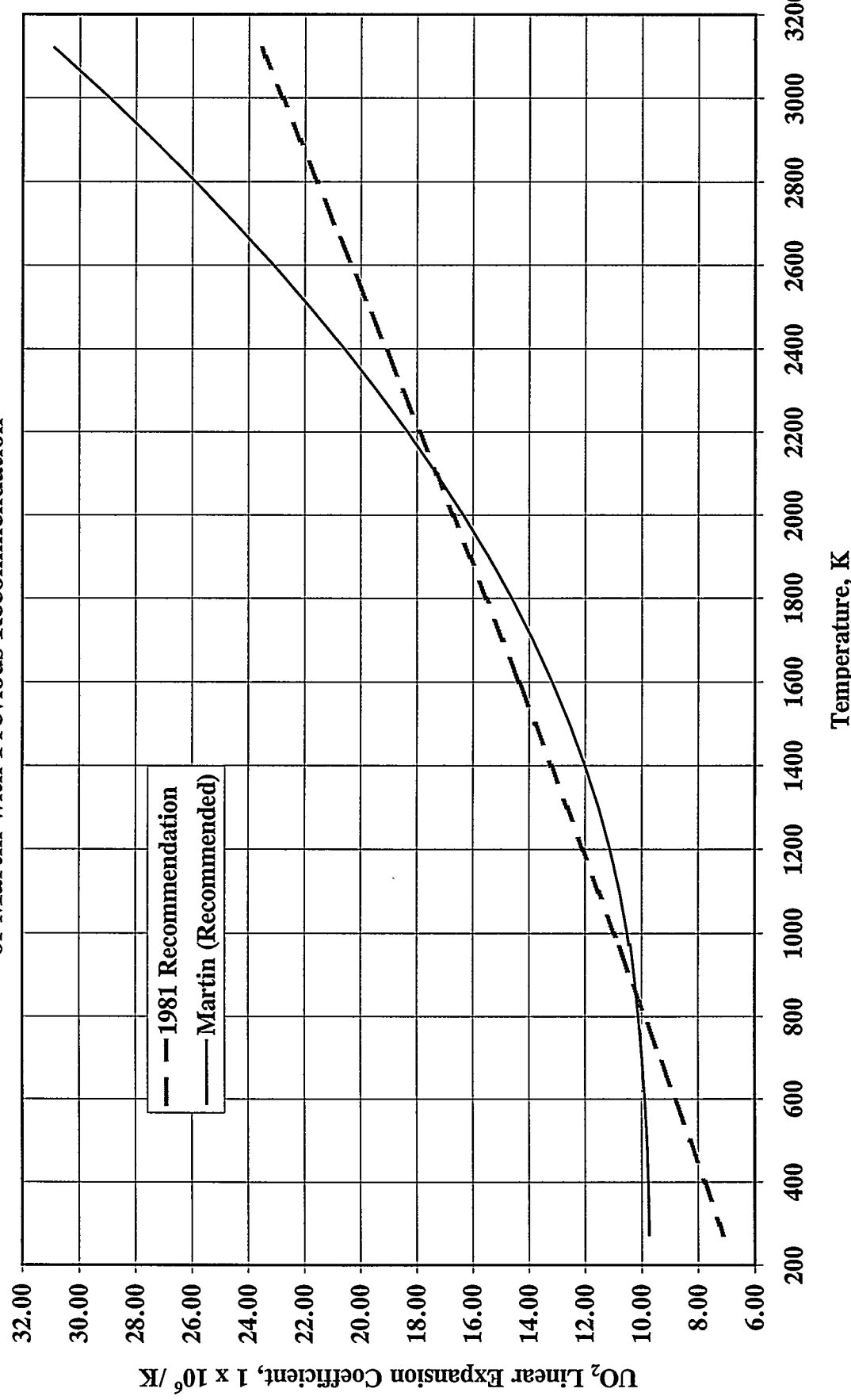
Figure 4.1.8 UO$_{2+x}$ Thermal Expansion Data Compared with Recommendation
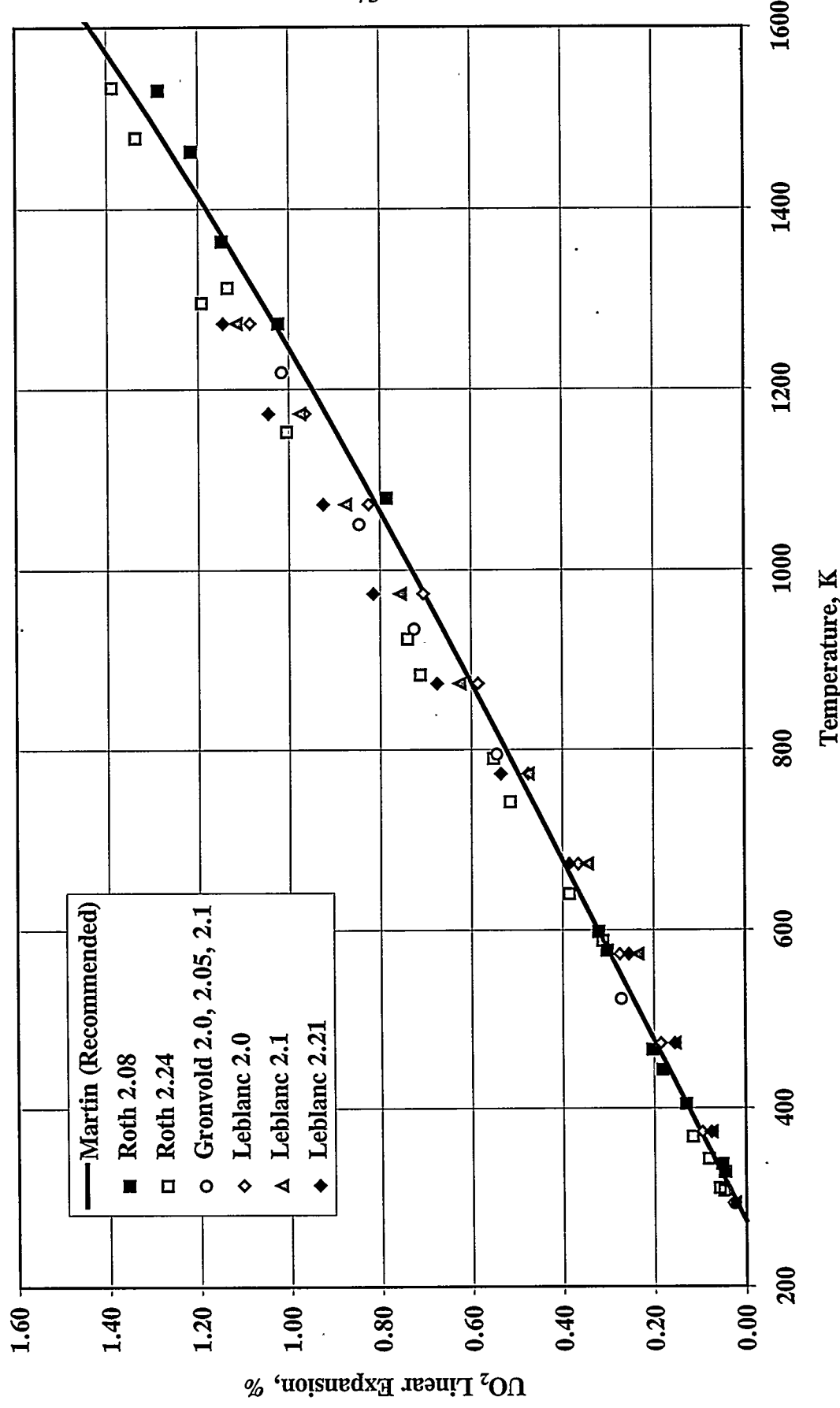
4.2 DENSITY OF SOLID UO$_2$

Recommended Equations

The recommended equations for the density of solid uranium dioxide are based on the lattice parameter value of 0.54704 nm obtained by Gronvold[1] at 293 K and the 1988 assessment of thermal expansion by D. G. Martin.[2] They are in agreement with the 1989 recommendations of Harding, Martin, and Potter.[3] The lattice parameter of Gronvold is in good agreement with recent measurements by Hutchings.[3] Assuming the molecular weight of UO$_2$ is 270.03, this lattice parameter gives a UO$_2$ density at 293 K of 10.96 Mg · m^{-3}. Applying the thermal expansion recommendation of Martin, the density at 273 K is 10.963 Mg · m^{-3}.

The density as a function of temperature may be calculated from

$$\rho(T) = \rho(273) \left(\frac{L(273)}{L(T)} \right)^3 \tag{1}$$

where $\rho(273)$ is the density at 273 K; $L(273)$ and $L(T)$ are the lengths at 273 K and at temperature T(K), respectively. The ratio of the length at 273 K to the length at temperature T(K) may be calculated from Martin's equations for the thermal expansion of solid UO$_2$:

For 273 K $\leq$ T $\leq$ 923 K,

$$L(T) = L(273) \, (9.9734 \times 10^{-1} + 9.802 \times 10^{-6} T - 2.705 \times 10^{-10} T^2$$
$$+ 4.291 \times 10^{-10} T^3); \tag{2}$$

For 923 K $\leq$ T $\leq$ 3120 K,

$$L(T) = L(273) \, (9.9672 \times 10^{-1} + 1.179 \times 10^{-5} T - 2.429 \times 10^{-9} T^2$$
$$+ 1.219 \times 10^{-12} T^3); \tag{3}$$

The densities as a function of temperature of solid UO_2 are given in Table 4.2.1.

From assessment of the available data on hyperstoichiometric uranium dioxide (UO_{2+x}), Martin recommended using the same equations for the linear thermal expansion of UO_2 and of UO_{2+x} for x in the ranges 0 to 0.13 and 0.23 to 0.25. Therefore, equations (1) through (3) are recommended for the density of UO_{2+x} for x in the ranges 0 to 0.13 and 0.23 to 0.25.

No data on the effect of burn-up on density or thermal expansion of UO_2 are currently available. In the absence of data, equations (1) through (3) are recommended for UO_2 during irradiation, in accord with the recommendation of Harding, Martin, and Potter.[3]

Uncertainties

The recommended uncertainty in the density of UO_2 is 1% for the entire temperature range. The uncertainties in the density of UO_2 calculated from the thermal expansion uncertainties given by Martin[2] are less than 1%. The 1% uncertainty is based on comparison of the recommended density with those of previous recommendations based on different data. Figure 4.2.1 shows the recommended density, the 1% uncertainty, and the 1981 recommended values[5] that are based on the thermal expansion values of Olsen[6] and a density at 298.15 K of 10.97 $Mg \cdot m^{-3}$.

REFERENCES

1.   F. Gronvold, J. Inorganic and Nucl. Chem. **1** 357, (1955).

2.   D. G. Martin, *The Thermal Expansion of Solid UO₂ and (U,Pu) Mixed Oxides - A Review and Recommendations,* J. Nucl. Mater. **152,** 94-101 (1988).

3.   J. H. Harding, D. G. Martin, and P. E. Potter, *Thermophysical and Thermochemical Properties of Fast Reactor Materials,"* Commission of European Communities Report **EUR 12402** (1989).

4.   M. T. Hutchings, *High-Temperature Studies of UO₂ and ThO₂ Using Neutron Scattering Techniques,* J. Chem. Soc. Faraday Trans. II **83,** 1083-1103 (1987).

5.   J. K. Fink, M. G. Chasanov, and L. Leibowitz, *Thermophysical Properties of Uranium Dioxide,* J. Nucl. Mater. **102** 17-25 (1981).

6.   C. S. Olsen, *Fuel Thermal Expansion (FTHEXP)* in *MATPRO- Version 11: A Handbook of Materials Properties for Use in the Analysis of Light Water Reactor Fuel Rod Behavior,* ed. D. R. Hagraman and G. A. Reymann, US Nuclear Regulatory Commission Rep. **NUREG/CR-0497** (February 1979); also revision (1981).

Table 4.2.1 Density of Solid Uranium Dioxide

Temperature, K	Density, $Mg \cdot m^{-3}$
273	10.96
298	10.95
300	10.95
400	10.92
500	10.89
600	10.86
700	10.83
800	10.79
900	10.76
1000	10.73
1100	10.69
1200	10.66
1300	10.62
1400	10.58
1500	10.54
1600	10.50
1700	10.46
1800	10.42
1900	10.37
2000	10.32
2100	10.27
2200	10.21
2300	10.16
2400	10.10
2500	10.03
2600	9.96
2700	9.89
2800	9.82
2900	9.74
3000	9.66
3100	9.57
3120	9.56

Figure 4.2.1 Density of Solid UO$_2$
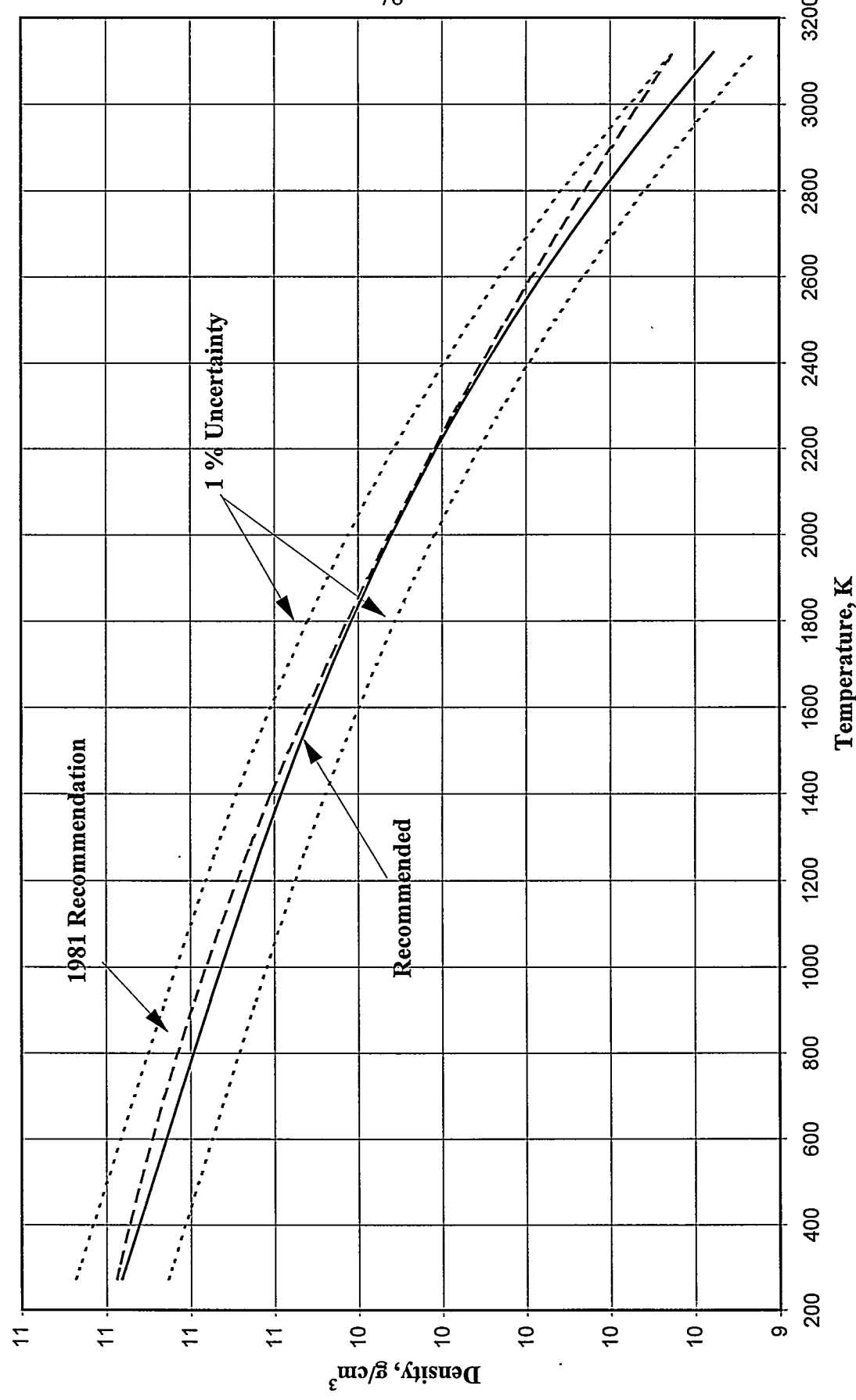
4.3   THERMAL EXPANSION COEFFICIENT OF LIQUID UO$_2$

Recommended Equation

The recommended equation for the thermal expansion coefficient of liquid uranium dioxide is based on the in-pile effective equation of state measurements of the vapor pressure, density, and isothermal compressibility of liquid (U, Pu)O$_2$ by Breitung and Reil.[1] From these measurements, the density and thermal expansion coefficient as functions of temperature were obtained from the melting point to 7600 K. The equation of Breitung and Reil for the thermal expansion coefficient of UO$_2$ and (U, Pu)O$_2$ for mole fractions of Pu $\leq$ 0.25 is in good agreement with the equation for the thermal expansion coefficient of UO$_2$ from experiments by Drotning,[2] which had been recommended in the 1981 assessment by Fink et al.[3,4]

The recommended equation for the instantaneous volumetric thermal expansion coefficient of UO$_2$ as a function of temperature is

$$\alpha_P = \frac{0.9285}{8860 - 0.9285\,(T - 3120)} \tag{1}$$

where the thermal expansion coefficient (α_P) is in K^{-1} and temperature (T) is in K. Values for the density and the instantaneous volumetric thermal expansion coefficient of UO$_2$ are given in Table 4.3.1. Figure 4.3.1 shows the recommended values for the instantaneous volumetric thermal expansion coefficient of UO$_2$, the uncertainties determined by Breitung and Reil,[1] and the instantaneous volumetric thermal expansion coefficients of UO$_2$ calculated from equations of Drotning,[2] of Christensen,[5] and of Harding.[6]

Uncertainties

Breitung and Reil determined experimental uncertainties from the uncertainty in the fuel mass ($\delta m/m = 10\%$), the uncertainty in the test volume ($\delta V/V = 2.5\%$), and the uncertainty in the fuel enthalpy ($\delta h/h = 6\%$). From these uncertainties, they obtained upper and lower limiting cases which they used to define uncertainties in the parameters in Eq. (1). The liquid density at the melting point, 8860 kg·m^{-3}, has an uncertainty of $\pm$ 120 kg·m^{-3}. The slope of the density, ($d\rho/dT$) = 0.9285 kg·m^{-3}·K^{-1}, has uncertainties of + 0.036 kg·m^{-3}·K^{-1} and - 0.135 kg·m^{-3}·K^{-1}. The upper and lower uncertainty limits calculated using the uncertainties in these parameters are shown in Figure 4.3.1.

They correspond to uncertainties of

+10% and -12% at 3120 K;

+10% and -13% at 3500 K;

+12% and -15% at 4500 K;

+13% and -17% at 5500 K;

+15% and -20% at 6500 K;

+18% and -27% at 7600 K.

Discussion of the Recommended Equation

Thermodynamic Relations - The instantaneous volumetric thermal expansion coefficient (α_p) is related to the density (ρ) by the thermodynamic relation

$$\alpha_P = -\frac{1}{\rho}\left(\frac{\partial\rho}{\partial T}\right)_\sigma + \beta_T\left(\frac{\partial P}{\partial T}\right)_\sigma \qquad (2)$$

where β_T is the isothermal compressibility and P is the vapor pressure. The subscript σ on the partial derivatives indicates that they are along the saturation curve. Breitung and Reil[1] stated that the magnitude of the second term in Eq. (2) is much smaller than the first term and only contributes a few percent at 8000 K. This is because along the saturation curve, the volume change due to the pressure change is much smaller than the corresponding volume change due to thermal expansion. Thus, for UO_2 and $(U,Pu)O_2$, the thermal expansion coefficient may be evaluated from the density/ temperature relation using the first term in Eq. (2).

The linear instantaneous thermal expansion coefficient is one third of the instantaneous volumetric thermal expansion coefficient, given by Eq. (1). Equations relating the instantaneous volumetric thermal expansion coefficient and density to other expansion parameters are given in the Section 4.5, "Density and Thermal Expansion Relations."

Comparison with Other Measurements and Assessments - Three experiments have provided data on the density and thermal expansion of liquid UO_2. Breitung and Reil[1] determined the density of UO_2 and $(U,Pu)O_2$ from the melting point (3120 K) to 7600 K from measurements of the pressure rise of a sealed capsule during a transient in-pile pulse. Their vapor pressure measurements using ultrapure UO_2, reactor grade UO_2, and reactor grade $(U,Pu)O_2$ showed no significant difference for

the vapor pressures of all three fuel types. Drotning[2] determined the density of UO_2 with O/M ratios ranging from 2.01 to 2.04 as a function of temperature using gamma ray attenuation measurements. Christensen measured the thermal expansion of solid and liquid UO_2 and the volume change on melting using gamma radiographs to determine the sample dimensions.

The variation of density with temperature from all three measurements is in good agreement. The slope ($d\rho/dT$) used in the first term of Eq. (2) is

- 0.9285 kg m^{-3} K^{-1} (Breitung & Reil)

- 0.916 kg m^{-3} K^{-1} (Drotning)

- 0.918 kg m^{-3} K^{-1} (Christensen)

The thermal expansion of Drotning[2] was recommended in the 1981 assessment by Fink et al.[3,4] The instantaneous volumetric thermal expansion coefficient calculated from Drotning's density equation using the first term in Eq. (2) is

$$\alpha_P = \frac{0.916}{8860 - 0.916\,(T - 3120)} \qquad (3)$$

where the thermal expansion coefficient (α_P) is in K^{-1} and temperature (T) is in K. Values of thermal expansion calculated with this equation are shown in Figure 4.3.1.

In their 1989 review of the data on density of liquid UO_2, Harding, Martin, and Potter[6] also recommended the change in density with temperature measured by Drotning. However, they recommended 8640 ± 60 kg·m^{-3} for the liquid density at 3120 K. So, the thermal expansion coefficient calculated from the density recommended by Harding et al. using the first term in Eq. (2) is

$$\alpha_P = \frac{0.893}{8640 - 0.893\,(T - 3120)} \qquad (4)$$

where the volumetric thermal expansion coefficient (α_P) is in K^{-1} and temperature (T) is in K. Because both Eq. (3) and Eq. (4) are based on the variation of density with temperature measured

by Drotning, the values of the thermal expansion coefficient calculated using Eq. (4) are almost identical to those calculated using Eq. (3). Differences are 0.03% from the melting point to 4800 K, 0.04% from 4900 to 6600 K, and 0.05% from 6700 to 7600 K.

The instantaneous volumetric thermal expansion coefficient calculated from the liquid density of Christensen and his change of density with temperature is

$$\alpha_P = \frac{0.918}{8740 - 0.918(T - 3120)} \tag{5}$$

where the thermal expansion coefficient (α_P) is in K^{-1} and temperature (T) is in K. Values of the volumetric thermal expansion coefficient determined from the measurements of Christensen have been included in Figure 4.3.1.

Figure 4.3.2 shows the deviations of the recommended thermal expansion coefficients of Breitung and Reil from the thermal expansion coefficients determined from measurements of Christensen[5] and of Drotning.[2] Percent deviations in Figure 4.3.2 are defined as

$$Deviation(\%) = \frac{\alpha_P(Eq) - \alpha_P(Breitung)}{\alpha_P(Breitung)} \cdot 100\% \tag{6}$$

Extrapolations of the thermal expansion coefficients from the low temperature measurements of Christensen[5] and Drotning[2] to 7600 K show good agreement throughout the temperature range. Deviations of recommended values from those determined from measurements by Drotning range from -1.4% at the melting point to -2.5% at 7600 K. Christensen's values deviate from those of Breitung and Reil by 0.2% at the melting temperature and by 0.4% at 7600 K. Figure 4.3.2 shows that all deviations are well within the uncertainty limits given by Breitung and Reil.

REFERENCES

1.   W. Breitung and K. O. Reil, *The Density and Compressibility of Liquid (U,Pu)-Mixed Oxide,* Nuclear Science and Engineering **105**, 205-217 (1990).

2.   W. D. Drotning, *Thermal Expansion of Molten Uranium Dioxide,* Proceedings of the 8th Symp. On Thermophysical Properties, Gaithersburg, Maryland, June 15-18, 1981, National Bureau of Standard (1981).

3.   J. K. Fink, M. G. Chasanov, and L. Leibowitz, *Thermophysical Properties of Uranium Dioxide,* J. Nucl. Mater. **102** 17-25 (1981).

4.   J. K. Fink, M. G. Chasanov, and L. Leibowitz, *Properties for Reactor Safety Analysis,* **ANL-CEN-RSD-80-3**, Argonne National Laboratory Report (April, 1981).

5.   J. A. Christensen, *Thermal Expansion and Change in Volume of Uranium Dioxide on Melting,* J. Am. Ceram. Soc. **46**, 607-608 (1963).

6.   J. H. Harding, D. G. Martin, and P. E. Potter, *Thermophysical and Thermochemical Properties of Fast Reactor Materials, "* Commission of European Communities Report **EUR 12402 (1989).**

Table 4.3.1 Density and Volumetric Thermal Expansion Coefficient for Liquid UO$_2$

Temperature K	Density Mg m^{-3}	Thermal Expansion α_p x 10^5, K^{-1}
3120	8.86	10.48
3200	8.79	10.57
3300	8.69	10.68
3400	8.60	10.80
3500	8.51	10.91
3600	8.41	11.03
3700	8.32	11.16
3800	8.23	11.28
3900	8.14	11.41
4000	8.04	11.54
4100	7.95	11.68
4200	7.86	11.82
4300	7.76	11.96
4400	7.67	12.10
4500	7.58	12.25
4600	7.49	12.40
4700	7.39	12.56
4800	7.30	12.72
4900	7.21	12.88
5000	7.11	13.05
5100	7.02	13.22
5200	6.93	13.40
5300	6.84	13.58
5400	6.74	13.77
5500	6.65	13.96
5600	6.56	14.16
5700	6.46	14.36
5800	6.37	14.57
5900	6.28	14.79
6000	6.19	15.01
6100	6.09	15.24
6200	6.00	15.47
6300	5.91	15.72
6400	5.81	15.97
6500	5.72	16.23
6600	5.63	16.50
6700	5.54	16.77
6800	5.44	17.06
6900	5.35	17.35
7000	5.26	17.66
7100	5.16	17.98
7200	5.07	18.31
7300	4.98	18.65
7400	4.89	19.00
7500	4.79	19.37
7600	4.70	19.75

Figure 4.3.1 Coefficient of Thermal Expansion for Liquid UO$_2$
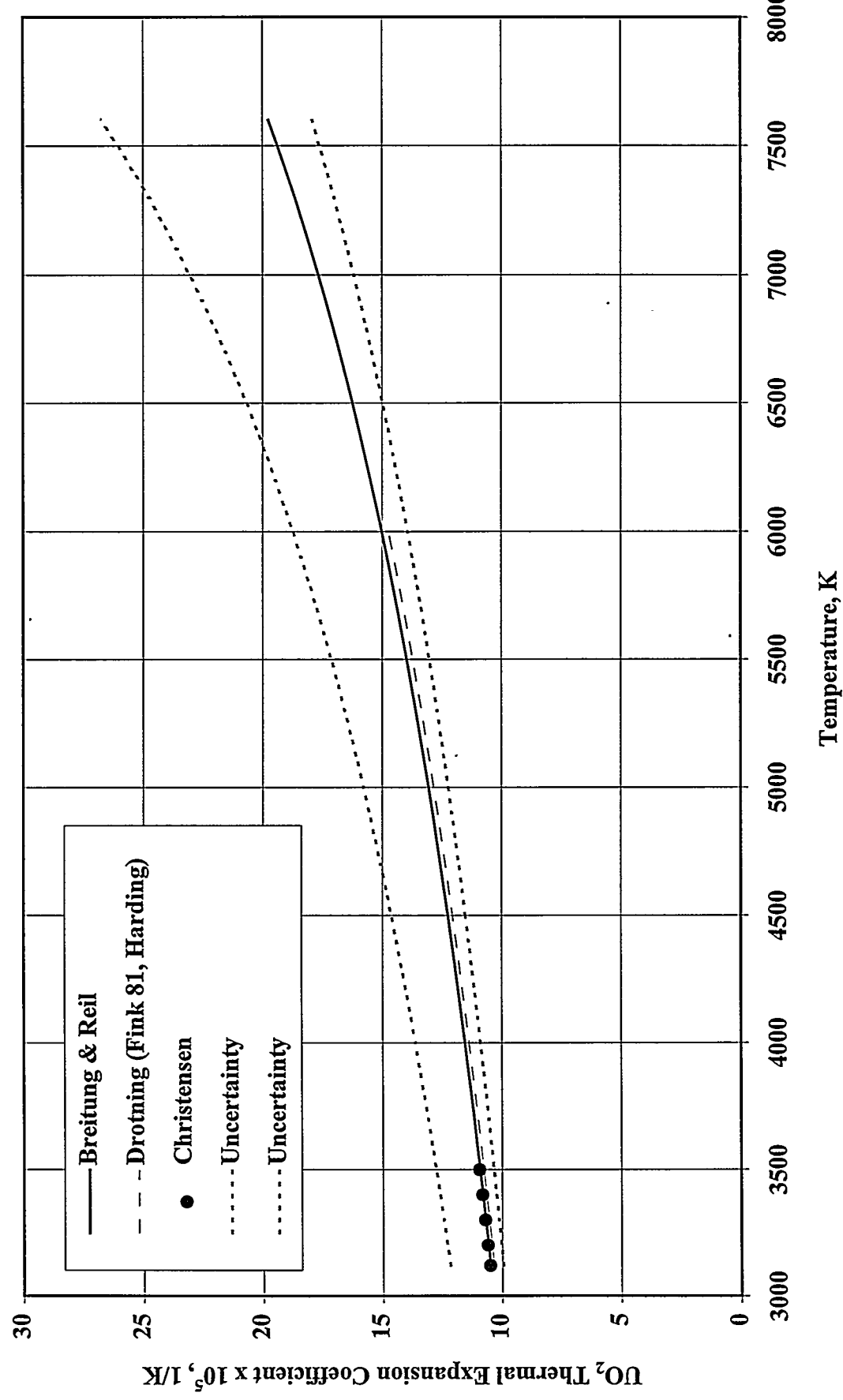
Figure 4.3.2 Deviations from $(U,Pu)O_2$ Liquid Thermal Expansion of Breitung & Reil
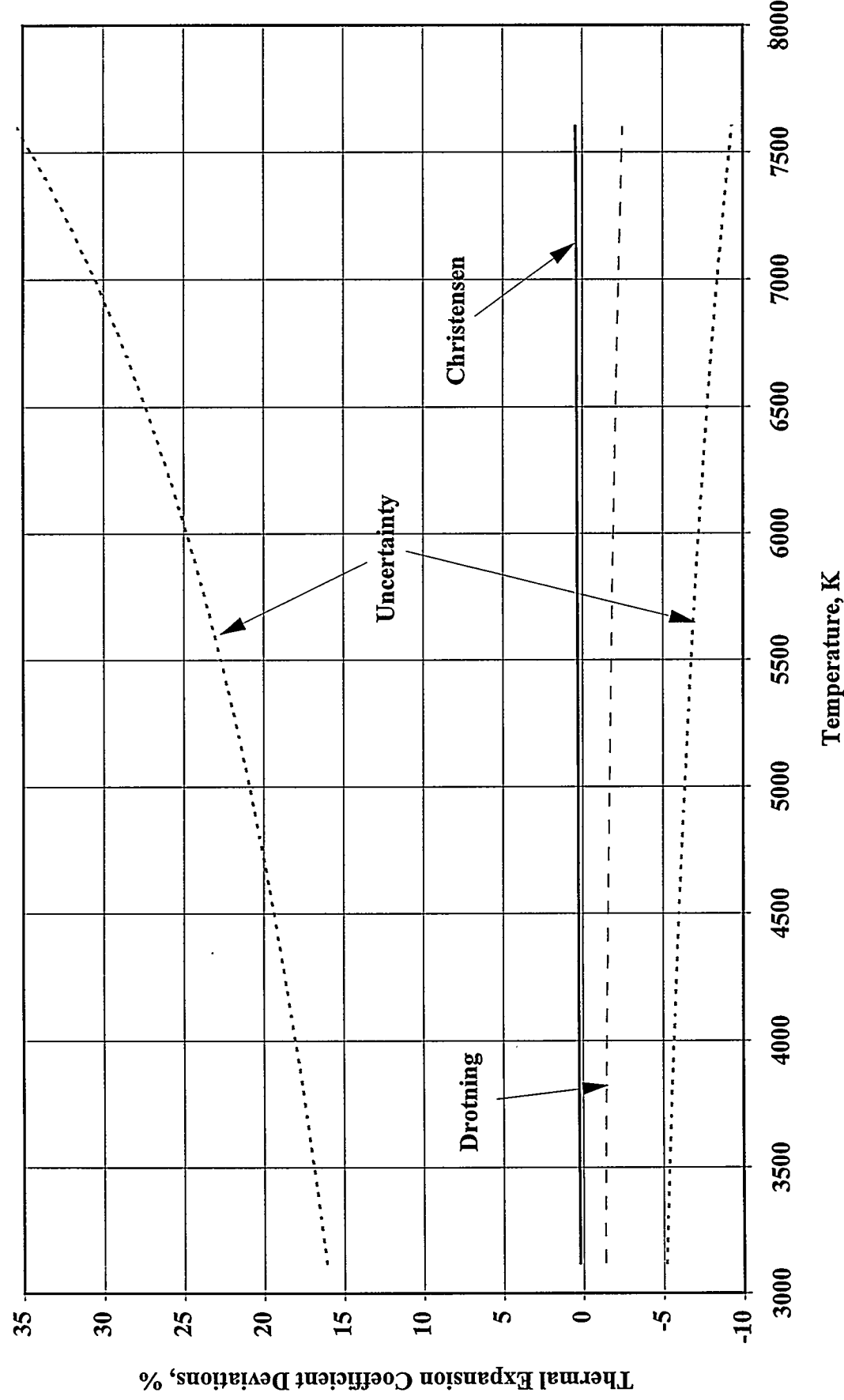
4.4   DENSITY OF LIQUID UO$_2$

Recommended Equation

The recommended equation for the density of liquid uranium dioxide is based on the in-pile effective equation-of-state measurements of the vapor pressure, density, and isothermal compressibility of liquid (U, Pu)O$_2$ by Breitung and Reil.[1] Measurements of density as a function of enthalpy and as a function of temperature were obtained from the melting point (3120 K) to 7600 K. The equation of Breitung and Reil for the density of UO$_2$ and (U, Pu)O$_2$ for mole fractions of Pu $\leq$ 0.25 is in good agreement with the equation for the density of UO$_2$ from experiments by Drotning,[2] which had been recommended in the 1981 assessment by Fink et al.[3,4]

The recommended equation for the density of UO$_2$ as a function of temperature is

$$\rho = 8.860 - 9.285 \times 10^{-4} (T - 3120) \qquad (1)$$

where density (ρ) is in Mg/m^3 and temperature (T) is in K. Values for the density and the instantaneous thermal expansion coefficient of UO$_2$ are given in Table 4.4.1. Figure 4.4.1 shows the recommended values for the density of UO$_2$, the uncertainties determined by Breitung and Reil,[1] and the UO$_2$ density data of Drotning[2] and of Christensen.[5]

Uncertainties

Breitung and Reil determined experimental uncertainties from the uncertainty in the fuel mass ($\delta m/m = 10\%$), the uncertainty in the test volume ($\delta V/V = 2.5\%$), and the uncertainty in the fuel enthalpy ($\delta h/h = 6\%$). From these uncertainties, they obtained upper and lower limiting values in addition to the most probable reference values. Their uncertainty bands correspond to uncertainties in the coefficients in Eq. (1) given by

$$\rho = (8.860 \pm 0.120) + \left[-9.285 \left(\begin{array}{c} +0.036 \\ -0.135 \end{array} \right) \right] \times 10^{-4} (T - 3120) \qquad (2)$$

The upper and lower uncertainty limits calculated from Eq. (2) are shown in Figure 4.4.1. They correspond to uncertainties of

$\pm$ 1.4% at 3120 K;

+1.6% and -2% at 3500 K;

+2.2% and -4% at 4500 K;

+3% and -6.3% at 5400 K;

+4.2% and -10% at 6500 K;

+6% and -15.4% at 7600 K.

Discussion of the Recommended Equation

Measurements and Assessments - Three experiments have provided data on the density and thermal expansion of liquid UO_2. Breitung and Reil[1] determined the density of UO_2 and $(U,Pu)O_2$ from the melting point to 7600 K from measurements of the pressure rise of a sealed capsule during a transient in-pile pulse. Their vapor pressure measurements using ultrapure UO_2, reactor grade UO_2, and reactor grade $(U,Pu)O_2$ showed no significant difference for the vapor pressures of all three fuel types. Drotning[2] determined the density of UO_2 with O/M ratios ranging from 2.01 to 2.04 as a function of temperature using gamma-ray attenuation measurements. Christensen measured the thermal expansion of solid and liquid UO_2 and the volume change on melting using gamma radiographs to determine the sample dimensions.

UO_2 liquid densities at the melting point measured by Drotning ranged from 8.779 to 8.939 Mg/m^3 with an average of 8.860 Mg/m^3 and a deviation of ± 0.061 Mg/m^3 or 0.7%. His equation for the density of UO_2 in Mg/m^3 from 3120 to 3250 K is

$$\rho = (8.860 \pm 0.06) - (9.16 \pm 0.43) \times 10^{-4} (T-3120) \tag{3}$$

where temperature is in K. This equation was recommended in the 1981 assessment by Fink et al.[3,4]

The change of density of UO_2 at the melting point measured by Christensen was 9.6%. In the liquid range, he measured densities from the melting point (which he measured as 3073 K rather than 3120 K) to 3373 K. At the melting point, he gave solid and liquid densities of 9.67 ± 0.13 Mg/m^3 and 8.74 ± 0.16 Mg/m^3, respectively. His equation for the liquid density of UO_2 adjusted to a melting point of 3120 K is

$$\rho = 8.74 - 9.18 \times 10^{-4} (T-3120) \tag{4}$$

where density is in Mg/m^3 and temperature is in K.

In their 1989 review of the data on density of liquid UO_2, Harding, Martin, and Potter[6] used the solid density at the melting point recommended by Martin[7] (9.56 ± 0.04 Mg/m^3) and the change in density at melting determined by Christensen (9.6%) to obtain 8.64 ± 0.06 Mg/m^3 for the liquid density at 3120 K. Because of the higher accuracy of Drotning's liquid density measurements compared with the thermal expansion measurements of Christensen, Harding et al.[6] based the slope of their density equation on the slope given by Drotning corrected to the different density at the melting point, 3120 K. They recommended the equation

$$\rho = (8.64 \pm 0.06) - (8.93 \pm 0.42) \times 10^{-4}(T-3120) \tag{5}$$

for the density of UO_2 in Mg/m^3, where temperature is in K. The liquid density at the melting point given by this equation is lower than the lowest density measured by Drotning but is above Christensen's lower uncertainty of 8.58 Mg/m^3.

Breitung and Reil set their melting point density of UO_2 and $(U,Pu)O_2$ to 8.860 Mg/m^3, the density of UO_2 at the melting point given by Drotning[2] because of the smaller error in Drotning's measurements ($\pm 0.7\%$) than in Christensen's measurements ($\pm 2\%$). The densities of Christensen and of Drotning agree within their experimental uncertainties. The uncertainty (± 0.120 Mg/m^3) given by Breitung and Reil for this parameter in their density equation is large enough to include the melting point density given by Christensen. The liquid density at the melting point recommended by Fink, Chasanov, and Leibowitz[3,4] was also 8.860 Mg/m^3.

Equation Selection - The equation given by Breitung and Reil, Eq. (1), has been recommended because it is a careful analysis of the experimental data with experimental uncertainties for the largest temperature range and is consistent with the measurements of Drotning. Figure 4.4.2 compares the recommended equation of Breitung and Reil with the equations of Drotning,[2] Christensen,[5] and Harding et al.[6] and the experimental data of Drotning and of Christensen. In Figure 4.4.2, the data of Christensen has been corrected for his temperature offset at the melting point. Figure 4.4.2 shows that the slope of the density equation recommended by Breitung and Reil is also consistent with that of Christensen. However, the equation of Harding

et al. is consistently lower than that of Breitung and Reil in this temperature region due to the melting point density selected by Harding et al. Because the solid density data of Christensen has been shown, by Martin's analysis[7] of the thermal expansion of solid UO_2, to be inconsistent with later more accurate measurements of Hutchings,[8] there is some question with regard to the reliability of his determination of the change of density on melting. Because the liquid densities at the melting point determined by Drotning and by Christensen are consistent within their error limits and the uncertainties for Drotning's data are less than those for Christensen's, the melting point density of Drotning is preferred to using the density change on melting given by Christensen and the solid density at the melting point given by Martin.[7]

Deviations from Recommended Equation - Percent deviations of the densities given by the equations of Drotning,[2] Christensen,[5] and Harding et al.[6] from the recommended values given by the equation of Breitung and Reil are shown in Figure 4.4.3. Percent deviations in Figure 4.4.3 are defined as

$$Deviation(\%) = \frac{\rho(Eq) - \rho(Breitung)}{\rho(Breitung)} \cdot 100\% \tag{6}$$

The uncertainties given by Breitung and Reil are included in Figure 4.4.3, expressed as percents, for comparison with the deviations. Figure 4.4.3 shows that all the equations are within the uncertainties of Breitung and Reil except for the equation of Harding et al. for the temperature range 3120 K through 3700 K. Absolute values of the percent deviations for the equation of Harding et al. decrease from a maximum deviation of -2.5% at the melting point to -1.3% at 7600 K. Percent deviations for the density equation of Christensen show little variation with temperature. They range from -1.4% at 3120 K to -1.6% at 7600 K. The smallest deviations occur for Drotning's equation, which gives densities within 1% of those given by Breitung and Reil from the melting point through 7200 K. At 7600 K, the percent deviation for these equations is 1.2%. Thus, for the entire temperature range of interest in severe accidents, the recommended densities of Breitung and Reil are in good agreement with those given by the equation of Drotning, which was recommended in the 1981 assessment by Fink et al.[3,4]

REFERENCES

1.   W. Breitung and K. O. Reil, *The Density and Compressibility of Liquid (U,Pu)-Mixed Oxide,* Nuclear Science and Engineering **105**, 205-217 (1990).

2.   W. D. Drotning, *Thermal Expansion of Molten Uranium Dioxide,* Proceedings of the 8th Symp. On Thermophysical Properties, Gaithersburg, Maryland, June 15-18, 1981, National Bureau of Standard (1981).

3.   J. K. Fink, M. G. Chasanov, and L. Leibowitz, *Thermophysical Properties of Uranium Dioxide,* J. Nucl. Mater. **102** 17-25 (1981).

4.   J. K. Fink, M. G. Chasanov, and L. Leibowitz, *Properties for Reactor Safety Analysis,* **ANL-CEN-RSD-80-3**, Argonne National Laboratory Report (April, 1981).

5.   J. A. Christensen, *Thermal Expansion and Change in Volume of Uranium Dioxide on Melting,* J. Am. Ceram. Soc. **46**, 607-608 (1963).

6.   J. H. Harding, D. G. Martin, and P. E. Potter, *Thermophysical and Thermochemical Properties of Fast Reactor Materials,"* Commission of European Communities Report **EUR 12402** (1989).

7.   D. G. Martin, *The Thermal Expansion of Solid UO_2 and (U,Pu) Mixed Oxides - A Review and Recommendations,* J. Nucl. Mater. **152** 94-101 (1988).

8.   M. T. Hutchings, *High-Temperature Studies of UO_2 and ThO_2 Using Neutron Scattering Techniques,* J. Chem. Soc. Faraday Trans. II **83,** 1083-1103 (1987).

Table 4.4.1 Density of Liquid UO_2

Temperature K	Density Mg m^{-3}
3120	8.86
3200	8.79
3300	8.69
3400	8.60
3500	8.51
3600	8.41
3700	8.32
3800	8.23
3900	8.14
4000	8.04
4100	7.95
4200	7.86
4300	7.76
4400	7.67
4500	7.58
4600	7.49
4700	7.39
4800	7.30
4900	7.21
5000	7.11
5100	7.02
5200	6.93
5300	6.84
5400	6.74
5500	6.65
5600	6.56
5700	6.46
5800	6.37
5900	6.28
6000	6.19
6100	6.09
6200	6.00
6300	5.91
6400	5.81
6500	5.72
6600	5.63
6700	5.54
6800	5.44
6900	5.35
7000	5.26
7100	5.16
7200	5.07
7300	4.98
7400	4.89
7500	4.79
7600	4.70

Figure 4.4.1 Liquid Density of UO$_2$
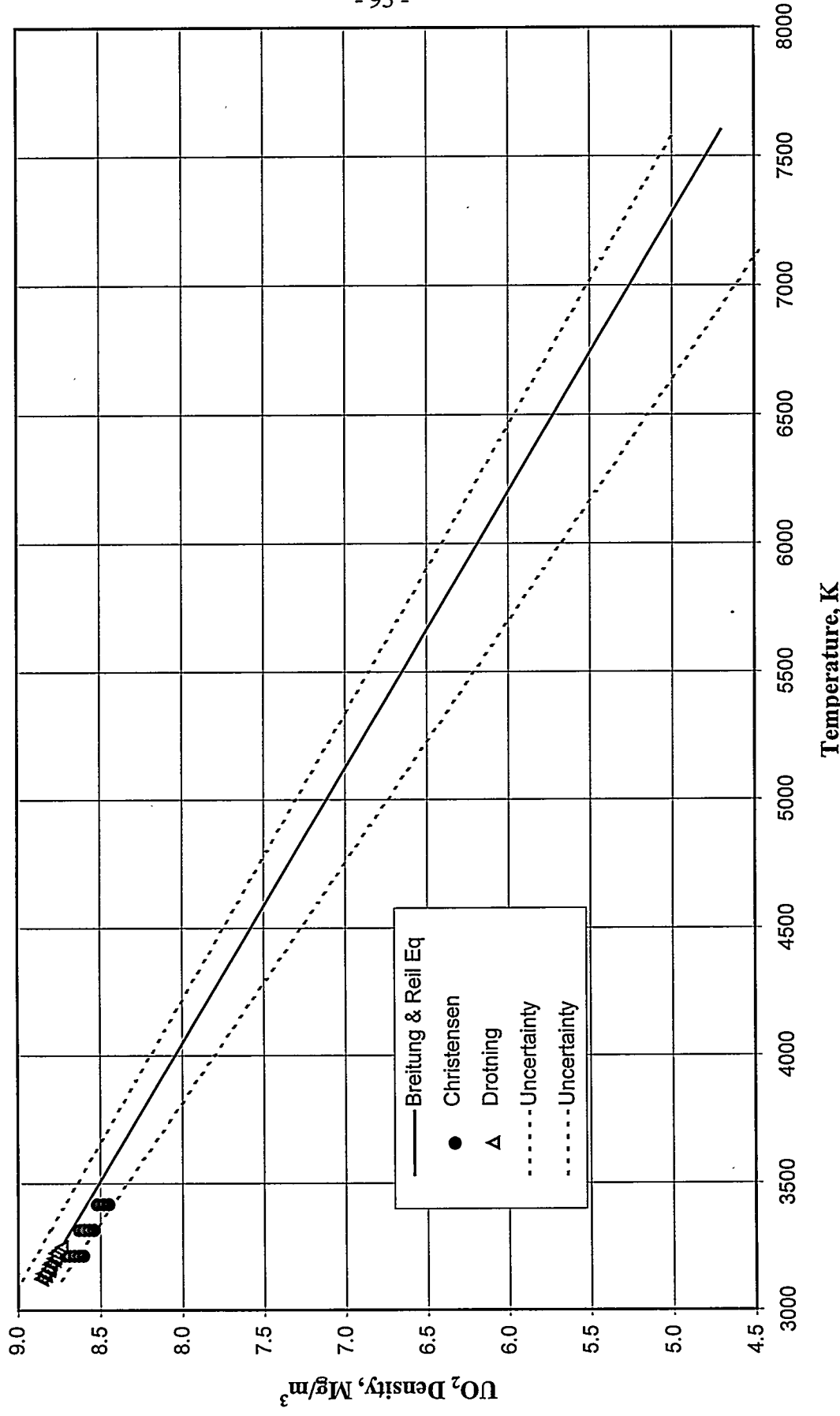
Figure 4.4.2 Liquid Density of UO$_2$
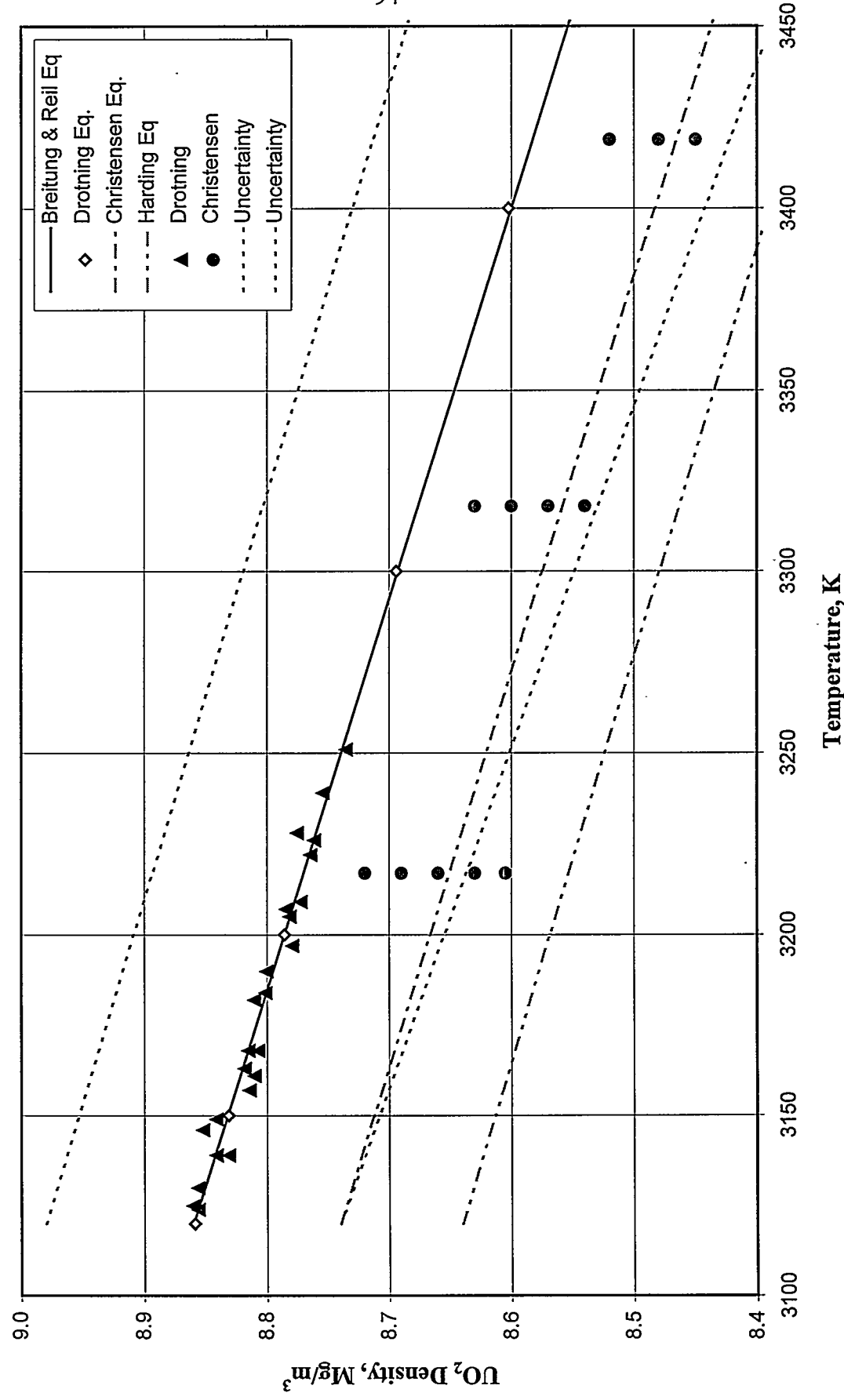
Figure 4.4.3 Deviations from $(U,Pu)O_2$ Liquid Density Eq. of Breitung & Reil

Legend:
- — — — Drotning Eq.
- — · · — Christensen Eq.
- — · — Harding Eq
- ———— Uncertainty
- ———— Uncertainty

X-axis: Temperature, K
Y-axis: Density Deviations, %
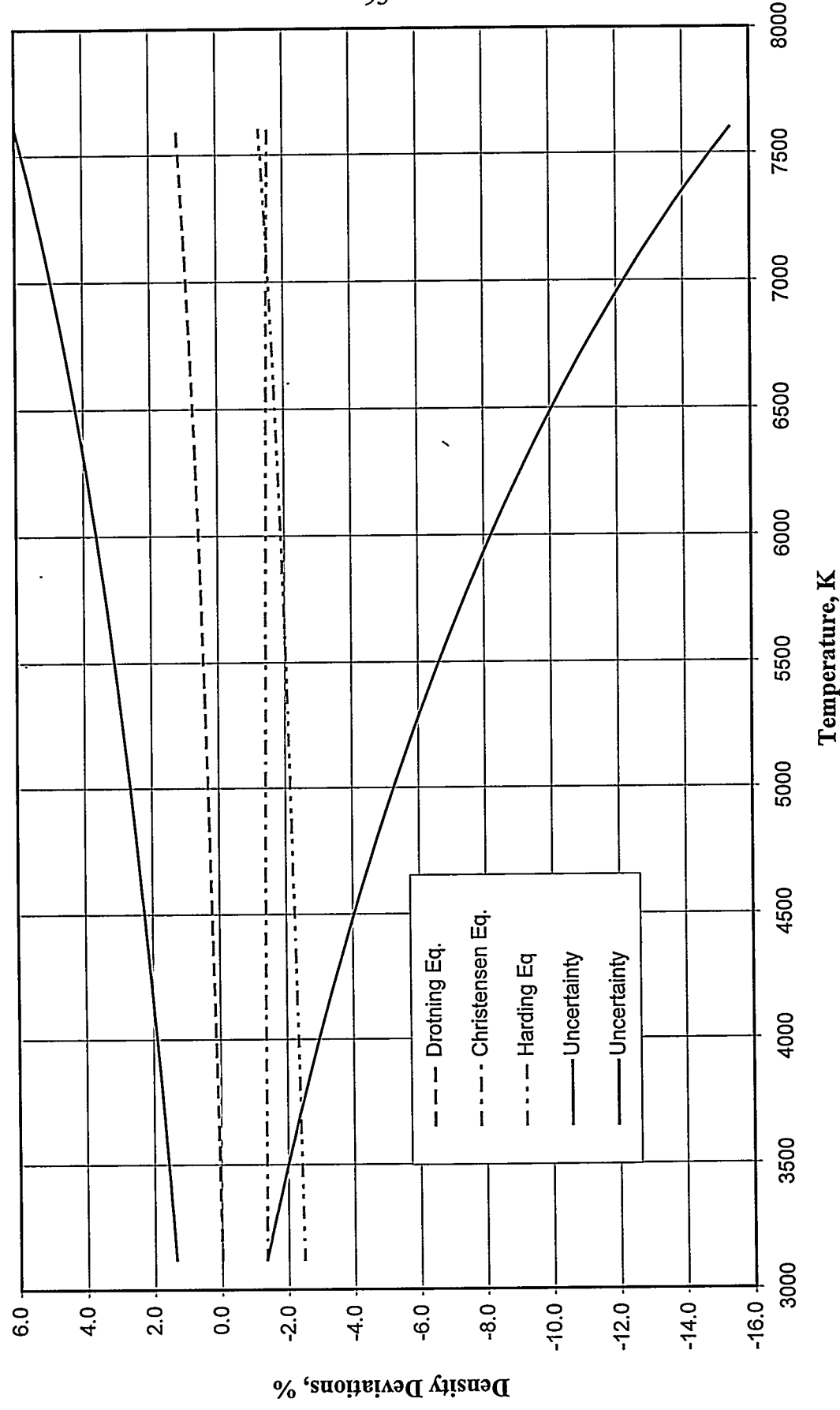
4.5   DENSITY AND THERMAL EXPANSION RELATIONS

The thermal-expansion coefficient (α_P) is a thermodynamic quantity defined as

$$\alpha_P = \frac{1}{V}\left(\frac{\partial V}{\partial T}\right) \tag{1}$$

where P, V, and T are, respectively, pressure, volume, and temperature. We will refer to α_P as the instantaneous volumetric thermal-expansion coefficient. For simplicity, the subscript P has been eliminated from the thermal-expansion coefficients in the following discussion with the understanding that constant pressure is implied in all the following equations.

The mean volumetric thermal-expansion coefficient is defined as

$$\bar{\alpha} = \frac{1}{V_o}\left(\frac{V - V_o}{T - T_o}\right) \tag{2}$$

where V and V_o are the volumes at temperatures T and T_o respectively.

Because many measurements of thermal expansion involve measurement of a length change, it is common to find tabulations of the fractional (or percent) change in length,

$$\frac{\Delta L}{L_o} = \left(\frac{L - L_o}{L_o}\right) \tag{3}$$

where L and L_o are respectively the sample lengths at temperatures T and T_o.

The instantaneous linear thermal-expansion coefficient is

$$\alpha_\ell = \frac{1}{L}\left(\frac{\partial L}{\partial T}\right) \tag{4}$$

The mean linear thermal-expansion coefficient is:

$$\bar{\alpha}_\ell = \frac{1}{L_o}\left(\frac{L - L_o}{T - T_o}\right) = \frac{1}{\Delta T}\left(\frac{L}{L_o} - 1\right) \tag{5}$$

The instantaneous volumetric thermal-expansion coefficient is just three times the instantaneous linear thermal-expansion coefficient; i.e., $\alpha = 3\alpha_\ell$. The same relation does not hold for the mean thermal-expansion coefficients, as the following considerations show. The mean volumetric thermal-expansion coefficient may be written as:

$$\bar{\alpha} = \frac{1}{\Delta T}\left(\frac{V}{V_o} - 1\right) \tag{6}$$

Since $V = L^3$ the definition of the mean linear thermal-expansion coefficient in Eq. (5) gives

$$\frac{V}{V_o} = (1 + \bar{\alpha}_\ell\Delta T)^3 \tag{7}$$

When this is substituted in Eq. (6) and expanded, the relationship between the mean volumetric and mean linear coefficient is:

$$\bar{\alpha} = 3\bar{\alpha}_\ell + 3\Delta T\bar{\alpha}_\ell^2 + \Delta T^2\bar{\alpha}_\ell^3 \tag{8}$$

The error introduced by taking only the first term in this equation will generally be small in many applications. For example for $\Delta T = 1000$ and $\bar{\alpha}_\ell = 1 \times 10^{-5}$, only a 1% error will be introduced by ignoring the last two terms.

The relation between linear thermal expansion and density is

$$\frac{\Delta\rho}{\rho_o} = \frac{1 - (1 + \Delta L/L_o)^3}{(1 + \Delta L/L_o)^3} \tag{9}$$

where $\Delta\rho = \rho - \rho_o$ is the difference between densities at temperatures T and T_o.

Equation (9) can be derived from the definition of density

$$\rho = \frac{m}{V} = \frac{m}{V_o\left(1 + \dfrac{\Delta V}{V_o}\right)} \tag{10}$$

giving

$$\frac{\Delta\rho}{\rho_o} = \frac{\dfrac{-\Delta V}{V_o}}{\left(1 + \dfrac{\Delta V}{V_o}\right)}$$

(11)

and the relation between fractional change in volume and fractional change in length

$$1 + \frac{\Delta V}{V_o} = \left(1 + \frac{\Delta L}{L_o}\right)^3$$

(12)

5.   SURFACE TENSION AND SURFACE ENERGY OF URANIUM DIOXIDE

Summary and Recommendation

Surface Tension of Liquid UO$_2$ - In 1987, Hall, Mortimer, and Mortimer[1] reported results of a critical review of available data on the surface tension of liquid UO$_2$ and on the surface energy of solid UO$_2$. Because no new data have been reported since this review, the results of this critical review are recommended. The recommended surface tension of liquid UO$_2$ at the melting point is the average of measurements by Schins,[2] Christensen,[3] and Bates[4] with a temperature dependence based on an equation derived by Nikopoulos and Schulz:[5]

$$\gamma_{LV} = 0.513 - 0.19 \times 10^{-3}(T-3120) \tag{1}$$

where the surface tension, γ_{LV}, is in J m^{-2} and temperature, T, is in K.

Surface Energy of Solid UO$_2$ - From review of the multi-phase equilibrium measurements of the surface energy of UO$_2$, Hall et al.[1] concluded that from 273 to 3120 K the surface energy (γ_{SV}) in J m^{-2} of solid UO$_{2.00}$ probably lies between two lines defined as follows:

Line 1:

$$\gamma_{SV} = 1.5 - 2.82 \times 10^{-4}(T-273) \tag{2}$$

Line 2:

$$\gamma_{SV} = 0.20 \tag{3}$$

with the mean line between these given by:

$$\gamma_{SV} = 0.85 - 1.40 \times 10^{-4}(T-273) \tag{4}$$

where temperature, T, is in K.

Hall et al.[1] gave the dependence of the solid surface energy on stoichiometry as:

$$\left(\gamma_{SV}\right)_x - \gamma_{SV} = 6.8x \quad (0 \leq x \leq 0.05;\ 0<T<2170K) \tag{5}$$

where $(\gamma_{SV})_x$ is the surface energy of $UO_{2\pm x}$ in J m^{-2}.

Hall et al.[1] concluded that the effective surface energy for pores in UO_2, γ_P, is different from γ_{SV}. It is given by:

$$\gamma_P = 0.41\gamma_{SV} \tag{6}$$

Uncertainties

Surface Tension of Liquid UO_2 - The standard error in the average of four measurements[2-4] of the surface tension of liquid UO_2 at the melting point is ± 0.085 J m^{-2}, which is an uncertainty of approximately $\pm 17\%$.

Surface Energy of Solid UO_2 - Because experimental estimates of the surface energy of solid UO_2 in the temperature range of 1773 to 2173 K from multi-phase equilibration techniques are uncertain up to $\pm 70\%$ and the sign of the temperature dependence is not unambiguously determined, Hall et al. gave the uncertainty in Eq. (4) as $\pm 70\%$. Although the uncertainty in the dependence on stoichiometry is $\pm 15\%$, the $UO_{2\pm x}$ surface energy uncertainty is $> \pm 70\%$ because of the UO_2 surface energy uncertainty.

Table 5.1 Measurements of the Surface Tension of Liquid UO_2 at the Melting Point

Surface Tension, J m^{-2}	Method	Experimenter	Reference
0.615 ± 0.180	liquid drop measurements	Schins	2
0.441 ± 0.210	liquid meniscus shape measurements	Bates	4
0.445 ± 0.210	droplet photographs	Christensen	3
$0.550. \pm 0.210$	droplet photographs	Christensen	3
0.420^*	shape of frozen menisci	Chasanov	6

*Not included in the determination of the recommended surface tension.

<u>Discussion</u>

Surface Tension of Liquid UO$_2$ - The measurements of the surface tension of liquid UO$_2$ at the melting point are given in Table 5.1. The value given by Chasanov has no estimate of uncertainty and has not been included in the assessment by Hall.[1] Therefore, the recommended value for the surface tension at the melting point, 0.513 ± 0.085 J m^{-2}, is the average of the surface tensions given in the first four rows of Table 5.1. Nikolopoulos and Schulz[5] calculated the surface tension of liquid UO$_2$ at three temperatures near the melting point using a theory for ionic liquids developed by Furth.[7] Their calculated values at 3125, 3175 and 3225 K are respectively 0.521, 0.514, and 0.502 J m^{-2}. These values are consistent with the average experimental value of the measurements by Schins, Bates, and Christensen. The value obtained by Chasanov[6] is low relative to this calculation. Inclusion of the value, 0.420 J m^{-2}, given by Chasanov in the average would give 0.494 J m^{-2} for the surface tension at the melting point. This value, recommended by Fink, Leibowitz, and Chasanov,[8] is low relative to the calculation of Nikopoulos and Schulz.[5]

Nikopoulos and Schulz[5] used their calculations to estimate the temperature dependence of the surface tension of liquid UO$_2$ near the melting point as $d\gamma_{SV}/dT = -0.19 \times 10^{-3}$ J m^{-2}. Combining this result and the average experimental value at the melting point, 0.513 ± 0.085 J m^{-2}, gives the recommended equation for the surface tension of liquid UO$_2$, Eq. (1). This equation, recommended by Hall et al.,[1] is also recommended in the assessment by Harding et al.[9]

Surface Energy of Solid UO$_2$ - The experimental data have been most recently reviewed by Hall et al.[1] The variations between the published data are much larger than the published error bars. The large variations in the data have been attributed to stoichiometry variations and to errors in the measurements of the angles (contact angle, grain boundary groove angle, and dihedral angle) from which the surface energy is calculated. Hall et al.[1] commented that the error in the dihedral angle dominates the uncertainty.

Surface energies obtained from multi-phase equilibration studies have been reported by Hodkin and Nicholas[10] (Cu on UO$_2$), by Nikolopoulos, Nazare and Thummler[11] (Ni on UO$_2$), and by Bratton and Beck[12] (Ni on UO$_2$). Hodkin and Nicholas[13] used sessile drop measurements of Cu-Th alloys on UO$_{2\pm x}$ to study the effect of stoichiometry. Published data from these studies, shown in Figure 5.1, illustrate the large variation in the available data. Figure 5.1 includes the two

bounding lines and the mean line defined by Hall et al.[1] (Hall Line 1, Hall Line 2, and Hall Mean), which are given in Eqs. (2-4), as well as estimates at the melting point. Eberhart[14] used the surface tension of liquid UO_2 to estimate the solid surface energy at the melting point as 0.56 ± 0.09 J m^{-2}. Deshpande, Desai, and Solomon[15] report the surface tension at the melting point as 0.805 ± 0.06 J m^{-2} based on an estimate made by Skapski.[16] Hall et al. commented that both estimation methods are more appropriate for metals than for UO_2 and, in the absence of a theoretical critique, used an average of the two values (0.68 ± 0.06 J m^{-2}) in their assessment. Hertzian indentation studies reported by Matzke et al.[17-19] gave surface energies at room temperature as a function of O:M ratio. Their published values have been included in Figure 5.1.

Hall et al.[1] have analyzed the various individual parameters that go into the calculations for the surface energies and tried to estimate best values of each. This analysis has the effect of smoothing out each parameter. Figure 5.2 shows the surface energies published by Hodkin and Nicholas, Nikolopoulos et al., Bratton and Beck, and Matzke et al., and the recalculated values obtained by Hall et al. Note that this re-analysis by Hall et al. has reversed the slope of the data of Nikolopoulos et al. and increased the magnitude of the slope of the data by Hodkin and Nicholas. Hall et al. stated that indentation results tend to be high because there is often plastic deformation rather than the elastic behavior assumed in the model. Indentation measurements on ThO_2 showed that the surface energy was reduced by 35% if the sample had been preheated so that the oxygen becomes mobile.[17] Assuming a similar effect in UO_2 would reduce the surface energy from 1.8 ± 0.3 J m^{-2} to 1.2 ± 0.3 J m^{-2}. In their re-analysis, Hall et al. applied this correction to the indentation data, as shown in Figure 5.2.

The re-analyzed data given by Hall et al. with estimated error bars are shown in Figure 5.3. They commented that the mean value they assumed for the surface energy at the melting point could be in considerable error and the room temperature surface energy for stoichiometric UO_2 is very dependent on the assumed 35% correction for relaxation. They stated that their analysis supports the conclusion made by Fink et al.[8] that, in view of the scatter in the measurements, there is no clear indication of the temperature dependence within the solid phase. However, their analysis indicates that the surface energy of $UO_{2.00}$ is likely to lie in a wedge defined by the two lines given in Eq. (2) and Eq. (3) and shown as dashed lines in Figure 5.3. Since some of the data, both before and after

re-analysis, lie outside this wedge, this recommendation has been made with great reserve. The best values would be expected to lie in the band between these two lines. The mean line in this band is given by Eq. (4) and is shown as a solid line in Figure 5.3.

Hall et al. also assessed the available data on the variation of surface energy with stoichiometry to obtain Eq. (5). For x > 0.05, the dependence is more pronounced than given by Eq. (5).

The ratio of the grain boundary energy to surface energy on the free surface is a function of the grain boundary groove angle only and is therefore better known than the grain boundary energy. Hall et al. define this ratio as

$$\frac{\gamma_{GB}}{\gamma_{SV}} = 0.58 \pm 0.05 \tag{7}$$

where γ_{GB} is the grain boundary energy and γ_{SV} is the surface energy. This relation is assumed by Hall et al.[1] to be correct over the entire temperature range of solid UO_2. Because the error in the surface energy is so large, $\pm 70\%$, the uncertainty in the grain boundary energy calculated from this relation is also large.

Hall et al. discussed pore geometry and defined an empirical surface energy of pores, γ_P, which they related to the grain boundary surface energy γ_{GB} by

$$\frac{\gamma_{GB}}{\gamma_P} = 1.40 \pm 0.02 \tag{8}$$

Substitution of Eq. (7) into Eq. (8) gives the relation of the surface energy of pores and the surface energy of UO_2 given in Eq. (6).

Further experimental measurements are needed to determine more accurate values of these quantities. To reduce the uncertainty in the surface tension of liquid UO_2, measurements are needed under controlled conditions. To obtain better data for the solid surface energy using the multi-phase

equilibration technique, methods must be developed for greater accuracy in the measurements of the angles, which now have errors on the order of 3°. Surface energy values accurate to $\pm 10\%$ require that the dihedral angle must be reproducible to 0.05°.

REFERENCES

1. R. O. A. Hall, M. J. Mortimer, and D. A. Mortimer, *Surface Energy Measurements on UO₂, A Critical Review,* J. Nucl. Mater. **148**, 237-256 (1987); see also *A. Critical Review of the Surface Energy of UO₂,* J. Less-Common Metals **121**, 341-345 (1986);and R. O. A. Hall and M. J. Mortimer, *Effect of Changes in Stoichiometry on the Surface Energy of UO₂,* J. Nucl. Mater. **137**, 77-85 (1985).

2. H. Schins, *On the Surface Tension of Liquid UO₂,* J. Nucl. Mater. **78**, 215-216 (1978).

3. J. A. Christensen, Battelle-Northwest Laboratory Report, Richland, WA, **BNWL-SA-588884-A** (1966).

4. J. L. Bates, C. E. McNeilly and J. J. Rasmussen, Material Science Research **5**, 11 (1971); see also Battelle-Northwest Laboratory Report **BNWL-SA-3579** (1970).

5. O. Nikolopoulos and B. Schulz, *Density, Thermal Expansion of Stainless Steel and Interfacial Properties of UO₂ - Stainless Steel Above 1690 K,* J. Nucl. Mater. **82**, 172-178 (1979).

6. M. G. Chasanov, L. Leibowitz, and S. D. Gabelnick, J. Nucl. Mater. **49**, 129 (1974).

7. R. Furth, Proc. Cambr. Phil. Soc. **37**, 252 (1941) as referenced by O. Nikolopoulos and B. Schulz, J. Nucl. Mater. **82**, 172-178 (1979).

8. J. K. Fink, M. G. Chasanov, and L. Leibowitz, *Thermodynamic Properties of Uranium Dioxide,* Argonne National Laboratory Report **ANL-CEN-RSD-80-3** (1981).

9. J. H. Harding, D. G. Martin, and P. E. Potter, *Thermophysical and Thermochemical Properties of Fast Reactor Materials,* Commission of the European Communities Report **EUR 12402 EN** (1989).

10. E. N. Hodkin and M. G. Nicholas, *The Surface and Interfacial Energies of Stoichiometric Uranium Dioxide,* J. Nucl. Mater. **47**, 23 (1973).

11. P. Nikolopoulos, S. Nazare, and F. Thummler, *Surface Grain Boundary and Interfacial Energies in UO₂ and UO₂-Ni,* J. Nucl. Mater. **71**, 89-94 (1977); see also *Comments on "Surface Grain Boundary and Interfacial Energies in UO₂ and UO₂-Ni,"* J. Nucl. Mater. **78**, 213-214 (1978).

12. R. J. Bratton and C. W. Beck, *Surface Energy of Uranium Dioxide,* J. Am. Ceram. Soc. **54**, 379-381 (1971).

13.   E. N. Hodkin and M. G. Nicholas, *Surface and Interfacial Properties of Non-Stoichiometric Uranium Dioxide,* J. Nucl. Mater. **67**, 171-180 (1977); see also *Comments on "Surface Grain Boundary and Interfacial Energies in UO$_2$ and UO$_2$-Ni" by P. Nikolopoulos et al.,* J. Nucl. Mater. **74**, 178 (1978);

14.   J. G. Eberhart, J. Nucl. Mater. **25**, 103 (1968).

15.   M. S. Deshpande, P. D. Desai, and A. Solomon, High Temp. Sci. **17** 303 (1984).

16.   A. S. Skapski, Acta Metall. **4** 576 (1956), as referenced by R. O. A. Hall, M. J. Mortimer, and D. A. Mortimer, J. Nucl. Mater. **148**, 237-256 (1987).

17.   H. Matzke, T. Inoue, and R. Warren, *The Surface Energy of UO$_2$ as Determined by Hertzian Indentation,* J. Nucl. Mater. **91**, 205-220 (1980).

18.   H. Matzke, J. Mater. Sci. **15**, 739 (1980).

19.   H. Matzke, *The Fracture Surface energy of $(U_{0.8} Pu_{0.2})O_2$,* J. Nucl. Mater. **113**, 273-275 (1983).

11/96

Figure 5.1 Comparison of Published Data on Surface Energy of Solid UO$_2$

Send Comments to:
jkfink@anl.gov

Version 0 for Peer Review
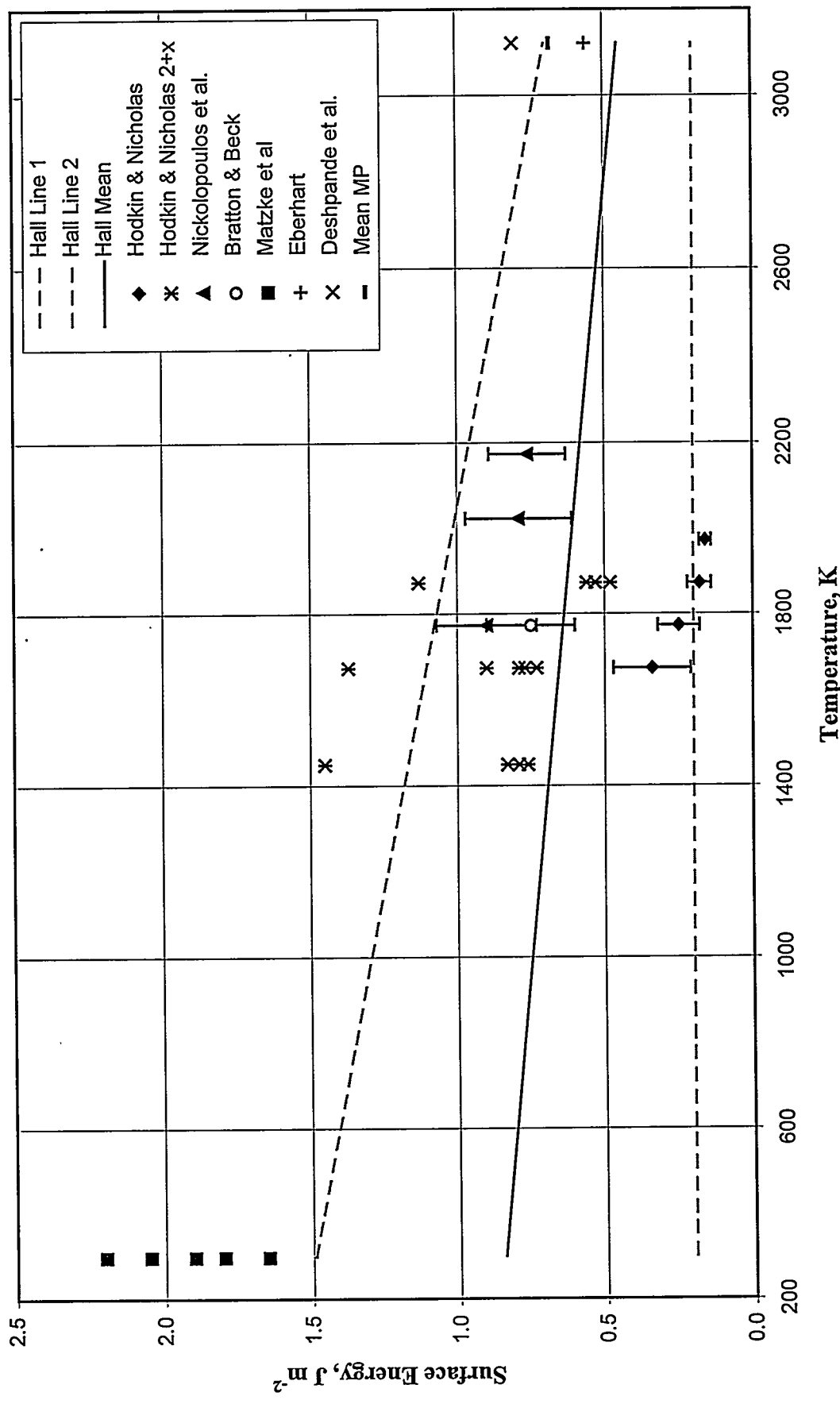
Figure 5.2 Corrections by Hall et al. to UO₂ Surface Energy Data
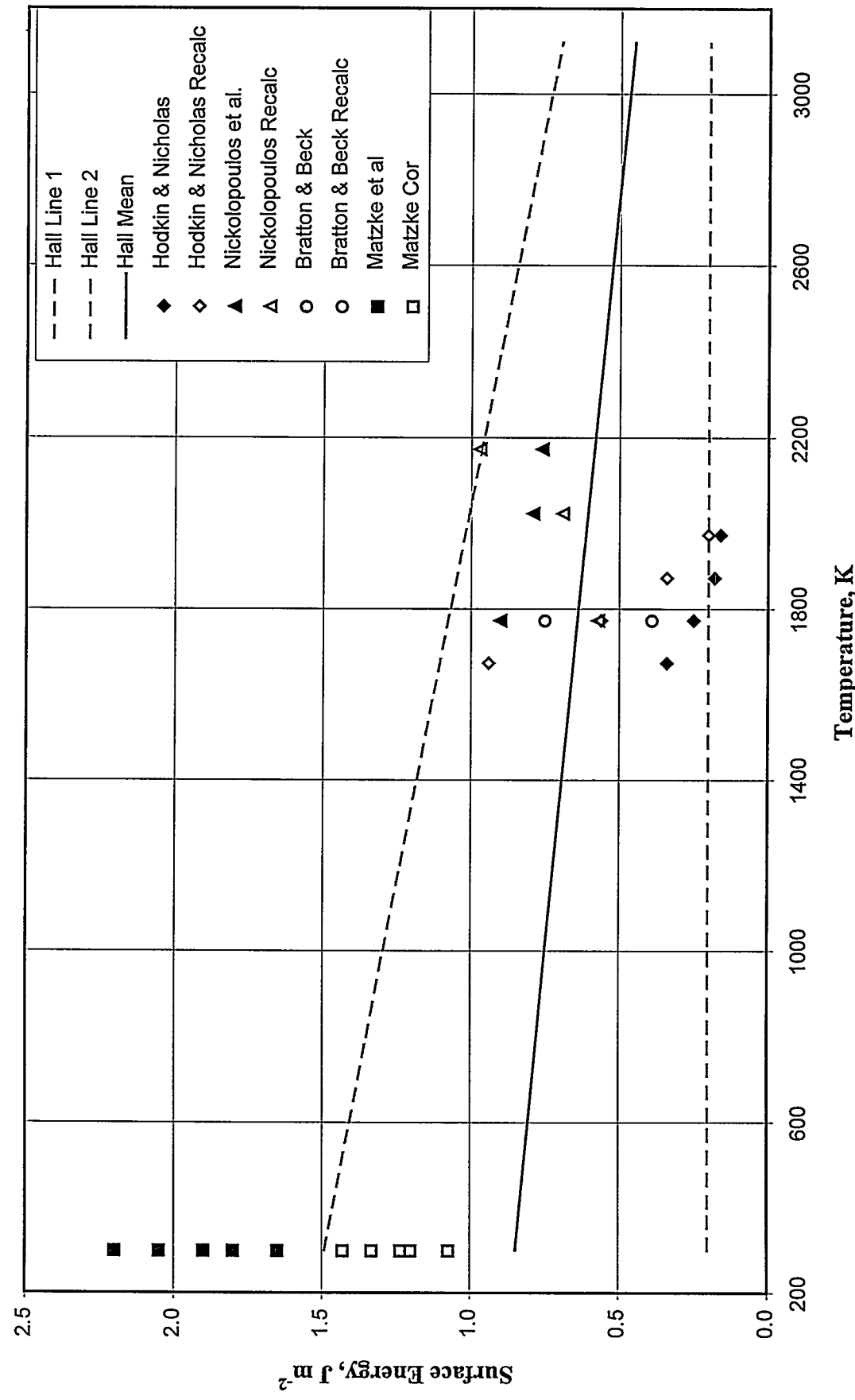
Figure 5.3 Surface Energy of Solid UO$_2$ of Hall et al. and Corrected Data
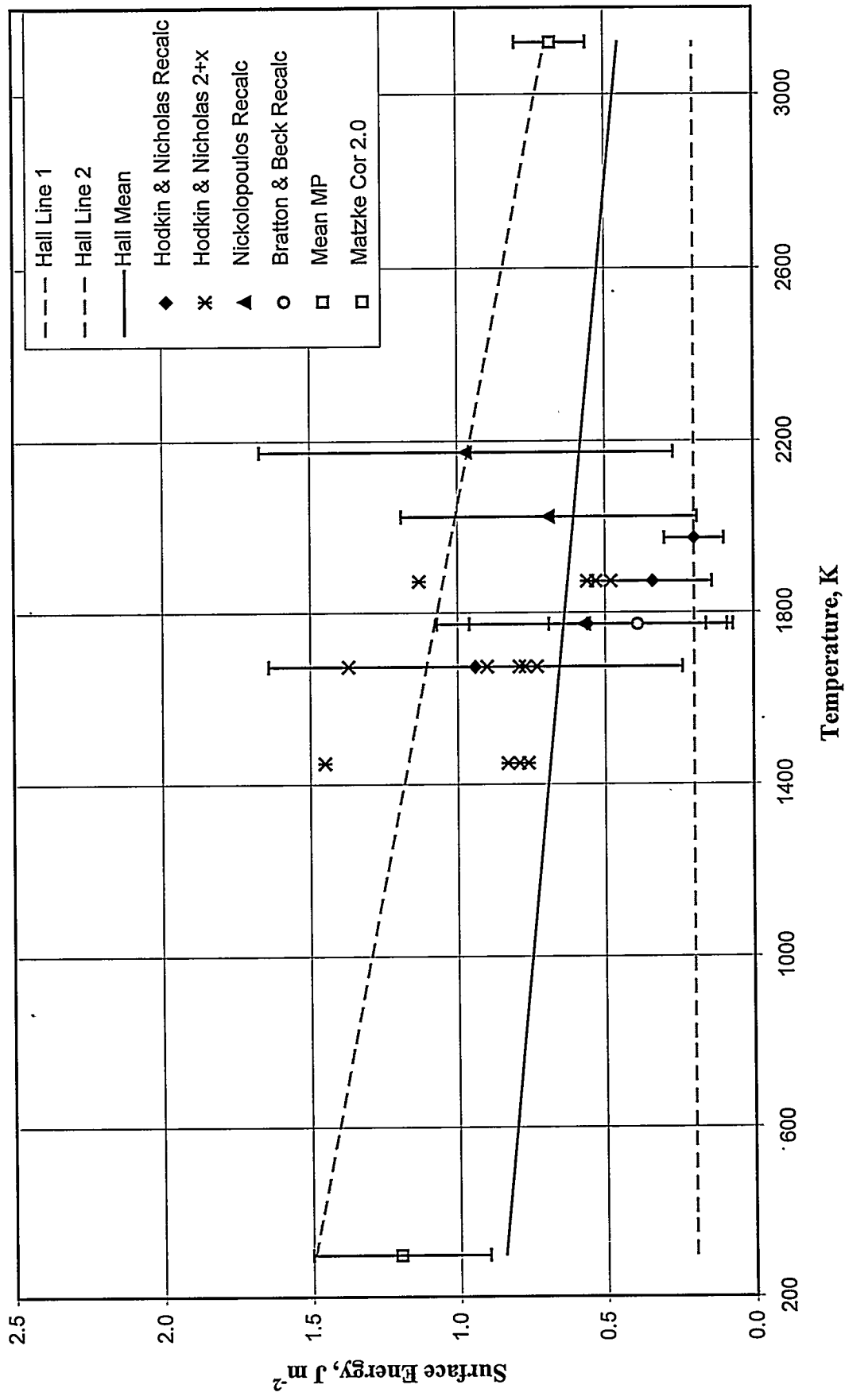
6. VAPOR PRESSURE OF URANIUM DIOXIDE

<u>Summary of Recommendations</u>

Vapor Pressure over Liquid UO_2 - The recommended equation for the total vapor pressure

$$\log_{10} P = -\frac{31284}{T} + 7.616 \tag{3}$$

The vapor pressure of $UO_2(g)$ calculated using the equation of Ackermann et al.[2] and the total vapor pressure over $UO_2(s)$ calculated using the equation of Tetenbaum and Hunt[4] are tabulated as a function of temperature in Table 6.2 and shown with estimated uncertainties in Figure 6.2.

Uncertainties

The estimated uncertainties in total vapor pressure over liquid UO_2 calculated from Eq. (1) range from -40%/+60% at 3120 K to -45%/+80% at 6000 K. From 3120 to 6000 K, the negative uncertainties are assumed to decrease linearly: $\Delta P/P \ (\%) = -[34.58 + 1.7 \times 10^{-3} T]$. The positive uncertainties are assumed to increase linearly from +60% at 3120 K to +80% at 4500 K: $\Delta P/P \ (\%) = 14.78 + 0.0145 T$. Above 4500 K, the positive uncertainties are assumed constant (+80%). The uncertainties in the pressure of $UO_2 \ (g)$ over solid UO_2 calculated from Eq. (2) and in the total vapor pressure over solid UO_2 calculated using Eq. (3) are estimated as -40%/+60% from 1700 to 3120 K.

Stoichiometry

Uranium dioxide can exist over a wide range of compositions (hypostoichiometric to hyperstoichiometric with respect to oxygen), which are temperature dependent. The total vapor pressure depends on the oxygen-to-uranium ratio of the condensed phase, so that the total vapor pressure over $UO_{2\pm x}$ will depend on the value of x. The vaporization of UO_2 is not congruent because the O:U ratio in the gas phase is greater than in the condensed phase. The total vapor pressure above solid and liquid UO_2 includes contributions from $UO_2(g)$, $UO(g)$, $UO_3(g)$, $U(g)$, $O(g)$, and $UO(g)$.

Discussion: Vapor Pressure over Liquid UO_2

Breitung and Reil[1] have recently reviewed the experimental measurements of the total vapor pressure of liquid UO_2. The data used in their assessment are summarized in Table 6.3. They included both pressure-temperature measurements and pressure-enthalpy measurements in their assessment.

Pressure-Temperature Measurements - The transpiration measurements of Reedy and Chasanov[5] were weighted high in the assessment of Breitung and Reil[1] for the following reasons: (1) they are the only measurements on both solid and liquid UO_2, (2) the technique produces true equilibrium data, and (3) the experimental uncertainties are very small (± 10% in pressure; ± 1% in temperature). In these experiments, the UO_2 was contained in tungsten, which limited the temperature range (2615 - 3390 K). At 2615 and 2860 K, the O:U ratio of the condensed phase was 1.98. At 3390 K, the O:U ratio of the liquid was 1.94.

The laser-heated vapor pressure measurements listed in Table 6.3 may be divided into two groups: (1) measurements performed far from thermodynamic equilibrium[6-13] and (2) measurements close to thermodynamic equilibrium.[14,15] Measurements far from thermodynamic equilibrium consist of experiments in which the fuel vapor expands into a vacuum or a rare gas environment. Such experiments require a theoretical model to convert properties of the expanding nonequilibrium plasma into saturation vapor pressures. The large scatter in the data from different experiments of this type is indicative of the difficulty of obtaining saturation vapor pressure data from these nonequilibrium measurements. Measurements close to equilibrium use a boiling point technique that determines the temperature at which a laser-generated UO_2 vapor cloud begins to expand against a xenon cover gas of a given pressure. At this temperature, the UO_2 vapor pressure is assumed to be equal to the gas pressure. The xenon gas atoms initially confine the laser-generated vapor cloud so that evaporation proceeds close to thermodynamic equilibrium. The recent boiling-point experiments by Bober and Singer[15] included corrections for optical absorption (by the vapor cloud) of thermal radiation emitted from the liquid surface. Breitung and Reil concluded that the recent measurements by Bober and Singer are the most reliable saturation vapor pressure data for liquid UO_2 from the laser experiments.

In-Reactor Experiments - The first in-reactor measurements of vapor pressure as a function of adiabatic fuel enthalpy by Reil[16] determined upper and lower bounds for the vapor pressure. Later calculations showed that these values were overly conservative.[1] Benson[17] measured the isobaric expansion of a 25-μm-thick layer of UO_2 powder confined by two movable pistons as it was heated to a certain internal energy in one microsecond. Results of this experiment were inconsistent with the expansion of a single-component liquid-vapor system. An unknown source of pressure, such as

water vapor, adsorbed by the fine UO_2 powder is believed to have contributed to the measured pressure. Fission heating was used in the eight Commissariat a l'Energie Atomique (CEA) experiments by Limon et al.[18] to heat a thin solid UO_2 disk to boiling under constant argon pressure. The boiling point was determined by the sudden increase in pressure. The average energy deposited in the UO_2 was assumed to be equal to the fuel enthalpy in the boiling zone. This assumption led to deviations of only a few percent in six high-enthalpy tests but the actual enthalpy in the boiling zone may have been on the order of 10% higher for the two low-enthalpy tests.[1]

Breitung and Reil[1] measured the saturation vapor pressure of pure $UO_{2.01}$, reactor grade $UO_{2.08}$, and reactor grade $(U_{0.77} Pu_{0.23})O_{2.09}$ as a function of enthalpy for enthalpies from 2000 to 3700 kJ kg^{-1}. Their six effective equation-of-state experiments at the annular core research reactor at Sandia National Laboratories determined the saturation vapor pressure as a function of enthalpy at conditions that are very close to those of the disassembly phase of a core disruptive accident. These experiments gave very reproducible results. They found that under these conditions

(1)   the fuel saturation vapor pressure for fuel containing uranium-plutonium mixed oxide was essentially identical to that of pure UO_2;

(2)   fuel impurities from fabrication did not noticeably contribute to the pressure;

(3)   stoichiometry variations have no strong influence on the saturation vapor pressure for $UO_{2.01}$, and $UO_{2.08}$;

(4)   replacement of uranium by plutonium in concentrations equivalent to mixed oxide fuel, e.g., $(U_{0.77} Pu_{0.23})O_{2.09}$, does not significantly affect the measured vapor pressure.

From the data obtained in these six experiments, Breitung and Reil developed an equation for the vapor pressure for all three fuels:

$$\log_{10}P(z) = -9.7652 + 8.0934 \times 10^{-3}z - 2.0515 \times 10^{-6}z^2 + 1.9013 \times 10^{-10}z^3 \qquad (4)$$

where $z = h - h_{298}$ is the enthalpy increment in kJ kg^{-1} and P is the saturation pressure in MPa. This equation fits their data for all three fuel types within their experimental uncertainties of ± 0.5 MPa in pressure and $\pm 3\%$ in enthalpy. Breitung and Reil[1] converted their pressure-enthalpy equation to

a pressure-temperature equation, Eq. (1), using Fischer's[20] theoretical prediction for the saturation pressure as a function of internal energy of liquid UO_2 and the melting point enthalpy given by Fink et al.[21] (1398.6 kJ/kg). Their equation for pressure as a function of temperature, Eq. (1), is slightly different from an earlier equation given by Breitung and Reil[22, 23] (which was recommended by Harding et al.[24]) because different equations were used to convert from pressure-enthalpy to pressure-temperature. Breitung and Reil[1] stated that the main uncertainty in the conversion is the choice of equation for the heat capacity. The large variations in the available equations for the heat capacity of liquid UO_2 are shown in Figure 6.3. The data in Figure 6.3 are those determined by Ronchi et al.[25] from their cooling curve experiments. In the analysis of these experiments, Ronchi et al. assumed a constant thermal conductivity of 2.5 W m^{-1} K^{-1}. The solid line is the fit by Ronchi et al.[25] to their data. The dashed line labeled "H+Cp Fit Fink" is a combined fit to the enthalpy data[26, 27] and the heat capacity data of Ronchi et al.[25] from 3100 to 4500 K. The line labeled "Rand et al." is the constant heat capacity obtained from the linear fit by Rand et al.[28] to the enthalpy data.[26, 27] The heat capacities of Fischer[20] were preferred by Breitung and Reil to the equation they used previously (labeled "Breitung and Reil KfK 3939") because the model used by Fischer was anchored at experimental results for the vapor pressure and density of liquid UO_2. Figure 6.1.3 shows that values from both equations used by Breitung and Reil are high relative to the values given by Ronchi et al.[25] Harding et al.[24] have pointed out that the heat capacity may be varied without significant effect on the vapor pressure at a given temperature. They stated that a 20% variation in heat capacity at 6000 K gives a 30% change in the vapor pressure.

Comparison of Recommended Equation with Data - In Figure 6.4, the recommended equation of Breitung and Reil for the total vapor pressure over liquid UO_2 is compared with the most recent and reliable vapor pressure data from each experimental method, with the equation formulated by the 1978 IAEA International Working Group on Fast Reactors (IWGFR),[29] and with vapor pressures calculated by Green and Leibowitz.[3] The IWGFR equation was based on a review of the data available in 1978 and was recommended for use up to 5000 K. The vapor pressures and vapor compositions above uranium dioxide calculated by Green and Leibowitz[3] are based on a statistical-mechanical calculation of the thermodynamic functions of the individual vapor species using molecular energy levels from spectroscopic data and an oxygen potential model. Experimental data

included in Figure 6.4 are: transpiration data of Reedy and Chasanov,[5] the boiling-point data of Bober and Singer,[15] data from the most recent laser-heating vaporization experiments of Ohse et al.,[12, 13] and data from the in-pile experiments of Limon et al.[18] The equation recommended by Limon et al. to best describe their data has also been included. Breitung and Reil's earlier vapor pressure equation that was obtained by using a different heat capacity[22,23] to convert their data has been included in Figure 6.4 to show the effect of differences in choice of heat capacity on the final vapor pressure equation. It is labeled "Breitung KfK3939." Figure 6.4 shows that at high temperatures, it gives lower pressures than the recommended equation of Breitung and Reil. Therefore, the recommended equation is in better agreement with the high-temperature data of Limon et al.

The IWGFR equation is consistent with the total pressures calculated by Green and Leibowitz[3] and with the early laser-vaporization data, which were higher than the 1980 data of Ohse et al.[12.] The datum at 4220 K from the 1980 measurements of Ohse et al.[12] is a factor of 3.3 higher than the vapor pressure at 4220 K calculated using the recommended equation of Breitung and Reil.[1] At 4000 K, vapor pressures obtained from the IWGFR equation and calculations by Green and Leibowitz[3] are, respectively, factors of 2.1 and 1.6 higher than the vapor pressure calculated with the equation of Breitung and Reil.[1] The recommended equation of Breitung and Reil is in good agreement with the vapor pressures determined from laser-vaporization experiments in 1985 by Ohse et al.,[13] with the low-temperature data of Reedy and Chasanov,[5] with the high-temperature data of Limon et al.,[18] and with the data of Bober and Singer.[15] It is a good representation of all equilibrium in-pile and out-of-pile data.

Breitung and Reil[1] noted that if the two low-temperature CEA data points of Limon et al.[18] are disregarded, all in-pile results are located close to an almost linear extension of the transpiration data of Reedy and Chasanov[5] and the laser boiling point data of Bober and Singer.[15] All these methods provide conditions very close to equilibrium vaporization so that the slope of the line connecting these data should give the heat of vaporization. They attributed the steeper slopes obtained from the earlier laser-vaporization experiments (as characterized by the 1980 data of Ohse et al.) to the use of nonequilibrium pressure models to reduce the data and/or to the neglect of

optical absorption of thermal surface radiation in the vapor cloud. Application of the Clausius - Clapeyron equation to their vapor pressure equation gives an effective heat of vaporization:

$$\Delta H_{vap} = 516382 - 22.946T \qquad (5)$$

where ΔH_{vap} is in J mol^{-1} and T in K ranges from 3120 to 8000 K. The heat of vaporization at the normal boiling point (3815.1 K) is 413.5 kJ mol^{-1}.

Discussion: Vapor Pressure over Solid UO$_2$

Although the total vapor pressure above solid UO_2 includes contributions from $UO_2(g)$, $UO(g)$, $UO_3(g)$, $U(g)$, $O(g)$, and $UO(g)$, the greatest contribution is from $UO_2(g)$. Ackermann et al.[2] measured the vapor pressure of $UO_2(g)$ above solid UO_2 from 1800 to 2600 K and commented that $UO_2(g)$ comprises 94% of the total pressure at 2150 K. Tetenbaum and Hunt[4] determined the total vapor pressure above UO_{2-x} in the temperature range 2080 to 2705 K. Green and Leibowitz[3] used models for the partial Gibbs free energy of oxygen above UO_2 to determine the contributions of the various vapor species above hypostoichioeteric uranium dioxide for $UO_{2.00}$ through $UO_{1.90}$.

Measurements of the total vapor pressure above solid UO_2 by Knudson effusion,[30-33] Langmuir surface evaporation,[35] and transpiration[4,36] methods and have been reviewed by Ackermann et al.[2] and compared with measurements of the vapor pressure due to $UO_2(g)$ determined from mass-spectrometric measurements by Pattoret et al.[37] and by Ackermann et al.[2] They found reasonable agreement between the different measurements. Table 6.4 shows the vapor pressures at 2150 K determined from the experiments included in the assessment by Ackermann et al.[2] Ackermann et al. corrected the data of Alexander et al.[36] for a systematic error. Consequently, the vapor pressure attributed to Alexander et al. in Table 6.4. (which is from the table of Ackermann et al.[2]) differs from the value given in the original paper by Alexander et al.[36] The average of the values, excluding the value from the 1979 mass spectroscopy measurements by Ackermann et al.,[2] is 1.38 x 10^{-7} MPa. This is in good agreement with the vapor pressure of $UO_2(g)$ (1.32 x 10^{-7} MPa) determined by Ackermann et al. in 1979.

The recommended equation for the vapor pressure of $UO_2(g)$ over UO_2, Eq. (2), is from the 1979 measurements and assessment of Ackermann et al.[2] It is in reasonable agreement with other data and was derived with considerations for consistency with the thermodynamic functions for solid

UO_2 and the enthalpy of sublimation from the solid. It is consistent with a heat capacity that has a phase transition at 2670 K. In Figure 6.5, this recommended equation of Ackermann et al.[2] for the vapor pressure of $UO_2(g)$ over solid UO_2 is compared with vapor pressure equations and data from earlier measurements and with the vapor pressure of $UO_2(g)$ and the total vapor pressure over $UO_{2.00}$ calculated by Green and Leibowitz.[3] In the legend for Figure 6.5, the notation "UO_2" has been included to distinguish measurements or calculations of the pressure due to the vapor species $UO_2(g)$ from the total vapor pressure over UO_2. Below 2450 K, the 1956 low-temperature data of Ackermann et al.[30] and the equation of Tetenbaum and Hunt[4] are in excellent agreement with the recommended equation of Ackermann et al.[2] Above 2615 K, the equation of Tetenbaum and Hunt for the total vapor pressure over UO_2 gives higher vapor pressures than the equation of Ackermann et al. for the vapor pressure of $UO_2(g)$. Two data from transpiration measurements of the total vapor pressure over $UO_{1.98}$ by Reedy and Chasanov[5] have been included in Figure 6.5. These are the only vapor pressure measurements over uranium dioxide in both the liquid and solid phases. The Reedy and Chasanov datum at 2615 K is in good agreement with the equation of Ackermann et al. but their datum at 2860 K is higher than values from both the equation of Ackermann et al. and the equation of Tetenbaum and Hunt. Total vapor pressures over UO_2 measured by Ohse et al.[32] are in good agreement with the equation of Ackermann et al. at low temperatures but are higher at high temperatures. Above 2500 K, the data of Ohse et al. approach total pressures calculated by Green and Leibowitz. The contribution to the total vapor pressure from $UO_2(g)$ calculated by Green and Leibowitz is in good agreement with the equation of Ackermann et al.[2] above 2600 K. However, the total vapor pressure over UO_2 calculated by Green and Leibowitz is consistently higher than the $UO_2(g)$ pressure given by the equation of Ackermann et al. The difference between these values increases with temperature. The contribution to the total vapor pressure from $UO_2(g)$ calculated by Green and Leibowitz descreases with increasing temperature. It is 70% at 2100 K, 54% at 2500 K, and only 37% at 3100 K. These comparisons indicate that the equation for the vapor pressure of $UO_2(g)$ over solid UO_2 is a reasonable approximation of the total vapor pressure over solid UO_2 up to 2600 K but not at higher temperatures. At higher temperatures, extrapolation of the equation of Tetenbaum and Hunt [Eq. (3)] is a better approximation to the total vapor pressure over solid UO_2.

The logarithm to the base 10 of the vapor pressures determined from a number of vapor pressure equations near the solid/liquid phase boundary are compared in Figure 6.6. Equations included in Figure 6.6 are: the 1978 IWGFR equation[29] for the vapor pressure over liquid UO_2, the equation of Breitung and Reil[2] for the vapor pressure over liquid UO_2, the equation of Ackermann et al. for the vapor pressure of $UO_2(g)$ over solid UO_2, the equation of Tetenbaum and Hunt[4] for the total vapor pressure over solid UO_2, and a modified equation of Tetenbaum and Hunt.[21] The equation of Tetenbaum and Hunt was modified by Fink, Leibowitz, and Chasanov[21] for continuity at the solid/liquid interface with the IWGFR equation[29] for the vapor pressure over liquid urania. The logarithms of the total vapor pressures over UO_2 calculated by Green and Leibowitz[3] are also shown in Figure 6.6. The total vapor pressure data of Reedy and Chasanov[5] that spans this temperature range and the 1985 liquid vapor pressure data of Ohse et al.[13] have also been included in the figure. Harding et al.[24] have recommended the equation of Ackermann et al.[2] as an approximation to the total vapor pressure over solid UO_2 up to the melting point. However, Figure 6 shows that extrapolation of the equation of Ackermann et al. to the melting point gives vapor pressures that are lower than the experimental data and 47% lower than the liquid vapor pressures at the melting point calculated from the equation of Breitung and Reil. Extrapolation of the equation of Tetenbaum and Hunt[4] into the liquid region gives vapor pressures that are consistent with the vapor pressures over the liquid determined in 1985 by Ohse et al.[13] but the vapor pressure at the melting point calculated with this extrapolated equation is 17% lower than that calculated using the equation of Breitung and Reil. The modified equation of Tetenbaum and Hunt[21] is consistent with the IWGFR equation and with the data of Reedy and Chasanov but the vapor pressure at the melting point calculated with this modified equation is 19% higher than the vapor pressure calculated with the equation of Breitung and Reil. Thus, the deviations from the equation of Breitung and Reil by the original equation of Tetenbaum and Hunt[4] and the modified equation of Tetenbaum and Hunt[21] are similar in magnitude but opposite in sign. The original equation of Tetenbaum and Hunt[4] is preferred to the modified equation of Tetenbaum and Hunt[21] because the original equation of Tetenbaum and Hunt was based on experimental data and it agrees better with the low-temperature vapor pressure data over solid UO_2 and with the equation of Ackermann et al. below 2450 K.

REFERENCES

1.   W. Breitung, and K. O. Reil, *Vapor Pressure Measurements on Liquid Uranium Oxide and (U,Pu) Mixed Oxide,* Nucl. Sci. Eng. **101**, 26-40 (1989).

2.   R. J. Ackermann, E. G. Rauh, and M. H. Rand, *A Re-Determination and Re-Assessment of the Thermodynamics of Sublimation of Uranium Dioxide,* Symp. on Thermodynamics of Nuclear Materials Julich 1979, Vol.1, IAEA, pp.11-27, Vienna (1980).

3.   D. W. Green and L. Leibowitz, *Vapor Pressures and Vapor Compositions in Equilibrium with Hypostoichiometric Uranium Dioxide at High Temperatures,* Argonne National Laboratory Report **ANL-CEN-RSD-81-1** (June 1981); also J. Nucl. Mater. **105**, 94 (1982).

4.   M. Tetenbaum and P. D. Hunt, *Total Pressure of Uranium-Bearing Species over Oxygen-Deficient Urania,* J. Nucl. Mater. **34**, 86-91 (1970).

5.   G. T. Reedy and M. G. Chasanov, *Total Pressure of Uranium-Bearing Species over Molten Urania,* J. Nucl. Mater. **42** 341-344 (1972).

6.   M. Bober, H. U. Karow, and K. Schretzmann, *Evaporation Experiments to Determine the Vapor Pressure of UO2 Fuel (3000 -5000 K),* IAEA Symp. on Thermodynamics of Nuclear Materials, Vol. 1, 295 (1975); Nucl. Technol. **26**, 237 (1975).

7.   M. Bober, W. Breitung, H. U. Karow, and K. Schretzmann, *Evaporation Studies of Liquid Oxide Fuel at Very High Temperatures Using Laser Beam Heating,* **KFK-2366**, Kernforschungszentrum Karlsruhe (1976).

8.   R. W. Ohse, P. G. Berrie, H. G. Bogensberger, and E. A. Fischer, Thermodyn. Nucl. Mater. **1**, 307 (1975).

9.   J. F. Babelot, G. D. Brumme, P. R. Kinsman, and R. W. Ohse, Atomwirtsch. Atomtech., **12**, 387 (1977), as referenced by W. Breitung, and K. O. Reil,, Nucl. Sci. Eng. **101**, 26-40 (1989).

10.   H. C. Tsai, A. Convington, and D. R. Olander, *Laser Vaporization of UO$_2$,* in *Materials and Molecular Research Division Annual Report* **LBL-6016**, Lawrence Berkeley Laboratory, University of California, Berkeley (1976).

11.   M. Bober, W. Breitung, and H. U. Karow, *Thermodynamic Calculation and Experimental Determination of the Equation of State of Oxide Fuels up to 5000 K,* **KFK-2689**, Kernforschungszentrum Karlsruhe (1978).

12.   R. W. Ohse, J. F. Babelot, A. Frezzotti, K. A. Long, and J. Magill, *Equation of State of Uranium Oxide: Mach-disk Investigation of Transient Laser-induced Vaporization of UO$_2$ up to 5000 K,* High Temp.-High Pressures **12**, 537 (1980).

13.   R. W. Ohse, J. F. Babelot, C. Cercignani, J. P. Hiernaut, M. Hoch, G. J. Hyland, and J. Magill, J. Nucl. Mater. **130**, 165 (1985).

14.   M. Bober and M. Trapp, *Bestimmung des Dampfdrucks von flussigem Uranoxid mittels Laseraufheizung,* Kernforschungszentrum Karlsruhe (unpublished), as referenced by W. Breitung, and K. O. Reil,, Nucl. Sci. Eng. **101**, 26-40 (1989).

15.   M. Bober and J. Singer, Nucl. *Vapor Pressure Determination of Liquid UO$_2$ Using a Boiling Point Technique,* Nucl. Sci. Eng. **97**, 344-352 (1987).

16.   K. O. Reil, *Effective Equation of State Measurements on Uranium Dioxide,* Dissertation, University of New Mexico (May 1977), as referenced by W. Breitung, and K. O. Reil, Nucl. Sci. Eng. **101**, 26-40 (1989).

17.   D. A. Benson, *Application of Pulsed Electron Beam Vaporization to Studies of UO$_2$,* **SAND77-0429**, Sandia National Laboratories (1977).

18.   R. Limon, G. Sutren, P. Combetter, and F. Barbry, *Equation of State of Non-Irradiated UO$_2$,* Proc. ENA/ANS Topical Meeting on Reactor Safety Aspects of Fuel Behavior, Sun Valley, Idaho, August 2-6, 1981, Vol. 2, pp. 2-576 to 2-583, CEA-CONF-5816, American Nuclear Society (1981).

19.   S. A. Wright, D. H. Worledge, G. L. Cano, P. K. Mast, and F. Briscoe, *Fuel-Disruption Experiments Under High-Ramp-Rate Heating Conditions,* **SAND81-0413**, Sandia National Laboratories (Oct. 1983).

20.   E. A. Fischer, *Evaluation of the Urania Equation of State Based on Recent Vapour Pressure Measurements,* **KfK- 4084** Kernforschungszentrum Karlsruhe (Sept. 1987).

21.   J. K. Fink, M. G. Chasanov, and L. Leibowitz, *Thermodynamic Properties of Uranium Dioxide,* J. Nucl. Mater. **102**, 17-25 (1981); see also *Thermophysical Properties of Uranium Dioxide*, **ANL-CEN-RSD-80-3**, Argonne National Laboratory (April 1981).

22.   W. Breitung and K. O. Reil, *In-Pile Vapor Pressure Measurements on UO$_2$ and (U,Pu)O$_2$ from 5000 to 8000 K,* Proc. of Conf. on Science and Technology of Fast Reactor Safety, Guernsey, U. K., May 12-16, 1986, p. 501.

23.   W. Breitung and K. O. Reil, *In-Pile Vapor Pressure Measurements on UO$_2$ and (U,Pu)O$_2$,* **KfK-3939** Kernforschungszentrum Karlsruhe (Aug. 1985).

24.   J. H. Harding, D. G. Martin, and P. E. Potter, *Thermophysical and Thermochemical Properties of Fast Reactor Materials,* Commission of the European Communities Report **EUR 12402 EN** (1989).

25.   C. Ronchi, J. P. Hiernaut, R. Selfslag, and G. J. Hyland, *Laboratory Measurement of the Heat Capacity of Urania up to 8000 K: I. Experiment,* Nucl. Sci. Eng. **113**, 1-19 (1993).

26.   L. Leibowitz, M. G. Chasanov, L. W. Mishler, and D. F. Fischer, *Enthalpy of Liquid Uranium Dioxide to 3500 K,* J. Nucl. Mater. **39** 115-116 (1971).

27.   R. A. Hein and P. N. Flagella, *Enthalpy Measurements of UO_2 and Tungsten to 3260 K,* General Electric Report **GEMP-578** (February 16, 1968).

28.   M. H. Rand, R. J. Ackermann, F. Gronvold, F. L. Oetting, and A. Pattoret, *The Thermodynamic Properties of the Urania Phase,* Rev. Int. Hautes Temp. Refract. **15**, 355-365 (1978).

29.   International Working Group on Fast Reactors, Specialists' Meeting on Equations of State of Materials of Relevance to the Analysis of Hypothetical Fast Breeder Reactor Accidents, Harwell, U. K., June 19-23, 1978, **IWGFR/26**, IAEA (1978).

30.   R. J. Ackermann, P. W. Giles, R. H. Thorn, J. Chem. Phys. **25**, 1089 (1956).

31.   V. E. Ivanov, A. A. Kruglykh, V. S. Pavlov, G. P. Kovtin, and V. M. Amonenko, Proc. Symp. On Thermodynamics of Nuclear Materials, Vienna, 1962, IAEA, p. 735, Vienna (1962).

32.   R. W. Ohse, J. Chem. Phys. **44**, 1375 (1966).

33.   Y. A. Gorban, L. V. Pavlinov, and V. N. Vykov, At. Ehnerg. **22**, 465 (1955), as referenced by R. J. Ackermann, E. G. Rauh, and M. H. Rand, *A Re-Determination and Re-Assessment of the Thermodynamics of Sublimation of Uranium Dioxide,* Proc. Symp. on Thermodynamics of Nuclear Materials, Julich, 1979, Vol.1, IAEA, pp.11-27, Vienna (1980).

34.   R. J. Ackermann, E. G. Rauh, and M. S. Chandrasekhariah, J. Phys. Chem. **73**, 762 (1969).

35.   N. M. Voronov, A. S. Danilin, I. T. Kovalev, Symp. on Thermodynamics of Nuclear Materials Vienna 1962, IAEA, p. 789, Vienna (1962).

36.   C. A. Alexander, J. S. Ogden, and G. C. Cunningham, Battelle Memorial Institute Report **BMI-1789** (Jan. 1967), as referenced by R. J. Ackermann, E. G. Rauh, and M. H. Rand, *A Re-Determination and Re-Assessment of the Thermodynamics of Sublimation of Uranium Dioxide,* Proc. Symp. on Thermodynamics of Nuclear Materials, Julich, 1979, Vol. 1, IAEA, pp. 11-27, Vienna (1980).

37.   A. Pattoret, J. Drowart, and J. Smoes, Proc. Symp. Thermodynamics of Nuclear Materials, Vienna 1967, IAEA, p. 613, Vienna (1968).

Table 6.1   Total Vapor Pressure Over Liquid UO$_2$

Temperature, K	Pressure, MPa	Pressure, atm
3120	0.00469	0.0463
3200	0.00720	0.0711
3300	0.0119	0.118
3400	0.0191	0.188
3500	0.0297	0.293
3600	0.0450	0.444
3700	0.0664	0.656
3800	0.0960	0.948
3900	0.136	1.34
4000	0.189	1.86
4100	0.257	2.54
4200	0.346	3.41
4300	0.457	4.51
4400	0.595	5.87
4500	0.765	7.55
4600	0.972	9.60
4700	1.22	12.1
4800	1.52	15.0
4900	1.87	18.4
5000	2.28	22.5
5100	2.75	27.1
5200	3.29	32.5
5300	3.91	38.6
5400	4.62	45.6
5500	5.41	53.4
5600	6.30	62.2
5700	7.29	71.9
5800	8.38	82.7
5900	9.58	94.6
6000	10.91	107.6

Table 6.2   Vapor Pressure Over Solid UO_2 Calculated from Equations
of Ackermann et al. and of Tetenbaum and Hunt

Temperature K	UO₂ Pressure MPa (Ackermann et al.)	Total Pressure MPa (Tetenbaum & Hunt)
1800	2.05×10^{-10}	-
1900	1.67×10^{-09}	-
2000	1.10×10^{-08}	9.42×10^{-09}
2100	5.98×10^{-08}	5.23×10^{-08}
2200	2.77×10^{-07}	2.49×10^{-07}
2300	1.12×10^{-06}	1.03×10^{-06}
2400	3.96×10^{-06}	3.81×10^{-06}
2500	1.26×10^{-05}	1.27×10^{-05}
2600	3.62×10^{-05}	3.83×10^{-05}
2700	9.54×10^{-05}	1.07×10^{-04}
2800	2.31×10^{-04}	2.77×10^{-04}
2900	5.22×10^{-04}	6.74×10^{-04}
3000	1.10×10^{-03}	1.54×10^{-03}
3100	2.17×10^{-03}	3.34×10^{-03}

Table 6.3   Vapor Pressure Measurements Over Liquid UO_2

Experimenter	Method	Year	Reference
	Out-of-Pile Experiments		
Reedy & Chasanov	Transpiration	1972	5
Bober et al.	Laser-heating, expansion into vacuum	1975 1976	6,7
Ohse et al.	Laser-heating, vacuum	1975 1977	8, 9
Tsai et al.	Laser-heating, vacuum	1976	10
Bober, Breitung, & Karow	Laser-heating, vaporization	1978	11
Ohse et al.	Laser-heating, evaporation	1980	12
Ohse et al.	Laser-heating, evaporation	1985	13
Bober & Trapp	Laser-heating in xenon	1984	14
Bober & Singer	Laser-heating in xenon, Boiling point method	1987	15
	In-Pile Experiments		
Reil	Adiabatic enthalpy vs pressure	1977	16
Benson	Isobaric expansion	1977	17
Limon et al.	UO_2 Fission-heated in argon	1981	18
Wright et al.	In-pile fuel disruptive exp'ts	1983	19
Breitung & Reil	Effective equation of state technique	1985-1989	1

Table 6.4   Measurements of the Vapor Pressure of UO_2 at 2150 K

Vapor Pressure at 2150 K, 10^7MPa	Experimenter	Year	Method	Temperature Range, K
1.23	Ackermann et al. [30]	1956	mass effusion	1758 - 2378
1.94	Ivanov et al. [31]	1962	mass effusion	1930 - 2160
0.58	Voronov et al. [35]	1962	Langmuir	1723 - 2573
1.34	Ohse [32]	1966	mass effusion	2200 - 2800
0.93	Alexander et al. [36]	1967	transpiration	2090 - 2900
2.00	Gorban et al. [33]	1967	mass effusion	1873 - 2573
1.83	Pattoret et al. [37]	1968	mass spectroscopy	1890 - 2420
1.18	Tetenbaum & Hunt [4]	1970	transpiration	2080 - 2705
1.32	Ackermann et al. [2]	1979	mass spectroscopy	1813 - 2463

Figure 6.1 Total Vapor Pressure Over Liquid UO$_2$
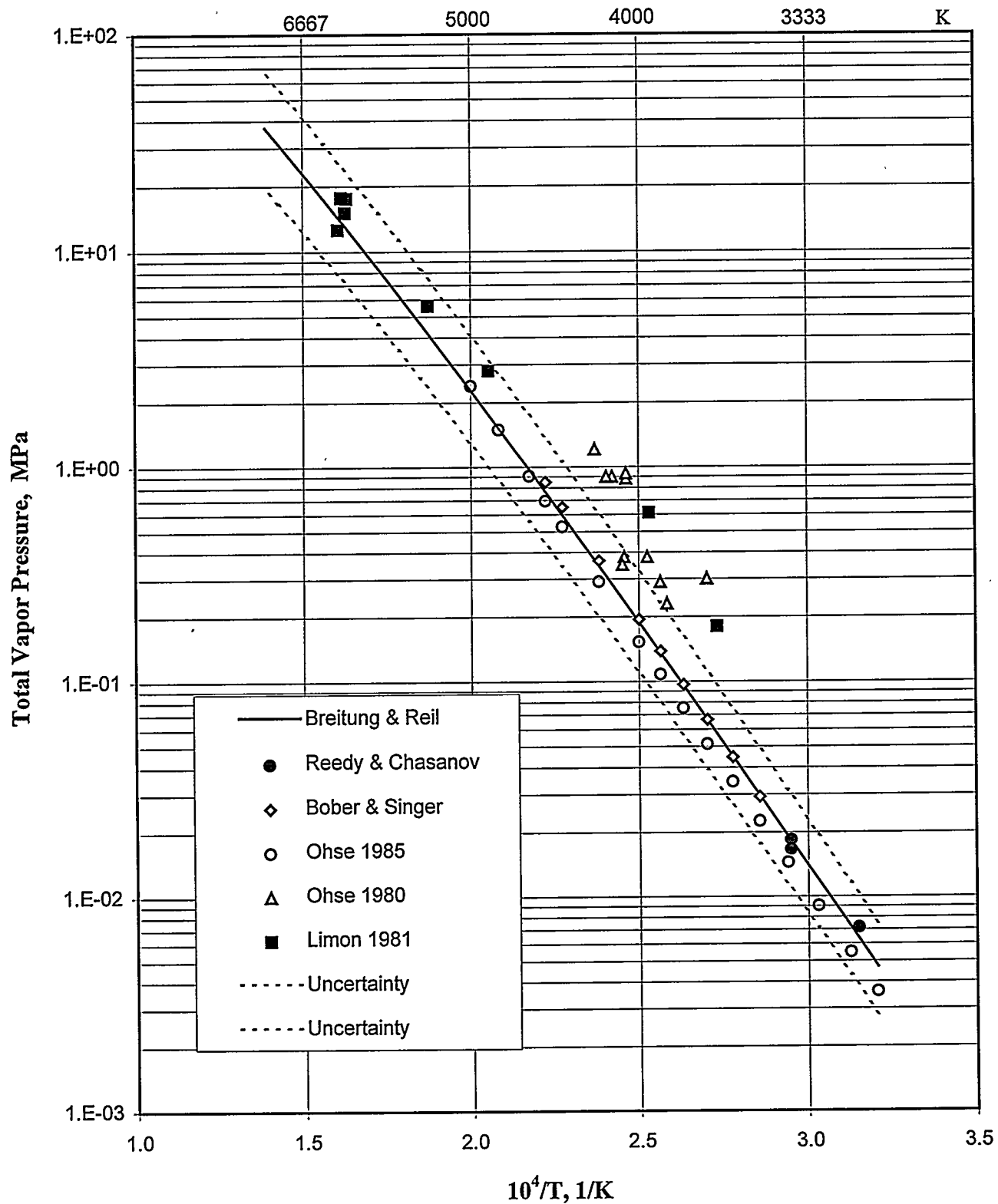
Figure 6.2 Vapor Pressure Over Solid UO$_2$
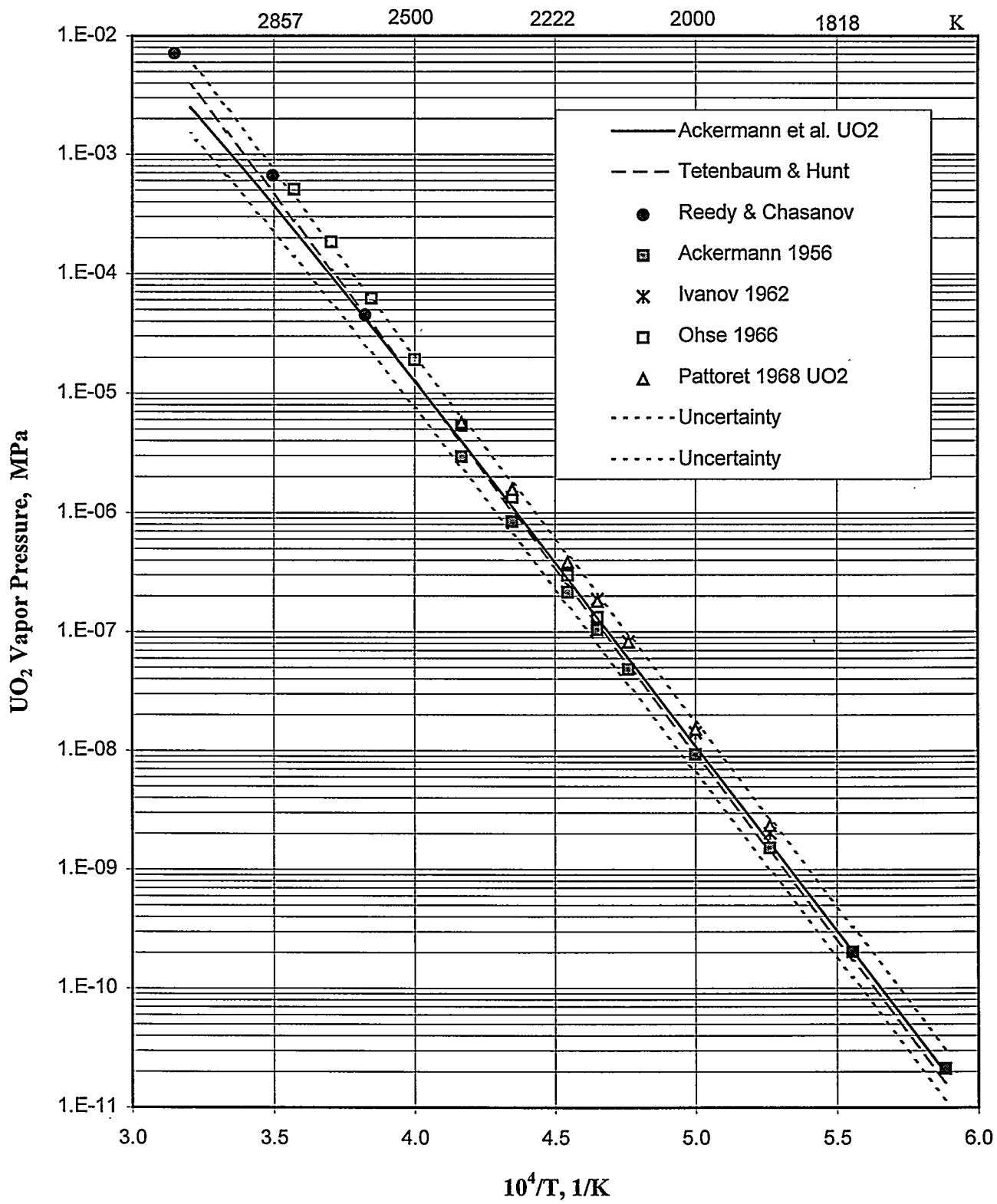
## Figure 6.3 Comparison of Liquid UO$_2$ Heat Capacity Data and Equations
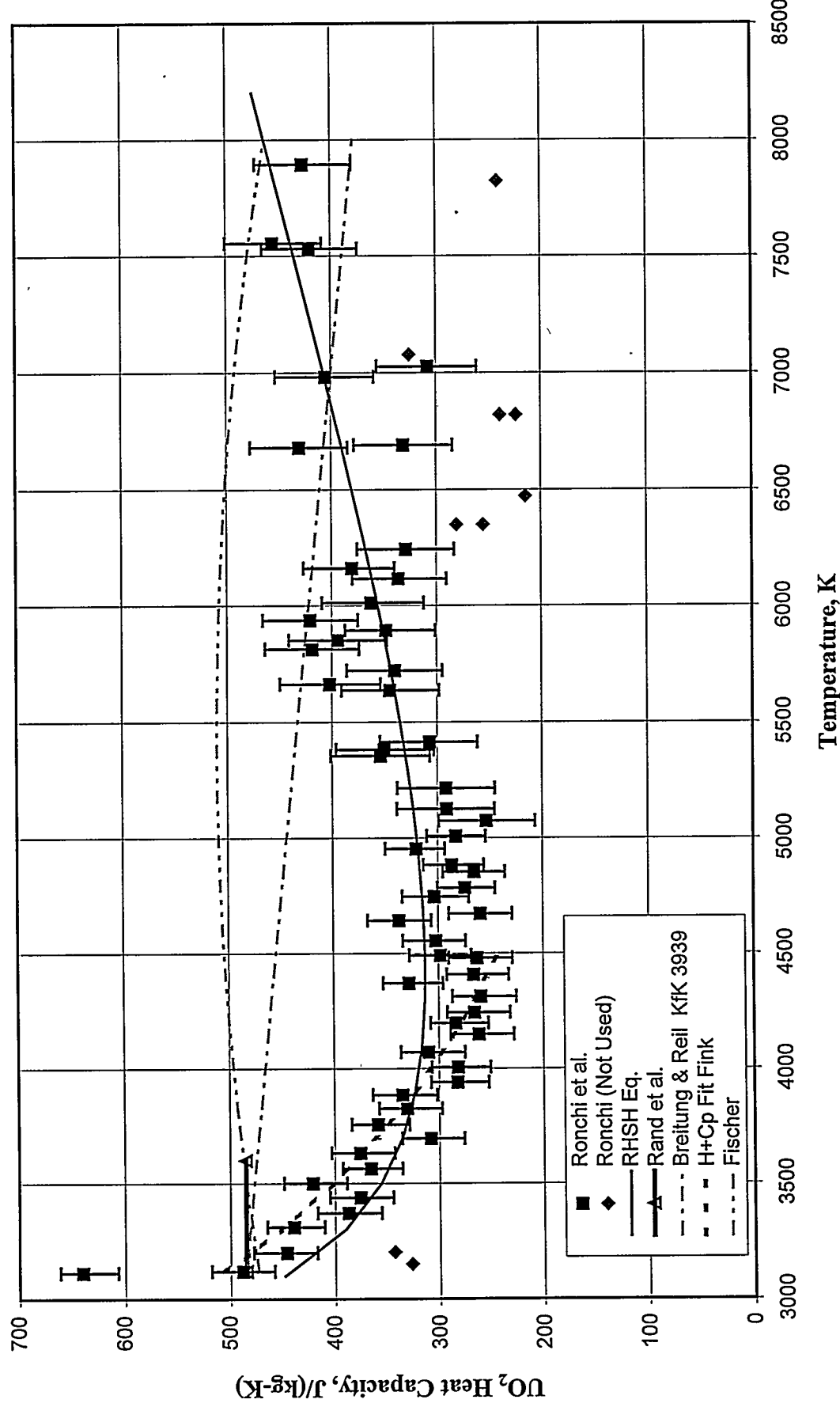
Figure 6.4 Total Vapor Pressure Over Liquid UO$_2$
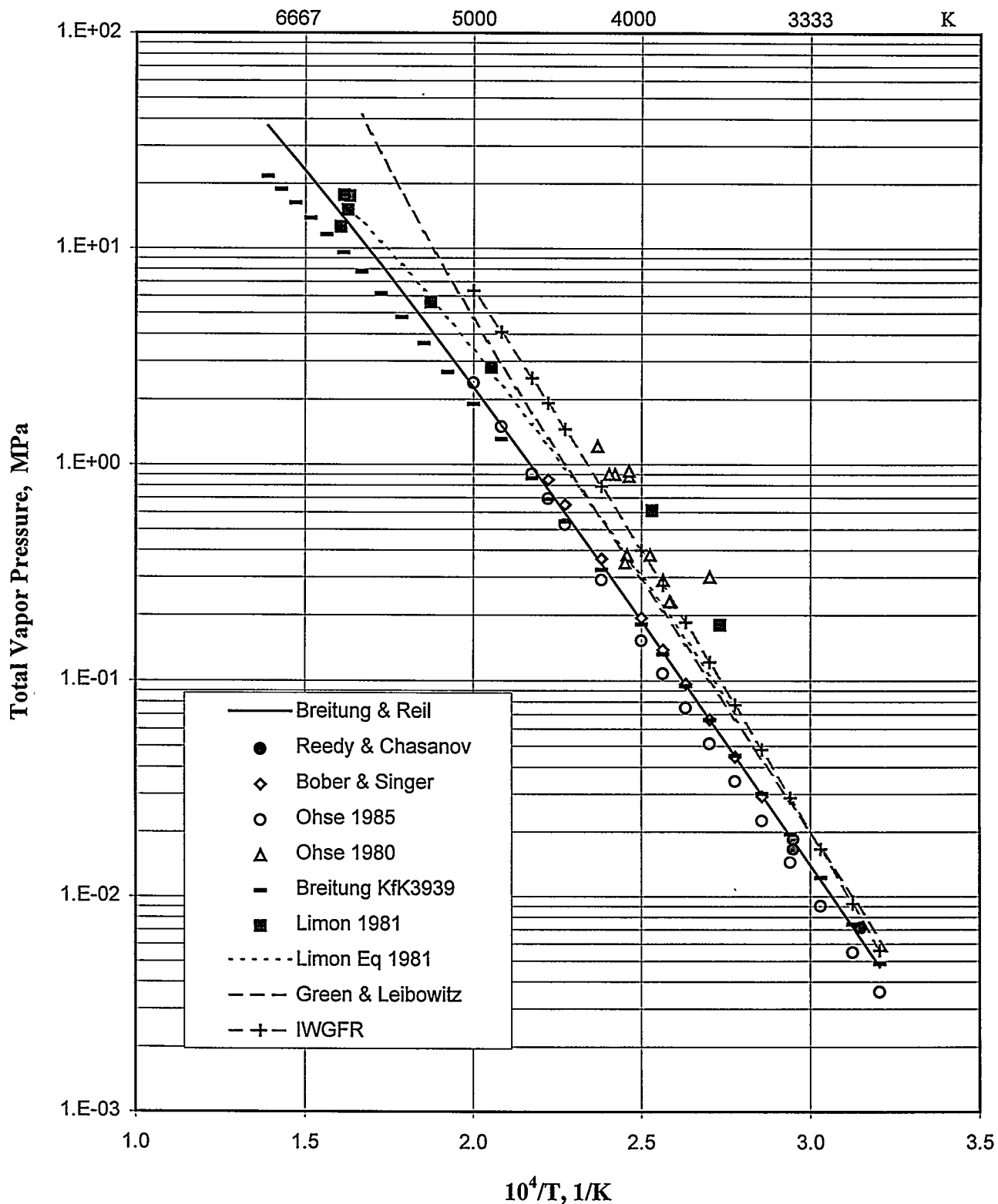
Figure 6.5 Vapor Pressure Over Solid UO$_2$

Send Comments to:
jkfink@anl.gov
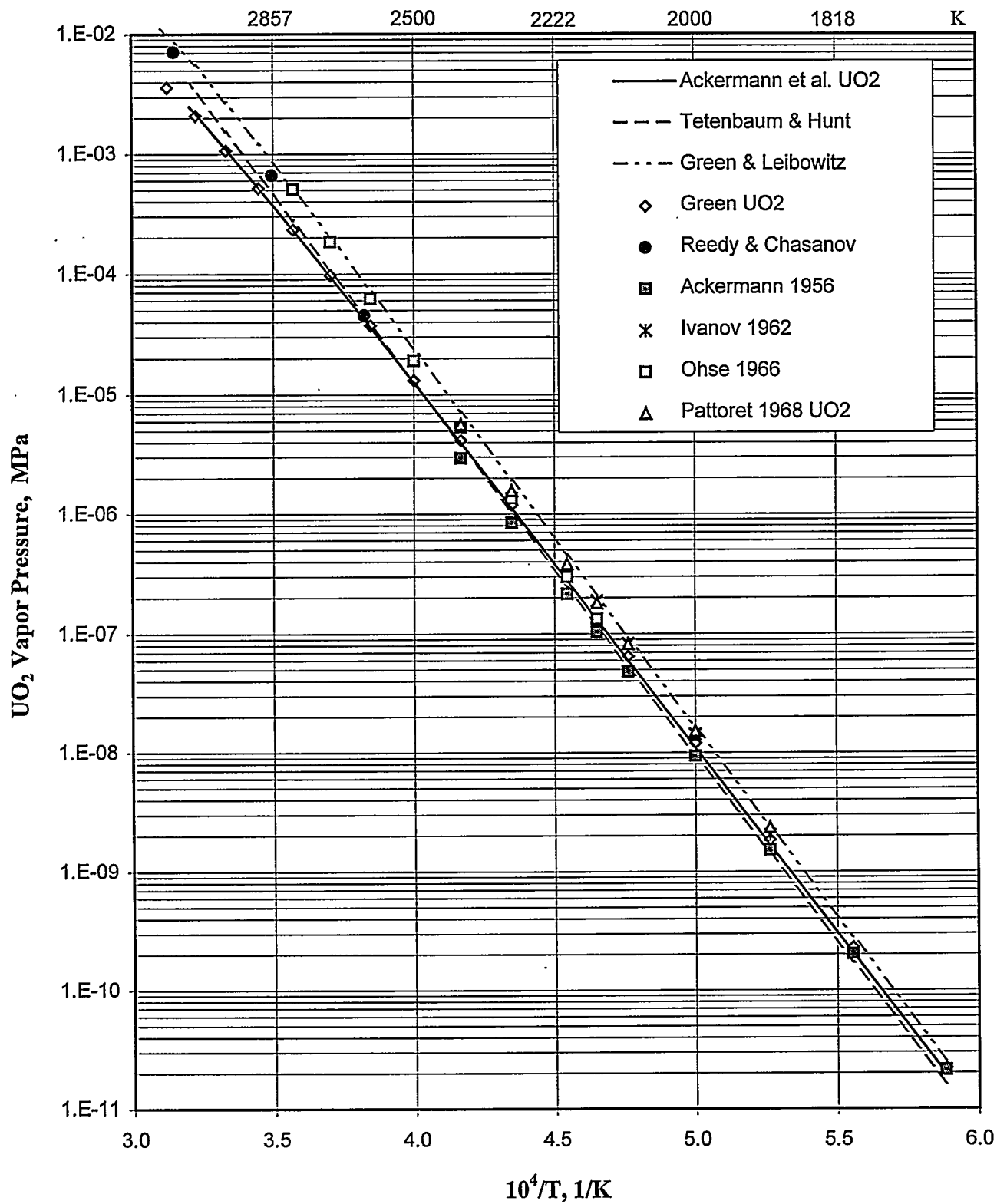
Figure 6.6 Vapor Pressure Over UO$_2$ at Solid/Liquid Interface
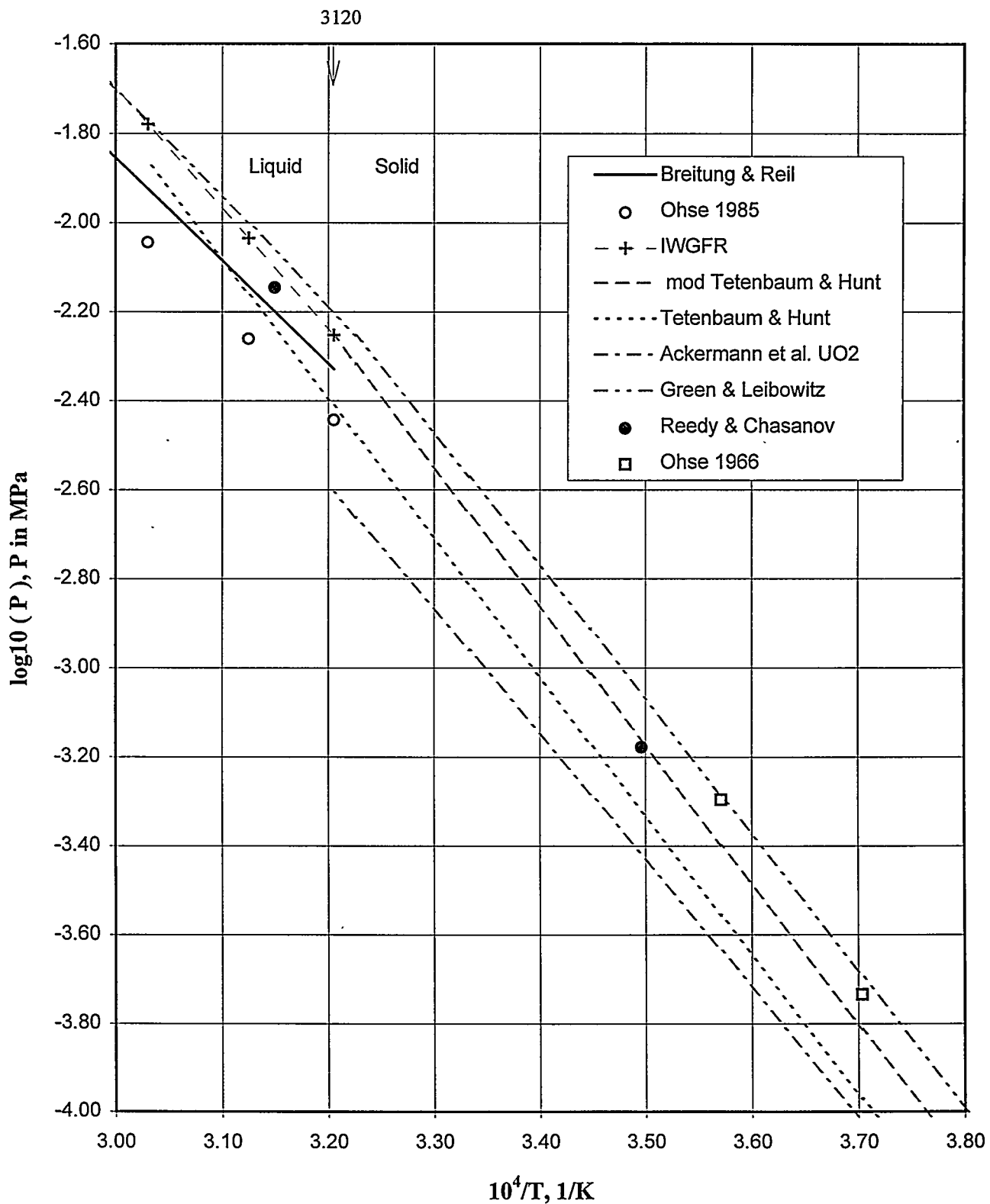
TRANSPORT PROPERTIES

7. THERMAL CONDUCTIVITY AND DIFFUSIVITY OF URANIUM DIOXIDE

7.1 THERMAL CONDUCTIVITY OF SOLID UO$_2$

<u>Summary and Recommended Equation</u>

The recommended equation for the thermal conductivity of fully dense solid UO$_2$ is from Harding and Martin[1] who have carefully considered the theoretical aspects related to the thermal conductivity of fully dense UO$_2$ to obtain a physically based equation for the temperature range of 773 K to the melting point, 3120 K. This equation was selected because it is the best equation available from a theoretical aspect, it is in good agreement with earlier equations that are based on statistical fits to the experimental data, and it is consistent with in-reactor measurements of the integral to melting. Although this equation is recommended only for the temperature range for which it was derived (773 to 3120 K), it is in good agreement with other equations that fit the experimental data below 773 K. The recommended equation of Harding and Martin for the thermal conductivity, k, in W m^{-1} K^{-1} is:

$$k = (0.0375 + 2.165x10^{-4}T)^{-1} + \frac{4.715x10^9}{T^2} \exp\left(\frac{-16361}{T}\right) \tag{1}$$

where the temperature, T, is in K. The first term in this equation represents the contribution from phonons. The second term represents the small polaron contribution. Values of the thermal conductivity for fully dense solid UO$_2$ calculated from Eq. (1) are tabulated as a function of temperature in Table 7.1.1 and shown graphically in Figure 7.1.1. Figure 7.1.1 also includes uncertainty bands.

<u>Uncertainties</u>

Harding and Martin[1] estimate the uncertainties in thermal conductivities calculated with their equation as 7% from 773 to 1800 K increasing to 15% at 3120 K. The increase in uncertainty from 7% at 1800 K to 15% at 3120 K, shown in Figure 7.1.1, is assumed to be linear in accord with the equation: % Uncertainty = - 3.9 + 0.0061 T, where T is the temperature in K.

Discussion of Recommendation

In 1982, Martin[2] reviewed the equations of Washington,[3] Brandt and Neuer,[4] Ainscough,[5] and Killeen[6] with respect to the experimental data, the integral to melting, and the physical models. Martin[2] pointed out that the MATPRO[7] equation, although used extensively, is not physically based. Therefore, it was not recommended. Martin included the polynomial equation of Ainscough, which has no physical basis, in his assessment because it represents the best fit to the low-temperature data and was significant in the development of the physically-based equation given by Killeen. Since the review by Martin, Fink et al.[8,9] reviewed the available thermal conductivity and thermal diffusivity data, converted the diffusivity data to conductivities and fit the combined data to a two term equation to account for the phase transition at 2670 K that appears in heat capacity data but not in either thermal diffusivity or density data. Differences between the physically based equations of Washington,[3] Brandt and Neuer,[4] Killeen,[6] and Fink et al.[8,9] arise from differences in the physical processes included in the equations used to represent the thermal conductivity and differences in the data sets included in the fits.

Washington's equation[3] for thermal conductivity in W m^{-1} K^{-1} and T in K is:

$$k = (0.035 + 2.25x10^{-4}T)^{-1} + 83.0x10^{-12}T^3 \qquad (2)$$

The first term of Washington's equation is the contribution due to phonons. The form of the second term is consistent with a contribution due to radiation implying that the increase in thermal conductivity at high temperatures arises from thermal radiation rather than electronic excitation. The limitations of Washington's equation are: the form of this second term and the minimum conductivity which is about 8% higher than most experiments but within the experimental uncertainty. Washington included integral-to-melting data in his fitting procedure to ensure good agreement with the available in-reactor data.

The equation given by Brandt and Neuer[4] is:

$$k = (0.0439 + 2.16x10^{-4}T)^{-1} + 11.2x10^{-2}T\exp\left(-\frac{1.18}{k_BT}\right)$$

$$-4.18x10^5\exp\left(-\frac{3.29}{k_BT}\right) \tag{3}$$

where k_B is the Boltzmann constant (8.6144×10^{-5} eV K^{-1}), T is in K, and thermal conductivity is in W m^{-1} K^{-1}. The first term in Eq. (3) gives the phonon contribution, the second term gives the contribution from electronic conduction, and the third term gives the decrease in conduction due to dislocations at high temperature. Martin[2] commented that this equation appears to be overly complicated and gives low values for the integral-to-melting. At low temperatures, thermal conductivities calculated with the equation of Brandt and Neuer[4] are slightly lower than the mean experimental values but are consistent with both the Round Robin experimental data[10] (based on UO_2 with O/M in the range of 2.002-2.007) and with the more recent low-temperature data of Weilbacher.[11,12]

The Ainscough equation[5] is a polynomial fit given by:

$$k = 9.851 - 8.803x10^{-3}T + 3.301x10^{-6}T^2 - 3.727x10^{-10}T^3 \tag{4}$$

where T is in K and thermal conductivity is in W m^{-1} K^{-1}. Although the equation given by Ainscough represents the best fit to the low-temperature data, it deviates at high temperatures and gives low integral-to-melting values of 6.3 kW/m for 95% dense fuel and 6.8 kW/m for 100% dense fuel.

Killeen's equation[6] is:

$$k = (0.0375 + 2.165x10^{-4}T)^{-1} + 3.861x10^{-3}T\exp\left(\frac{-1.07}{k_BT}\right) \tag{5}$$

where k_B is the Boltzmann constant (8.6144×10^{-5} eV K^{-1}), T is in K, and thermal conductivity is in W m^{-1} K^{-1}. The first term in Killeen's equation is the phonon contribution. The parameters were chosen to give a best fit to Ainscough's low-temperature thermal conductivities. The second term represents thermal transport by electronic charge carriers with both electrons and holes contributing

to the conduction. The form is a modified Wiedemann-Franz relationship for intrinsic semi-conductors. Killeen's physically based equation is a good representation of the low-temperature data and gives good integral-to-melting values but gives high thermal conductivities at high temperatures.

The equations of Fink et al. are:

For T ≤ 2670 K,

$$k = (6.8337x10^{-2} + 1.6693x10^{-4}T + 3.1886x10^{-8}T^2)^{-1} + 1.2783x10^{-1}T \exp\left(\frac{-1.1608}{k_B T}\right) \quad (6)$$

For T ≥ 2670 K,

$$k = 4.1486 - 2.2673x10^{-4}T \quad (7)$$

where k_B is the Boltzmann constant (8.6144×10^{-5} eV K^{-1}), T is in K, and thermal conductivity is in W m^{-1} K^{-1}. The first term in Eq.(6) gives the phonon contribution. The second term, which gives the electronic contribution, has the same form as that of Killeen. The discontinuity at 2670 K arises from conversion of the thermal diffusivity measurements of Weilbacher[11,12] and Bates[10] to thermal conductivity. As pointed out by Harding et al.,[13] there is currently no basis for a discontinuity in thermal conductivity at the Bredig transition but there is only one experimental thermal conductivity datum above 2670 K (at 2777 K by Stora et al.[14]). Although this equation gives a better overall fit to the experimental data than that of Brandt and Neuer, like the equation of Brandt and Neuer, it gives a low integral-to-melting value.

Hyland[15] has published a detailed critique and recommendation for the thermal conductivity of UO$_2$ that discusses the lattice, radiation, and electronic contributions to the thermal conductivity and the errors in the theories and the experimental data. However, he gives no equation to represent the thermal conductivity for the entire temperature range. Hyland comments that the electronic contribution is from small polarons and is not well represented by the intrinsic semiconductor contribution used by Killeen. Hyland assumed that at temperatures above 2000 K, the lattice contribution to the thermal conductivity was constant and equal to the value at 2000 K where the total thermal conductivity reaches a minimum value. This was based on Schmidt's[16] comment that as temperatures increase, the phonon component decreases as the mean free path between scattering

events decreases. Schmidt estimated that by 2323 K the mean free path had fallen to values equal to the inter-ionic separation. Since smaller mean free paths have no physical meaning, Schmidt recommended that above 2323 K the phonon lattice contribution should be a constant equal to the value at 2323 K. Hyland calculated the electrical contribution due to small polarons using the electrical conductivity data of Killeen[17] to obtain the temperature dependence. The radiation contribution was included to account for the increase in thermal conductivity at high temperatures.

The first term of the equation of Harding and Martin, Eq. (1), is identical with that given by Killeen, which gives a good fit to the low-temperature thermal conductivity data. Because Schmidt's determination of the mean-free path was based on extrapolated elastic constants, his calculation was repeated by Harding and Martin using recent elastic constant measurements.[18] They concluded that the mean free path is always greater than the inner-ionic spacing, suggesting that the phonon contribution given by the first term of Killeen's equation could be used at all temperatures up to the melting point. They commented that there is no experimental evidence indicating whether the phonon contribution reaches a minimum and remains a constant or continues to decrease until the melting point. ThO_2 thermal conductivity, which has no electronic contribution at high temperatures, shows a monotonic decrease up to 2800 K. However, this is still far from the 3640 K melting point of ThO_2. The second term of the equation of Harding and Martin is the contribution due to small polarons. It has been calculated from the activation energy for the formation of electron-hole pairs and the electrical conductivity using data related to the hole mobility from Dudney et al.[19] and from the recommendations by Hampton et al.[20] and the high-temperature electrical conductivity data of Bates.[21] This term has a different temperature dependence than the small polaron contribution given by Hyland and gives higher values. The integral to melting for 95% theoretically dense UO_2 was calculated by Harding and Martin assuming a porosity correction factor of (1-2.5 p) where p is the porosity. They obtained 6.8 kW m^{-1} for the integral to melting, which is the value recommended by Marchandise.[22]

Comparison with Recommendation

The recommended equation of Harding and Martin[1] [Eq. (1)] is compared in Figure 7.1.2 with curves from the calculation of Hyland,[15] and equations of Killeen,[6] Fink et al.,[8,9] Brandt and Neuer,[4] Washington,[3] Ainscough,[5] and MATPRO.[7] Below 600 K, it is consistent with the equation

of Killeen, which is high relative to the equation of Ainscough. However, the equations of Ainscough, Brandt and Neuer, Washington, Killeen, and Harding and Martin are recommended only from 773 to 3120 K, so the differences below 600 K are not surprising. Above the solid-solid phase transition at 2670 K, the equation of Harding and Martin is consistent with values given by the equation of Brandt and Neuer which fit the high-temperature data of Weilbacher. Thus, at high temperatures, the equation of Harding and Martin gives lower values than the equation of Killeen and slightly higher values than calculated by Hyland. Figure 7.1.3 shows percent deviations of the calculation by Hyland and the equations of Killeen, Fink et al., Brandt and Neuer, Washington, Ainscough, and MATPRO from the recommended equation of Harding and Martin. These deviations are defined by:

$$Deviation(\%) = \frac{k(Other) - k(Recommended)}{k(Recommended)} \cdot 100\% \qquad (8)$$

From 1000 to 2800 K, percent deviations are greatest for the MATPRO equation. The unusual deviations near 2670 K in the values from the equations of Fink et al. are due to the inclusion of a discontinuity at the solid-solid phase transition and the use of a linear equation above that transition.

Above 2670 K, the only experimental data available are the thermal diffusivity measurements of Weilbacher[11,12] and Bates[10] and a single datum from the thermal conductivity measurements of Stora et al.[14] Since Brandt and Neuer[4] fit these data, new equations have been determined for the heat capacity[23] and density[24] of UO_2. The heat capacity equations[23] are consistent with the experimental data that confirm a solid-solid phase transition at 2670 K. At high temperatures, the density equation[24] has been based on the recent high-temperature data from Hutchings.[25] To compare these high-temperature diffusivity measurements with the recommended equation of Harding and Martin, the thermal diffusivity data of Weilbacher and Bates have been converted to thermal conductivity using these new equations for density and heat capacity and the relation:

$$k = \delta \, C_P \, \rho \qquad (9)$$

where δ is the thermal diffusivity, C_P is the heat capacity, and ρ is the density. In Figure 7.1.4, the equation of Harding and Martin is compared with the thermal conductivities obtained from the data

of Weilbacher and of Bates and the thermal conductivity values of Stora et al. Uncertainty bands based on the uncertainty recommendations of Harding and Martin have been included in the figure. The thermal conductivities of Stora et al. and all the thermal conductivities from the thermal diffusivities of Weilbacher except for the datum of Weilbacher at 3023 K are within the 15% uncertainty. However, conductivities calculated from the thermal diffusivities of Bates are lower than the 15% uncertainty. The recent measurements of Weilbacher are considered more reliable than the older high-temperature measurements of Bates.

<u>Effect of Porosity</u>

The recommended equation of Harding and Martin is for fully dense stoichiometric UO_2. Although the effect of porosity on thermal conductivity of UO_2 has been studied experimentally, a large spread exists in the experimental results. This is due to differences in the shape and orientation of the porosity depending on the history of the fuel. The influence of porosity on the thermal conductivity of irradiated UO_2 has been determined by Bakker et al.[26] using the finite element method which considers the effects of shape, orientation, and distribution of the pores in the fuel. They found good agreement between their calculations and the analytical equations derived by Schulz,[27] which approximate the shape of the pores by ellipsoids and assume that the pores are randomly positioned. Schulz used general relationships for the thermal conductivity of two-phase materials to obtain equations for thermal conductivity of porous materials. These equations require data on the structure (dispersion or penetration), the porosity (P) and whether it is open or closed, the shape of the pores, the orientation of the pores, and the thermal conductivity of the pure phases. Equations recommended by Schulz for the thermal conductivity for closed and open porosity are:

Closed Porosity:

$$k = k_0(1-P)^X \tag{10}$$

$$X = \frac{1-\cos^2\alpha}{1-F} + \frac{\cos^2\alpha}{2F} \tag{11}$$

Open Porosity:

$$(1-P)(k_0-k)\left[\frac{2(1-\cos^2\alpha)}{k_0+k} + \frac{\cos^2 apha}{k}\right] = P(2-\cos^2\alpha) \qquad (12)$$

where k is the thermal conductivity of the porous material, k_0 is the thermal conductivity of the theoretically dense material, P is the porosity, and F and $\cos^2\alpha$ are shape and orientation factors for the pores. In general, the pores are treated as three-dimensional ellipsoids which leads to complex integrals for the shape and orientation factors as given by Bakker et al.[26] The complexity of these equations of Schulz limit their usefulness.

A number of simpler equations have been suggested based on measurements on unirradiated fuel. A modified Loeb relation has been recommended by a number of analysts including Washington and by Brandt and Neuer. The modified Loeb relation is:

$$k = k_0\ (1-\alpha P) \qquad (13)$$

where k_0 is the thermal conductivity of fully dense fuel and P is the fractional porosity. Washington recommended $\alpha = 2.5$; Brandt and Neuer proposes that α is a linear function of temperature given by $\alpha = 2.6 - 0.5 \times 10^{-5}\ T$, where T in °C. The porosity correction proposed in MATPRO is the Maxwell-Eucken equation:

$$k = k_0\ \frac{1-P}{1+\beta P} \qquad (14)$$

where k_0 is the thermal conductivity of fully dense fuel and P is the fractional porosity. The factor β is a linear function of temperature, T in K:

$$\beta = \beta_0 + \beta_1 T \qquad (15)$$

Mean values given in MATPRO for β_0 and β_1 are: 6.5 and - 0.00469, respectively. Martin[2] recommended a modified Loeb relation with $\alpha = 2.5$ for fractional porosity values less than 0.1. For higher porosities, Martin recommended a Maxwell-Euken relationship with $\beta = 2$.

Harding et al.[13] commented that the Loeb equation and the Maxwell-Euken equation may be replaced to an acceptable accuracy with the single equation:

$$k = k_0(1-P)^{2.5} \qquad (16)$$

where P is the fractional porosity. However, this equation as well as Eqs. (14) and (15) have the defect that the correction factors are means of values that have been determined from measurements on fuels from different laboratories that have possible differences in manufacturing that could result in genuine differences in pore structure in the different fuels. In addition, no consideration has been made for irradiated fuel which has different pore structures from unirradiated materials. Consequently, Harding et al. recommended an equation, based on the work of J. R. Mathews, which accounts for the pore structure by splitting the porosity into a number of components. Their equation for the thermal conductivity of fuel containing porosity is:

$$k = k_0(1-P_1)\ (1-P_2-P_3)^{2.5}\ (1-P_4-P_5)^{3.5} \qquad (17)$$

where k_0 is the conductivity for theoretically dense fuel and the various P's refer to volume fractions of different types of pore:

P_1 = large spherical pores,

P_2 = small spherical manufacturing pores,

P_3 = small spherical intragranular gas bubbles or pores,

P_4 = lenticular grain face bubbles or pores, and

P_5 = toroidal grain edge bubbles or pores.

In these definitions, large (small) refer to pores greater than (less than) 5 μm in diameter. The first term $(1-P_1)$ comes from measurements on UO_2 containing large, spherical pores that were deliberately introduced in the sample. The 2.5 exponent is based on the experimental evidence that led to Eq. (17). The higher power of 3.5 for the third bracket is a recognition that the aspect ratios of lenticular and toroidal pores are higher than those associated with small spherical pores. Because this equation has more physical basis than the simpler Loeb and Maxwell-Euken equations and also Eq. (17) and does not have the complexity of Schulz's analytical expressions, it is recommended.

REFERENCES

1.   J. H. Harding and D. G. Martin, *A Recommendation for the Thermal Conductivity of UO₂*, J. Nucl. Mater. **166**, 223-226 (1989).

2.   D. G. Martin, *A Re-Appraisal of the Thermal Conductivity of UO₂ and Mixed (U,Pu) Oxide Fuels*, J. Nucl. Mater. **110**, 73-94 (1982).

3.   ` A. B. G. Washington, *Preferred Values for the Thermal Conductivity of Sintered Ceramic Fuel for Fast Reactor Use*, UKAEA Report **TRG Report 2236 (D)** (1973).

4.   R. Brandt and G. Neuer, *Thermal Conductivity and Thermal Radiation Properties of UO₂*, J. Non-Equilib. Thermodyn. **1**, 3-23 (1976).

5.   J. B. Ainscough, Springfields Nuclear Power Development Laboratories, unpublished work (1972) as referenced by M. Martin in J. Nucl. Mater. **110**, 73-94 (1982).

6.   J. G. Killeen, Berkeley Nuclear Laboratories, unpublished work (1980) as shown by M. Martin in J. Nucl. Mater. **110**, 73-94 (1982).

7.   J. K. Horhorst, editor, *SCADAP/RELAP5/MOD2 Code Manual Vol. 4: MATPRO - a library of materials properties for light-water-reactor accident analysis*, EG&G Idaho Report **NUREG/CR-5273** (1990).

8.   J. K. Fink, M. G. Chasanov, and L. Leibowitz, *Thermal Conductivity and Thermal Diffusivity of Solid UO₂*, Argonne National Laboratory Report **ANL-CEN-RSD-81-3** (June 1981).

9.   J. K. Fink, M. G. Chasanov, and L. Leibowitz, *Thermophysical Properties of Uranium Dioxide*, J. Nucl. Mater. **102,** 17-25 (1981); also as ANL Report **ANL-CEN-RSD-80-3**, Argonne National Laboratory (April 1981).

10.   J. L. Bates, *High-Temperature Thermal Conductivity of 'Round Robin' Uranium Dioxide*, Battelle Memorial Institute Pacific Northwest Laboratories, Richland, Washington (July 1970).

11.   J. C. Weilbacher, *Measurement of Thermal Diffusivity of Mixed Uranium Plutonium Oxides*, CEA Report **CEA-R-4572**, Centre d'Etudes Nucléairs de Fontenay-aux Roses, France (1974).

12.   J. C. Weilbacher, *Diffusivité Thermique de l'Oxyde d'Uranium et de l'Oxyde de Thorium à Haute Temperature,* High Temp.-High Pressures 4, 431-438 (1972).

13.   J. H. Harding, D. G. Martin, and P. E. Potter, *Thermophysical and Thermochemical Properties of Fast Reactor Materials,* Commission of the European Communities Report **EUR 12402 EN** (1989).

14.   J. C. Stora, B. de Bernardy de Sigoyer, R. Delmas, P. Deschamps, B. Lavaud, and C. Ringot, *Conductibilite Thermique de l'UO₂ Fritté dans les Conditions d'Utilisation en Pile,* CEA Report **CEA-R-2586,** Centre d'Etudes Nucléaires de Saclay, France (1964).

15.   G. J. Hyland, *Thermal Conductivity of Solid UO₂: Critique and Recommendation,* J. Nucl. Mater. **113,** 125-132 (1983).

16.   H. E. Schmidt, *Some Considerations on the Thermal Conductiivty of Stoichiometric Uranium Dioxide at High Temperatures,* J. Nucl. Mater **39,** 234-237 (1971)

17.   J. C. Killeen, *The Effect of Niobium Oxide Additions on the Electrical Conductivity of UO₂,* J. Nucl. Mater **88,** 185-192 (1980).

18.   D. G. Martin, *The Elastic Constants of Polycrystalline UO2 and (U,Pu) Mixed Oxides: A Review and Recommendations,* High Temp.-High Pressures **21,** 13-24 (1989).

19.   N. J. Dudney, R. L. Coble, and H. L. Tuller, *electrical Conductivity of Pure and Yttria-Doped Uranium Dioxide,* Am. Ceram. Soc. **64,** 627-631 (1981).

20.   R. N. Hampton, G. A. Saunders, A. M. Stoneham and J. H. Harding, *The Electrical Impedance of Single-Crystal Urania at Elevated Temperatures,* J. Nucl. Mater **154,** 245-252 (1988).

21.   J. L. Bates, *Electrical Conductivity of UO₂,* Pacific Northwest Laboratory Report **BNWL-296 Pt. 2** (November 1967).

22.   H. Marchandise, *Conductibilite Thermique du Dioxyde d'Uranium,* Commission of the European Communities Report **EUR4568f** (November 1970).

23.   J. K. Fink, *Enthalpy and Heat Capacity of the Actinide Oxides,* Int. J. Thermophys. 3(2), 165-200 (1982).

24.   D. G. Martin, *The Thermal Expansion of solid UO₂ and (U,Pu) Mixed Oxides - A Review and Recommendations,* J. Nucl. Mater. **152** 94-101 (1988).

25.   M. T. Hutchings, *High-Temperature Studies of UO₂ and ThO₂ using Neutron Scattering Techniques,* J. Chem. Soc. Faraday Trans. II **83,** 1083-1103 (1987).

26.   K. Bakker, H. Kwast, and E. H. P. Cordfunke, *Determination of a Porosity Correction Factor for the Thermal Conductivity of Irradiated UO$_2$ Fuel by Means of the Finite Element Method,* J. Nucl. Mater. **226** 128-143 (1995).

27.   B. Schulz, *Thermal Conductivity of Porous and Highly Porous Materials,* High Temp.-High Pressure **13**, 649-660 (1981)and KFK 1988 (1974).

Table 7.1.1 Recommended Thermal Conductivity of Theoretically Dense UO$_2$

Temperature K	Thermal Conductivity W m^{-1} K^{-1}
298.15	9.80
300	9.76
400	8.06
500	6.86
600	5.97
700	5.29
800	4.75
900	4.30
1000	3.94
1100	3.63
1200	3.37
1300	3.14
1400	2.96
1500	2.80
1600	2.67
1700	2.57
1800	2.50
1900	2.46
2000	2.45
2000	2.45
2100	2.47
2200	2.52
2300	2.59
2400	2.69
2500	2.81
2600	2.95
2670	3.06
2700	3.11
2800	3.29
2900	3.49
3000	3.69
3100	3.91
3120	3.95

Figure 7.1.1 Recommended Thermal Conductivity of Solid UO$_2$ with Uncertainties
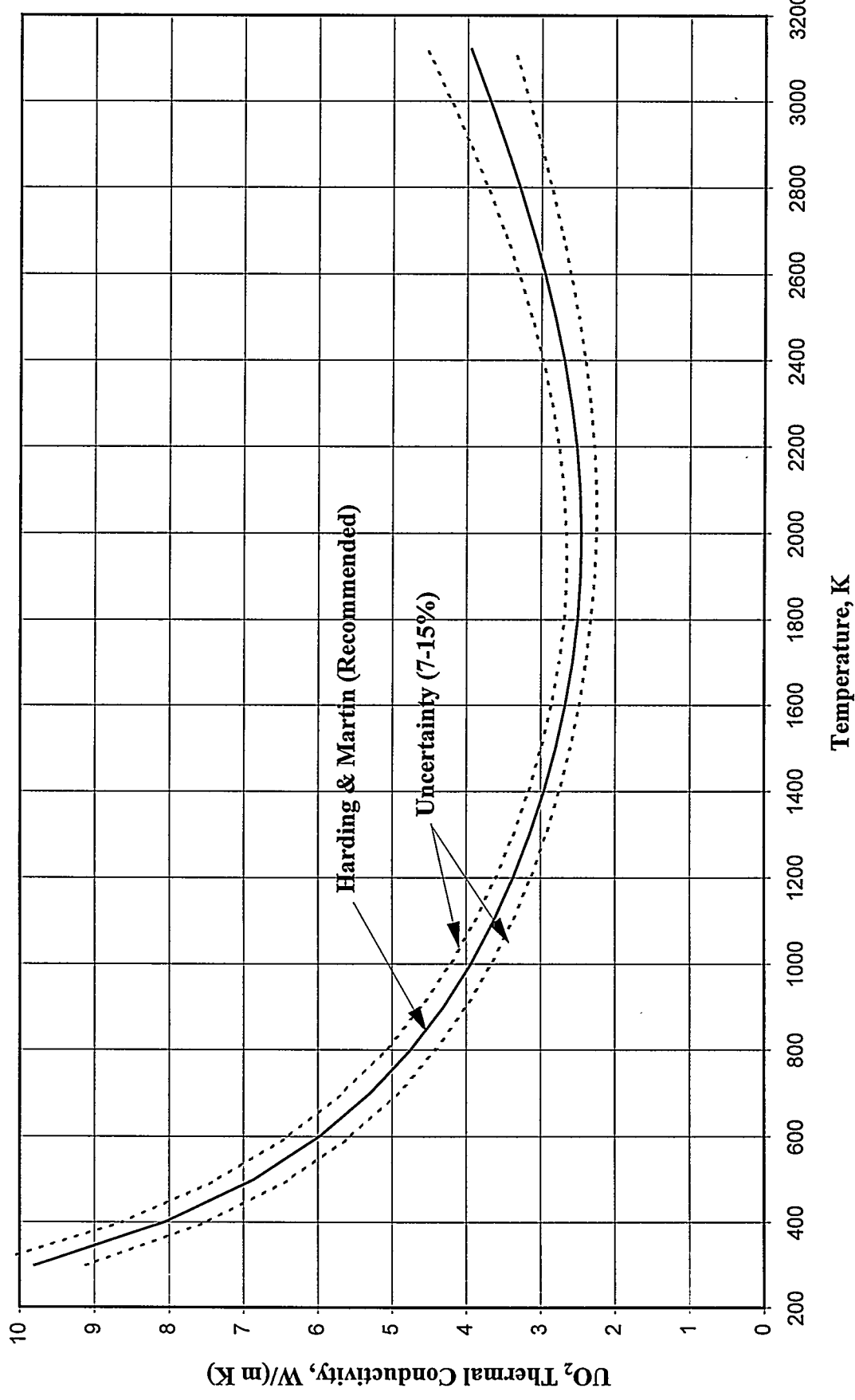
## Figure 7.1.2 Comparison of Equations for the Thermal Conductivity of Solid UO$_2$
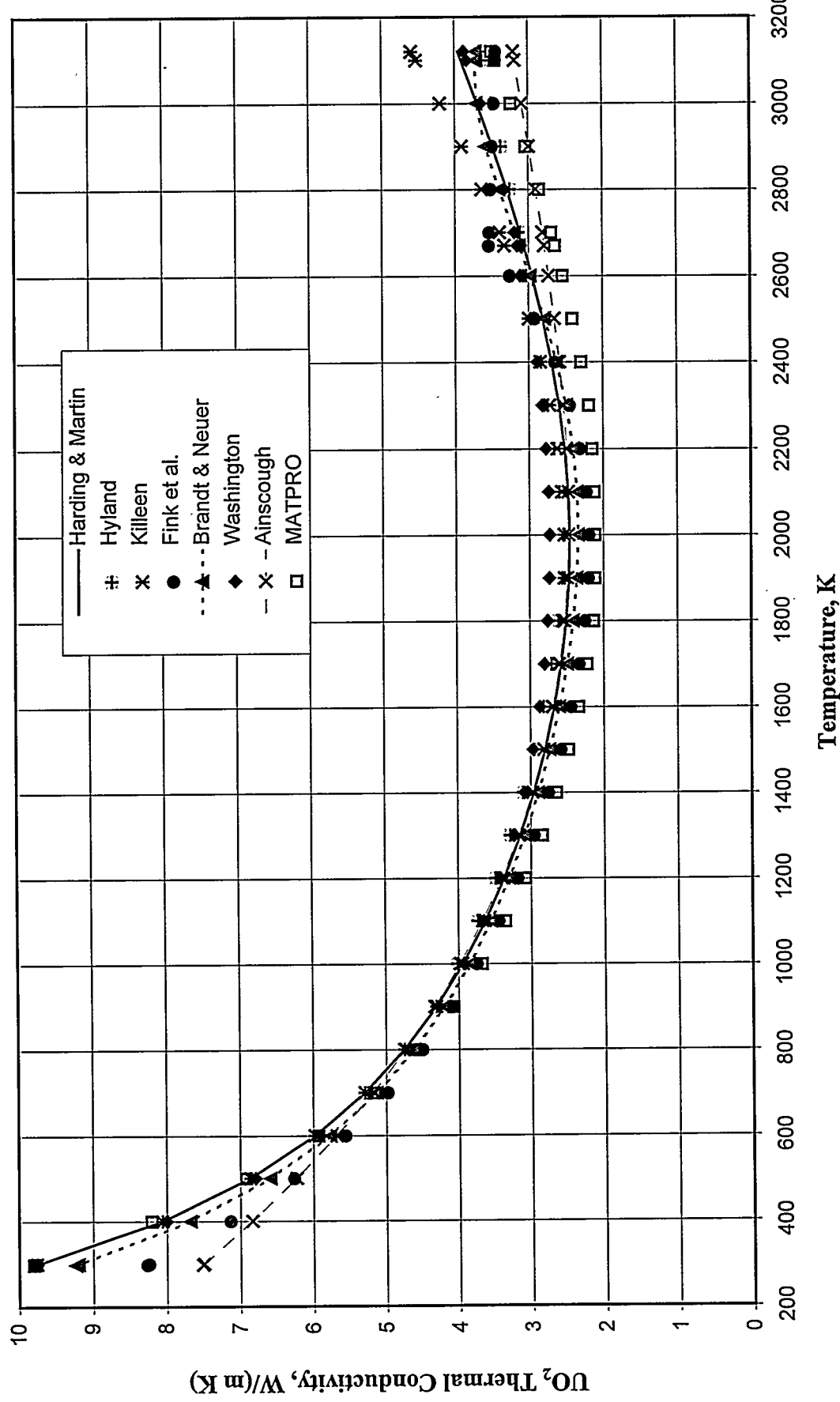
Figure 7.1.3 Deviations from UO$_2$ Thermal Conductivity Eq. of Harding & Martin
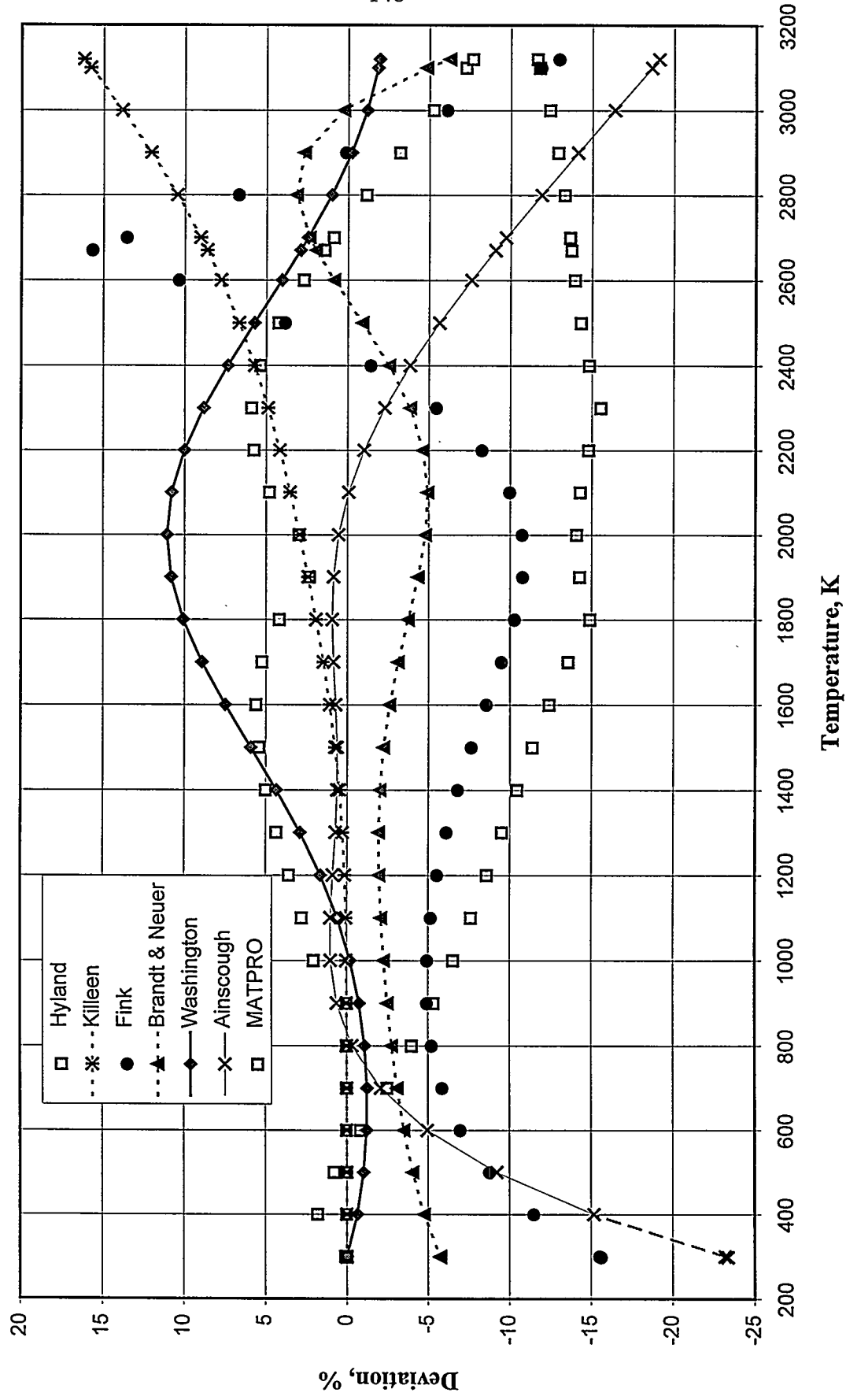
Figure 7.1.4 Thermal Conductivity of UO$_2$
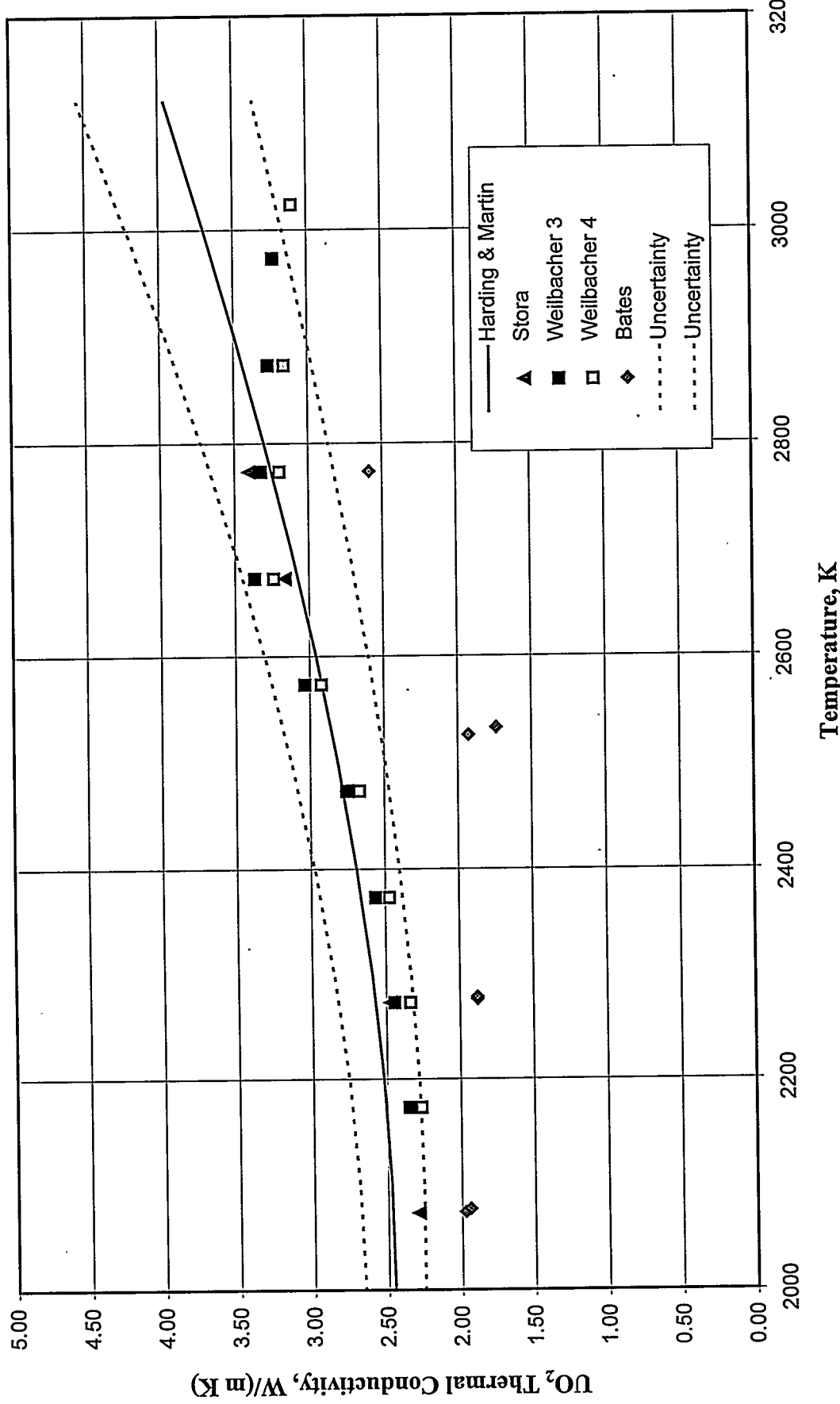
7.2   THERMAL CONDUCTIVITY AND DIFFUSIVITY OF LIQUID UO$_2$

Preliminary Recommendation

Based on an initial review of the limited data[1-4] on the thermal conductivity and thermal diffusivity of liquid UO$_2$, the liquid thermal conductivity is in the range of 2.5 to 3.6 W m^{-1} K^{-1}. Liquid thermal diffusivities range from 6 x 10^{-7} to 11 x 10^{-7} m^2 s^{-1}.

Experiments

The available data on the thermal conductivity (k) and thermal diffusivity (α) of liquid UO$_2$ are summarized in Table 7.2.1. Measurements of thermal diffusivity were made by Kim et al.[1] and by Otter and Damien.[2] Tasman et al.[3,4] measured thermal conductivity. The measurements by Kim et al. and by Otter and Damien were based on standard methods for obtaining the thermal diffusivity.

Kim et al.[1] used a modulated electron beam technique to measure the thermal diffusivity of UO$_2$ in the temperature range of 3187 to 3310 K. A thin UO$_2$ sample clad in tungsten was heated by two electron beams. The top beam was modulated sinusoidally and the difference in phase between the top and bottom temperatures was measured. The thermal diffusivity was determined from the phase changes. Measurements were made on two thicknesses of UO$_2$ (0.813 and 1.219 mm) and three modulated frequencies: 0.25 Hz (π/2 rad s^{-1}), 0.50 Hz (π rad s^{-1}), and 0.75 Hz (3π/2 rad s^{-1}). The tungsten above and below the UO$_2$ layer was 1.397 and 1.016 mm thick. In the reanalysis[5] of the data of Kim et al.,[1] an error was found in the original analysis by Kim et al.[1] The reanalysis included (1) the ideal calculation done by Kim et al., (2) an ideal model using a three-dimensional unsteady-state heat transfer code that assumed infinite slabs with no sidewalls, and (3) the real case accounting for heat transfer in the tungsten sidewalls using a transient 3-dimensional unsteady-state heat transfer code. No radiative heat transfer within the liquid was modeled based on the comment of Bober[7] that radiative heat transfer in the liquid would be small and could not account for the increase in thermal conductivity of the liquid. The heat transfer analysis using ideal and real models of the UO$_2$ in the tungsten cell showed that if the thermal conductivity was low, then the ideal model was not a good approximation because wall conductivity becomes important as the conductivity of the liquid layer decreases. As shown in Table 7.2.1, a statistically significant difference was found between the thermal conductivities of the thick and thin layers. Although tungsten contamination of the samples could affect the conductivity, it would have a greater effect

Table 7.2.1. Thermal Conductivity of Liquid UO_2 from Measurements of Thermal Diffusivity and Thermal Conductivity

Experiment	Kim et al. [1]	Otter & Damien [2]	Tasman et al. [3,4]
Property Measured	Thermal Diffusivity	Thermal Diffusivity	Thermal Conductivity
Method	Periodic Heat Flow	Laser Flash	Laser Heating - Melt & Ablate UO_2 self-contained sample
Sample	UO_2 in tungsten 3 -layers; UO_2 layer: 0.8 mm, 1.2 mm	UO_2 in tungsten 3 -layers; UO_2 layer: 0.7 mm	UO_2 6 mm diam disc partially molten; molten layer: 0.2 mm
k reported, $W\ m^{-1}\ K^{-1}$	11	8.5	2.0-2.4; mean 2.2 [3]
Re-evaluated 3-dim. transient heat transfer model [5] k, $W\ m^{-1}\ K^{-1}$	5.5 (mean) 4.8 (thin 0.8 mm) 6.2 (thick 1.2 mm)	6.7	4.5
Corrected 3-dim transient heat transfer calculation [5] using Cp of Ronchi et al. [6] k, $W\ m^{-1}\ K^{-1}$	3.9 (thin) 5.1 (thick)	5.8	3.3
Re-measurement & finite-element-method analysis under unsteady conditions; k, $W\ m^{-1}\ K^{-1}$ [4]			2.5 [4]

in the thin cell than in the thick cell and give the larger conductivity for the thin cell. Lack of good contact between the tungsten and the liquid could also affect the experimental results. The difference between the thin and thick cell results is analogous to differences observed in diffusivity measurements of materials in which radiation is important and cannot be neglected.[8,9] The main uncertainties in this experiment are effects from radiative heat transfer in the liquid and effects from changes in the O/M ratio in the UO_2 due to tungsten contamination in the liquid UO_2 sample.

Otter and Damien[2] measured the thermal diffusivity of a 0.7-mm layer of liquid UO_2 encased in tungsten using a laser flash method in the temperature range of 3133 to 3273 K. Although this

method is well established, analysis of the data becomes more complex at high temperatures with liquids encased in metal cells because of the necessity of including thermal losses to the environment and the need for properties such as heat capacity, density, and thermal conductivity of the metal containment.[10] The reanalysis[5] of their experiment gave lower thermal conductivities than those originally reported by Otter and Damien. Insufficient information is available regarding their experiment and heat losses to determine if the differences are due to different treatment of heat losses in the reanalyzed three-dimensional transient heat transfer calculation. Radiation within the sample was not included in the reanalysis. If radiative heat transfer was significant in the experiments of Kim et al., it would also affect the experiment of Otter and Damien. In addition, errors from tungsten contamination of the sample cannot be ruled out.

Tasman et al.[3] determined the thermal conductivity of liquid UO_2 from a steady-state finite element analysis of the heat transfer in a partially molten, self-contained sample. A UO_2 disc (6 mm in diameter by 1.2- to 3-mm thick) was heated in an argon atmosphere at 4 bar (0.4 MPa) using three continuous-wave CO_2 laser beams. One laser beam was focused on a 4 mm diameter area on the bottom of the disc; two laser beams were focused on area 2 mm in diameter on the top of the disc. The sample was heated with only the bottom beam until it reached 1800°C (2073 K). Then the upper beams were turned on and a molten pool was formed on the top of the sample. Temperatures were measured with optical pyrometers and a fast scanning device. During heating, only the bottom temperature was measured. The peak top temperature was 3200°C (3473 K). Because of extensive vaporization of the sample, the top of the sample could be heated for only 4-5 sec. When heated longer, extensive evaporation created a deep pit in the top center of the sample and part of the ejected material was deposited in crystalline form along the center crater edge. Even on short (5-sec) exposures, recondensed crystals were found. Sample loss from evaporation was limited to less than 2 mg (0.5%) if the exposure to the upper beams was limited to 5 sec. However, it is not clear how much sample mass was redistributed by vaporization and condensation on cooler parts of the sample during the 5 sec exposure to the upper beam. Significant vaporization of UO_2 began at 2300°C (2573 K), which is well below the melting point, 3120 K. Tasman et al.[3] stated that the largest uncertainty in their experiment was the temperature measurement and temperature profile of the top and bottom faces. Because these profiles are critical input in the analysis of the experiment, there

is significant uncertainty in the calculated results. The precision of the experiment is limited by the presence of very high radial temperature gradients and axial asymmetries. However, the error is bounded by the depth of the molten layer, which was determined after solidification from examination of cross sections of the sample. The reliability of visual observation of the liquid depth was questioned[5] based on (1) low melting points (2661 and 2699 K) obtained by early investigators[11] from the appearance of residues and (2) the observed[12] softening and plasticity of UO_2 above about 2500 K where the Frenkel oxygen lattice disorder increases as the phase transition is approached. Above 2670 K, the creep rate also increases significantly,[12, 13] so UO_2 readily deforms to the shape of its container. Ronchi[14] commented that in the short duration of the experiment of Tasman et al. (~ 10 sec), the grain growth is approximately 10 μm at 2700 K[13] and is estimated to be only 5 times larger at 3050 K. He, therefore, concluded that the solid grains are still recognizable at temperatures near the melt front so that the liquid phase is readily distinguished. The reanalysis of this experiment by Fink and Leibowitz[5] indicated that the assumption of steady state conditions made by Tasman et al.[3] makes a significant difference in the resulting thermal conductivity.

Tasman[4] repeated his experiment using a rapid 2D temperature-scanning device and included unsteady transport in the 2D finite-element method (f.e.m.) analysis. His correction was less than that reported by Fink and Leibowitz.[5] He claimed that perturbations that cannot be accounted for in his analysis would lead to lower values in the thermal conductivity.[14] He concluded that the thermal conductivity of liquid UO_2 is 2.5 ± 1 W m^{-1} K^{-1}, which is lower than the thermal conductivity of the solid at the melting point given by Harding and Martin[15] (3.95 W m^{-1} K^{-1}) and by Hyland[16] (3.65 W m^{-1} K^{-1}). The thermal conductivity equation for solid UO_2 of Harding and Martin includes a phonon lattice contribution and an electronic contribution from small polarons, whereas Hyland also included a radiation contribution. At the melting point, the electronic contribution calculated by Harding and Martin is 2.56 W m^{-1} K^{-1}, which is slightly higher than the value for the thermal conductivity of the liquid obtained by Tasman. The electronic, radiation, and lattice contributions to the solid thermal conductivity at the melting point determined by Hyland are 1.55 W m^{-1} K^{-1}, 0.2 W m^{-1} K^{-1}, and 2.1 W m^{-1} K^{-1}, respectively. The radiative contribution calculated by Hyland was 0.48 W m^{-1} K^{-1}, but he assumed a 50% uncertainty because this value was

higher than needed for good agreement with experimental total thermal conductivities. Differences in the lattice and electronic contributions to the thermal conductivity of the solid in these two calculations are related to the different data used in the models. Because of these differences, no conclusions with regard to the reliability of the measurement of Tasman can be made from comparison with contributions to the solid thermal conductivity at the melting point.

Discussion

Ronchi et al.[6] determined the heat capacity of liquid UO_2 from the melting point to 8000 K by heating sintered 0.5- to 1-mm diameter microspheres by four tetrahedrally oriented laser beams in an inert autoclave at pressures up to 1000 bar. The samples were suspended by a tungsten needle during pulses of a few milliseconds duration. The heat capacity was calculated numerically from the energy input, the sample temperature during and after laser pulse heating, the energy loss rates, the cooling mechanisms (radiation and convection), and the heat transport within the sample. The accuracy of the calculation depended on the symmetry (of the temperature field from the lasers and the sample shape) and the accuracy of the physical properties (density and thermal conductivity) used in the heat transport analysis. In the calculations, Ronchi et al.[6] used 2.5 W m^{-1} K^{-1} for the thermal conductivity of liquid UO_2. However, they commented that selection of a higher value for the thermal conductivity of the liquid would result in a lower heat capacity. The thermal conductivity values in the next-to-the-last row of Table 7.2.1 are the values of thermal conductivity from the reanalysis of Fink and Leibowitz[5] adjusted for the heat capacities of Ronchi et al. Although the new heat capacity values reduce the thermal conductivities calculated by Fink and Leibowitz,[5] the calculated thermal conductivities are not as low as the value reported by Tasman.[4] However, the corrected value calculated for the experiment of Tasman et al.[3] is within the original uncertainty given by Tasman et al.[3, 4]

Because the heat capacities obtained by Ronchi et al.[6] are a function of the value selected for the thermal conductivity and are consistent with the value reported by Tasman[4] and all other data in Table 7.2.1 are from thermal diffusivity measurements, thermal diffusivities should be compared instead of thermal conductivities. The temperature at which the thermal conductivity of liquid UO_2 was remeasured by Tasman[4] has not been reported by Ronchi et al.[6,14] In their analysis of their heat capacity data, Ronchi et al.[13] assumed that the liquid thermal conductivity is constant at 2.5

$Wm^{-1}K^{-1}$ for the liquid temperature range (3120 - 8000 K). It is not clear if their observed variation in heat capacity with temperature is real or is due, in part, to this assumption of constant thermal conductivity. In any case, the thermal diffusivity calculated using the heat capacities (C_P) of Ronchi et al.[6,13] and constant thermal conductivity (k) of 2.5 W m^{-1} K^{-1} is consistent with the analytical treatment of the heat capacity data of Ronchi et al.[6,13] The liquid UO_2 densities (ρ) of Breitung and Reil,[17] which agree with the values of Drotning,[18] have been used in the conversion to thermal diffusivity (α) via the relationship

$$\alpha = \frac{k}{C_P \, \rho} \qquad (1)$$

Thermal diffusivities from the most recent measurements of Tasman[4] and the thermal diffusivity experiments of Otter and Damien[2] and Kim et al.[1] are given in Table 7.2.2.

Ronchi[14] commented that diffusivity in crystals decreases with temperature due to increased anharmonic vibrations caused by defects, impurities, and lattice strains. Below 2500 K, the behavior of the thermal diffusivity of UO_2 is in accord with this crystalline behavior. As the λ phase transition at 2670 K is approached, the number of phonon scattering centers increases. Above the λ phase transition, the concentration of Frenkel pairs in the oxygen sublattice approaches 0.2,[13] so the lattice has a very high degree of disorder similar to an amorphous or glassy material. Ronchi[14] commented that materials that have both crystalline and glassy forms (e.g., SiO_2) have a different temperature dependence for the thermal diffusivity in the two forms (decreasing for the crystal; increasing for the glassy phase).[14] In metals and alloys that undergo order/disorder λ transitions, the slope of thermal diffusivity, changes at the λ transition from decreasing to increasing. If no transition exists, the reversal of slope normally occurs at the melting point and is often accompanied by a discontinuity in thermal diffusivity upon melting. For materials with a premelting order/disorder transition, the thermal diffusivity typically increases continuously across the melting point.[14] In Figure 7.2.1, the thermal diffusivities of liquid UO_2 from the measurements of Kim et al.,[1] Otter and Damien,[2] and Tasman[4] are compared with thermal diffusivities of solid UO_2 near the melting point. The solid values are from thermal diffusivity measurements by Weilbacher[19, 20] and the thermal conductivity equations of Harding and Martin[15] and of Hyland.[16] The thermal

**Table 7.2.2   Thermal Diffusivity of Liquid UO_2 from Measurements
of Thermal Diffusivity and Thermal Conductivity**

Experiment	Kim et al. [1]	Otter & Damien [2]	Tasman et al. [3,4]
Property Measured	Thermal Diffusivity	Thermal Diffusivity	Thermal Conductivity
Method	Periodic Heat Flow	Laser Flash	Laser Heating - Melt & Ablate UO_2 self-contained sample
Sample	UO_2 in tungsten 3 -layers; UO_2 layer: 0.8 mm, 1.2 mm	UO_2 in tungsten 3 -layers; UO_2 layer: 0.7 mm	UO_2 6 mm diam disc partially molten; molten layer: 0.2 mm
Reported α, $m^2 s^{-1}$	19×10^{-7} - 33×10^{-7} *	16×10^{-7} - 25×10^{-7}	-
Re-evaluated 3-dim. transient heat transfer model [5]	11×10^{-7} (thin) 15×10^{-7} (thick)	16×10^{-7}	
Re-measurement & f.e.m. analysis under unsteady conditions; α, $m^2 s^{-1}$ [4]			6×10^{-7} - 8×10^{-7}

* In the assessment by Fink and Leibowitz, an error was found in the original analysis that indicated that these values reported by Kim et al. are high by about a factor of two.

conductivities were converted to thermal diffusivities using Eq. (1) and the heat capacities from the assessment by Fink[21] and the densities from the assessment of Martin.[22] Thermal diffusivities calculated from the thermal conductivity of Tasman[4] are between the solid values of Martin and of Hyland. Based on the behavior of other materials with premelting transitions, Ronchi[14] concluded that the thermal diffusivity obtained from the thermal conductivity measurement of Tasman is the most consistent with the thermal diffusivities of solid UO_2.

If the λ transition at 2670 K results in sufficient disorder for the thermal diffusivity to follow glassy behavior, then internal radiation, which is important for glassy materials, must also be

considered for UO_2 above this transition. In his critical analysis of the thermal conductivity of solid UO_2, Hyland[16] included a contribution from radiation. At the melting point, 0.48 W m^{-1} K^{-1} is the radiative contribution to the thermal conductivity of solid UO_2 calculated by Hyland[16] using the method given by Browning[23] and the optical property data for solid UO_2 measured by Bober et al.[7] This result for the solid and the statistically significant difference between the thermal diffusivities of the thin and thick UO_2 layers, which is indicative of internal radiation,[8,9] imply that the radiative contribution should also be considered for the liquid. The radiative contribution to the thermal conductivity for an optically thick sample is

$$k_r = \frac{16n^2 \sigma T^3}{3\kappa_R} \tag{2}$$

where n is the refractive index (1.72 for liquid UO_2)[7], κ_R is the Rosseland absorption coefficient, and σ is the Stephan-Boltzmann constant. Following Hyland,[16] the value of κ_R was obtained from Figure 4 of Browning,[23] which includes the contributions beyond the absorption edge of the material. For the liquid at the melting point, the radiative contribution to the thermal conductivity in the optically thick limit is 0.28 W m^{-1} K^{-1}. This corresponds to corrections to the thermal diffusivity of 0.7 x 10^{-7} to 0.9 x 10^{-7} m^2 s^{-1} between 3120 and 3400 K, assuming constant thermal conductivity and thermal diffusivity variations with temperature in accord with changes in density and heat capacity. In Figure 7.2.2, the curve labeled *"Tasman + Radiation"* includes the optically thick radiative contribution to the thermal conductivity of Tasman. If the assumption is made that the difference in thermal diffusivities between the thick and thin layers of UO_2 in the experiment of Kim et al. arises from failure to include the radiative term in the analysis, and the radiative contribution scales according to the thickness of the UO_2 layer, the experimental thermal diffusivity of a 0.2 mm thickness of UO_2 (thickness of the molten layer in the experiment of Tasman[3]) can be estimated. For the temperatures of 3250 and 3277 K, this estimate gives thermal diffusivities in the range of 5.8 x 10^{-7} m^2 s^{-1} and 6.7 x 10^{-7} m^2 s^{-1}. These values, shown in Figure 7.2.2, are slightly lower than the values calculated from the thermal conductivity of Tasman[4] using the heat capacities of Ronchi et al.[6] and densities of Breitung and Reil.[17] This scaled correction is larger than the calculated

radiative contribution due to an optically thick layer. Figure 7.2.2 includes the positive uncertainty of Tasman and a corresponding negative uncertainty (-40%) in the thermal diffusivities from the 0.813-mm layer measurements of Kim et al. These uncertainty bands overlap.

Conclusion

From these comparisons, it is reasonable to assume that 2.5 W m^{-1} K^{-1} (the new value reported by Tasman[4]) represents a lower limit of the thermal conductivity of liquid UO$_2$. An upper limit of 3.6 W m^{-1} K^{-1} is consistent with the error limit given by Tasman and with the lower value obtained from the experiments of Kim et al. with the optically thick radiative contribution (0.3 W m^{-1} K^{-1}) subtracted. Clearly, the data of Kim et al. must be reanalyzed with radiative contributions for the thickness of the UO$_2$ layers included. Although the data of Kim et al. show systematic differences between the thick and thin layers of UO$_2$ and the data of Otter and Damien appear to be high, these measurements are consistent in that they show little variation in thermal diffusivity with temperature. However, thermal diffusivities calculated using the constant thermal conductivity of Tasman[4] and the heat capacities of Ronchi et al.[6] show significant increases with temperature. From the experiments of Ronchi et al.[6] it is unclear how much of the temperature variation in C$_p$ arises from the change in thermal conductivity with temperature. (Thermal conductivity was assumed to be constant in their analysis). Ronchi[14] states that glassy ceramics show a slight increase in the thermal diffusivity with temperature and the thermal diffusivity usually increases continuously across the melting point. Because no information is available with respect to the recent thermal conductivity measurements of Tasman,[4, 14] the temperature of the measurement is uncertain. If the thermal diffusivity was assumed to be constant, the thermal conductivity data of Tasman and the heat capacity of Ronchi et al. at 3473 K would give 8.2 m^2 s^{-1} for the thermal diffusivity of liquid UO$_2$. At the melting point, this would correspond to a thermal conductivity of 3.2 W m^{-1} K^{-1}. This is within the range of recommended values.

Uncertainty

The uncertainty in the thermal conductivity and thermal diffusivity of liquid UO$_2$ is approximately 40%, the uncertainty given by Tasman et al.[3,4]

REFERENCES

1.   C. S. Kim, R. A. Haley, J. Fischer, M. G. Chasanov, and L. Leibowitz, *Measurement of Thermal Diffusivity of Molten UO$_2$*, Proc. Seventh Symp. On Thermophysical Properties, A. Cezairliyan, Ed., ASME, New York, p. 338-343 (1977).

2.   C. Otter and D. Damien, *Mesure de la Diffusivité Thermique de UO$_2$ Fondu*, High Temp.-High Pressures **16**, 1-6 (1984).

3.   H. A. Tasman, D. Pel, J. Richter, and H. E. Schmidt, *Measurement of the Thermal Conductivity of Liquid UO$_2$*, High Temp.-High Pressures **15**, 419-431 (1983).

4.   H. A. Tasman, *Thermal Conductivity of Liquid UO$_2$*, Commission of the European Communities Joint Research Centre Annual Report **TUAR88**, Karlsruhe, Germany (1988); as referenced by C. Ronchi in *On the Thermal Conductivity and Diffusivity of Solid and Liquid Uranium Dioxide*, J. Phys. Condens. Matter **6**, L561-L567 (1994).

5.   J. K. Fink and L. Leibowitz, *An Analysis of Measurements of the Thermal Conductivity of Liquid Urania*, High Temp.- High Pressures **17**, 17-26 (1985).

6.   C. Ronchi, J. P. Hiernaut, R. Selfslag, and G. J. Hyland, *Laboratory Measurement of the Heat Capacity of Urania up to 8000 K: I. Experiment*, Nuclear Science and Engineering **113**, 1-19 (1993).

7.   M. Bober, J. Singer, and K. Wagner, *Determination of the Optical Constants of Liquid UO$_2$ from Reflectivity Measurements*, Proc. Eighth Symp. On Thermophysical Properties, J. V. Sengers, Ed., ASME, New York, Vol. II, p. 234-244 (1981).

8.   K. C. Mills, and W. A. Wakeham, *Effect of Radiation on Thermal Transport Measurements*, High Temp.-High Pressures **17**, 343-348 (1985).

9.   S. Fischer, and E. Obermeier, *Influence of Radiative Heat Transfer on the Effective Thermal Conductivity of Liquids: Experimental and Theoretical Investigation*, High Temp.-High Pressures **17**, 699-705 (1985).

10.   C. Otter and J. Vandevelde, *Contribution à l'Etude du Probleme de Thermocinétique lie à la Mesure de la Diffusivité Thermique des Materiaux Liquides a Haute Temperature par la Méthode du <<Flash Laser>>*, Rev. Int. Hautes Temp. Refract. **19**, 41-53 (1982).

11.   R. J. Ackermann, *The High Temperature, High Vacuum Vaporization and Thermodynamic Properties of Uranium Dioxide*, Argonne National Laboratory Report **ANL-5482** (1955).

12. M. T. Hutchings, *High-Temperature Studies of UO₂ and ThO₂ Using Neutron Scattering Techniques,* J. Chem. Soc., Faraday Trans. II **83**, 1083-1103 (1987).

13. C. Ronchi and G. J. Hyland, *Analysis of Recent Measurements of the Heat Capacity of Uranium Dioxide,* J. of Alloys and Compounds **213/214** 159-168 (1994).

14. C. Ronchi, *On the Thermal Conductivity and Diffusivity of Solid and Liquid Uranium Dioxide,* J. Phys. Condens. Matter **6**, L561-L567 (1994).

15. J. H. Harding and D. G. Martin, *A Recommendation for the Thermal Conductivity of UO₂,* J. Nucl. Mater. **166**, 223-226 (1989).

16. G. J. Hyland, *Thermal Conductivity of Solid UO₂: Critique and Recommendation,* J. Nucl. Mater. **113**, 125-132 (1983).

17. W. Breitung and K. O. Reil, *The Density and Compressibility of Liquid (U,Pu)-Mixed Oxide,* Nucl. Sci. and Eng. **105**, 205-217 (1990).

18. W. D. Drotning, *Thermal Expansion of Molten Uranium Dioxide,* Proceedings of the Eighth Symp. Thermophysical Properties, Gaithersburg, Maryland, June 15-18, 1981, J. V. Sengers, Ed., ASME, New York, Vol. II, pp 245-249 (1981).

19. J. C. Weilbacher, *Measurement of Thermal Diffusivity of Mixed Uranium Plutonium Oxides,* CEA Report **CEA-R-4572**, Centre d'Etudes Nucleairs de Fontenay-aux Roses, France (1974).

20. J. C. Weilbacher, *Diffusivité Thermique de l'Oxyde d'Uraium et de l'Oxyde de Thorium à Haute Temperature,* High Temp.-High Pressures **4**, 431-438 (1972).

21. J. K. Fink, *Enthalpy and Heat Capacity of the Actinide Oxides,* Int. J. Thermophys. **3**(2), 165-200 (1982).

22. D. G. Martin, *The Thermal Expansion of Solid UO₂ and (U,Pu) Mixed Oxides - A Review and Recommendations,* J. Nucl. Mater. **152** 94-101 (1988).

23. P. Browning, *On the Relative Importance of the Electronic and Radiative Contributions to the Thermal Conductivity of Uranium Dioxide,* J. Nucl. Mater. **92** 33-38 (1982).

Figure 7.2.1 UO$_2$ Thermal Diffusivity
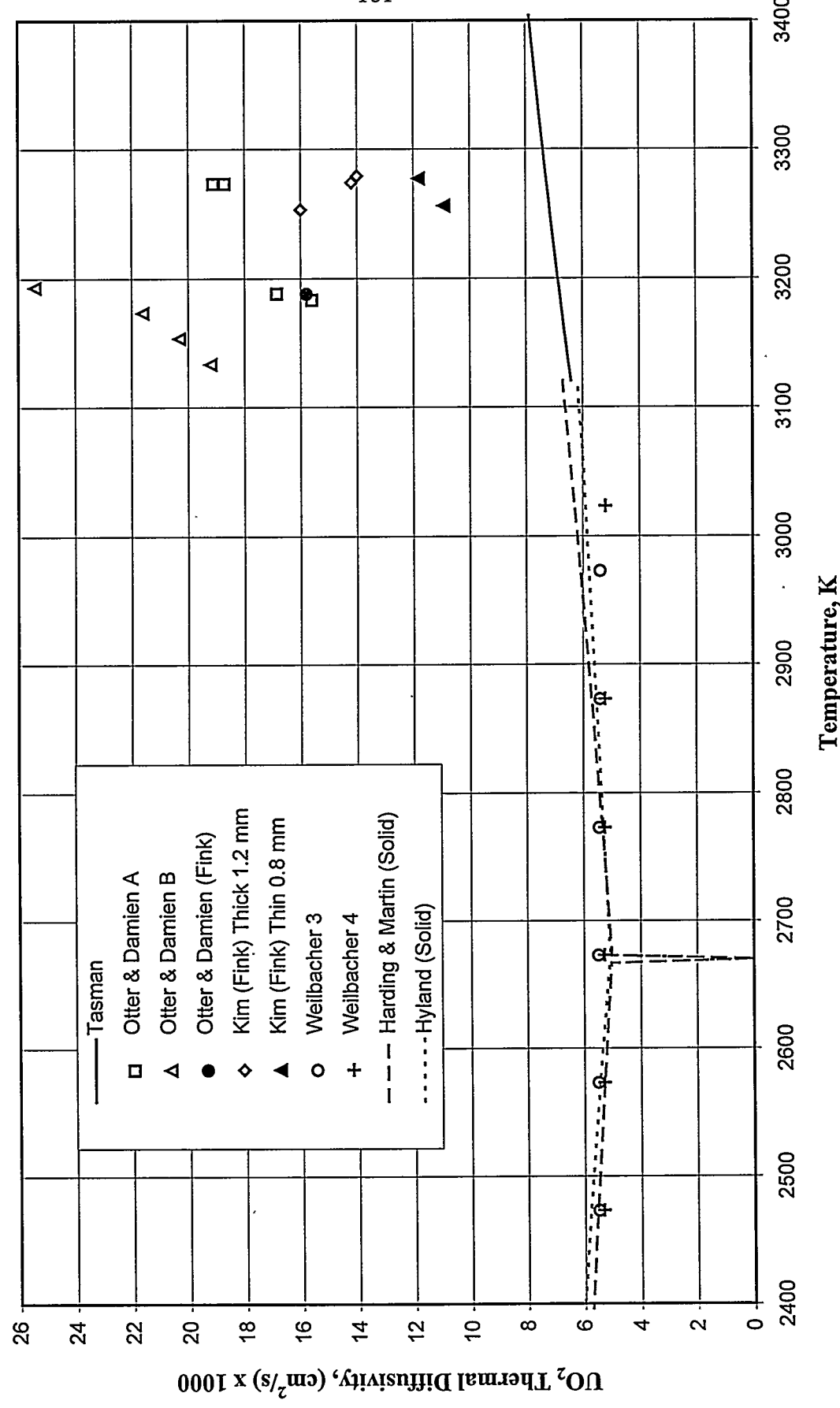
Figure 7.2.2 UO₂ Thermal Diffusivity
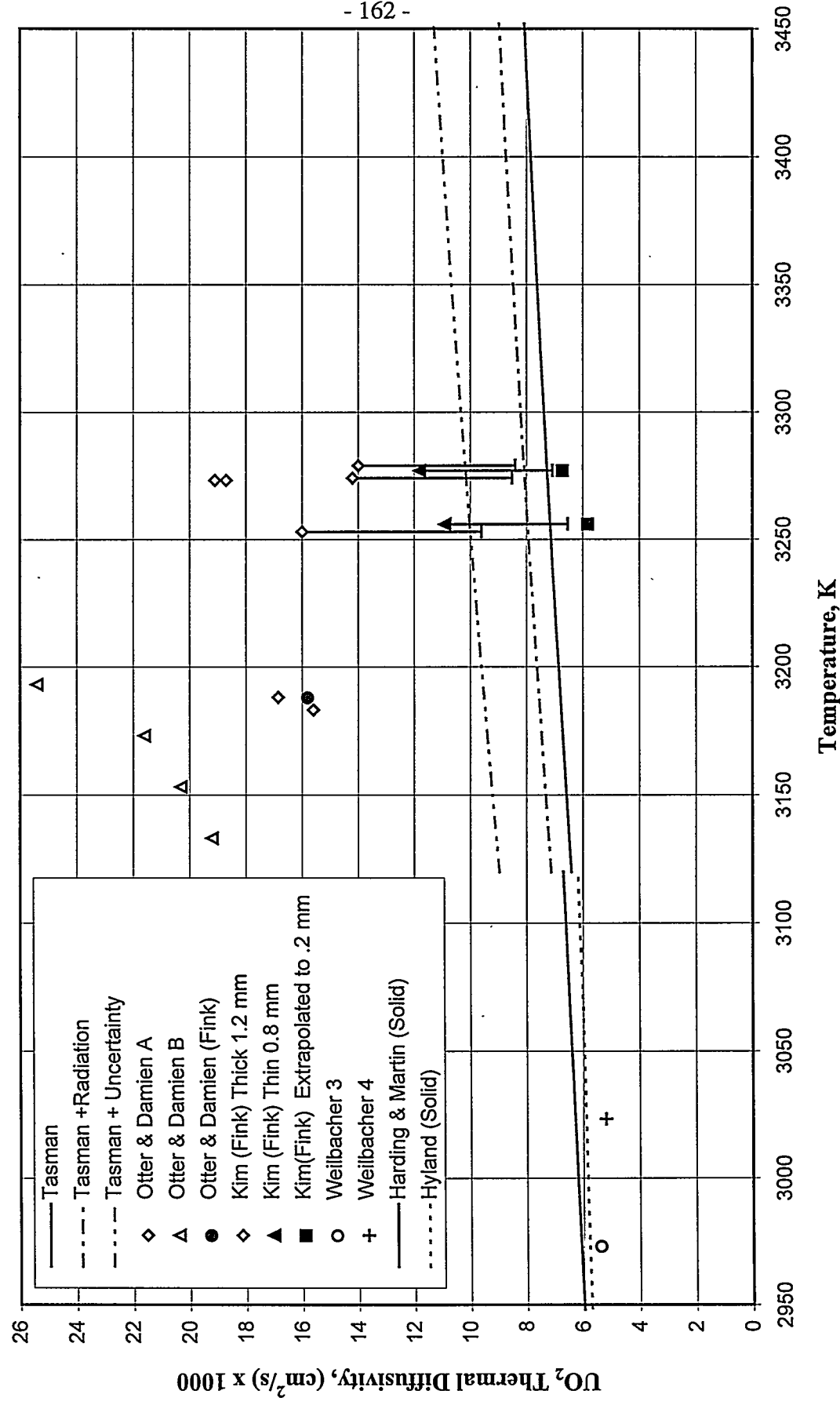
8.   VISCOSITY OF LIQUID URANIUM DIOXIDE

Summary and Recommendation

Viscosities of liquid uranium dioxide have been measured in the temperature range of 3143 to 3303 K by Woodley,[1] at the melting point (3120 K) by Palinski,[2] and from 3083 to 3328 K by Tsai and Olander.[3] The recommended equation is that of Woodley because of the greater precision of his data and the agreement between Woodley and Palinski. The Woodley equation is

$$\eta = 0.988 \exp\left(\frac{4620}{T}\right) \tag{1}$$

where the kinematic viscosity, η, is in centipoise (mPa s) and T is in K. Recommended values are given in Table 8.1 as a function of temperature and graphed in Figure 8.1. The data of Woodley,[1] Palinski,[2] and Tsai and Olander[3] as well as estimated uncertainties have been included in Figure 8.1.

Uncertainties

The uncertainty in the available data is difficult to estimate because of the lack of high-temperature viscosity standards. For the temperature range of 3120 to 3400 K, the error is estimated as ± 25%. The uncertainty of extrapolated viscosities in the temperature range of 3400 to 4000 K is estimated as ± 50%.

Discussion

Figure 8.2 shows the viscosity data of Woodley,[1] Tsai and Olander,[3] and Palinski.[2] Tsai and Olander made measurements on two different samples. Their viscosities are higher than the values of Woodley and of Palinski and lack the precision of the data of Woodley. In addition, the Tsai and Olander data for the second sample are consistently higher than for the first sample, indicating a possible systematic error. Tsai and Olander gave the melting point of UO_2 as 3073 K (not 3120 K) so that their lowest temperature datum, 9.2 cP (mPa s) at 3083 K, is at a temperature that they consider to be completely liquid. They commented that their low melting point may be due to temperature measurement errors, change in stoichiometry of their samples, or contamination of their melt by the tungsten crucible. Figure 8.2 shows that Woodley's two series of measurements on the same encapsulated sample are in good agreement and in reasonable agreement with the datum of Palinski. The viscosity of $UO_{2.003}$ at the melting point measured by Palinski[2] is 4.6 cP (4.6 mPa s)

which is within 7% of the value (4.3 cP) obtained with Eq. (1), given by Woodley. Thus, the equation based on the Woodley data is preferred. This equation has also been recommended in the assessment by Harding, Martin, and Potter.[4]

The viscosity of UO_2 was also measured by Nelson et al.[5] at 3028 K and at 3068 K, which they believed was just above the melting point. Their viscosity values at these temperatures are 46 cP and 36 cP, respectively, which are about a factor of 10 above the viscosity at 3120 K calculated with Eq. (1). The temperatures and viscosities obtained by Nelson et al.[4] suggest that these measurements were made below the melting point of UO_2. Thus, these data have not been included in this analysis.

REFERENCES

1.   R. E. Woodley, *The Viscosity of Molten Uranium Dioxide*, J. Nucl. Mater. **50**, 103-106 (1974).

2.   R. Palinski, *Core Melts - Measurement of Some Thermophysical Properties of Liquid Reactor Materials at High Temperatures*, Commission of European Communities Joint Research Centre, Ispra Establishment, Italy Report **EUR 7002 EN** (1980).

3.   H. C. Tsai and D. R. Olander, *The Viscosity of Molten Uranium Dioxide*, J. Nucl. Mater. **44**, 83-86 (1972).

4.   J. H. Harding, D. G. Martin, and P. E. Potter, *Thermophysical and Thermochemical Properties of Fast Reactor Materials*, Commission of the European Communities Report **EUR 12402 EN (1989)**.

5.   R. P. Nelson, J. J. Rasmussen, and O. D. Slagle, *Properties of Molten Fast-Reactor Oxide Fuels*, pp. 2-4 to 2.26 of Battelle-Northwest Laboratory Report **BNWL-1279** (February 1970); this study is also briefly described by J. L. Bates, C. E. McNeilly and J. J. Rasmussen, Materials Research **5**, 11 (1971).

Table 8.1 Viscosity of Liquid Uranium Dioxide

Temperature K	Viscosity mPa s
3120	4.34
3150	4.28
3200	4.19
3250	4.09
3300	4.01
3350	3.92
3400	3.84
3450	3.77
3500	3.70
3550	3.63
3600	3.57
3650	3.50
3700	3.44
3750	3.39
3800	3.33
3850	3.28
3900	3.23
3950	3.18
4000	3.14

Viscosities at temperatures ≥ 3400 K are extrapolated.

Figure 8.1 Viscosity of Liquid UO$_2$
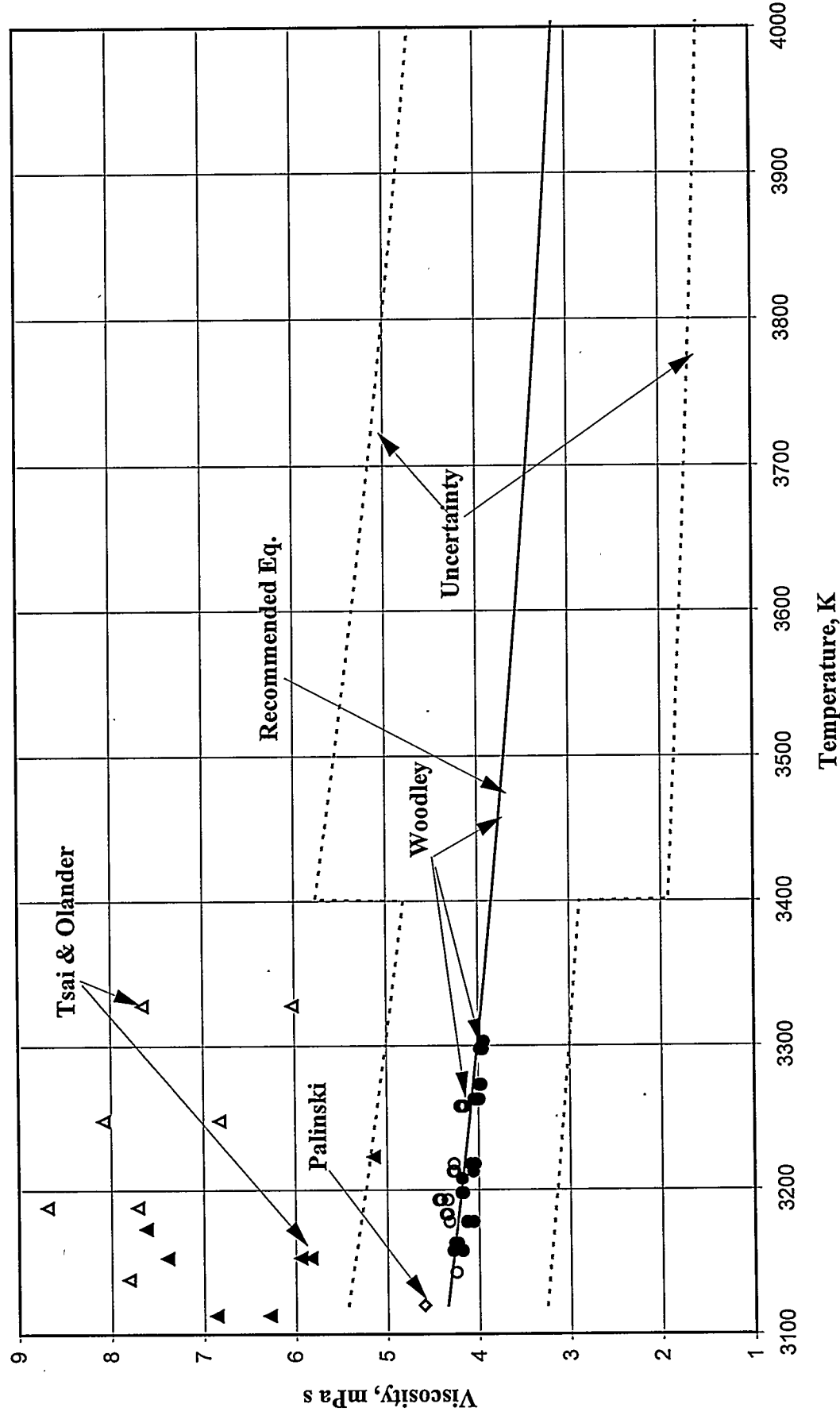
Figure 8.2 Viscosity of Liquid UO$_2$
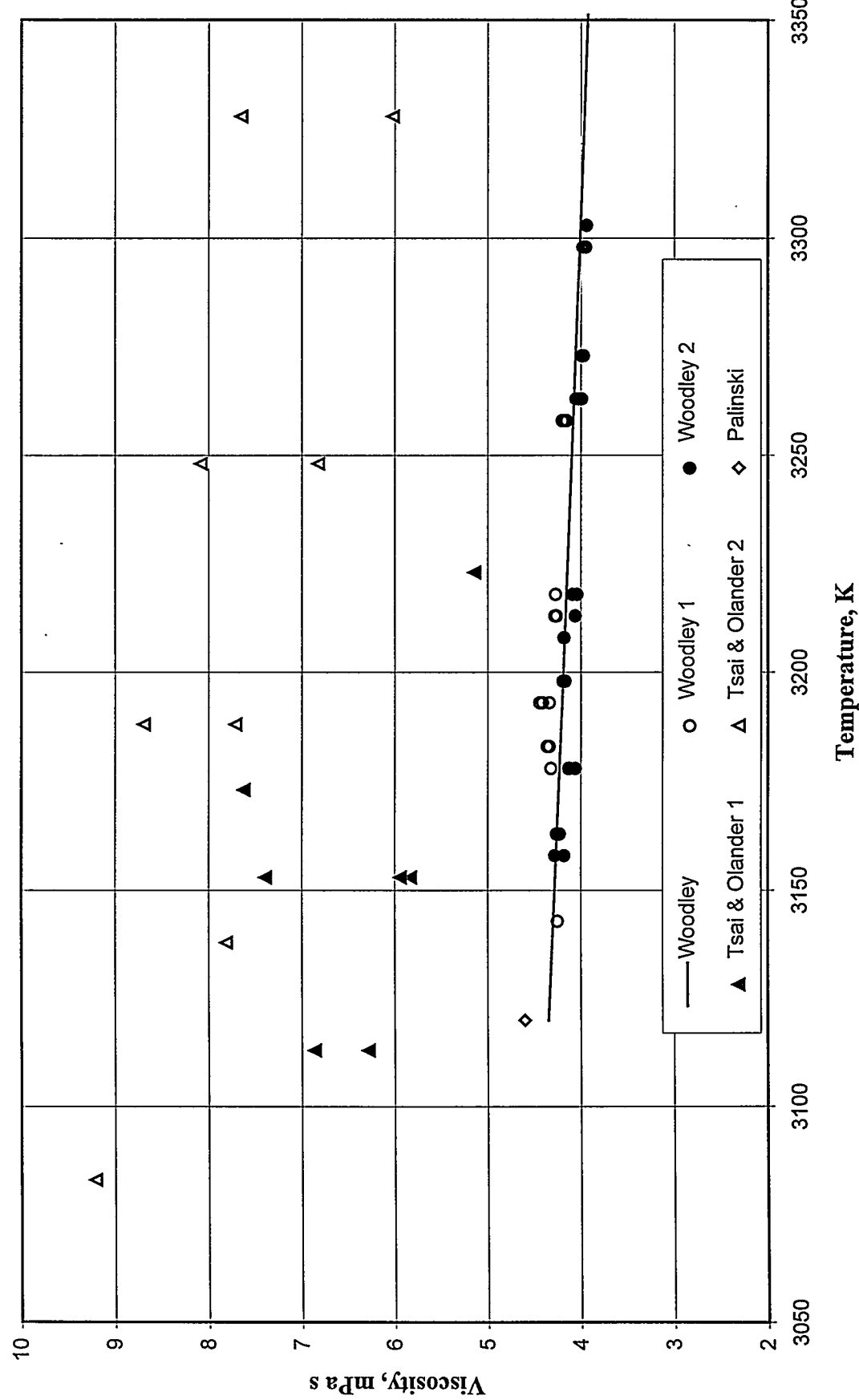
9.   EMISSIVITY AND OPTICAL CONSTANTS OF URANIUM DIOXIDE

<u>Summary of Recommendations</u>

Emissivity - The experiments of Bober et al.[1-6] for the emissivity, reflectivity, and optical constants of UO$_2$ in the solid and liquid phases provide the most reliable data for these properties. Bober, Karow, and Mueller[3] commented that, within the limits of experimental error, their data for solid UO$_2$ agree with earlier emissivity measurements by Cabannes et al.,[7] Held and Wilder,[8] and Schoenes.[9] The data in the range of 1000 K to the melting temperature (3120 K) indicate that the emissivity of both sintered and premelted solid UO$_2$ varies little with temperature and is only a weak function of wavelength. Thus, the constant total hemispherical emissivity (ϵ^h) that was suggested by Gentry[10] and also by Harding et al.[11] is recommended:

$$\epsilon^h = 0.85 \pm 0.05 \tag{1}$$

The equation given by Bober, Karow, and Muller[3] for the normal spectral emissivity of premelted solid UO$_2$ at the wavelength of 630 nm is recommended for wavelengths in the visible range:

For 1000 K $\leq T \leq$ 3120 K and 400 nm $\leq \lambda \leq$ 700 nm,

$$\epsilon(\lambda = 630nm) = 0.836 + 4.321 x 10^{-6}(T - 3120) \tag{2}$$

where *T* is in K. Values from this equation are given in Table 9.1 and shown in Figure 9.1.

The emissivity of liquid UO$_2$ is a function of both wavelength and temperature. For wavelengths in the visible range, however, the normal spectral emissivity of liquid UO$_2$ is approximately independent of wavelength. The recommended values as a function of temperature for this wavelength range are those calculated from an equation for a wavelength of 630 nm determined by Fink et al.[12]:

For 3120 K $\leq T \leq$ 6000 K and 400 nm $\leq \lambda \leq$ 700 nm,

$$\epsilon(\lambda = 630nm) = 1 - 0.16096 \exp\left[-3.7897 x 10^{-4}\Delta T - 3.2718 x 10^{-7}(\Delta T)^2\right] \tag{3}$$

where $\Delta T = T - 3120$ K. Normal spectral emissivities calculated with this equation are tabulated in Table 9.2 and are included in Figure 9.1. Although Eq. (3) was derived to fit the data of Bober, Karow, and Muller3 at a wavelength of 630 nm, it also gives a good fit to more recent data[1,2] at

wavelengths of 548, 514.5, 647, and 752.5 nm. However, the behavior of the emissivity in the infrared region differs considerably from Eq. (3). Bober et al.[3, 6] found that the normal spectral emissivity at a wavelength of 10600 nm falls from 0.85 at 3120 K to 0.64 at 3670 K and to 0.4 at 4000 K. Further emissivity measurements of liquid UO_2 are needed in the infrared and far infrared region to confirm these results.

Optical Constants - Provisional recommendations are available from measurements by Bober, Singer, and Wagner.[1, 2] They determined the optical constants for liquid UO_2 from 3100 to 3600 K and for single-crystal UO_2 at room temperature from reflectivity measurements in the spectral range of 450 to 750 nm. Their room temperature index of refraction values confirm the values of Ackermann et al.[13] The average values for the index of refraction (n) and absorption coefficient (k) of UO_2 at room temperature and in the liquid region are

For T = 300 K,

$$n = 2.2; \quad k = 0.7. \tag{4}$$

For $3100 < T \le 3600$ K,

$$n = 1.7; \quad k = 0.8. \tag{5}$$

Uncertainties

The uncertainty in the total hemispherical emissivity is $\pm$ 0.05.[10,11] Experimental uncertainties given by Karow and Bober[6] for the normal spectral emissivity of premelted solid UO_2 at the wavelength of 630 nm increase from ~1% at 1500 K to 2% at 3000 K. In the liquid region, their uncertainties are 2.5 to 3%. Uncertainties of +3%/-10% are suggested[12] for extrapolation of Eq. (2) above 4200 K. Large scatter in the reflectivity data from which the optical constants are derived lead to uncertainties in the refractive index (n) of $\pm$10% and in the absorption constant (k) of $\pm$20%.

Discussion

Emissivity of Solid UO_2 - Data of Bober et al.[1-6] provide normal spectral emissivities of solid and molten UO_2 from 1000 to 4200 K and optical constants of molten UO_2 from 3000 to 4000 K. These are the most recent and reliable data and cover the largest temperature range. The normal spectral emissivities at a wavelength of 630 nm determined by Bober et al.[3, 6] are in reasonable

agreement with normal spectral emissivities of Cabannes et al.[7] at a wavelength of 650 nm, and of Held and Wilder[8] at wavelengths of 656 and 700 nm but disagree with earlier data of Claudson[14,15] and of Ehlert and Margrave,[15,16] as shown in Figure 9.1. The data of Claudson,[14,15] which show a decrease in the emissivity in the temperature range of 1000 to 2000 K, have been rejected in reviews by Fink et al.,[12] Gentry,[10,11] and Harding et al.[11] Cabannes et al.[7] have suggested that the decrease with temperature observed by Claudson[14,15] was due to errors in the experimental technique. Unlike the data of Held and Wilder,[8] which decrease with temperature above 2000 K, the data of Bober et al.[3,6] show little temperature dependence and no decrease with temperature above 2000 K.

Bober, Karow, and Muller[3] found that the normal spectral emissivity of sintered UO_2 at a wavelength of 630 nm is slightly higher than that for premelted UO_2. From 1000 to 3120 K, they obtained an emissivity of 0.87 for sintered UO_2 and recommended Eq. (1) to represent the emissivity of premelted UO_2. Their data are supported by the measurements of Babelot et al.,[17] who obtained an emissivity of 0.84 at a wavelength of 650 nm at the melting point, 3120 K.

Cabannes et al.[7] determined emissivities at 300, 1200, and 1600 K for wavelengths ranging from 500 nm to the infrared region (10000 nm). They found little variation in emissivity with wavelength or temperature. From these data, they obtained total emissivities of 0.86, 0.90, and 0.90 at 300, 1200 and 1600 K, respectively. These total emissivities are consistent with the recommendation of Gentry[10,11] for a total emissivity of 0.85 ± 0.05. The temperature-dependent total emissivity for solid UO_2 determined by Mason[18] is given in MATPRO:[19]

$$\epsilon = 0.7856 + 1.5263 x 10^{-5} T \tag{6}$$

Total emissivities calculated with Eq. (6) increase from 0.79 at 300 K to 0.80 at 1000 K and 0.83 at 3120 K. These emissivities are consistently lower than the value given by Gentry.[10,11] However, above 700 K, they are within the uncertainty for the total emissivity recommended by Gentry.

Emissivity of Liquid UO_2 - Bober, Karow, and Muller[3] fit their data for the normal spectral emissivity of liquid UO_2 at a wavelength of 630 nm to a quartic equation:

$$\epsilon(\lambda = 630nm) = 0.843 + 1.4465 x 10^{-4} \Delta T + 1.6497 x 10^{-7} \Delta T^2$$
$$- 1.3136 x 10^{-10} \Delta T^3 + 2.899 x 10^{-14} \Delta T^4 \tag{7}$$

where $\Delta T = T - 3120K$, and T is in K. Although Eq. (7) represents the experimental data of Bober, Karow, and Muller,[3] this equation should not be used to extrapolate beyond 4200 K because it goes through an inflection point at 4831 K followed by an increasing slope that results in values greater than unity for temperatures above 5668 K. Consequently, Fink et al.[12] fit the data of Bober, Karow, and Muller[3] to an equation with a functional form appropriate for extrapolation beyond the range of experimental data without introducing unphysical behavior. That equation is the recommended equation, Eq. (3). In the temperature range of experimental data, Eq. (3) reproduces the values given by Eq. (7) to within 0.14%. Equation (3) also provides a good fit to liquid emissivity data for other wavelengths in the visible range ($\lambda = 459, 514.5, 647$, and 752.5 nm).

The normal spectral emissivity of liquid UO_2 at wavelengths in the far infrared range shows an entirely different temperature behavior from that at wavelengths in the visible range. Data of Karow and Bober[3,6] show that for $\lambda=10600$ nm the normal spectral emissivity of liquid UO_2 falls from 0.85 at 3120 K to 0.64 at 3670 K and to 0.4 at 4000 K. Further data are required at wavelengths in the infrared region to confirm these results and determine total emissivities for the liquid.

Optical Constants - Optical constants of single-crystal UO_2 were determined at 300 K by Bober et al.[1,2,4] for comparison with values obtained by Ackermann et al.[13] Ackermann et al. determined the index of refraction at room temperature in the ultraviolet region (at the wavelength of 260 nm) and in the visible range (at wavelengths from 450 to 800 nm). Figure 9.2 shows refraction indexes obtained from these measurements at wavelengths in the visible range. Room temperature values obtained from measurements by Ackermann et al. are consistently higher than those given by Bober et al. but these data are usually within the estimated 10% experimental uncertainty. The average of the values for the room temperature index of refraction from the data of Bober et al.[1] is 2.24. The average index of refraction from the values of Ackermann et al.[13] is 2.45. These averages are within the 10% uncertainty given by Bober et al.[1,2] They are both higher than the room temperature index of refraction at a wavelength of 260 nm given by Ackermann et al. (1.95). Figure 9.2 shows that they are also consistently higher than values for liquid UO_2 at wavelengths in the visible spectrum. Absorption coefficients for UO_2 at room temperature, determined by Bober et al., decreased from 0.84 at a wavelngth of 458 nm to 0.60 at a wavelength

of 752.5 nm with an average value of 0.7.

Bober, Singer, and Wagner[1, 2] determined the optical constants for liquid UO_2 from reflectivity measurements with polarized light in the temperature range of 3000 to 4000 K at four visible wavelengths (458, 514.5, 647, and 752.5 nm) and at three angles of incidence (45°, 58°, and 71°). Reflectivities measured as a function of temperature and wavelength showed considerable scatter with angle of incidence. Optical constants were calculated from the reflectivities at each temperature and wavelength for each of the three possible pairs of measurement angles (45° and 58°, 45° and 71°, 58° and 71°). Then these three sets of values were averaged to obtain optical constants for each wavelength and temperature. Figures 9.3 and 9.4 show, respectively, the average refractive index and average absorption coefficient for liquid UO_2 for four visible wavelengths as a function of temperature. Both optical constants decrease with increasing temperature. Based on these data, Bober et al.[1, 2] proposed average values for the refractive index and absorption coefficient for wavelengths in the visible range and temperatures from 3100 to 3600 K. Their average values are n=1.7 and k = 0.8.

From the scatter in their reflectance data, Bober et al.[1,2] estimated the uncertainty in the refractive index, n, as ± 10% and the uncertainty in the absorption coefficient, k, as ± 20%. Bober et al.[1] commented that the accuracy of the absorption coefficient, k, is influenced more by measurement errors than that of the refractive index, n. The equations used to calculate the optical constants are based on the assumption of an ideal optically smooth surface, which is difficult to attain. Scatter in the experimental data was attributed to imperfections of the reflecting surface, variations in the angle of incidence arising from oscillations of the liquid surface, and the formation of a meniscus. With increased temperature, surface disturbances from vaporization and gas bursts added to the difficulty of the measurements. The increased difficulty is apparent in the decreased consistency in the reflectance data above 3500 K.

REFERENCES

1. M. Bober, J. Singer, and K. Wagner, *Determination of the Optical Constants of Liquid UO₂ from Reflectivity Measurements,* Proc. Eighth Symp. on Thermophysical Properties, Gaithersburg, MD, 1981, Vol II, pp. 234-244, ASME (1982).

2. M. Bober, J. Singer, and K. Wagner, *Bestimmung der Optischen Konstanten von Geschmolzenen Kernbrennstoffen,* J Nucl. Mater. **124**, 120-128 (1984).

3. M. Bober, H. U. Karow, and K. Muller, *Study of the Spectral Reflectivity and Emisssivity of Liquid Ceramics,* High Temp. - High Pressures **12**, 161-168 (1980).

4. M. Bober, *Spectral Reflectivity and Emissivity of Solid and Liquid UO₂ as a Function of Wavelength, Angle of Incidence, and Polarization,* High Temp. - High Pressures **12**, 297-306 (1980).

5. M. Bober and H. U. Karow, *Measurements of Spectral Emissivity of UO₂ Above the Melting Point,* Proc. Seventh Symp. on Thermophysical Properties, Gaithersburg, MD, 1977, pp. 344-350, ASME (1978).

6. H. U. Karow, and M. Bober, *Experimental Investigations into the Spectral Relectivities and Emissivities of Liquid UO₂, UC, ThO₂, and Nd₂O₃,* Thermodynamics of Nuclear Materials 1979 Vol I, Proc. Symp. Julich, 1979, pp. 155-169, IAEA (1980).

7. F. Cabannes, J. P. Stora, and J. Tsakiris, *Facteurs de Reflexion et d'Emission de UO₂ a Haute Temperature,* C. R. Acad. Sc. Paris, **264B**, 45-48 (1967).

8. P. C. Held and D. R. Wilder, *High-Temperature Hemispherical Spectral Emittance of Uranium Oxides at 0.65 and 0.70 μm,* J. Am. Ceramic Society **52**, 152-185 (1969).

9. J. Schoenes, *Optical Properties and Electronic Structure of UO₂,* J. Appl. Phys. **49** 1463-1465 (1978).

10. P. J. Gentry, Report **ND-P-6887 (W)** (1981), as referenced by J. H. Harding, D. G. Martin, and P. E. Potter, *Thermophysical and Thermochemical Properties of Fast Reactor Materials,* Commission of the European Communities Report **EUR 12402 EN** (1989).

11. J. H. Harding, D. G. Martin, and P. E. Potter, *Thermophysical and Thermochemical Properties of Fast Reactor Materials,* Commission of the European Communities Report **EUR 12402 EN** (1989).

12. J. K. Fink, M. G. Chasanov, and L. Leibowitz, *Transport Properties of Uranium Dioxide,* **ANL-CEN-RSD-80-4**, Argonne National Laboratory (April 1981).

13.   R. J. Ackermann, R. J. Thorn, and G. H. Winslow, *Visible and Ultraviolet Absorption Properties of Uranium Dioxide Films,* J. Opt. Soc. Am. **49**, 1107 (1959).

14.   T. T. Claudson, *Emissivity Data for Uranium Dioxide,* Report **AW-55414** (Nov. 1958), as referenced in *Uranium Dioxide Properties and Nuclear Applications,* J. Belle, Ed.,. pp. 196-197, US AEC (1961)

15.   J. Belle, Ed., *Uranium Dioxide Properties and Nuclear Applications,* pp. 196-197, US AEC (1961)

16.   T. C. Ehlert and J. L. Margrave, *Melting Point and Spectral Emissivity of Uranium Dioxide,* J. Am. Ceram. Soc. **41**, 330 (1958), as referenced in *Uranium Dioxide Properties and Nuclear Applications,* J. Belle, Ed., pp. 196-197, USAEC (1961).

17.   J. F. Babelot, G. D. Brunne, P. R. Kinsman, and R. W. Ohse, Atomwirt-Atomtech **22**, (No. 7-8), 387 (1977).

18.   R. E. Mason, *Fuel Emissivity,* **CDAP-TR-78-039**, Idaho Engineering Laboratory (1978).

19.   J. K. Hohorst, Ed., *SCADAP/RELAP5/MOD2 Code Manual, Vol. 4: MATPRO- a Library of Materials Properties for Light-Water-Reactor Accident Analysis,* **NUREG/CR-5273** (1990).

Table 9.1 Normal Spectral Emissivity of Premelted UO_2 at $\lambda = 630$ nm

Temperature , K	Emissivity ($\lambda = 630$ nm)
300	0.82
500	0.82
1000	0.83
1500	0.83
2000	0.83
2500	0.83
3000	0.84
3120 (s)	0.84

Table 9.2 Normal Spectral Emissivity of Liquid UO_2 at $\lambda = 630$ nm

Temperature , K	Emissivity ($\lambda = 630$ nm)
3120	0.84
3500	0.87
4000	0.91
4500	(0.95)*
5000	(0.98)*
5500	(0.99)*
6000	(0.99)*

* Extrapolated beyond the range of experimental data

Figure 9.1 UO$_2$ Emissivity
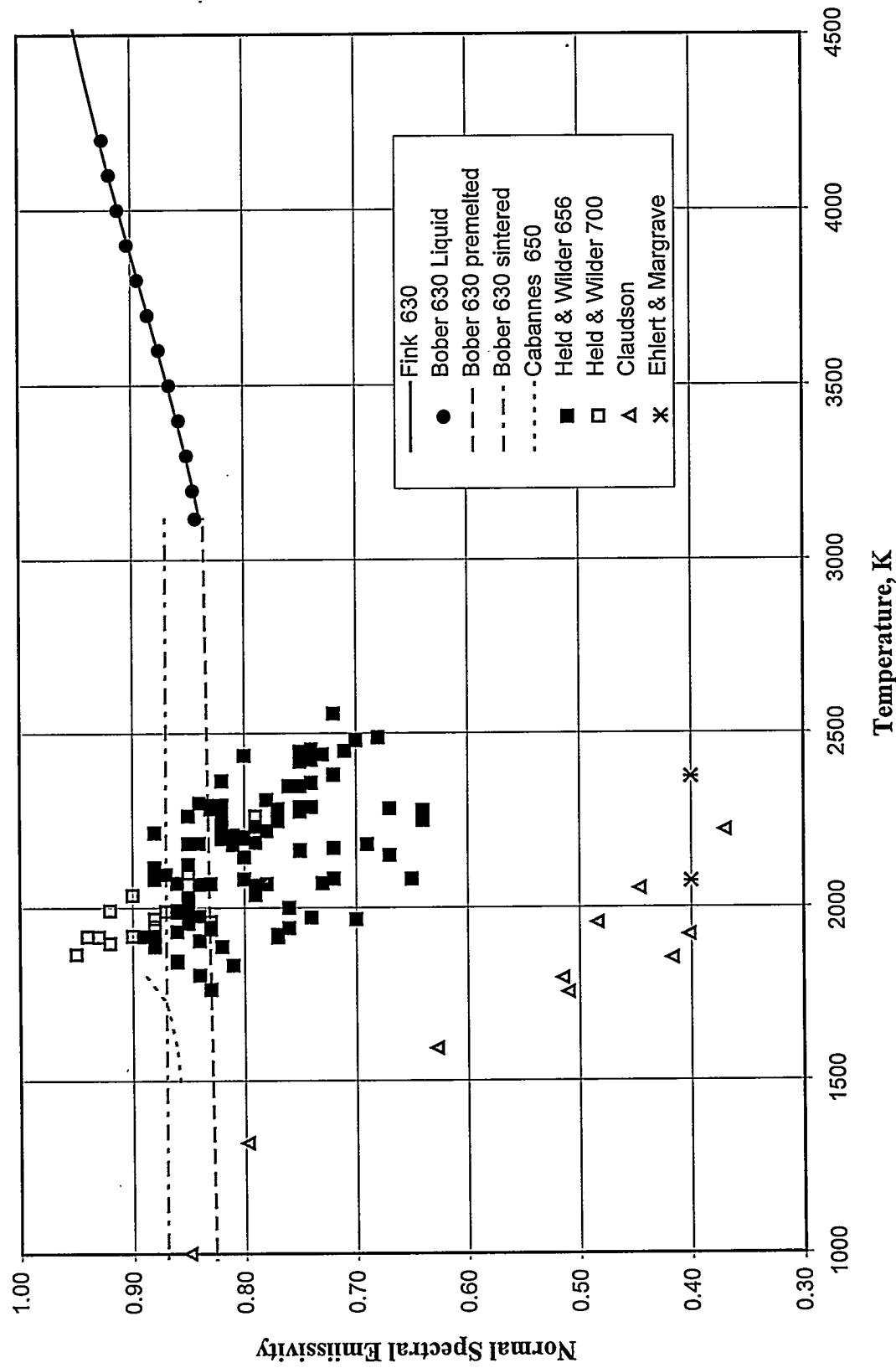
Figure 9.2 Average Refractive Index of UO$_2$
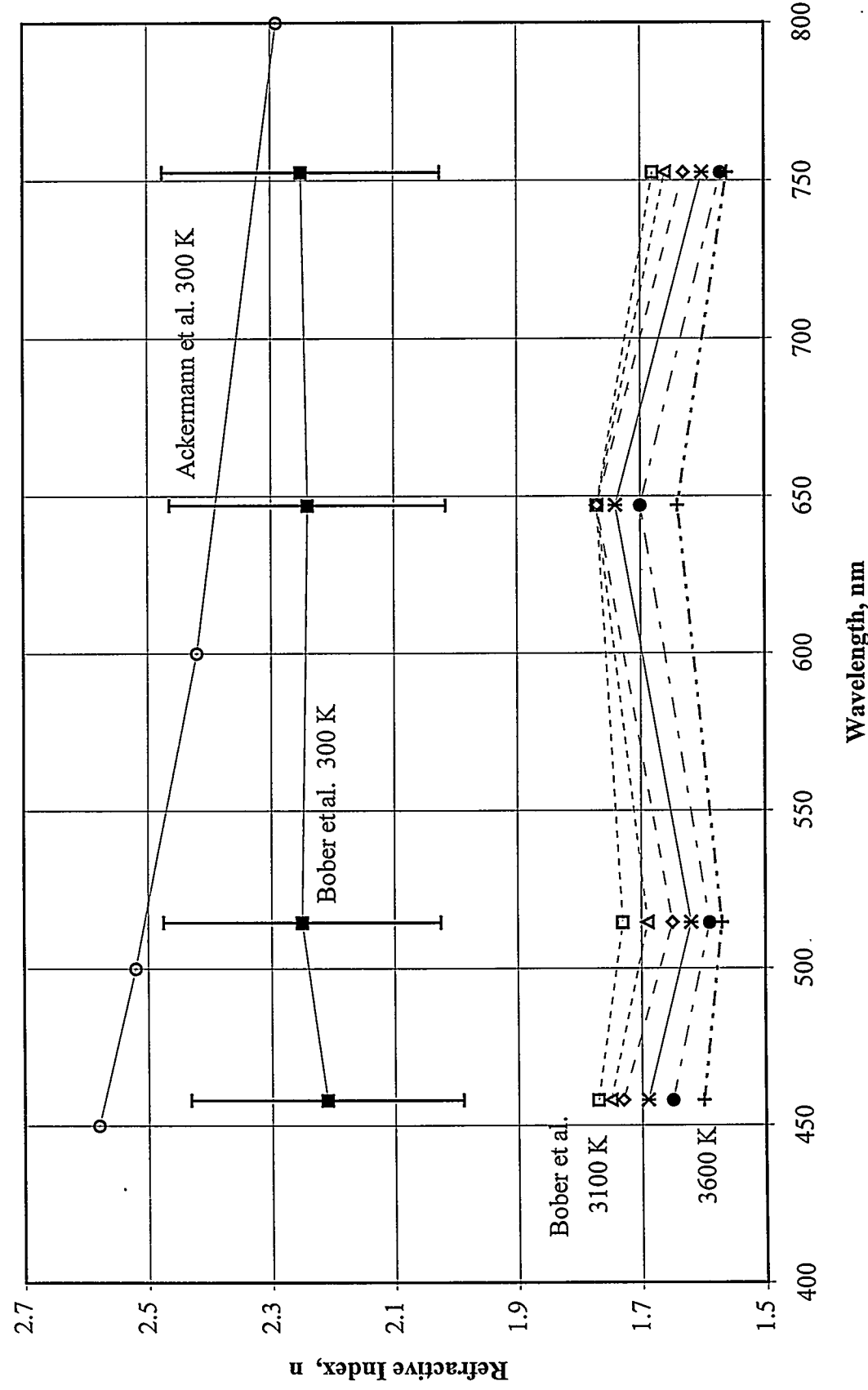
Figure 9.3 Average Refractive Index of UO$_2$ from Measurements of Bober et al.
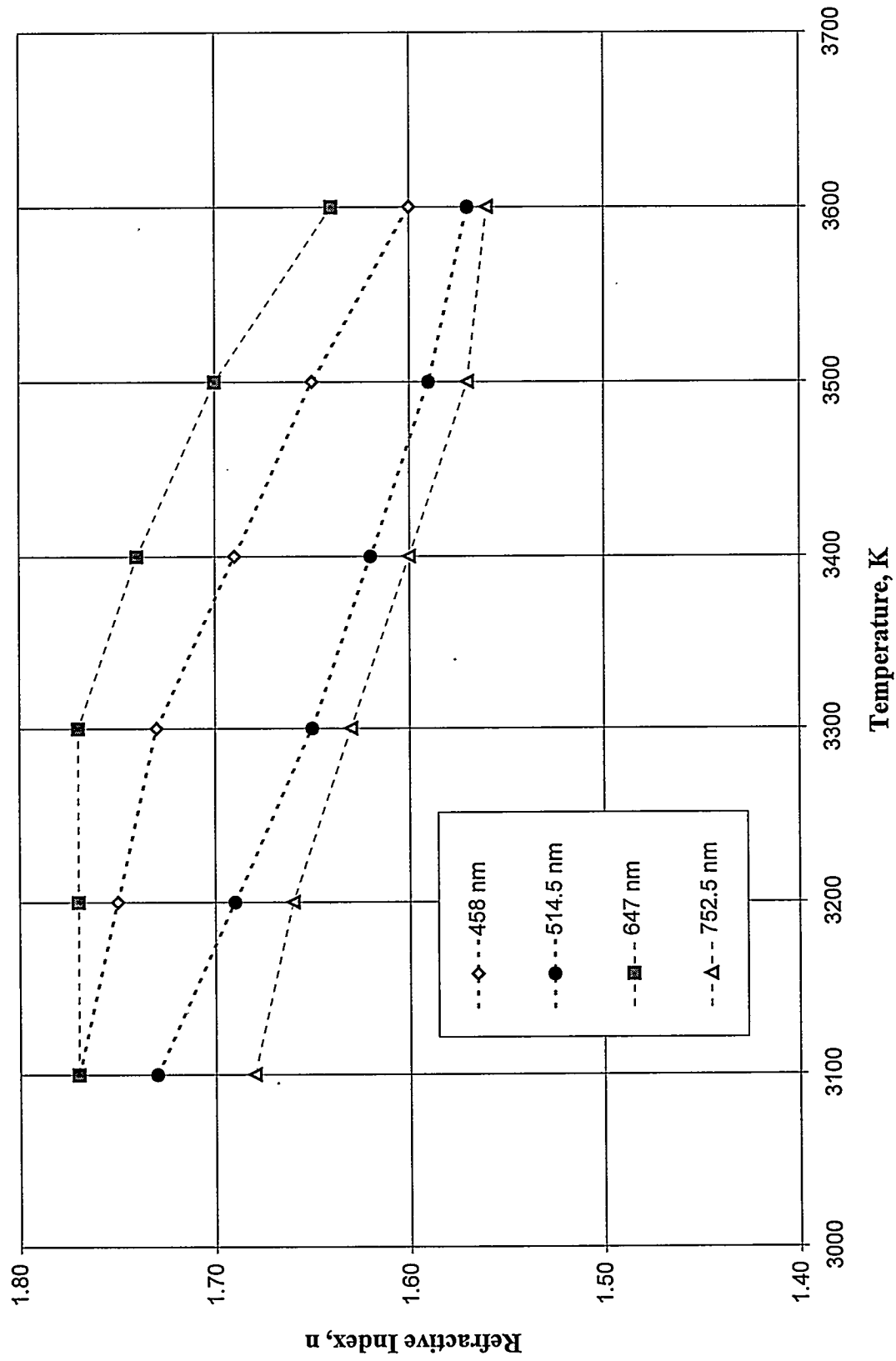
Figure 9.4 Average UO$_2$ Absorption Coefficient from Measurements of Bober et al.

ACKNOWLEDGMENTS